

# **EUROCODE 2**

# **COMMENTARY**





# **EUROCODE 2**

# **COMMENTARY**

Copyright: European Concrete Platform ASBL, June 2008

All rights reserved. No part of this publication may be reproduced, stored in a retrieval system or transmitted in any form or by any means, electronic, mechanical, photocopying, recording or otherwise, without the prior written permission of **the European Concrete Platform ASBL**.

Published by the European Concrete Platform ASBL  
Editor: Jean-Pierre Jacobs  
8 rue Volta  
1050 Brussels

Layout & Printing by  
The European Concrete Platform

All information in this document is deemed to be accurate by the European Concrete Platform ASBL at the time of going into press. It is given in good faith.

Information on European Concrete Platform document does not create any liability for its Members. While the goal is to keep this information timely and accurate, the European Concrete Platform ASBL cannot guarantee either. If errors are brought to its attention, they will be corrected.

The opinions reflected in this document are those of the authors and the European Concrete Platform ASBL cannot be held liable for any view expressed therein.

All advice or information from the European Concrete Platform ASBL is intended for those who will evaluate the significance and limitations of its contents and take responsibility for its use and application. No liability (including for negligence) for any loss resulting from such advice or information is accepted.

Readers should note that all European Concrete Platform publications are subject to revision from time to time and therefore ensure that they are in possession of the latest version.

This publication is based on the publication: "Guida all'uso dell'eurocodice 2" prepared by AICAP; the Italian Association for Reinforced and Prestressed Concrete, on behalf of the the Italian Cement Organization AITEC, and on background documents prepared by the Eurocode 2 Project Teams Members, during the preparation of the EN version of Eurocode 2 (prof A.W. Beeby, prof H. Corres Peiretti, prof J. Walraven, prof B. Westerberg, prof R.V. Whitman).

Authorization has been received or is pending from organisations or individuals for their specific contributions.

## FOREWORD

The introduction of Eurocodes is a challenge and opportunity for the European cement and concrete industry. These design codes, considered to be the most advanced in the world, will lead to a common understanding of the design principles for concrete structures for owners, operators and users, design engineers, contractors and the manufacturers of concrete products. The advantages of unified codes include the preparation of common design aids and software and the establishment of a common understanding of research and development needs in Europe.

As with any new design code, it is important to have an understanding of the principles and background, as well as design aids to assist in the design process. The European cement and concrete industry represented by CEMBUREAU, BIBM and ERMCO recognised this need and set up a task group to prepare two documents, Commentary to EN 1992 and Worked Examples to EN 1992. The Commentary to EN 1992 captures the background to the code and Worked Examples to EN 1992 demonstrates the practical application of the code. Both the documents were prepared by a team led by Professor Giuseppe Mancini, Chairman of CEN TC 250/SC2 Concrete Structures, and peer reviewed by three eminent engineers who played a leading role in the development of the concrete Eurocode: Professor Narayanan, Professor Spehl and Professor Walraven.

This is an excellent example of pan-European collaboration and CEMBUREAU, BIBM and ERMCO are delighted to make these authoritative documents available to design engineers, software developers and all others with an interest in promoting excellence in concrete design throughout Europe. As chairman of the Task Group, I would like to thank the authors, peer reviewers and members of the joint Task Force for working efficiently and effectively in producing these documents.

Dr Pal Chana

Chairman, CEMBUREAU/BIBM/ERMCO TF 5.5 "Eurocodes"



## **Attributable Foreword to the Commentary and Worked Examples to EC2**

Eurocodes are one of the most advanced suite of structural codes in the world. They embody the collective experience and knowledge of whole of Europe. They are born out of an ambitious programme initiated by the European Union. With a wealth of code writing experience in Europe, it was possible to approach the task in a rational and logical manner. Eurocodes reflect the results of research in material technology and structural behaviour in the last fifty years and they incorporate all modern trends in structural design.

Like many current national codes in Europe, Eurocode 2 (EC 2) for concrete structures draws heavily on the CEB Model Code. And yet the presentation and terminology, conditioned by the agreed format for Eurocodes, might obscure the similarities to many national codes. Also EC 2 in common with other Eurocodes, tends to be general in character and this might present difficulty to some designers at least initially. The problems of coming to terms with a new set of codes by busy practising engineers cannot be underestimated. This is the backdrop to the publication of 'Commentary and Worked Examples to EC 2' by Professor Mancini and his colleagues. Commissioned by CEMBUREAU, BIBM, EFCA and ERMCO this publication should prove immensely valuable to designers in discovering the background to many of the code requirements. This publication will assist in building confidence in the new code, which offers tools for the design of economic and innovative concrete structures. The publication brings together many of the documents produced by the Project Team during the development of the code. The document is rich in theoretical explanations and draws on much recent research. Comparisons with the ENV stage of EC2 are also provided in a number of cases. The chapter on EN 1990 (Basis of structural design) is an added bonus and will be appreciated by practioners. Worked examples further illustrate the application of the code and should promote understanding.

The commentary will prove an authentic companion to EC 2 and deserves every success.

Professor R S Narayanan  
Chairman CEN/TC 250/SC2 (2002 – 2005)

## **Foreword to Commentary to Eurocode 2 and Worked Examples**

When a new code is made, or an existing code is updated, a number of principles should be regarded:

1. Codes should be based on clear and scientifically well founded theories, consistent and coherent, corresponding to a good representation of the structural behaviour and of the material physics.
2. Codes should be transparent. That means that the writers should be aware, that the code is not prepared for those who make it, but for those who will use it.
3. New developments should be recognized as much as possible, but not at the cost of too complex theoretical formulations.
4. A code should be open-minded, which means that it cannot be based on one certain theory, excluding others. Models with different degrees of complexity may be offered.
5. A code should be simple enough to be handled by practicing engineers without considerable problems. On the other hand simplicity should not lead to significant lack of accuracy. Here the word “accuracy” should be well understood. Often so-called “accurate” formulations, derived by scientists, cannot lead to very accurate results, because the input values can not be estimated with accuracy.
6. A code may have different levels of sophistication. For instance simple, practical rules can be given, leading to conservative and robust designs. As an alternative more detailed design rules may be offered, consuming more calculation time, but resulting in more accurate and economic results.

For writing a Eurocode, like EC-2, another important condition applies. International consensus had to be reached, but not on the cost of significant concessions with regard to quality. A lot of effort was invested to achieve all those goals.

It is a rule for every project, that it should not be considered as finalized if implementation has not been taken care of. This book may, further to courses and trainings on a national and international level, serve as an essential and valuable contribution to this implementation. It contains extensive background information on the recommendations and rules found in EC2. It is important that this background information is well documented and practically available, as such increasing the transparency. I would like to thank my colleagues of the Project Team, especially Robin Whittle, Bo Westerberg, Hugo Corres and Konrad Zilch, for helping in getting together all background information. Also my colleague Giuseppe Mancini and his Italian team are gratefully acknowledged for providing a set of very illustrative and practical working examples. Finally I would like to thank CEMBURAU, BIBM, EFCA and ERMCO for their initiative, support and advice to bring out this publication.

Joost Walraven  
Convenor of Project Team for EC2 (1998 -2002)



## **Authorisation to use the Background Document(s) of EN 1992**

I hereby agree to grant the European Concrete Platform, its founding members and for their respective members as well as for future European branch associations to become member of the European Concrete Platform and their members, the licence to use the following documents hereinafter collectively referred to as "the Material" as specified below:

Background documents prepared as part of my work in the Project Team for EN 1992-1-1 (2004).

The European Concrete Platform, its founding members and for their respective members as well as for future European branch associations to become member of the European Concrete Platform and their members, are authorised, for free, worldwide, for the whole duration over which an intellectual property right protects the Material to reproduce such Material, including to adapt, translate into any language, combine with other documents, summarise and to communicate to the public such Material, whatever the technique or the format used e.g. via Internet, paper or electronic, via web, CD-ROM, etc.

I hereby warrant and guarantee that I hold all the necessary rights over the Material in order to grant European Concrete Platform, its founding members and for their respective members as well as for future European branch associations to become member of the European Concrete Platform and their members, the above mentioned licence and, if need be, I have obtained all necessary authorisations from any third party which may hold an intellectual property right over the Material.

Consequently, I shall keep European Concrete Platform, its founding members and for their respective members as well as for future European branch associations to become member of the European Concrete Platform and their members, collectively or/and individually immune from any liability and/or claim based on any violation of an intellectual or contractual right by the use by European Concrete Platform, its founding members and for their respective members as well as for future European branch associations to become member of the European Concrete Platform and their members, of the Material as provided for in this agreement.

Done in Stockholm, in 1 exemplar.

On June 12, 2008



Bo Westerberg

16 JUN 2008

# Eurocode 2 Commentary – Reading key

## SECTION 2 BASIS OF DESIGN

### 2.1 Requirements

Clause 2.1 of the EN 1992-1-1

Comment on Clause 2.1  
of EN 1992-1-1

## SECTION 2 BASIS OF DESIGN

### C2.1 Requirements

Eurocode 2, Section 2, Part 1.1 states that concrete structures should be designed in accordance with the general rules of EN1990 and with actions defined in EN 1991. EN 1992 has some additional requirements.

In particular, the basic requirements of EN1990 Section 2 are deemed to be satisfied for all concrete structures if limit state design is carried out with the partial factor method in accordance with EN1990, and if actions are defined in accordance with EN1991, and if combinations of actions in accordance with EN1990, and finally if resistance, durability and serviceability are dealt with in accordance with EN1992.

Comment on Clause 5.8.3  
of EN 1992-1-1

5.8.3 Simplified criteria for  
second order effects  
5.8.3.1 Slenderness criterion  
for isolated members

### C5.8.3. Simplified criteria for ignoring 2nd order effects

#### C5.8.3.1 Slenderness limit for isolated members

##### 5.8.3.1.1 General

The load bearing capacity of a member in compression for low slenderness ratios is illustrated in figure 3-1 by means of interaction curves, calculated according to the general method in 5.8.6.

(See chapter 6 in this report for more details about interaction curves and the general method.)

without "C": first paragraph of the  
comment on clause 5.8.3.1

## COMMENTARY TO EUROCODE 2 - SUMMARY

<b>SECTION 1 SYMBOLS</b> .....	<b>1-1</b>
<b>SECTION 2 BASIS OF DESIGN</b> .....	<b>2-1</b>
2.1 REQUIREMENTS .....	2-1
2.2 PRINCIPLES OF LIMIT STATE DESIGN .....	2-5
2.3 BASIC VARIABLES .....	2-6
2.4 VERIFICATION BY THE PARTIAL FACTOR METHOD .....	2-10
2.5 DESIGN ASSISTED BY TESTING .....	2-14
2.6 SUPPLEMENTARY REQUIREMENTS FOR FOUNDATIONS .....	2-14
2.7 REQUIREMENTS FOR FASTENINGS .....	2-14
<b>SECTION 3 MATERIALS</b> .....	<b>3-1</b>
3.1 CONCRETE .....	3-1
3.2 REINFORCING STEEL .....	3-11
3.3 PRESTRESSING STEEL .....	3-12
3.4 PRESTRESSING DEVICES .....	3-13
<b>SECTION 4 DURABILITY AND COVER TO REINFORCEMENT</b> .....	<b>4-1</b>
<b>SECTION 5 STRUCTURAL ANALYSIS</b> .....	<b>5-1</b>
5.1 GENERAL .....	5-1
5.2 GEOMETRIC IMPERFECTIONS .....	5-1
5.3 IDEALISATION OF THE STRUCTURE .....	5-2
5.4 LINEAR ELASTIC ANALYSIS .....	5-4
5.5 LINEAR ANALYSIS WITH LIMITED REDISTRIBUTION .....	5-4
5.6 PLASTIC ANALYSIS .....	5-5
5.7 NON-LINEAR ANALYSIS .....	5-5
5.8 ANALYSIS OF SECOND ORDER EFFECTS WITH AXIAL LOAD .....	5-6
5.9 LATERAL INSTABILITY OF SLENDER BEAMS .....	5-34
5.10 PRESTRESSED MEMBERS AND STRUCTURES .....	5-34
5.11 ANALYSIS FOR SOME PARTICULAR STRUCTURAL MEMBERS .....	5-34
<b>SECTION 6 ULTIMATE LIMIT STATES (ULS)</b> .....	<b>6-1</b>
6.1 BENDING WITH OR WITHOUT AXIAL FORCE .....	6-1
6.2 SHEAR .....	6-12

<b>6.3 TORSION</b>	<b>6-25</b>
<b>6.4 PUNCHING</b>	<b>6-26</b>
<b>6.5 DESIGN WITH STRUT AND TIE MODELS</b>	<b>6-32</b>
<b>6.6 ANCHORAGES AND LAPS</b>	<b>6-32</b>
<b>6.7 PARTIALLY LOADED AREAS</b>	<b>6-32</b>
<b>6.8 FATIGUE</b>	<b>6-32</b>
<b>SECTION 7. SERVICEABILITY LIMIT STATES (SLS)</b>	<b>7-1</b>
<b>7.1 GENERAL</b>	<b>7-1</b>
<b>7.2 STRESS LIMITATION</b>	<b>7-1</b>
<b>7.3 CRACK CONTROL</b>	<b>7-1</b>
<b>7.4 DEFLECTION CONTROL</b>	<b>7-15</b>
<b>SECTION 8 DETAILING OF REINFORCEMENT AND PRESTRESSING TENDONS - GENERAL</b>	<b>8-1</b>
<b>8.1 GENERAL</b>	<b>8-1</b>
<b>8.2 SPACING OF BARS</b>	<b>8-1</b>
<b>8.3 PERMISSIBLE MANDREL DIAMETERS FOR BENT BARS</b>	<b>8-1</b>
<b>8.4 ANCHORAGE OF LONGITUDINAL REINFORCEMENT</b>	<b>8-1</b>
<b>8.5 ANCHORAGE OF LINKS AND SHEAR REINFORCEMENT</b>	<b>8-1</b>
<b>8.6 ANCHORAGE BY WELDED BARS</b>	<b>8-1</b>
<b>8.7 LAPS AND MECHANICAL COUPLERS</b>	<b>8-1</b>
<b>8.8 ADDITIONAL RULES FOR LARGE DIAMETER BARS</b>	<b>8-1</b>
<b>8.9 BUNDLED BARS</b>	<b>8-1</b>
<b>8.10 PRESTRESSING TENDONS</b>	<b>8-1</b>
<b>SECTION 11 LIGHTWEIGHT CONCRETE</b>	<b>11-1</b>
<b>11.1 GENERAL</b>	<b>11-1</b>
<b>11.3 MATERIALS</b>	<b>11-1</b>

**SECTION 1 SYMBOLS****SECTION 1. SYMBOLS**

For the purposes of this document, the following symbols apply.  
Note: the notation used is based on ISO 3898:1987

*Latin upper case letters*

$A$	Accidental action
$A$	Cross sectional area
$A_c$	Cross sectional area of concrete
$A_p$	Area of a prestressing tendon or tendons
$A_s$	Cross sectional area of reinforcement
$A_{s,min}$	minimum cross sectional area of reinforcement
$A_{sw}$	Cross sectional area of shear reinforcement
$D$	Diameter of mandrel
$D_{Ed}$	Fatigue damage factor
$E$	Effect of action
$E_c, E_c(28)$	Tangent modulus of elasticity of normal weight concrete at a stress of $\sigma_c = 0$ and at 28 days
$E_{c,eff}$	Effective modulus of elasticity of concrete
$E_{cd}$	Design value of modulus of elasticity of concrete
$E_{cm}$	Secant modulus of elasticity of concrete
$E_c(t)$	Tangent modulus of elasticity of normal weight concrete at a stress of $\sigma_c = 0$ and at time $t$
$E_p$	Design value of modulus of elasticity of prestressing steel
$E_s$	Design value of modulus of elasticity of reinforcing steel
$EI$	Bending stiffness
EQU	Static equilibrium
$F$	Action
$F_d$	Design value of an action
$F_k$	Characteristic value of an action
$G_k$	Characteristic permanent action
$I$	Second moment of area of concrete section
$L$	Length
$M$	Bending moment
$M_{Ed}$	Design value of the applied internal bending moment
$N$	Axial force
$N_{Ed}$	Design value of the applied axial force (tension or compression)
$P$	Prestressing force
$P_0$	Initial force at the active end of the tendon immediately after stressing
$Q_k$	Characteristic variable action
$Q_{fat}$	Characteristic fatigue load
$R$	Resistance
$S$	Internal forces and moments
$S$	First moment of area
SLS	Serviceability limit state
$T$	Torsional moment
$T_{Ed}$	Design value of the applied torsional moment
ULS	Ultimate limit state
$V$	Shear force
$V_{Ed}$	Design value of the applied shear force

*Latin lower case letters*

$a$	Distance
$a$	Geometrical data
$\Delta a$	Deviation for geometrical data
$b$	Overall width of a cross-section, or actual flange width in a T or L beam
$b_w$	Width of the web on T, I or L beams
$d$	Diameter; Depth
$d$	Effective depth of a cross-section
$d_g$	Largest nominal maximum aggregate size
$e$	Eccentricity
$f_c$	Compressive strength of concrete

$f_{cd}$	Design value of concrete compressive strength
$f_{ck}$	Characteristic compressive cylinder strength of concrete at 28 days
$f_{cm}$	Mean value of concrete cylinder compressive strength
$f_{ctk}$	Characteristic axial tensile strength of concrete
$f_{ctm}$	Mean value of axial tensile strength of concrete
$f_p$	Tensile strength of prestressing steel
$f_{pk}$	Characteristic tensile strength of prestressing steel
$f_{p0,1}$	0,1% proof-stress of prestressing steel
$f_{p0,1k}$	Characteristic 0,1% proof-stress of prestressing steel
$f_{0,2k}$	Characteristic 0,2% proof-stress of reinforcement
$f_t$	Tensile strength of reinforcement
$f_{tk}$	Characteristic tensile strength of reinforcement
$f_y$	Yield strength of reinforcement
$f_{yd}$	Design yield strength of reinforcement
$f_{yk}$	Characteristic yield strength of reinforcement
$f_{ywd}$	Design yield of shear reinforcement
$h$	Height
$h$	Overall depth of a cross-section
$i$	Radius of gyration
$k$	Coefficient; Factor
$l$ (or $l$ or $L$ )	Length; Span
$m$	Mass, reduced moment
$n$	reduced axial force
$r$	Radius
$1/r$	Curvature at a particular section
$t$	Thickness
$t$	Time being considered
$t_0$	The age of concrete at the time of loading
$u$	Perimeter of concrete cross-section, having area $A_c$
$u, v, w$	Components of the displacement of a point
$x$	Neutral axis depth
$x, y, z$	Coordinates
$z$	Lever arm of internal forces

#### Greek lower case letters

$\alpha$	Angle; ratio
$\beta$	Angle; ratio; coefficient
$\gamma$	Partial factor
$\gamma_A$	Partial factor for accidental actions $A$
$\gamma_C$	Partial factor for concrete
$\gamma_F$	Partial factor for actions, $F$
$\gamma_{F,fat}$	Partial factor for fatigue actions
$\gamma_{C,fat}$	Partial factor for fatigue of concrete
$\gamma_G$	Partial factor for permanent actions, $G$
$\gamma_M$	Partial factor for a material property, taking account of uncertainties in the material property itself, in geometric deviation and in the design model used
$\gamma_P$	Partial factor for actions associated with prestressing, $P$
$\gamma_Q$	Partial factor for variable actions, $Q$
$\gamma_S$	Partial factor for reinforcing or prestressing steel
$\gamma_{S,fat}$	Partial factor for reinforcing or prestressing steel under fatigue loading
$\gamma_f$	Partial factor for actions without taking account of model uncertainties
$\gamma_g$	Partial factor for permanent actions without taking account of model uncertainties
$\gamma_m$	Partial factors for a material property, taking account only of uncertainties in the material property
$\delta$	Increment/redistribution ratio
$\zeta$	Reduction factor/distribution coefficient
$\epsilon_c$	Compressive strain in the concrete
$\epsilon_{c1}$	Compressive strain in the concrete at the peak stress $f_c$
$\epsilon_{cu}$	Ultimate compressive strain in the concrete
$\epsilon_u$	Strain of reinforcement or prestressing steel at maximum load
$\epsilon_{uk}$	Characteristic strain of reinforcement or prestressing steel at maximum load
$\theta$	Angle
$\lambda$	Slenderness ratio

$\mu$	Coefficient of friction between the tendons and their ducts
$\nu$	Poisson's ratio
$\nu$	Strength reduction factor for concrete cracked in shear
$\xi$	Ratio of bond strength of prestressing and reinforcing steel
$\rho$	Oven-dry density of concrete in kg/m <sup>3</sup>
$\rho_{1000}$	Value of relaxation loss (in %), at 1000 hours after tensioning and at a mean temperature of 20°C
$\rho_l$	Reinforcement ratio for longitudinal reinforcement
$\rho_w$	Reinforcement ratio for shear reinforcement
$\sigma_c$	Compressive stress in the concrete
$\sigma_{cp}$	Compressive stress in the concrete from axial load or prestressing
$\sigma_{cu}$	Compressive stress in the concrete at the ultimate compressive strain $\epsilon_{cu}$
$\tau$	Torsional shear stress
$\phi$	Diameter of a reinforcing bar or of a prestressing duct
$\phi_n$	Equivalent diameter of a bundle of reinforcing bars
$\varphi(t, t_0)$	Creep coefficient, defining creep between times $t$ and $t_0$ , related to elastic deformation at 28 days
$\varphi(\infty, t_0)$	Final value of creep coefficient
$\psi$	Factors defining representative values of variable actions
$\psi_0$	for combination values
$\psi_1$	for frequent values
$\psi_2$	for quasi-permanent values

**SECTION 2 BASIS OF DESIGN****2.1 Requirements****2.1.2 Reliability management****SECTION 2 BASIS OF DESIGN****C2.1 Requirements**

Eurocode 2, Section 2, Part 1.1 states that concrete structures should be designed in accordance with the general rules of EN1990 and with actions defined in EN 1991. EN 1992 has some additional requirements.

In particular, the basic requirements of EN1990 Section 2 are deemed to be satisfied for all concrete structures if limit state design is carried out with the partial factor method in accordance with EN1990, and if actions are defined in accordance with EN1991, and if combinations of actions in accordance with EN1990, and finally if resistance, durability and serviceability are dealt with in accordance with EN1992.

**C2.1.2 Reliability management**

EC2 points 2.1.2 and 2.1.3 refer to EN1990 section 2 for all rules in relation to reliability, design working life and quality management measures. These rules, as well as the basic concepts of structural reliability, will be referred to later.

By the definition given by EN1990, structural reliability is the ability of a structure or a structural member to fulfil the specified requirements for which it has been designed; it includes structural safety, serviceability and durability.

Given the random nature of quantities involved in structural design (actions, geometry, restraints, strength of materials, etc.), the assessment of structural reliability cannot be set up by deterministic methods, but requires a probabilistic analysis. The objective of safety verification is therefore to keep failure probability, i.e. probability that a certain danger condition is attained or exceeded, below a fixed value. This value is determined as a function of type of construction, influence on safety of people and damage to goods.

Every situation which is dangerous for a construction is referred to as a "limit state". Once a construction has attained this condition, it is no longer able to fulfil the functions for which it has been designed. Limit states are of two types: ultimate limit states and serviceability limit states - depending on the gravity of their consequences. Exceeding the first causes collapse of the whole structure or of part of it, exceeding the second causes limited damage that makes the structure unfit for the requirements of the project. Exceeding serviceability limit states can be reversible or irreversible: in the first case, no consequences of actions exceeding the specified service requirements will remain once those actions are removed; in the second, case, some consequences will remain. For example, a crack width limit state with limited width is a reversible limit state, whereas one defined by a high width is irreversible (in fact, if the crack width is high, once the actions are removed the cracks cannot close).

For a given limit state, let us define S and R as two random variables representing respectively stress and strength. We recall that by 'stress' we mean any effect produced in the structural members by actions applied or by any other effect such as strain, cracking, increase of reinforcing steel corrosion. 'Strength', on the other hand, means the capacity of a structure to respond to a given stress. A rigorous assessment of structural safety against a relevant limit state can be carried out by first introducing a safety factor  $F_s$ , defined as the ratio between strength R and stress S, or alternatively by a safety margin  $M_s$ , defined as the difference between R and S:

$$\text{either } F_s = R/S, \quad \text{or } M_s = R - S,$$

Both these factors are random variables like R and S. The distribution of  $F_s$  or  $M_s$  is then determined on the basis of the statistical distribution of actions, strengths and geometrical dimensions of the structure, also taking account of the randomness of the structural scheme. Finally, the probability of failure is related to a fixed reference period of time T through one of the following expressions:

$$P_f = P\{R/S \leq 1\} = P\{F_s \leq 1\} \quad \text{or} \quad P_f = P\{R - S \leq 0\} = P\{M_s \leq 0\}.$$

$P_f$  represents the probability that failure arises, i.e. that the considered limit state is attained or exceeded at least once during T.

This analysis (known as level 3 method) is very complex. Because of the difficulty of calculation and of the limitation of available data (data which often fail to give the probabilistic distributions



necessary for calculation), this method is of limited applicability to the design practice.

Alternatively, if only the first and second order moments (averages and standard deviations) of the random variables R and S, but not their statistical distributions, are known, the probability of failure can be estimated based on a  $\beta$  index, called the “reliability index”. Assuming that  $M_S$  is linear, it was first defined by Cornell as the ratio between the average value  $\mu_M$  of  $M_S$  and its standard deviation  $\sigma_M$ :

$$\beta = \mu_M / \sigma_M .$$

In circumstances where R and S are not correlated (note that in case of normal distributions non-correlation is equivalent to statistical independence),  $\beta$  is expressed as follows:

$$\beta = (\mu_R - \mu_S) / \sqrt{\sigma_R^2 + \sigma_S^2} , \text{ where } \mu_R, \mu_S, \sigma_R, \sigma_S \text{ are the averages and standard deviations of R and S.}$$

This method (known as “level 2” method or “ $\beta$ -method”) does not generally allow assessment of the probability of failure, with the exception of the particular case where the relation between  $M_S$  and the random variables of the problem is linear and the variables have normal distribution. The probability of failure, i.e. the probability that the safety margin  $M_S$  assumes non-positive values, is given by the distribution function  $\Phi_M$  of  $M_S$  calculated in 0:

$$P_f = P \{M_S \leq 0\} = \Phi_M (0)$$

Introducing m as the normalized variable of the safety margin  $M_S$ ,

$$m = \frac{M_S - \mu_M}{\sigma_M}$$

the result:  $M_S = \mu_M + m \cdot \sigma_M$  substituted in the expression of  $P_f$  gives:

$$P_f = P \{M_S \leq 0\} = P \{\mu_M + m \cdot \sigma_M \leq 0\} = P \{m \leq -\mu_M / \sigma_M\} = P \{m \leq -\beta\} = \Phi_m(-\beta) = 1 - \Phi_m(\beta)$$

where  $\Phi_m$  indicates the distribution function of m.

The reliability index may be expressed in geometrical terms. In fact, if we introduce the normalized strength and stress variables [ $r = (R - \mu_R) / \sigma_R$  and  $s = (S - \mu_S) / \sigma_S$ ], the limit condition ( $M_S = 0$ ) is represented in the r - s plane by a line that divides the plane into a safe region and an unsafe region (Figure 2.1). The distance from the origin of the axis of this line equals the reliability index (in circumstances where R and S are not correlated), so the verification of safety is carried out by assigning a given value to this distance.

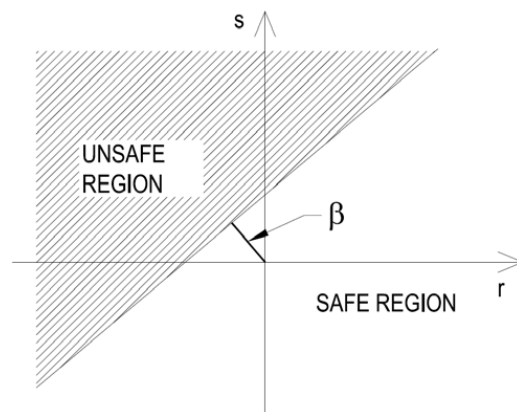


Figure 2.1. Geometric representation of the reliability index in the r-s plane

The level 2 method is also difficult to apply in practical design because the necessary data are often not available, so that another method is used: the partial factor method or semi-probabilistic method (level 1 method).

This method is based on the compliance with a set of rules that ensure the required reliability of the structure by using “characteristic values” of the problem variables and a series of “safety elements”. These are represented by partial safety factors,  $\gamma$  which cover the uncertainties in actions and materials, and by additional elements  $\Delta$  for uncertainties in geometry, e.g. to allow for the randomness of cover to reinforcement and therefore of the effective depth of a reinforced concrete section.

This method does not require that the designer has any probabilistic knowledge, because the probabilistic aspects of the question of safety are already taken into account in the method calibration process, i.e. in the choice of characteristic values, partial safety factors etc., fixed in the Standards. The method is based on the following assumptions:

1. strength and stress are independent random variables;
2. characteristic values of strength and stress are fixed as fractiles of given order of the respective distributions, on the basis of a given probability;
3. other uncertainties are taken into account by transforming characteristic values into design values, by applying partial safety factors and additional elements;
4. the assessment of safety is positive if the design action effects don't exceed the design strengths.

It has to be pointed out that the characteristic values of actions are fixed as those values with a given probability of being exceeded during the service life of the structure only if statistical data are available. Otherwise, characteristic values are fixed as the nominal values prescribed in standards or specifications, or as target values, for example in the case of accidental actions such as impacts from road vehicles, explosions etc.

**2.1.3 Design working life, durability and quality management**

**C2.1.3 Design working life, durability and quality management**

Independently from the method used for safety evaluation, a structure can be defined as reliable if positive safety measures have been provided for all its limit states during the whole design working life  $T_u$ .  $T_u$  is defined as the period for which a structure is assumed to be usable for its intended purpose with anticipated maintenance but without major repair being necessary.

Table 2.1 gives the indicative values of design working life for different types of structures.

*Table 2.1. Indicative design working life [Table (2.1) - EN1990]*

<i>Design working life category</i>	<i>Indicative design working life (years)</i>	<i>Examples</i>
1	10	Temporary structures (*)
2	10 to 25	Replaceable structural parts, e.g. gantry girders, bearings
3	15 to 30	Agricultural and similar structures
4	50	Building structures and other common structures
5	100	Monumental building structures, bridges, and other civil engineering structures

(\*) Structures or parts of structures that can be dismantled with a view to being re-used should not be considered as temporary.

The reliability required for structures [within the scope and field of application of EN1990] shall be achieved through design in accordance with EN1990 to EN1999 and by appropriate execution and quality management measures.

EN1990 allows for the choice of different levels of reliability, both for structural resistance and for serviceability. The choice of the levels of reliability for a particular structure should take account of the relevant factors, including :

- the possible cause and /or mode of reaching a limit state;
- the possible consequences of failure in terms of risk to life, injury, potential economical losses;
- public aversion to failure;
- the expense and procedures necessary to reduce the risk of failure.

The levels of reliability relating to structural resistance and serviceability can be achieved by suitable combinations of protective measures (e.g. protection against fire, protection against corrosion, etc.), measures relating to design calculations (e.g. choice of partial factors), measures relating to quality management, measures aimed to reduce errors in design (project supervision) and execution of the structure (inspection in phase of execution) and other kinds of measures.

Point (B3.1) of EN1990 Annex B defines three classes based on the consequences of failure or malfunction of the structure (Table 2.2).

**Table 2.2. Consequences classes [Table (B1) - EN1990]**

Consequences Class	Description	Examples of buildings and civil engineering works
CC3	Serious consequences for loss of human life, or for economic, social or environmental concerns	Grandstands, public buildings where consequences of failure are high (e.g. a concert hall)
CC2	Moderate consequence for loss of human life; economic, social or environmental consequences considerable	Residential and office buildings, public buildings where consequences of failure are medium (e.g. an office building)
CC1	Low consequence for loss of human life; economic, social or environmental consequences small or negligible	Agricultural buildings where people do not normally enter (e.g. storage buildings), greenhouses

Classes CC1 and CC2 correspond to importance classes I, II, whereas CC3 corresponds to classes III and IV, as from EN1998.1, Table 4.3.

From this table it is apparent that it is the importance of the structure concerned which is the criterion for classification.

Three reliability classes (RC1, RC2, RC3) may be associated with the three consequence classes CC1, CC2 and CC3, depending on the reliability index  $\beta$  defined above. Table 2.3 gives values of  $\beta$  for different values of  $P_f$  (remembering that the  $\beta$  index allows the estimation of  $P_f$  values only if the relationship between  $M_s$  and the random variables of the problem is linear and the variables have normal distribution).

**Table 2.3. Relation between  $\beta$  and  $P_f$  [Table C1 - EN1990]**

$P_f$	$10^{-1}$	$10^{-2}$	$10^{-3}$	$10^{-4}$	$10^{-5}$	$10^{-6}$	$10^{-7}$
$\beta$	1,28	2,32	3,09	3,72	4,27	4,75	5,20

Recommended minimum values for  $\beta$  at ultimate limit states are given in Table 2.4, for reference periods of 1 year and 50 years.

A design using EN 1990 with the partial factors given in annex A1 and EN 1991 to EN 1999 is considered generally to lead to a structure with a  $\beta$  value greater than 3,8 for a 50 year reference period (Table 2.3), i.e. with a rough probability of attaining the ULS in 50 years of  $7,2 \cdot 10^{-5}$  (Table 2.3).

**Table 2.4. Recommended minimum values of the reliability index  $\beta$  (ultimate limit states) [Table (B2)-EN1990]**

Reliability Class	$\beta$ minimum values at ULS	
	1 year reference period	50 years reference period
RC3	5,2	4,3
RC2	4,7	3,8
RC1	4,2	3,3

For the serviceability limit states (irreversible), which are less dangerous and do not concern the safety of people, the failure probability values for structural elements of Class RC2 are roughly  $10^{-1}$  (1/10) in 50 years and  $10^{-3}$  (1/1000) in 1 year; this can be deduced from the relation between  $\beta$  and  $P_f$  (Table 2.3) for the values of  $\beta$  given in the last row of Table 2.5.

**Table 2.5. Target values of the reliability index for Class RC2 structural members [Table (C2)-EN1990]**

Limit state	Target reliability index	
	1 year reference period	50 years reference period
Ultimate	4,7	3,8
Fatigue	---	1,5 to 3,8
Serviceability (irreversible)	2,9	1,5

Design supervision and execution inspection measures being equal, reliability differentiation can be achieved by distinguishing classes of partial factors  $\gamma_F$  of actions to be used in combination of actions, and applying multiplication factor  $K_{F1}$ , different for each reliability class. Values for  $K_{F1}$  are given in Table 2.6.

**Table 2.6.**  $K_{F1}$  factor for actions [Table (B3)-EN1990]

$K_{F1}$ factor for actions	Reliability class		
	RC1	RC2	RC3
$K_{F1}$	0,9	1,0	1,1

Measures of design and execution management and quality control are aimed at eliminating failures due to gross errors, and at ensuring that the design resistance is achieved. Design supervision and execution inspection levels are given at Tables 2.7 and 2.8, with reference to each reliability class.

**Table 2.7.** Design supervision levels (DSL) [Table (B4)-EN1990]

Design supervision levels	Characteristics	Minimum recommended requirements for checking of calculations, drawings and specifications
DSL3 relating to RC3	Extended supervision	Checking performed by an organisation different from that which has prepared the design
DSL2 relating to RC2	Normal supervision	Checking by different persons than those originally responsible and in accordance with the procedure of the organisation.
DSL1 relating to RC1	Normal supervision	Self-checking: checking performed by the person who has prepared the design

**Table 2.8.** Inspection levels (IL) [Table (B5)-EN1990]

Inspection levels	Characteristics	Requirements
IL3 relating to RC3	Extended inspection	Third party inspection
IL2 relating to RC2	Normal inspection	Inspection in accordance with the procedures of the organisation
IL1 relating to RC1	Normal inspection	Self inspection

Design with partial factors given in EC2 and with the partial factors given in the EN1990 annexes results in a structure associated with the RC2 reliability class.

**2.2 Principles of limit state design**

**C2.2 Principles of limit state design**

Eurocodes adopt the partial factors method, or limit states semi-probabilistic method, as the method for the verification of structural safety.

EC2 point 2.2 refers to EN1990 Section 3 for limit state design rules. These are here repeated, partially repeating the description of the three safety verification methods in Par. 2.1.2.

Design for limit states shall be based on the use of structural and load models for relevant limit states. It shall be verified that no limit state is exceeded when relevant design values for actions, material and product properties and geometrical data are used in these models.

The verifications shall be carried out for all relevant design situations and load cases.

Two categories are defined by the consequences associated with the attainment of a limit state: ultimate limit state and serviceability limit state. Verification shall be carried out against both categories; verification of one of the two categories may be omitted only if it can be proven that it is satisfied by the verification of the other one.

The ultimate limit states are associated with loss of equilibrium of the whole structure, or failure or excessive deformation of a structural member and they generally concern safety of people.

For the verification of ultimate limit state design actions shall not exceed the design resistance of the structure. Table 2.9 shows the ULS classification according to EN1990 [(EN1990 point (6.4.1)).

**Table 2.9.** ULS classification

Notation	Definition
EQU	Loss of static equilibrium of the structure or any part of it considered as a rigid body, where : – minor variations in the value or the spatial distribution of actions from a single source are significant (e.g. self-weight variations) – the strengths of construction materials or ground are generally not governing
STR	Internal failure or excessive deformation of the structure or structural members, including footings, piles, basement walls, etc., where the strength of construction materials of the structure governs
GEO	Failure or excessive deformation of the ground where the strengths of soil or rock are significant in providing resistance
FAT	Fatigue failure of the structure or structural members.

Serviceability limit states correspond to conditions beyond which specified service requirements for a structure or structural member are no longer met. Exceeding these limits causes limited damage but means that the structures do not meet design requirements: functional requirements (not only of the structure, but also of machines and services), comfort of users, appearance (where the term “appearance” is concerned with high deformation, extensive cracking, etc.), damage to finishes and to non-structural members. Usually the serviceability requirements are agreed for each individual project.

EN1990 indicates three different types of combinations for serviceability limit states verifications: *characteristic combination* (called “rare combination” in the previous versions of Eurocodes), *frequent combination* and *quasi-permanent combination*.

The choice of combinations to be taken into account is related to the distinction between reversible and irreversible limit states: frequent and quasi-permanent combinations apply to the first case, characteristic combinations to the second case.

The definition of relevant limit states for a certain construction requires above all the analysis of the different situations to which it can be exposed.

The situations chosen for design shall cover all situations that can reasonably occur during the execution and working life of the structure.

In common cases, design situations are classified as:

- *persistent design situations*, referring to conditions of normal use;
- *transient situations*, referring to temporary conditions of the structure, e.g. during construction or repair;
- *accidental situations*, involving exceptional conditions of the structure or its exposure, including fire, explosion, impact, etc.;
- *seismic situations*, where the structure is subjected to a seismic event.

## 2.3 Basic variables

### 2.3.1 Actions and environmental influences

Each design situation is characterized by the presence of several types of actions on the structure. “Action” means, as EN1990 states, either a set of forces (loads) applied to the structure (direct actions), or a set of imposed deformations or accelerations caused for example, by temperature changes, moisture variation, uneven settlement or earthquakes (indirect action).

Actions are classified as:

- *permanent actions* ( $G$ ), the duration of which is continuous and equal to the design working life of the structure, or for which the variation in magnitude with time is negligible (e.g. self-weight). Those actions, like prestressing or concrete shrinkage, for which the variation is always in the same direction (monotonic) until the action attains a certain limit value, are also permanent actions;
- *variable actions* ( $Q$ ), divided in variable actions with discrete and regular occurrence in time (e.g. imposed load of people and low-duration imposed load in general on building floors); and variable actions characterized by variable and non-monotonic intensity or direction (e.g. snow, wind, temperature, waves);
- *accidental actions* ( $A$ ), which are not easily foreseeable and of low duration (e.g. explosions, impacts, fire).

Each permanent action with low variability has a single characteristic value  $G_k$ . This is the case of actions due to self-weight: they are generally represented through a nominal value calculated on the basis of the design drawings (structural and non-structural member dimensions) and of the average specific gravity of materials ( $G_k = G_m$ ).

If a permanent action has relevant uncertainties (coefficient of variation bigger than 10%, where the coefficient of variation is the ratio between standard deviation and average) and if sufficient statistical information is available, two characteristic values (upper,  $G_{k,sup}$ , and lower,  $G_{k,inf}$ ) should be used.  $G_{k,sup}$  is the 95% fractile and  $G_{k,inf}$  is the 5% fractile of the statistical distribution for  $G$ , which may be assumed to be Gaussian.

There is a 5% probability that these two values will be exceeded, the probability that the real value of action is more than  $G_{k,sup}$  or less than  $G_{k,inf}$  is less than 5% (fig. 2.2).

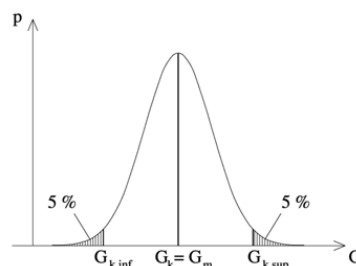


**Figure 2.2.** Characteristic value of a permanent action:  $G_k = G_m$  if the coefficient of variation is negligible; a lower and an upper characteristic value  $G_{k,inf}$  and  $G_{k,sup}$  are defined if the coefficient of variation is high

Each variable action has four representative values. The main representative value of a variable action is its characteristic value  $Q_k$ ; the other representative values are, in decreasing order:

- the combination value, represented as a product  $\psi_0 Q_k$ ,
- the frequent value, represented as a product  $\psi_1 Q_k$ ,
- the quasi-permanent value, represented as a product  $\psi_2 Q_k$ .

For simplicity, each of these last three values is defined as a fraction of the characteristic value, obtained by applying a reducing factor to  $Q_k$ . In reality, the frequent value and the quasi-permanent value are inherent properties of the variable action, and the  $\psi_1$  and  $\psi_2$  factors are simply the ratios between these values and the characteristic value. On the other hand, the  $\psi_0$  factor, called the combination factor, determines the level of intensity of a variable action when this action is taken into account, in design, simultaneously with another variable action, called "leading variable action", which is taken into account by its characteristic value.

The  $\psi_0$  factor takes therefore into account the low probability of simultaneous occurrence of the most unfavourable values of independent variable actions. It is used both for ULS verifications and for irreversible SLS verifications.

The frequent ( $\psi_1 Q_k$ ) and the quasi-permanent ( $\psi_2 Q_k$ ) values are used for ULS verifications including accidental actions and for reversible serviceability limit states.

Values of  $\psi$  factors for buildings are defined in the National Annex. Table 2.10 shows the values recommended by EN1990.

The characteristic value of a variable action has a defined probability, beforehand accepted, of being exceeded on the unfavourable side within a fixed reference period. This period is normally coincident with the design working life of the structure.

For the majority of climatic variable actions, as well as for service loads on building floors, the characteristic value is based upon the probability of 0,02 of its time-varying part being exceeded within a reference period of one year. In other words, this is equivalent to a mean return period of 50 years.

**Table 2.10. Recommended values of  $\psi$  factors for buildings [Table (A1.1)-EN1990]**

Imposed loads in buildings, category (see EN 1991-1-1)	$\psi_0$	$\psi_1$	$\psi_2$
Category A: domestic, residential areas	0,7	0,5	0,3
Category B: office areas	0,7	0,5	0,3
Category C: congregation areas	0,7	0,7	0,6
Category D: shopping areas	0,7	0,7	0,6
Category E: storage areas	1,0	0,9	0,8
Category F: traffic area, vehicle weight $\leq 30$ kN	0,7	0,7	0,6
Category G: traffic area, $30 \text{ kN} < \text{vehicle weight} \leq 160$ kN	0,7	0,5	0,3
Category H: roofs	0	0	0
Snow loads on buildings (see EN 1991-1-3)* in Finland, Iceland, Norway, Sweden and other CEN Member, for sites located at altitude $H > 1000$ m a.s.l.	0,7	0,5	0,2
Other CEN Member States, for sites located at altitude $H < 1000$ m a.s.l.	0,5	0,2	0
Wind load on buildings (see EN 1991-1-4)	0,6	0,2	0
Temperature (non-fire) in buildings (see EN 1991-1-5)	0,6	0,5	0
NOTE The $\psi$ values may be set by the National annex.			
* For countries not mentioned below, see relevant local conditions.			

The characteristic value of seismic action for ULS verification is fixed by Eurocode 8 (EN1998), based on a return period of 475 years, corresponding to a probability of 10% of being exceeded in 50 years. It is possible to modify the return period by means of an importance factor  $\gamma_1$ .

The frequent value and the quasi-permanent value of floor loads on building are determined so that the average periods of time within which they are exceeded are respectively 10% (ratios of the sum of intercepts of time BC, DE, FG, HI and the reference period of 50 years represented by segment AJ in Fig. 2.3) and 50% (ratio of listed segments and segment AJ). Figure 2.3 resumes the representative values of variable actions.



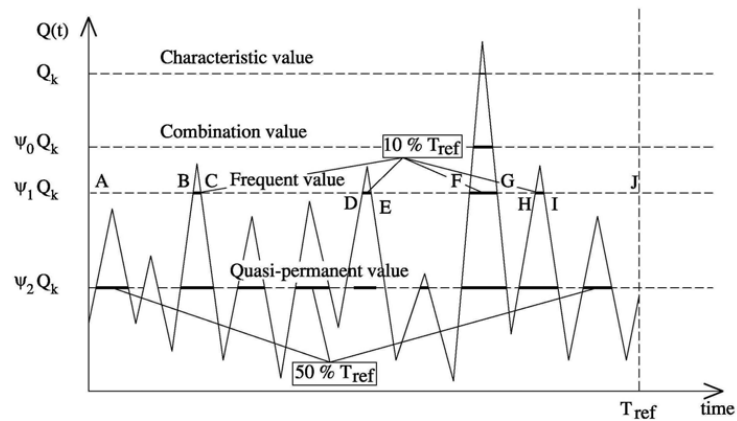


Figure 2.3. Schematic illustration of representative values of variable actions

For accidental actions, a single nominal value is determined because, due to the nature of these actions, sufficient information for the appropriate application of statistical methods is not available.

In order to take into account the uncertainties on the choice of characteristic values for actions and some uncertainties concerning the action modelling, design does not use characteristic values, but amplified values, called “design values”, which are obtained by multiplying characteristic values by a partial factor.

Symbols representing the design values are indicated with index d. Table 2.11 shows the steps to pass from the representative values of actions to the design values of their effects on construction.

Table 2.11. Procedure to determine the design values of effects on structures starting from the representative values of actions

Expression	Comment
$F_1$	Actions on the structure are identified
$F_{k,i}$ or $(\psi F_{k,i})$ where $(\psi = \psi_0, \psi_1, \psi_2)$	Representative values are assigned to actions: characteristic values or other (combination, frequent, quasi-permanent) values.
$F_{d,i} = \gamma_{f,i} F_{k,i}$ (or $\gamma_{f,i} \psi F_{k,i}$ ) where $(\psi = \psi_0, \psi_1, \psi_2)$	Design values of actions are determined by multiplying the representative values $F_{k,i}$ or $\psi F_{k,i}$ (where $\psi = \psi_0, \psi_1, \psi_2$ ) by a partial factor $\gamma_{f,i}$ . $\gamma_{f,i}$ is a partial factor generally covering the uncertainties related to the choice of characteristic values for actions and, sometimes, part of the uncertainties related to action modelling. In case of permanent actions, when it is necessary to split the action into a favourable and an unfavourable part, two different partial factors, indicated as $\gamma_{G,sup}$ and $\gamma_{G,inf}$ , are used.
$E_d = E(\gamma_{f,i} \psi F_{k,i}; a_d)$	Actions that can occur simultaneously are considered; combinations of actions are calculated and the effects of these combinations on the structure are assessed (e.g. action effect in a cross section). $a_d$ represents either the design value of the set of geometrical data (in general, values indicated on the design drawings) or data that take into account the possibility of geometrical imperfection liable to cause second order effects.
$E_d = \gamma_{Sd} E(\gamma_{f,i} \psi F_{k,i}; a_d)$	The design value of effects is obtained by multiplying the values produced by the design actions, by a partial factor $\gamma_{Sd}$ mainly covering the uncertainties of the structural model.
$E_d = E(\gamma_{F,i} \psi F_{k,i}; a_d)$	In normal cases, the previous expression is simplified in this one, where: $\gamma_{F,i} = f(\gamma_{Sd}, \gamma_{f,i})$ so that the model coefficient $\gamma_{Sd}$ does not explicitly appear. The product: $F_{d,i} = \gamma_{F,i} \cdot F_{k,i}$ or $(\gamma_{F,i} \psi F_{k,i}; \psi = \psi_0, \psi_1, \psi_2)$ is often directly assumed as the design value of the action $F_{k,i}$ .





2.3.1.2 Thermal effects

2.3.1.3 Differential settlements/movements

2.3.1.4 Prestress

2.3.2 Material and product properties

2.3.2.1 General

Several material properties are involved in structural design. The main one is strength, i.e. the ability to resist forces without breaking or failing.

Strength of materials is represented through a characteristic value, indicated as  $f_k$ . This is the value that has a given probability of not being attained or exceeded during a hypothetical unlimited test series. Eurocode EN1990 defines the characteristic value of a property of a material as the 5% fractile of its statistical distribution where a minimum value of the property is the nominal failure limit (general case), and as the 95% fractile where a maximum value is the limiting value.

For the structural stiffness parameters (moduli of elasticity, creep coefficient, thermal expansion coefficient, etc.), the characteristic value is taken as a mean value because, depending on the case, these parameters can be favourable or unfavourable.

Product properties are also represented by a single characteristic value or a set of characteristic values, according to their constituent materials.

Table 2.12 shows the steps to pass from the characteristic values of individual material strengths or product resistances to the design values of structural resistance.

Table 2.13 gives the values of partial safety factors to be assumed for concrete and steel for ULS, in case of persistent, transient and accidental load combinations.

**Table 2.12.** Procedure to determine the design values of resistances starting from the characteristic values of strength

Expression	Comment
$X_i$	Material strengths and product resistances involved in the verifications are identified.
$X_{k,i}$	Characteristic values of material strengths and product resistances are introduced.
$X_{d,i} = \eta \frac{X_{k,i}}{\gamma_{m,i}}$	The design value of a material property is determined on the basis of its characteristic value, through the two following operations: a) divide by a partial factor $\gamma_{m,i}$ , to take into account unfavourable uncertainties on the characteristic of this property, as well as any local defaults.; b) multiply, if applicable, by a conversion factor $\eta$ mainly aimed at taking into account scale effects.
$R \left( \eta \frac{X_{k,i}}{\gamma_{m,i}}; a_d \right)$	Determine the structural resistance on the basis of design values of individual material properties and of geometrical data.
$R_d = \frac{1}{\gamma_{Rd}} R \left( \eta \frac{X_{k,i}}{\gamma_{m,i}}; a_d \right)$	Following a procedure similar to the one for calculating the design value of action effects, the design value of structural resistance is determined on the basis of individual material properties and of geometrical data multiplied by a partial factor $\gamma_{Rd}$ that covers the model uncertainties of resistance and the geometrical data variations, if these are not explicitly taken into account in the model.
$R_d = R \left( \eta \frac{X_{k,i}}{\gamma_{M,i}}; a_d \right)$	As for the action effects, factor $\gamma_{Rd}$ is often integrated in the global safety factor $\gamma_{M,i}$ , by which the characteristic material strength is divided: $\gamma_{M,i} = f(\gamma_{Rd}, \gamma_{m,i})$ .

Fig. 2.4 summarise in a schematic way the relation between the single partial factors used in Eurocodes.

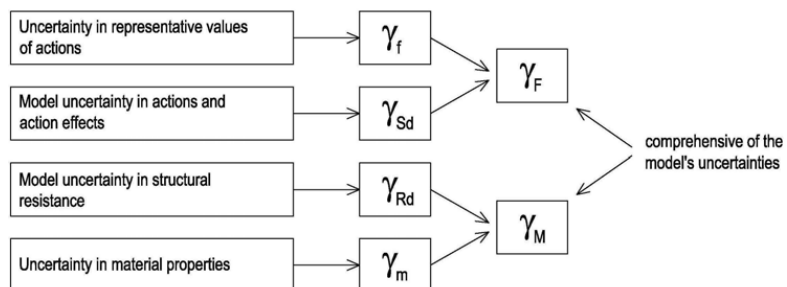


Figure 2.4. Relation between the single partial factors [Fig. (C3) - EN1990]

**2.3.2.2 Shrinkage and creep**

**2.3.3 Deformations of concrete**

**2.3.4 Geometric data**

**2.3.4.1 General**

**2.3.4.2 Supplementary requirements for cast in place piles**

**2.4 Verification by the partial factor method**

**2.4.1 General**

**2.4.2 Design values**

**2.4.2.1 Partial factor for shrinkage action**

**2.4.2.2 Partial factors for prestress**

**2.4.2.3 Partial factor for fatigue loads**

**2.4.2.4 Partial factors for materials**

*Table 2.13. Partial factors for concrete and steel for ultimate limit states [Table (2.1N)-EC2]*

Design situations	$\gamma_c$ for concrete	$\gamma_s$ for reinforcing steel	$\gamma_s$ for prestressing steel
Persistent and transient	1,5	1,15	1,15
Accidental	1,2	1,0	1,0

The values of partial factors given in the previous table were determined as:

$$\gamma_M = \exp(3,04 V_R - 1,64 V_f)$$

where:

$$V_R = \sqrt{(V_m^2 + V_G^2 + V_f^2)}$$

- $V_R$  coefficient of variation of resistance
- $V_m$  coefficient of variation of model uncertainty
- $V_G$  coefficient of variation of geometrical factor
- $V_f$  coefficient of variation of material strength

The basic values in EC2 may be considered to be based on the following assumptions:

For reinforcement	model uncertainty	$V_m = 2,5 \%$
	geometry	$V_G = 5 \%$
	steel strength	$V_f = 4 \%$
For these values the equation gives $\gamma_M = \gamma_s = 1,154$		
For concrete	Variation of model uncertainty	5 %
	Variation of geometry	5 %
	Variation of concrete strength	15 %

For these values the equation gives  $\gamma_M = \gamma_c = 1,30$ . Assuming an additional factor 1,15 to cover the uncertainty arising from the concrete being tested with test specimens specially made and cured for this purpose, rather than from the finished structure, the result is  $\gamma_c = 1,15 \cdot 1,30 = 1,50$ .

For serviceability limit states values of partial safety factors  $\gamma_c$  and  $\gamma_s$  are defined in the National Annex. The recommended value for situations not covered by specific parts of EC2 is 1,0.

Besides the partial safety factors for materials above, EC2 also defines partial factors for shrinkage, prestressing, fatigue loads and materials for foundations. These values are also defined in the National Annex. The table below gives the values recommended in EC2.

**Table 2.14. Recommended values of partial safety factors**

Shrinkage (e.g. for ULS verification of stability when second order effects are relevant)		$\gamma_{SH}$	1,0
Prestressing	favourable in persistent and transient situations	$\gamma_{P,fav}$	1,0
	Stability ULS with external prestressing if an increase of prestressing may be unfavourable	$\gamma_{P,unfav}$	1,3
	local effects	$\gamma_{P,unfav}$	1,2
Fatigue		$\gamma_{F,fat}$	1,0
Materials for foundations (amplified in order to obtain the design resistance of cast in place piles without permanent scaffolding)		$\gamma_{C,fond}$	1,1 $\gamma_C$

**2.4.2.5 Partial factors for materials for foundations**

**2.4.3 Combinations of actions**

The general formats for the ULS and SLS combinations of actions, as defined in EN 1990 Section 6, are given below.

It has to be pointed out that the combinations foreseen in EN 1990 cover static actions only, but there is no consideration of actions of dynamic type, such as actions caused by vibrating machinery (turbines, compressors, etc.).

It has also to be noted that EN 1990 considers the zero value a possible value of the partial factor of variable actions  $\gamma_Q$ , although  $\gamma_Q = 0$  has no probabilistic meaning. A zero value of  $\gamma_Q$  is therefore an expedient to remove from the combination of actions the favourable effect of variable actions (e.g. to maximize the positive bending moment in the central span of a three-span continuous beam, the variable imposed load shall be applied on the central span only, which is equivalent to setting  $\gamma_Q = 0$  in the two lateral spans, see Example 2.1).

ULS Combinations

Three types of combinations of actions should be considered for Ultimate Limit States: fundamental, accidental and seismic.

*Combinations of actions for persistent or transient design situations (fundamental combinations):*

$$\sum_{j \geq 1} \gamma_{G,j} G_{k,j} + \gamma_P P + \gamma_{Q,1} Q_{k,1} + \sum_{i > 1} \gamma_{Q,i} \psi_{0,i} Q_{k,i}$$

or alternatively for the STR and GEO limit states, the more unfavourable of the two following expressions:

$$\sum_{j \geq 1} \gamma_{G,j} G_{k,j} + \gamma_P P + \gamma_{Q,1} \psi_{0,1} Q_{k,1} + \sum_{i > 1} \gamma_{Q,i} \psi_{0,i} Q_{k,i}$$

$$\sum_{j \geq 1} \xi_j \gamma_{G,j} G_{k,j} + \gamma_P P + \gamma_{Q,1} Q_{k,1} + \sum_{i > 1} \gamma_{Q,i} \psi_{0,i} Q_{k,i}$$

where  $\xi_i$  are reduction factors for the unfavourable permanent actions G.

EN1990 introduces then the possibility to choose for the fundamental combination:

1. the traditional expression with a predominant variable action  $Q_{k,1}$  and the permanent actions (including prestressing P) introduced with its characteristic value, other concomitant variable actions introduced with their combination values;
2. or a system of two expressions, the most unfavourable of which should be adopted by the designer; these expressions are obtained by reducing the multiplying factor of the predominant variable action (through the  $\psi_0$  factor) in the first case, or by reducing the multiplying factors for permanent unfavourable actions (through the  $\xi$  factor that is in the range 0,85 ÷ 1,00).

The expression to be used for the fundamental combination is chosen in the National Annex.

*Combinations of actions for accidental design situations*

$$\sum_{j \geq 1} G_{k,j} + P + A_d + (\psi_{1,1} \text{ or } \psi_{2,1}) Q_{k,1} + \sum_{i > 1} \psi_{2,i} Q_{k,i}$$

where  $A_d$  is the accidental design action (for fire situations, it represents the design value of the indirect thermal action due to fire).

If a variable action may be present on the structure at the moment when the accidental action occurs, its frequent value ( $\psi_{1,1} Q_{k,1}$ ) will be used in the combination, otherwise its quasi-permanent value ( $\psi_{2,1} Q_{k,1}$ ) will be used; other variable actions are introduced in the combination with their quasi-permanent values ( $\psi_{2,i} Q_{k,i}$ ).

#### *Combinations of actions for seismic design situations*

$$\sum_{j \geq 1} G_{k,j} + P + A_{Ed} + \sum_{i \geq 1} \psi_{2,i} Q_{k,i}$$

where  $A_{Ed}$  is the design value of seismic action ( $A_{Ed} = \gamma_1 \cdot A_{Ek}$  with  $\gamma_1$  importance factor and  $A_{Ek}$  characteristic values of seismic action - see EN1998). Note that the seismic action is combined with the quasi-permanent value of variable actions, whereas permanent actions  $G_{k,j}$  are taken into account with their characteristic value, and prestressing with its representative value (see ch. 6).

#### SLS combinations

There are three combinations of actions for SLS: characteristic, frequent and quasi-permanent.

##### *Characteristic combination*

$$\sum_{j \geq 1} G_{k,j} + P + Q_{k,1} + \sum_{i > 1} \psi_{0,i} Q_{k,i}$$

##### *Frequent combination:*

$$\sum_{j \geq 1} G_{k,j} + P + \psi_{1,1} Q_{k,1} + \sum_{i > 1} \psi_{2,i} Q_{k,i}$$

##### *Quasi-permanent combination:*

$$\sum_{j \geq 1} G_{k,j} + P + \sum_{i \geq 1} \psi_{2,i} Q_{k,i}$$

Detailed expressions of the combinations of actions are given in the normative annexes to EN 1990 (Annex A1 for buildings, A2 for bridges, etc.), together with the recommended values of partial safety factors  $\gamma_F$  and of combination factors  $\psi$ .

The characteristic combination should be normally considered for short term limit states, associated with the one-time attainment of a fixed value of the effect considered (e.g. crack formation). It corresponds to those effects that have a probability of being exceeded which is close to the probability that the characteristic value of the predominant variable action  $Q_{k,1}$  will be exceeded. In other words, the characteristic combination should be considered for verification of irreversible serviceability limit states: e.g. the crack width limit state characterized by a 0,5 mm crack width is an irreversible limit state, because such a wide crack cannot completely close once the action that produced it is removed.

The frequent combination should be considered for long term limit states, associated with the attainment of a fixed value of the effect considered for a small fraction of the reference period or for its attainment a fixed number of times. It corresponds to those effects that are exceeded with a frequency or length of time close to the one of the frequent value  $\psi_{1,1} Q_{k,1}$  of the predominant variable action (e.g. the crack width limit state of a prestressed concrete beam with bonded tendons, XC2 exposure class, with design crack width not exceeding 0,2 mm).

The quasi-permanent combination should be considered for long term action effects, associated with the attainment of a fixed value of these limit states for a long fraction of the reference period (e.g. the crack width limit state for a reinforced concrete or prestressed concrete beam with unbonded tendons, with design crack width not exceeding 0,3 mm).

Frequent and quasi-permanent combinations must be considered for the verification of reversible limit states, i.e. limit states that will not be attained or exceeded once the actions that have caused attainment or exceeding are removed.

#### Combination of actions for fatigue limit state

The combination of actions for fatigue verification is given in [(6.8.3)-EC2]:

$$\left( \sum_{j \geq 1} G_{k,j} + P + \psi_{1,1} Q_{k,1} + \sum_{i > 1} \psi_{2,i} Q_{k,i} \right) + Q_{fat}$$

where  $Q_{fat}$  is the relevant fatigue load (e.g. traffic load or other cyclic load).

**2.6.1 Combinations of actions for the ultimate limit states verification of a building**

EN1990 Annex A1 gives rules for combinations of actions for buildings, on the basis of symbolic expressions and recommended values (or of values given in the National Annex) of partial factors to be applied to actions in the combinations. Eurocodes allow combinations of actions to contain two or more variable actions.

In general, for ultimate limit states, values of partial factors are subdivided in three sets (A, B and C), given in Tables [A1.2(A)-EN1990] to [A1.2(C)-EN1990], which are combined in the following table.

**Table 2.15.** Sets A, B and C of partial factors  $\gamma$  for actions

Actions		Permanent actions $G_k$		Predominant variable action $Q_{k,1}$ (Note 2)	Non predominant variable actions $Q_{k,i}$ (Note 2)
		Unfavourable	Favourable		
Set A		1,10	0,90	1,5	$1,5 \cdot \psi_{0,i}$
Set B (Note 1)	(eq.6.10)-EN1990	1,35	1,00	1,5	$1,5 \cdot \psi_{0,i}$
	or alternatively the most unfavourable between the two following:				
	(eq.6.10a)-EN1990	1,35	1,00	$1,5 \cdot \psi_{0,1}$	$1,5 \cdot \psi_{0,i}$
	(eq.6.10b)-EN1990	$0,85 \cdot 1,35$	1,00	1,5	$1,5 \cdot \psi_{0,i}$
Set C		1,00	1,00	1,30	1,30

*Note 1: eq.6.10 or alternatively the most unfavourable between eq.6.10a and eq.6.10b is used. The choice is made in the National Annex. In case of 6.10a and 6.10b, the National annex may in addition modify 6.10a to include permanent actions only.*

*Note 2: The partial factor of favourable variable actions should be taken as 0.*

Depending on the limit state under consideration, values from one or more sets should be used, as indicated in the following table.

**Table 2.16.** Sets of partial factors to be used for ULS

Limit state	Set of partial factors to be used
EQU – Static equilibrium	Set A
STR – Design of structural members not involving geotechnical actions	Set B
STR – Design of structural members involving geotechnical actions (foundations, piles, basement walls, etc.)	Approach 1(*): Apply in separate calculations design values from Set B and Set C to all actions. In common cases, the sizing of foundations is governed by Set C and the structural resistance is governed by Approach 2: Apply Set B to all actions
GEO – Breaking or excessive deformation of ground	Approach 3: Simultaneously apply, in the same calculation, Set B to actions on the structure and Set C to geotechnical actions

(\*) The choice of approach to be used for STR/GEO verification is given in the National Annex.

Combinations obtained with sets A, B and C of partial factors with EN 1990 recommended values are given below. Note that the partial factor of variable actions should be taken as 0 where these actions are favourable.

*Combinations of actions with Set A of partial factors (EQU)*

$$\sum_{j \geq 1} (1,1 \cdot G_{kj,sup} + 0,9 \cdot G_{kj,inf}) + 1,5 \cdot Q_{k,1} + \sum_{i > 1} 1,5 \cdot \psi_{0,i} Q_{k,i}$$

In this combination the favourable part of a same action is multiplied by 0,9 and the unfavourable by 1,1. For example, in the verification of holding down devices for the uplift of bearings of a continuous beam, the self weight of spans that give a stabilising effect should be multiplied by 0,9 whereas the self weight of spans that give destabilising effect should be multiplied by 1,1 (see Example 2.1).

*Combinations of actions with Set B of partial factors (STR/GEO)*

Either

$$\sum_{j \geq 1} (1,35 \cdot G_{kj,sup} + 1,0 \cdot G_{kj,inf}) + 1,5 \cdot Q_{k,1} + \sum_{i > 1} 1,5 \cdot \Psi_{0,i} Q_{k,i} \quad [\text{eq. (6.10)-EN1990}]$$

(where  $G_{kj,sup}$  are unfavourable permanent loads and  $G_{kj,inf}$  are favourable permanent loads)

or the less favourable of the two following expressions:

$$\sum_{j \geq 1} (1,35 \cdot G_{kj,sup} + 1,0 \cdot G_{kj,inf}) + 1,5 \cdot \Psi_{0,1} Q_{k,1} + \sum_{i > 1} 1,5 \cdot \Psi_{0,i} Q_{k,i} \quad [\text{eq. (6.10a)-EN1990}]$$

$$\sum_{j \geq 1} (1,15 \cdot G_{kj,sup} + 1,0 \cdot G_{kj,inf}) + 1,5 \cdot Q_{k,1} + \sum_{i > 1} 1,5 \cdot \Psi_{0,i} Q_{k,i} \quad [\text{eq. (6.10b)-EN1990}]$$

The National Annex decides whether eq. [(6.10)-EN1990] or the less favourable of [(6.10a)-EN1990] and [(6.10b)-EN1990] should be considered.

In these expressions  $G_{kj,sup}$  ( $G_{kj,inf}$ ) is a set of permanent actions from one source with an unfavourable (or favourable) resulting effect of the total action. For example, all actions originating from the self weight of the structure may be considered as coming from one source; this also applies if different materials are involved. Therefore in the verifications of resistance of the sections of a beam, its self weight should be taken with the same design value for the whole length of the beam ( $\gamma_G = 1,35$ ), whereas a different value of partial factor ( $\gamma_G = 1,0$ ) can be taken for permanent loads originating from a different source.

*Combinations of actions with Set C of partial factors (STR/GEO)*

$$\sum_{j \geq 1} (1,0 \cdot G_{kj,sup} + 1,0 \cdot G_{kj,inf}) + 1,3 \cdot Q_{k,1} + \sum_{i > 1} 1,3 \cdot \Psi_{0,i} Q_{k,i}$$

**2.4.4 Verification of static equilibrium - EQU**

**2.5 Design assisted by testing**

**2.6 Supplementary requirements for foundations**

**2.7 Requirements for fastenings**

See examples 2.1, 2.2, 2.3, 2.4, 2.5

**SECTION 3 MATERIALS**

**SECTION 3. MATERIALS**

Section 3 of Eurocode 2, dedicated to materials, is structured in the following paragraphs:

- 3.1 – Concrete
- 3.2 – Reinforcing steel. Annex C-EC2 is related to this paragraph
- 3.3 – Prestressing steel

**3.1 Concrete**

**C3.1.1 General**

**3.1.1 General**

This section deals with normal weight concrete, viz. according to EN 206-1 having density greater than 2000 but not exceeding 2600 kg/m<sup>3</sup>. "Light-weight" concrete is dealt with in Sect.11-EC2.

**3.1.2 Strength**

**C3.1.2 Strength**

Compressive strength is defined in [3.1.2(1)P-EC2], in accordance with EN 206-1, by the characteristic value  $f_{ck}$  (5% fractile of distribution) obtained through the elaboration of compression tests executed at 28 days on cylindrical specimens of diameter 150 mm and height 150 mm.

As in many countries testing is carried out on 150 mm cubic specimens, EN 206-1 admits  $f_{ck,cube}$  compressive strength, too.

Compressive strength classes are denoted by letter C followed by two numbers that indicate the cylinder and cube characteristic strength, expressed in N/mm<sup>2</sup>, for example C30/37.

EC2 contemplates 14 classes: from C12/15 to C90/105.

Table [3.1-EC2] gives the numeric values of strength and deformation characteristics associated with strength classes and the analytic relationship expressing such values in function of  $f_{ck}$ . Average values of compressive strength  $f_{cm}$ , of tensile strength  $f_{ctm}$  and of elasticity modulus  $E_{cm}$  are plotted in Fig. 3.1 in function of  $f_{ck}$ .  $E_{cm}$  is denoted by the inclination of the line secant of the  $\sigma$ - $\epsilon$  relation between points  $\sigma = 0$  and  $\sigma = 0,4 \cdot f_{cm}$  as indicated in [Fig. 3.2-EC2].

Clause [3.1.2(6)-EC2] deals with the development of compressive strength with time. Formula [(3.2)-EC2] allows to calculate the average strength  $f_{cm}$  at a time  $t$  (days) in function of the value at 28 days, which can be deduced from Table [3.1-EC2] and from the class of cement used. Cement classes conforming to EN 197 are:

- Class R (rapid hardening), including CEM 42,5R, CEM 52,5N and CEM 52,5R
- Class N (normal hardening) including CEM 42,5N and CEM 32,5R
- Class S (slow hardening) including CEM 32,5N.

Table 2.1 shows the development until 360 days of average strength  $f_{cm}$  of concrete produced with cement from the three classes, where the compressive strength at 28 days for each class,  $f_{cm}$ , equals 1.

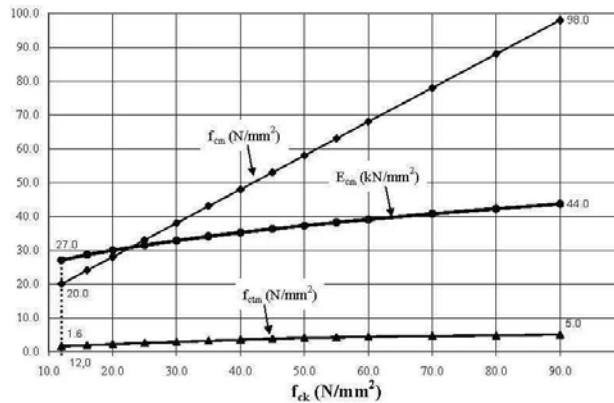


Figure 3.1. Values of  $f_{cm}$ ,  $f_{ctm}$  and  $E_{cm}$  in function of  $f_{ck}$

Table 3.1. Development of  $f_{cm}(t) / f_{cm,28}$  ratio

t (days)	Class R	Class N	Class S
1	0,42	0,34	0,19
2	0,58	0,50	0,35
3	0,66	0,60	0,46
7	0,82	0,78	0,68
14	0,92	0,90	0,85
<b>28</b>	<b>1,00</b>	<b>1,00</b>	<b>1,00</b>
90	1,09	1,11	1,18
360	1,15	1,19	1,31

**3.1.3 Elastic deformation**

**C3.1.3 Elastic deformation**

Clause [3.1.3-EC2] deals with the elastic deformation represented by the values of the modulus of elasticity  $E_{cm}$ . Note that the numerical values in Table [3.1-EC2] and here given in Fig 3.1 are referred to concrete produced with siliceous aggregate, at 28 days of curing. These values should be reduced, for concrete with limestone and sandstone aggregates, respectively by 10% and by 30%. For basaltic aggregates they should be increased by 10%.

The development of the E-modulus with time is deduced from the one of  $f_{cm}$  (Table 3.1) with formula [(3.5)-EC2]. Table 3.2 shows the development of  $E_{cm}$  up to 360 days as a ratio of  $E_{cm}$  at 28 days.

**Table 3.2. Development of modulus of elasticity  $E_{cm}$  with time**

t (days)	Class R	Class N	Class S
3	0,88	0,86	0,80
7	0,94	0,93	0,89
14	0,97	0,96	0,95
<b>28</b>	<b>1,00</b>	<b>1,00</b>	<b>1,00</b>
90	1,02	1,03	1,05
360	1,04	1,05	1,08

**3.1.4 Creep and shrinkage**

**C3.1.4 Creep and shrinkage**

Clause [3.1.4-EC2] is about creep and shrinkage.

These two phenomena are typical of concrete. The first relates to the increase in the deformation with time in presence of permanent actions, the second is a spontaneous variation of volume. The development of both phenomena depends on the ambient humidity, the dimensions of the element and the composition of the concrete. Creep is also influenced by the maturity of the concrete when the load is first applied and depends on the duration and magnitude of the loading.

3.1.4 (1-5)

**C3.1.4 (1-5)**

The creep deformation of concrete  $\epsilon_{cc}(\infty, t_0)$  at time  $t = \infty$  for a constant compressive stress  $\sigma_c$  applied at the concrete age  $t_0$ , is given by:

$$\epsilon_{cc}(\infty, t_0) = \varphi(\infty, t_0) \cdot \left( \frac{\sigma_c}{E_c} \right) \quad \text{[(3.6)-EC2]} \quad (2.1)$$

where  $\varphi(\infty, t_0)$  is the creep coefficient related to  $E_c$ , the tangent modulus, which may be taken as 1,05  $E_{cm}$  as from Table [3.1-EC2]. Annex B of the Eurocode gives detailed information on the development of creep with time. Where great accuracy is not required, the value found from Figure 3.1 may be considered as the creep coefficient, provided that the concrete is not subjected to a compressive stress greater than  $0,45f_{ck}(t_0)$  at an age  $t_0$ .

The values given in Figure 3.1 are valid for ambient temperatures between  $-40^\circ\text{C}$  and  $+40^\circ\text{C}$  and a mean relative humidity between  $\text{RH} = 40\%$  and  $\text{RH} = 100\%$ . Moreover, graphs are in function of the concrete  $t_0$ , expressed in days, at the time of loading, of the notional size  $h_0 = 2A_c/u$  where  $A_c$  is the concrete cross-sectional area and  $u$  is the perimeter of that part which is exposed to drying. They are also in function of the concrete class (e.g. C30/37) and of the class (R, N, S) of cement used, as detailed at clause [3.1.2(6)-EC2].

When the compressive stress of concrete at an age  $t_0$  exceeds the value  $0,45 f_{ck}(t_0)$  then the proportionality expressed by [(3.1)-EC2] does not subsist and creep non-linearity should be considered. In such cases the non-linear notional creep coefficient should be obtained as from the exponential expression [(3.7)-EC2].

3.1.4 (6)

**C3.1.4 (6)**

The total shrinkage strain  $\epsilon_{cs}$  is composed of two components:

$\epsilon_{cd}$ , the drying shrinkage strain, which develops slowly, since it is a function of the migration of the water through the hardened concrete and

$\epsilon_{ca}$ , the autogenous shrinkage strain, which develops during hardening of the concrete: the major part of it therefore develops in the early days after casting.

Autogenous shrinkage can be defined as "the macroscopic volume reduction of cementitious materials when cement hydrates after initial setting. Autogenous shrinkage does not include the volume change due to loss or ingress of substances, temperature variation, the application of an external force and restraint" [JCI, 1998]. Autogenous shrinkage specially has to be regarded for higher strength concrete's, since its value increases with decreasing water cement ratio. Autogenous shrinkage is negligible, in comparison to drying shrinkage, in concrete having a w/c ratio greater than 0.45, but it can represent 50% of the total shrinkage when w/c is 0.30. Its development in time is linked to the hardening process of the concrete. In high strength concrete there is a considerable strength development during the first days; therefore autogenous shrinkage specially has to be regarded in cases that imposed deformations can occur, such as in the case that new concrete is cast against old concrete. In Annex B of EC-2 the basic equations for both drying shrinkage and autogenous shrinkage are given. They are valid up to a concrete strength class C90.



Drying shrinkage is essentially a function of the ambient humidity and of the notional size  $h_0 = 2A_0/u$ . Clause [3.1.4(6)-EC2] gives formulae and tabled values normally used. Further information is given in Annex B (part B2).

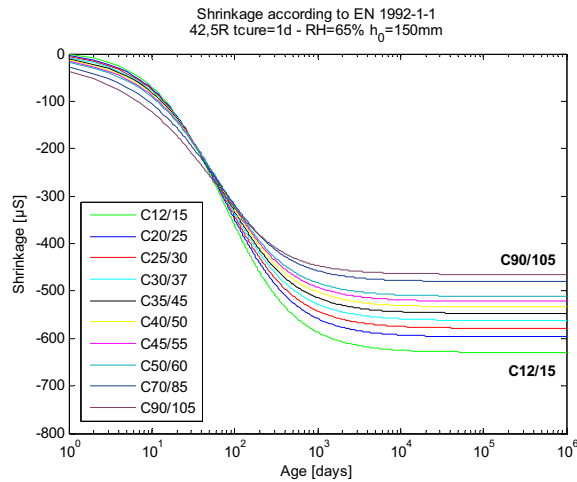


Figure 3.2. Development of shrinkage according to EC2

**3.1.5 Stress-strain relation for non-linear structural analysis**

**C3.1.5 Stress-strain relation for non-linear structural analysis**

Clause [3.1.5-EC2] gives the stress-strain relation for non-linear structural analysis as described by [Fig. 3.2-EC2] and by the expression [(3.14)-EC2].

In the ENV-1992-1-1 the following relation has been used in order to describe the mean stress strain relation:

$$\frac{\sigma_c}{f_{cm}} = \frac{\kappa\eta - \eta^2}{1 + (\kappa - 2)\eta} \tag{1}$$

where

$$\eta = \epsilon_c / \epsilon_{c1} \tag{2}$$

$$\epsilon_{c1\%} = 0.0022 \quad (\text{strain at peak compressive stress})$$

$$k = (1.1 E_c) \epsilon_{c1} / f_c \tag{3}$$

$E_c$  denotes the mean value  $E_{cm}$  of the longitudinal modulus of deformation, where

$$E_{cm} = (f_{ck} + 8)^{1/3} \tag{4}$$

In ENV 1992-1-1, however, only concrete strength classes up to C50/60 were considered.

High strength concrete is known to behave in a more brittle way and the formulation therefore cannot be extended to high strength concrete without modification.

Fig. 3.2 shows compressive stress–strain relations for concrete strength classes ranging from about C25 to C90

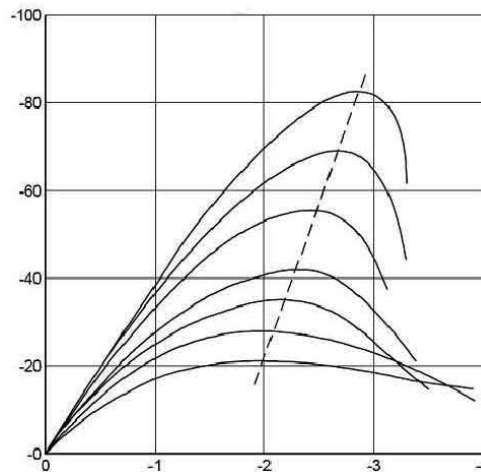


Figure 3.2 Stress-strain relation for concrete's different strength classes subjected to a constant strain rate (strain in horizontal axis in %, stress in vertical axis in MPa)

In [CEB, 1995], the following modifications have been proposed:

- Eq. (4) overestimates the E-modulus for HSC. An appropriate formulation for HSC is:

$$E_{cm} = 22.000 [(f_{ck} + \Delta f) / 10]^{0.3} \tag{5}$$

where the difference between mean and characteristic strength  $\Delta f$  is 8 MPa. This equation is also a good approximation for the E-modulus of normal strength concrete and could therefore be attributed general validity. (It should be noted that the given values are mean values and that the real modulus of elasticity can considerably be influenced by a component like the aggregate. If the modulus of elasticity is important and results from similar types of concrete are not known, testing of the concrete considered is recommended).

- To determine the ascending branch, using Eq. 1, the constant value  $\epsilon_{c1} = - 0.0022$  should for HSC be replaced by

$$\epsilon_{c1} (\%) = - 0.7 f_{cm}^{0.31} \text{ (} f_{cm} \text{ in MPa)} \tag{6}$$

This value can as well be used for normal strength concrete

- For HSC (>C50) the descending branch should be formulated by

$$\sigma_c = f_{cm} / [1 + \{(\eta_1 - 1) / (\eta_2 - 1)\}^2] \tag{7}$$

where  $\eta_1 = \epsilon_c / \epsilon_{c1}$  and  $\eta_2 = (\epsilon_{c1} + \epsilon_{c0}) / \epsilon_{c1}$  where  $\epsilon_{c0}$  is a value to be taken from Table 3.3.

**Table 3.3.** The parameter  $t$  for HSC

$f_{ck}$ (MPa)	50	60	70	80	90
$\epsilon_{c0}$ ( $10^{-3}$ )	0.807	0.579	0.338	0.221	0.070

A warning is given that the descending branch highly depends on the testing procedure and its formulation should be used with caution.

Using the relations (1,2,3,5,6,7) the diagram shown in Fig. 3.3 is obtained.

Since the descending branch for HSC is not very reliable, a simplified formulation is preferred, in that the lines according to Eq. (1) are continued beyond the top, Eq. 6, until a defined value  $\epsilon_{cu}$  is reached, according to

$$\epsilon_{cu} (\%) = 2.8 + 27 [(98 - f_{cm})/100]^4 \text{ for } f_{ck} \geq 55 \text{ Mpa} \tag{8}$$

In this way the simplified curves shown in Fig. 3.4 may be obtained.

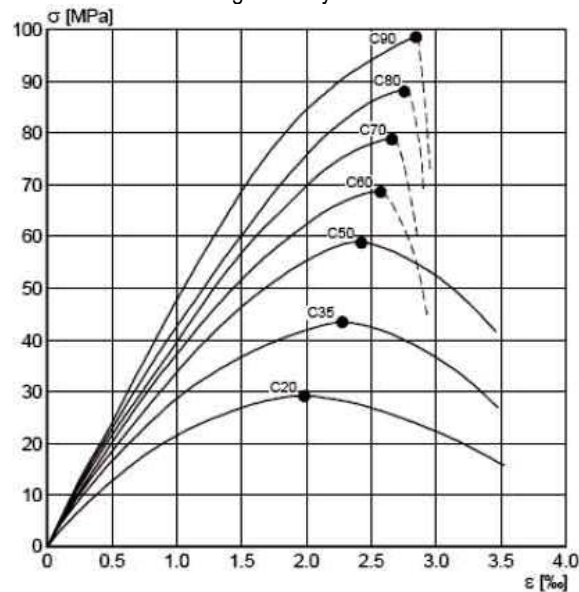


**Figure 3.3.** Mean stress-strain relations, obtained by combining Eq. (1-3) and (5-7).

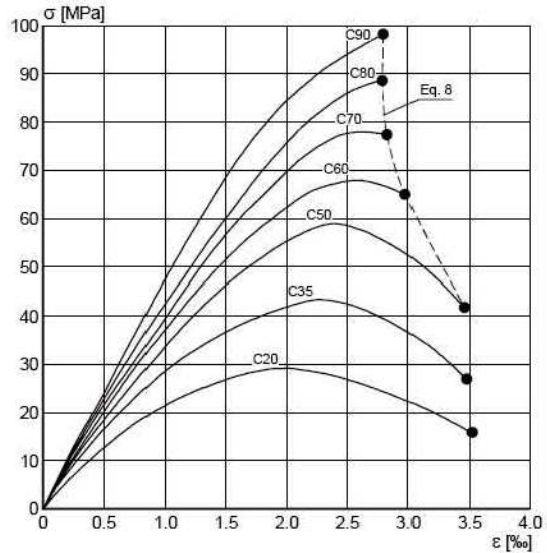


Figure 3.4. Simplified mean stress-strain relations, according to the new formulation, combining Eq. (5,6,8)

**3.1.6 Design compressive and tensile strengths**

**C3.1.6 Design compressive and tensile strengths**

The value of the design compressive strength  $f_{cd}$  is defined as

$$f_{cd} = \alpha_{cc} f_{ck} / \gamma_c \tag{3.15-EC2} \quad (2.2)$$

where

$\alpha_{cc}$  is the coefficient taking account of long term effects on the compressive strength and of unfavourable effects resulting from the way the load is applied;

$\gamma_c$  is the partial safety factor for concrete, which is 1,50 [Table 2.1N-EC2].

A well known research program focussing on the effects of long term loading was the one carried out by Rüschi [Rüschi, 1960]. He carried out tests on concrete prisms, which he loaded to a certain fraction of the short-term compressive strength: subsequently the load was kept constant for a long period. If the long-term loads were higher than about 80% of the short-term bearing capacity, failure occurred after a certain period. Fig. 3.5 reproduces Rüschi's diagrammatic representation of concrete strains as a function of the applied stresses for several loading times.

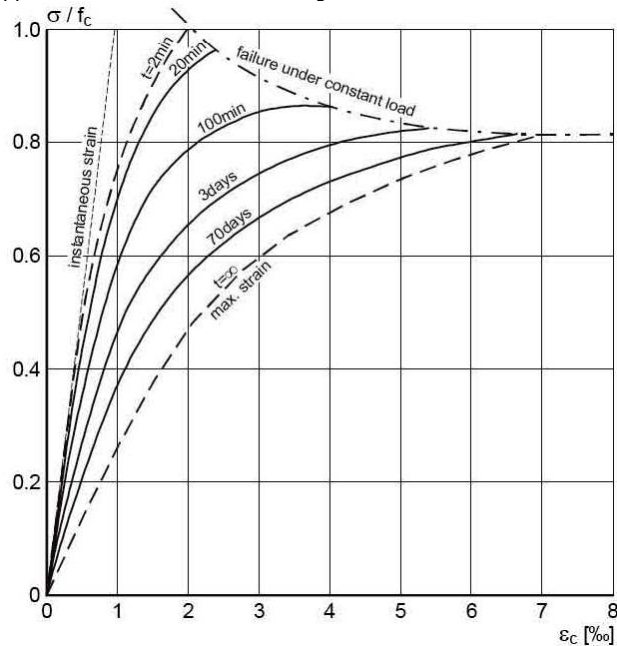


Figure 3.5. Stress-strain relations for several time durations of axial compressive loads (Rüschi, 1960)

As can be seen, the longer the loading time, the more the ultimate strength approaches the long-term value 80%. The tests carried out by Rüschi were limited to concrete's with a maximum cube strength of about 60Mpa. Tests by Walraven and Han on concrete's with cube strength's up to 100 Mpa showed that the sustained loading behaviour for high strength concrete is similar to that of conventional concrete's [Han/Walraven, 1993].

However, Rüschi's tests were carried out on concrete which had an age of 28 days at the time the load was applied. This condition will normally not hold for a structure in practice, which generally will be much older when subjected to a load. This means that the sustained loading effect is at least partially compensated by the increase in strength between 28 days and the age of loading. Fig. 3.6 shows the strength development in time according to eq. EC-3.3 for concrete's made with rapid hardening high strength cements RS, normal and rapid hardening cements N and R, and slowly hardening cements SL.

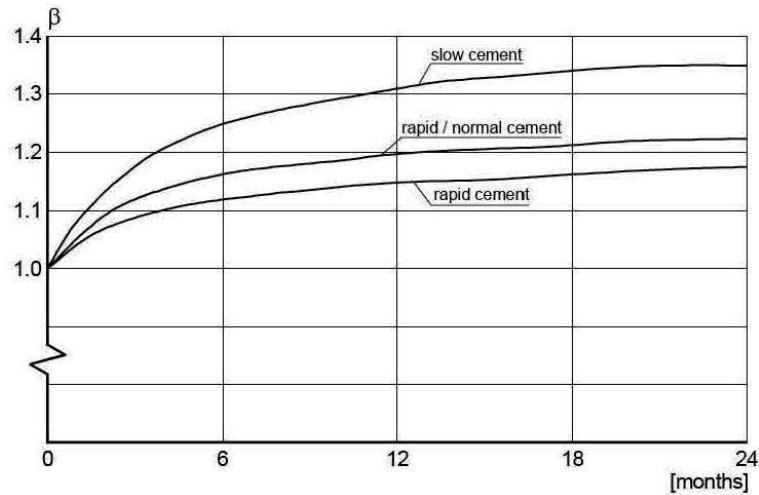


Figure 3.6. Compressive strength development of concrete made with various types of cement according to Eq. EC-3-3

Fig 3.6 shows, that the gain in strength in 6 months ranges from 12% for rapid hardening cements to 25% for slowly hardening cements. So, a considerable part of the sustained loading effect is compensated for by the increase in strength.

Furthermore the bearing capacity as formulated in building codes is generally based on experiments in laboratories (shear, punching, torsion, capacity of columns). Normally those tests have a duration of at least 1.5 hours. In Fig. 3.5 it can be seen that in a test with a loading duration of 100 minutes, the reduction of strength with regard to 2 minutes is already about 15%.

A certain sustained loading effect is therefore already included in the results of tests. It is therefore concluded that cases in which the sustained loading effect will really influence the bearing capacity of a structure in practice are seldom and do not justify a general reduction of the design strength with a sustained loading factor of 0.8. Therefore in clause 3.1.4 it is stated that "the value of  $\alpha_{cc}$  may be assumed to be 1, unless specified otherwise".

Such a case can for instance occur when, according to 3.1.2, the concrete strength is determined substantially after 28 days: in such a case the gain in strength may be marginal so that a value  $\alpha_{cc}$  smaller than 1 is more appropriate.

For tension similar arguments apply.

The value of the design tensile strength  $f_{ctd}$  is defined as

$$f_{ctd} = \alpha_{ct} f_{ctk, 0.05} / \gamma_c \tag{3.16)-EC2} \quad (2.3)$$

where

$\alpha_{ct}$  is a safety factor, similar to  $\alpha_{cc}$ , the value of which may be found in the National Annex;

$f_{ctk, 0.05}$  is the characteristic axial tensile strength of concrete, fractile 5%, which can be deducted from Table [3.1-EC2].

### 3.1.7 Stress-strain relations for the design of cross-sections

#### C3.1.7 Stress-strain relations for the design of cross-sections

Design stress-strain relations can be derived from the mean stress strain relations. This can principally be done using the relations given in 3.1.5, but now for the *characteristic* compressive strength ( $f_{ck}$ ) values and subsequently reducing the stress ordinate by a factor  $\gamma_c = 1.5$ . This means that principally not only the stress values but also the  $E_c$  values are divided by  $\gamma_c$ . In order to obtain consistent and sufficiently safe design relations the ultimate strains  $\epsilon_{cu}$  have also been slightly reduced in relation to Eq. 8. By choosing the expression

$$\epsilon_{cu} (\%) = 2.6 + 35 [(90 - f_{ck})/100]^4 < 3.5 \tag{9}$$

for concrete strength classes C55 and higher, all curves end approximately at their top (compare Fig. 3.3). The resulting curves are shown in Fig. 3.7.

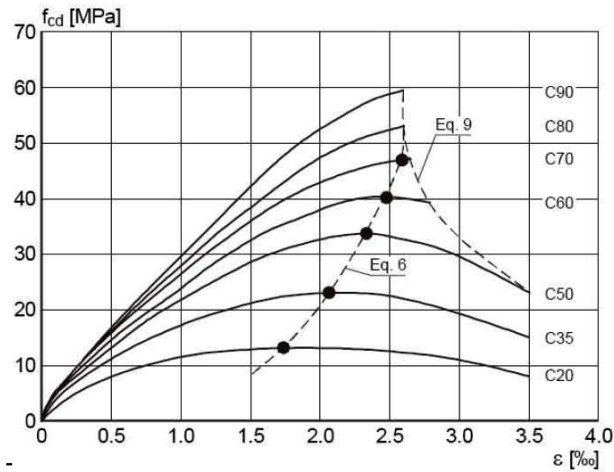


Figure 3.7. Basis for design diagrams

In the new version for EC-2 two alternative design curves are given: one on the basis of a parabola-rectangle relation (Fig. 3.8), and one on the basis of a bilinear relation (Fig. 3.9)

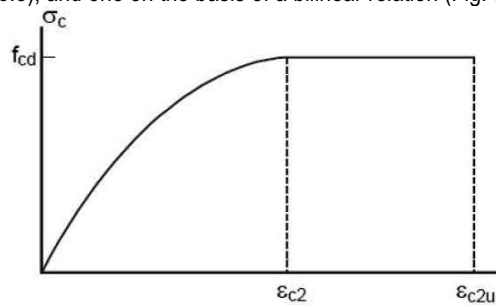


Figure 3.8. Parabola-rectangle design stress-strain relation

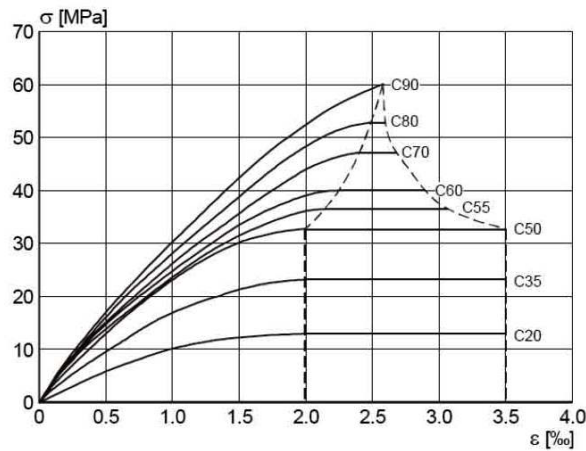


Figure 3.9. Design stress-strain curves for a parabola-rectangle formation

The parabola rectangle relation (Fig. 3.8) is expressed by

$$\sigma_c = f_{cd} \left[ 1 - \left( 1 - \frac{\epsilon_c}{\epsilon_{cu}} \right)^n \right] \quad \text{for } 0 \leq |\epsilon_c| \leq |\epsilon_{c2}|$$

$$\sigma_c = f_{cd} \quad \text{for } 0 \leq |\epsilon_c| \leq |\epsilon_{c2u}|$$

where n,  $\epsilon_{c2}$  and  $\epsilon_{c2u}$  follow from the table below:

Table 3.4. Parameters for the parabola-rectangle design stress-strain relation in compression

	C20	C35	C50	C55	C60	C70	C80	C90
$\epsilon_{c2}(\text{‰})$	2,0	2,0	2,0	2,2	2,3	2,4	2,5	2,6
$\epsilon_{cu2}(\text{‰})$	3,5	3,5	3,5	3,1	2,9	2,7	2,6	2,6
n	2	2	2	1,75	1,6	1,45	1,4	1,4

on the basis of the parabola – rectangle approach and the bilinear approach. The figure shows that there is good overall consistency. It could be argued that for the lowest concrete strength classes (see the figure for C20 in Fig. 3.12), the bilinear approach is slightly less accurate. This could be improved by reducing the values  $\epsilon_{c3}$  for the lower strength classes. This would however have a considerable disadvantage since then the shape of the design stress strain curves for all strength classes < C55 would be different which would render substantial complications for practical design (different shape factors and distance factors, large sets of design diagrams for various cases, where now only one diagram is sufficient). Since the loss of accuracy for practical calculations is very small the constant value  $\epsilon_{c3} = 1.75 \%$  should be maintained.

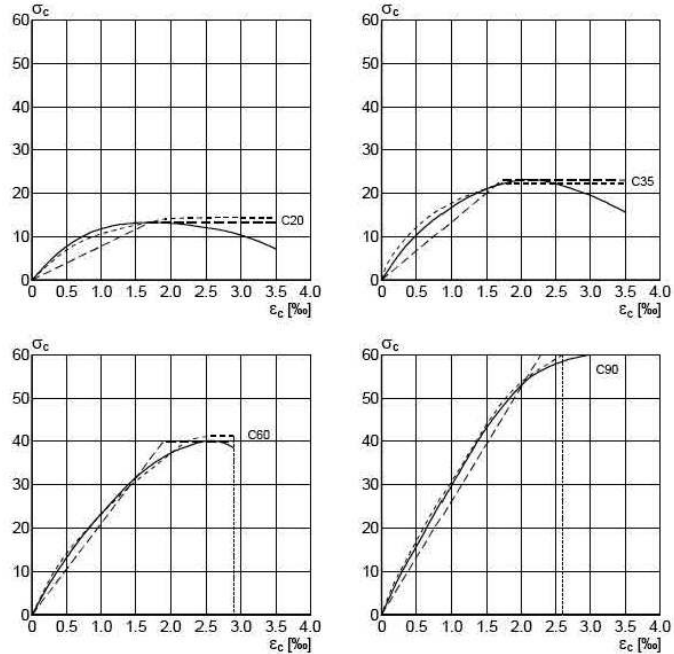


Figure 3.12. Comparison of "basic" and "approximate" design curves

In clause 3.1.6 (4) of EC2 as well the possibility is offered to work with a rectangular stress distribution, see fig. 12. This requires the introduction of a factor  $\lambda$  for the depth of the compression zone and a factor  $\eta$  for the design strength, see Fig. 3.13.

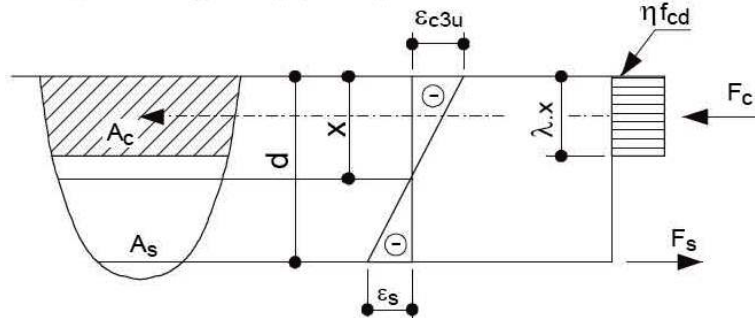


Figure 3.13. Rectangular stress distribution

As a basis for the derivation of  $\lambda$  and  $\eta$  the parabolic-rectangle stress strain relation is used, see Fig. 3.11. As an example the values  $\lambda$  and  $\eta$  are calculated for the strength classes C50 and lower. For concrete's in the strength classes  $\leq C50$  the characteristic strains are  $\epsilon_{c2} = 2.0 \text{ ‰}$  and  $\epsilon_{c2u} = 3.5 \text{ ‰}$ . Now a rectangular stress block is searched for, which gives the same resulting force at the same location.

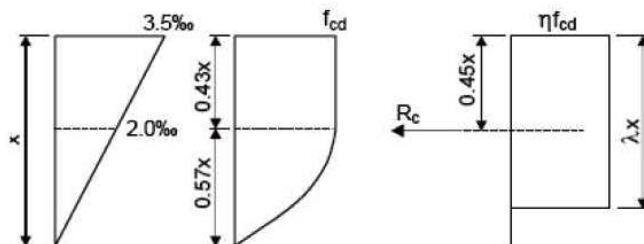


Figure 3.14. Derivation of rectangular stress block from the parabolic-rectangle stress distribution for concrete strength class  $\leq C50$

For the parabolic-rectangle stress distribution the resulting force is  $0.81 \times b f_{cd}$  and the distance of this force to the top is  $0.415x$ , where  $x$  is the height of the compression area.  
 In order to obtain a rectangular stress block with its resultant at the same position, the depth of the compression area should be  $\lambda x = 2 \times 0.415x = 0.83x$ , so  $\lambda = 0.83$ .  
 In order to get the same magnitude of the resultant, the maximum stress is defined as  $\eta f_{cd}$ .  
 The resultant force for the rectangular stress block is  $(\lambda x)b(\eta f_{cd})$ . Since this force should be equal to  $0.83 \times b f_{cd}$ , the value of  $\eta$  follows from  $\eta = 0.81/\lambda = 0.98$   
 Carrying out this calculation for all concrete strength classes, with the values for  $\epsilon_{c3}$  and  $\epsilon_{c3u}$  taken from table 3.5 [table 3.1 EC2], the values  $\eta$  and  $\lambda$  shown in fig. 3.15 are obtained.

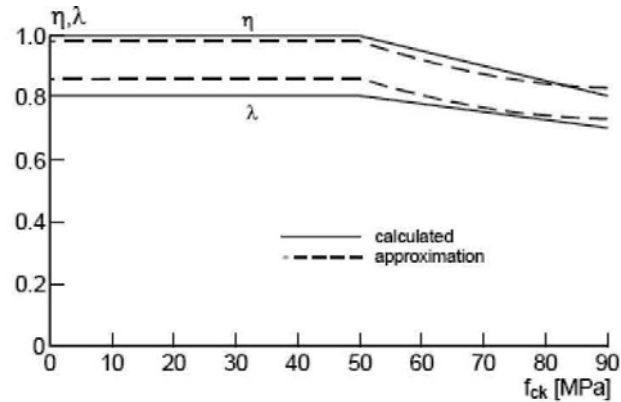


Figure 3.15. Values  $\eta$  and  $\lambda$  for the definition of the rectangular stress block

Approximate equations for  $\lambda$  and  $\eta$  are:

$$\lambda = 0,8 \quad \text{per } f_{ck} \leq 50 \text{ N/mm}^2$$

$$\lambda = 0,8 - \frac{(f_{ck} - 50)}{400} \quad \text{per } 50 < f_{ck} \leq 70 \text{ N/mm}^2$$

$$\eta = 1 \quad \text{per } f_{ck} \leq 50 \text{ N/mm}^2$$

$$\eta = 1,0 - \frac{(f_{ck} - 50)}{200} \quad \text{per } 50 < f_{ck} \leq 70 \text{ N/mm}^2$$

If the width of the compression zone decreases in the direction of the extreme compression fibre, the values given in Eq. 16a,b do not hold. This is investigated in Fig. 3.16.

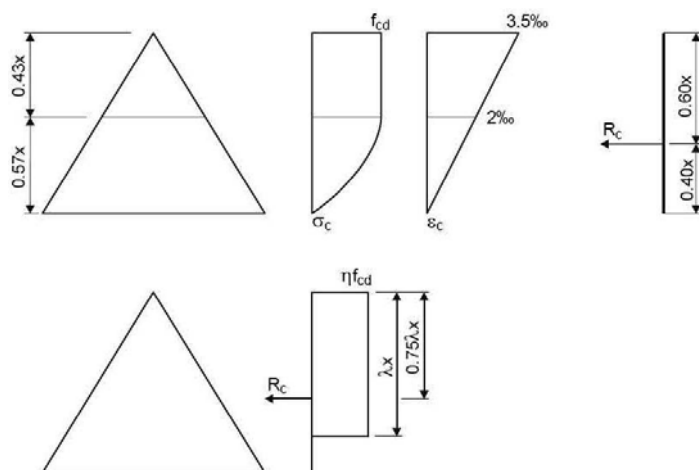


Figure 3.16. Derivation of rectangular stress block from bilinear stress block for a cross section width in the direction of the extreme compression fibre

Similar type of calculations has been carried out for this case. Fig. 3.17 shows for  $\eta$  as a function of the concrete strength. Three cases are considered:

- the calculated relations for a rectangular cross-section
  - the calculated relations for a triangular cross-section with the top at the extreme compressive strain
  - the design equation, derived for the case of the rectangular cross-section.
- It is shown that the design equation for  $\lambda$  is safe for both cases. However, the values for  $\eta$  for the triangular case are lower than the design values.  
 It is sufficient to reduce the values for  $\eta$  with 10% in order to cover as well the triangular case.

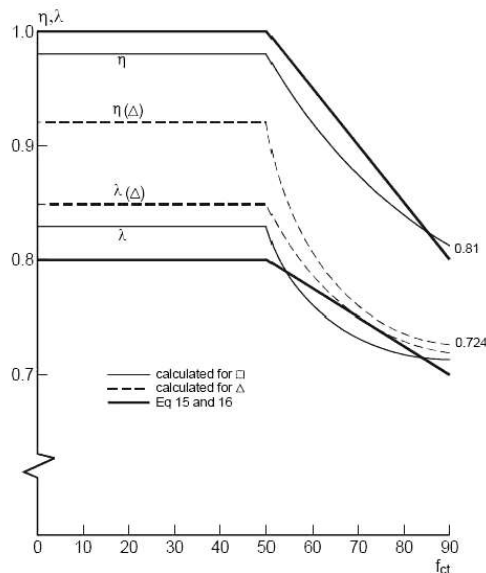


Figure 3.17. Calculated values for  $\eta$  and  $\lambda$  for a rectangular and triangular cross-section, in comparison with the design equation for the rectangular case.

**3.1.8 Flexural tensile strength**

**C3.1.8 Flexural tensile strength**

The flexural tensile strength is larger than the concentric tensile strength. This is caused by strain softening at cracking concrete. The size effect of concrete in bending is therefore the same as for concrete subjected to shear or punching (see f.i. Walraven, 1995), so that the size

factor  $k = 1 + \sqrt{\frac{200}{d}}$  may be expected to apply for the relation between flexural tensile strength and

concentric tensile strength as well. However, in this case the phenomenon is more sensitive to the effect of drying shrinkage, temperature gradients and imposed deformations.

Therefore the more conservative equation

$$f_{ctm,fl} = \left(1,6 - \frac{h}{100}\right) f_{ctm} \geq f_{ctm}$$

has been chosen.

**3.1.9 Confined concrete**

**C3.1.9 Confined concrete**

Having a uniform radial compressive stresses  $\sigma_2$  at the ULS as a result of confinement, the axial strength  $f_{ck,c}$  is:

$$f_{ck,c} = f_{ck} [1 + 5,000 (\sigma_2 / f_{ck})] \quad \text{for } \sigma_2 \leq 0,05 f_{ck} \quad [(3.24)\text{-EC2}] \quad (2.4)$$

$$f_{ck,c} = f_{ck} [1,125 + 2,5 (\sigma_2 / f_{ck})] \quad \text{for } \sigma_2 > 0,05 f_{ck} \quad [(3.25)\text{-EC2}] \quad (2.5)$$

Axial strength increases by 50% if the lateral compressive stresses are 15% of  $f_{ck}$ , it doubles if compressive stresses are 35% of  $f_{ck}$ . Also the strain at failure increase up to 3-4 times.

Lateral stresses may be achieved by confinement of the compressed member. Index c after  $f_{ck}$ , stands for "confined".

**3.2 Reinforcing steel**

**3.2.1 General**

**3.2.2 Properties**

**C3.2.2 Properties**

Clause [3.2.2(3P)-EC2] states that the design rules of Eurocode are valid when steel having characteristic yield  $f_{yk}$  between 400 and 600 N/mm<sup>2</sup> is used.

**3.2.3 Strength**

**3.2.4 Ductility characteristics**

**3.2.5 Welding**

**3.2.6 Fatigue**



**3.2.7 Design assumptions**

**C3.2.7 Design assumptions**

Safety factor  $\gamma_s$  for ultimate limit states is 1,15 according to Table [2.1N-EC2]. The design stress-strain diagram is shown in Fig. 3.18.

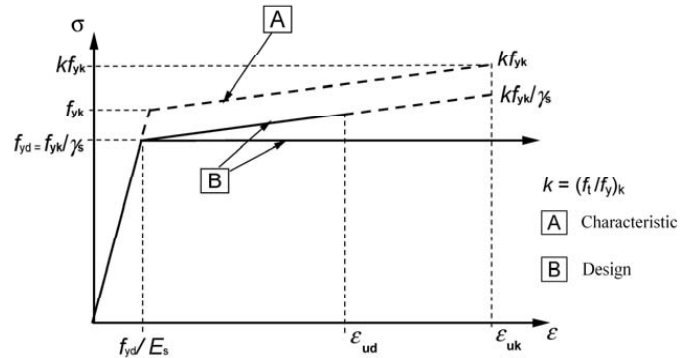


Figure 3.18. Idealised and design stress-strain diagrams for reinforcing steel [Fig. 3.8-EC2]

For normal design, either of the following assumptions may be made:

- c) an inclined top branch with a strain limit of  $\epsilon_{ud}$  and a maximum stress of  $k \frac{f_{yk}}{\gamma_s}$  where  $k = \left( \frac{f_t}{f_y} \right)_k$
- d) a horizontal top branch without the need to check the strain limit.

The recommended value of  $\epsilon_{ud}$  is 0,9  $\epsilon_{uk}$ .

The value of  $\left( \frac{f_t}{f_y} \right)_k$ , given in Annex C for class C steel, is between 1,15 and 1,35.

The value of the elasticity modulus  $E_s$  may be taken as 200000 Nmm<sup>-2</sup>.

**3.3 Prestressing steel**

**C3.3 Prestressing steel**

Data from EC2, integrated with those from EN 10138 which is referred to in EC2, are recalled hereafter.

**3.3.1 General**

Prestressing steel are geometrically classified as:

**3.3.2 Properties**

- wires with plain or indented surface, of diameter between 3,0 and 11,0 mm
- two-wire strands spun together over a theoretical common axis; nominal diameter of the strand between 4,5 and 5,6 mm
- three-wire strands spun together over a theoretical common axis; nominal diameter of the strand between 5,2 and 7,7 mm
- seven-wire strands of which a straight core wire around which are spun six wires in one layer; nominal diameter of the strand between 6,4 and 18,0 mm
- ribbed bars; nominal diameter between 15,0 and 50,0 mm.

**3.3.3 Strength**

Within each type, reinforcing steel is classified according to the following properties:

- Strength, denoting the value of tensile strength  $f_p$  and the value of the 0,1% proof stress ( $f_{p0,1k}$ ).
- Ductility, denoting the value of the ratio of tensile strength to proof strength ( $f_{pk}/f_{p0,1k}$ ), which should be at least 1.1, and elongation at maximum load ( $\epsilon_{uk}$ ). Although it's not indicated in EC2, in accordance with EN10138  $\epsilon_{uk}$  should be at least 0,035.
- Class, indicating the relaxation behaviour. Three classes are defined in the Eurocode:
  - Class 1: wire or strand – ordinary relaxation
  - Class 2: wire or strand – low relaxation
  - Class 3: hot rolled and processed bars

**3.3.4 Ductility characteristics**

The design calculations for the losses due to relaxation of the prestressing steel should be based on the value of  $\rho_{1000}$ , the relaxation loss (in %) at 1000 hours after tensioning and at a mean temperature of 20 °C. The value of  $\rho_{1000}$  is expressed as a percentage ratio of the initial stress and is obtained for an initial stress equal to 0,7 $f_p$ , where  $f_p$  is the actual tensile strength of the prestressing steel samples.  $\rho_{1000}$  values indicated in EC2 for structural design are: 8% for Class 1, 2,5% for Class 2, 4% for Class 3.

Clause [3.3.2(7)-EC2] gives the formulae for calculation of relaxation at different t times for the three above-mentioned classes. Annex [D-EC2] provides the elements needed for accurate calculations.

Fatigue: prestressing tendons are liable to fatigue. Relevant criteria and methods for verification are

### 3.3.5 Fatigue

given at clause [6.8-EC2].

### 3.3.6 Design assumptions

On top of strength and ductility values, the Eurocode provides the following design assumptions:

- Modulus of elasticity recommended for strands: 195000 N/mm<sup>2</sup>; for wires and bars: 205000 N/mm<sup>2</sup>
- Design stress-strain diagrams. As represented in Fig. 3.19, taken the safety factor  $\gamma_s = 1,15$ , the design diagram is made of a rectilinear part up to ordinate  $f_{pd}$  from which two ways start: a rectilinear inclined branch, with a strain limit  $\epsilon_{ud} = 0,9 \epsilon_{uk}$ , or 0,02; the other branch is a horizontal branch without strain limit.

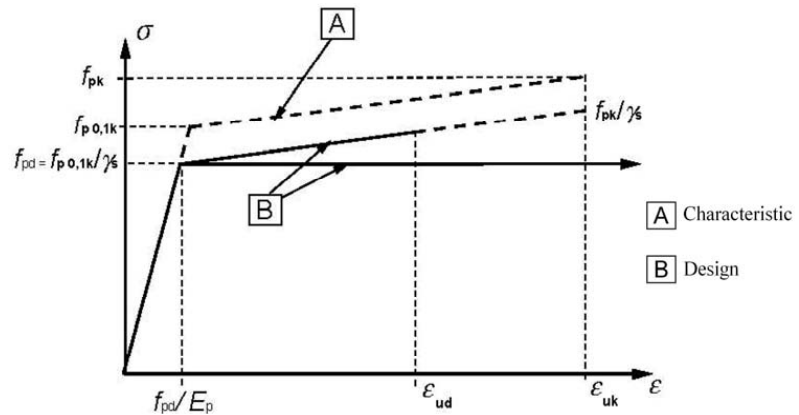


Figure 3.19. Idealised and design stress-strain diagrams for prestressing steel [Fig. 3.10-EC2]

### 3.3.7 Prestressing tendons in sheaths

### 3.4 Prestressing devices

#### LITERATURE

Aitcin, P., "Demystifying Autogenous Shrinkage", Concrete International, 1999, pp. 54-56.

CEB-Bulletin 228, "High Performance Concrete: Recommended Extensions to Model Code 90", Report on the CEB-FIP Working Group on High Strength Concrete", July 1995.

ENV 197-1 Cement – composition, specifications and conformity criteria – Part 1 Common cements, 1992

fib, "Structural Concrete: Text Book on Behaviour, Design and Performance, Upgraded Knowledge of the CEB/FIP Model Code

Han, N., "Time dependant behaviour of high strength concrete", PhD thesis, Delft University of Technology, The Netherlands", 1996.

JCI Technical Committee Report on Autogenous Shrinkage *Autogenous Shrinkage of Concrete: Proceedings of the International Workshop*, ed. Tazawa, E&FN Spon, London, 1998, pp. 3-63.

Koenders, E., van Breugel, K., "Second Stichtse Bridge – Concrete with high strength: experimental research into the creep and relaxation behaviour during the early stage of the hardening process", Report 25.5-96-2, Feb. 1996, TU Delft (in Dutch).

Müller, H.S., Küttner, C.H., "Creep of High Performance Concrete – Characterisation and Code Type Prediction Model", 4<sup>th</sup> International Symposium on Utilisation of Highstrength/ High Performance Concrete, Paris, 1996, pp. 377/386

Müller, H.S., Küttner, C.H., Kvitsel, V., "Creep and shrinkage models for normal and high performance concrete – a unified code type approach", *Revue Francaise du Genie Civil* (1999)

Neville, A.M., "Properties of concrete", Pitman Publishing Limited, London 1995,

In Table 3.4 the values for  $\epsilon_{c2u}$  follow from Eq. (6-9)

The values for  $\epsilon_{c2}$  and  $n$  are obtained by curve fitting to the relations shown in Fig. 3.7. An approximate expression for  $\epsilon_{c2}$  is:

$$\epsilon_{c2}(\text{‰}) = 2.0 \quad \text{for } f_{ck} \leq 50 \text{ Mpa} \quad (12a)$$

$$\epsilon_{c2}(\text{‰}) = 2.0 + 0.085 (f_{ck} - 50)^{0.53} \quad \text{for } f_{ck} > 50 \text{ Mpa} \quad (12b)$$

and for  $n$ :

$$n = 2.0 \quad \text{for } f_{ck} \leq 50 \text{ Mpa} \quad (13a)$$

$$n = 1.4 + 23.4 [(90 - f_{ck})/100]^4 \quad \text{for } f_{ck} > 50 \text{ MPa} \quad (13b)$$

The resulting design curves are shown in Fig. 3.10.

A second possibility is the use of a bilinear design stress-strain relation (Fig. 3.10). The values  $\epsilon_{c3}$  and  $\epsilon_{c3u}$  are obtained by curve fitting to the relations shown in Fig. 3.7, and are given in Table 3.5.

**Table 3.5.** Parameters for the bilinear design stress-strain relation in compression

	C20	C35	C50	C55	C60	C70	C80	C90
$\epsilon_{c3}(\text{‰})$	1,75	1,75	1,75	1,75	1,90	2,1	2,2	2,3
$\epsilon_{cu3}(\text{‰})$	3,5	3,5	3,5	3,1	2,9	2,7	2,6	2,6

The values for  $\epsilon_{c3u}$  are the same as for  $\epsilon_{c2u}$  and follow therefore from Eq. 9. An approximate expression for  $\epsilon_{c3}$  is

$$\epsilon_{c3}(\text{‰}) = 1.75 \text{ for } f_{ck} < 55 \text{ MPa} \quad (14a)$$

$$\epsilon_{c3}(\text{‰}) = 1.75 + 0.11 (f_{ck} - 55)0.42 \text{ for } f_{ck} \geq 55 \text{ MPa} \quad (14b)$$

The design stress-strain relations derived in this way are shown in Fig. 3.11.

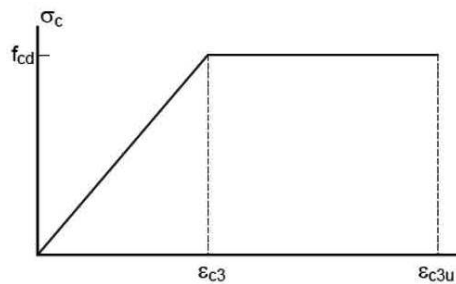


**Figure 3.10.** Bilinear design stress-strain relation

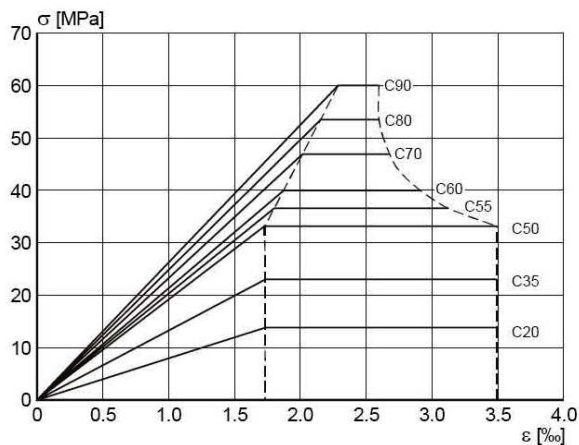


**Fig.3.11.** Design stress-strain curves with bilinear formation

Fig. 3.12 shows the comparison for the “basic” design stress – strain relations (derived from the mean curve by taking the characteristic value and dividing it by  $\gamma_c = 1.5$ ) and the “simplified” design curves,

Nilson, A., "High Strength Concrete- An Overview of Concrete Research", Proceedings of the Conference Utilisation of High Strength Concrete", Stavanger 1987.

Walraven, J.C., "High Performance Concrete Bridges", a European Perspective", Conference on Developments in Short and Medium Span Bridge Engineering, Calgary, Canada, '98, Proceedings, Part I, pp 1-14.

Walraven, J.C., "Size effects: their nature and their recognition in building codes", STUDI E RICERCHE – Vol. 16, 1995, pp. 113-134.

## SECTION 4 DURABILITY AND COVER TO REINFORCEMENT

## SECTION 4. DURABILITY AND CONCRETE COVER

**C4** The rules on design for durability in EC2 are substantially different than in the past. Previously the concrete cover was prescribed in dependence of the environmental class, but independent of the concrete quality. In the actual version of EC2 (EN 1992-1-1) the cover required depends not only on the environmental class, but as well on the concrete strength class, the required design working life and the quality control applied. In the following, background information is given with regard to those choices. The values for the cover in EN 1992-1-1 are a result of increased understanding in the processes of deterioration, as revealed by the Duracrete studies [1], and practical experience. In the following theoretical considerations the most important deterioration processes are explained and parameter studies illustrate the mutual dependencies. Further background information is found in FIB Bulletin n. 34 "Model code for service life design" [2].

### 4.1.1 Introduction

In a European research project [1] a probabilistic based durability design procedure of concrete structures has been developed with the objective to set up a similar concept as in structural design, where the resistance of the structure is compared to the acting load. Related to corrosion protection of reinforcement the resistance of a concrete structure is mainly determined by the thickness and the quality of the concrete cover.

In the European design code for concrete structures EN 1992-1-1 the designer has to determine the nominal concrete cover, which consists of the minimum concrete cover (dependent on the relevant environmental class) plus an allowance in design for tolerance. According to the first draft of prEN 1992-1 the allowance in design for tolerance was also dependent on the environmental class – 10 mm for XC0 and XC1 and 15 mm for all other classes. This rule was changed with respect to the general requirement that values or rules specified in other Eurocodes should not explicitly given again in EN 1992-1-1 but they should only be referred to. Thereafter in the December 99 draft of prEN 1992-1 the allowance in design for tolerance was determined with respect to the execution standard prENV 13670 where the execution tolerance is uniformly defined to 10 mm. This means a reduction of the nominal cover if the values for the minimum cover are not increased accordingly.

In order to find out which value for the nominal concrete cover is adequate a durability design was performed, based in the model in the European project. In particular, the reliability index  $\beta$  was determined and evaluated for different concrete mixes and different nominal concrete covers. The concrete mixes have been chosen with respect to the environmental classes given in EN 206-1.

### 4.1.2 Description of Deterioration Models and Probabilistic Durability Design

This chapter only gives a short overview on those models, since the deterioration models related to reinforcement corrosion and the safety concept of durability design have already been thoroughly described in the literature.

#### 4.1.2.1 Deterioration Models

The corrosion process can be divided into two time periods: the initiation period describes the time until the reinforcement is depassivated either by carbonation or by penetrating chlorides reaching a critical chloride content.

After depassivation, corrosion will start if sufficient oxygen and moisture are available. As a result of corrosion a reduction of the steel cross section, cracking or spalling of the concrete cover will occur. This time period is described as the propagation period.

In the literature deterioration models [2], by which the processes of the initiation period can be described, are well established. The process of the propagation period is much more complex and so far no unanimously accepted models exist.

In the following the time-dependent description of the carbonation progress and the time dependent diffusion-controlled penetration of chlorides are briefly presented.

#### 4.1.2.1.1 Carbonation-Induced Corrosion

The CEB Task Group V model by which the carbonation process in the initiation period can be predicted is given in equation (4.1):

$$x_c(t) = \sqrt{\frac{2 \cdot k_e \cdot k_c \cdot D_{\text{Eff},0} \cdot \Delta C}{a}} \cdot \sqrt{t} \cdot \left(\frac{t_0}{t}\right)^w \quad (4.1)$$

where:

$x_c(t)$  is the carbonation depth at time  $t$

$D_{\text{Eff},0}$  effective diffusion coefficient of dry concrete for carbon dioxide in defined environment (20°C, 65% rel. humidity)

a	the amount of CO <sub>2</sub> for complete carbonation [kgCO <sub>2</sub> /m <sup>3</sup> ]
ΔC	the concentration difference of CO <sub>2</sub> at the carbonation front and in the air, which usually means the carbon dioxide content of the surrounding air c <sub>0</sub>
k <sub>e</sub>	parameter for micro climatic conditions, describing the mean moisture content of concrete
k <sub>c</sub>	parameter to describe the curing conditions
w	parameter (exponent) for micro climatic conditions at the concrete surface, describing wetting and drying
t <sub>0</sub>	reference period,
√t	law valid (e.g. 1 year) t time

**4.1.2.1.2 Chloride-Induced Corrosion**

The model for predicting the initiation period in the case of chloride-induced reinforcement corrosion is defined by equation (4.2):

$$x(t) = 2C_{(crit)} \sqrt{k_t \cdot D_{RCM,0} \cdot k_e \cdot \left(\frac{t_0}{t}\right)^n \cdot t} \tag{4.2}$$

$$k_t D_{RCM,0} = D_0 \tag{4.3}$$

$$C_{(crit)} = \text{erf}^{-1} \left( 1 - \frac{C_{crit}}{C_{SN}} \right) \tag{4.4}$$

where:

x(t)	depth with a corresponding chloride content (here C <sub>(crit)</sub> ) at time (t)
D <sub>0</sub>	effective chloride diffusion coefficient under defined compaction, curing and environmental conditions, measured at time t <sub>0</sub> D <sub>RCM,0</sub> chloride migration coefficient under defined compaction, curing and environmental conditions, measured at time t <sub>0</sub>
C <sub>crit</sub>	chloride threshold level
n	factor which takes the influence of age on material property into account
k <sub>t</sub>	constant which transforms the measured chloride migration coefficient D <sub>RCM,0</sub> into a chloride diffusion coefficient D <sub>0</sub>
k <sub>e</sub>	constant which considers the influence of environment on D <sub>0</sub>
erf <sup>-1</sup>	inverse of the error function
C <sub>SN</sub>	surface chloride level
t	time
t <sub>0</sub>	reference period (28 days)

**4.1.2.2 Probabilistic Durability Design**

**4.1.2.2.1 Safety Concept**

The simplest design problems have only one resistance variable and one action variable. They are generally solved by facing the two variables R and S:

$$Z = R - S \tag{4.5}$$

where Z is the reliability of the structure, R the resistance and S the action: both variables R and S have their averages and standard deviations, and in this example they are normally distributed. Z is a variable itself (see Figure 4.1) and is also normally distributed with a mean μ<sub>Z</sub> and a standard deviation σ<sub>Z</sub> according to equations (4.6) and (4.7).

$$\mu_Z = \mu_R - \mu_S \tag{4.6}$$

$$\sigma_Z = \sqrt{\sigma_R^2 + \sigma_S^2} \tag{4.7}$$

In this simplest case with two variables, the reliability index is the difference between the mean values of R and S divided by the standard deviation of the variable Z or, alternatively the mean value of Z divided by the standard deviation of Z (see Equation 4.8, Figure 4.1):

$$p_f = \Phi\left(-\frac{\mu_z}{\sigma_z}\right) = \Phi(-\beta)$$

where  $\Phi(\cdot)$  stands for a normal distribution and  $p_f$  for the failure probability.

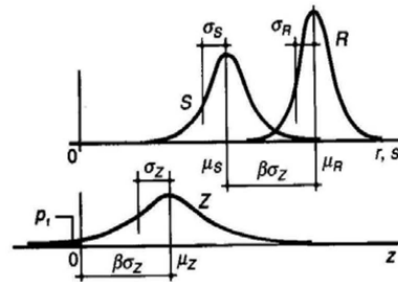


Figure 4.1 resistance, action, failure probability and reliability index

The numerical problems which are treated in the context of durability design are not as easy to calculate as this, because there are numerous variables which have to be statistically evaluated and they are often part of non-linear functions. Besides these aspects, variables are not always normally distributed. For this reason, computer programs are used to calculate these kinds of problems.

### 4.2. Definition of reliability levels

As already mentioned, the corrosion process can be divided into two time periods. For both periods, limit state conditions can be defined. Depassivation of the reinforcement (= end of the initiation period) is defined as a serviceability limit state (SLS), because after the end of the initiation period the corrosion process starts [1]. As the corrosion process in the propagation period can lead to severe consequences (loss of safety of people and structure), this situation is defined as ultimate limit state (ULS). Since the calculations performed in this study only concern the initiation period, the durability design presented here durability design is a SLS assessment.

Design limit states are often defined by means of the reliability index  $\beta$ . According to EN1990, the reliability index for SLS is determined to  $\beta = 1,5$ ; in other National Standards the reliability index is even higher. In the case of durability design a risk oriented grading of the reliability index is proposed. Because of the fact that only the initiation period is considered, the corrosion process itself is so far not included in durability design. A possible way of taking account of the different corrosion risks is to adjust the reliability index to the environmental classes. As a consequence, with respect to the corrosion process a moderate humid environment (e.g. XD1) or environments with cyclic wetting and drying (XC4, XD3, XS3) should fulfil higher safety requirements than totally dry or wet environments (e.g. XC1, XC2, XC3, XS2, XD2) and therefore a higher reliability index is proposed. For the same reason in chloride environments higher reliability indices should be applied due to the risk of higher corrosion rates compared to carbonation induced corrosion. A proposal is given in Table 4.1.

Environmental class	Reliability index $\beta_{SLS,50}$
XC4, XD1, XS1, XS3, XD3	2,0
XC2, XC3, XS2, XD2	1,5
XC1	0,5

Table 4.1: Required reliability index  $\beta_{SLS,50}$  for a life time of 50 years

### 4.3 Parametric Study

#### 4.3.1 General

The calculations are based on the models given in 4.2.1.1 and 4.2.2.2. All input values are given as stochastic variables (mean, standard deviation, type of distribution). The output of the program is the reliability index  $\beta$  as a function of the lifetime. In this study the reliability index  $\beta$  is considered for a lifetime of 50 years.

#### 4.3.2 Carbonation

The type of cement has a strong influence on the concrete resistance against carbonation. Concretes with Portland cement are exposed to carbonation they show a decreasing porosity in the carbonation zone resulting in higher resistance against ongoing carbonation. In concretes with blastfurnace cements or with cements with pozzolanic additions (e.g. fly ash), on contrary, the porosity of the concrete increases after carbonation and the carbonation of the concrete sometimes progresses faster (as the diffusion of  $CO_2$  takes place through the carbonated zone). The influence

of different types of cement is not considered. In the calculations two different concrete mixes (favourable and unfavourable) were studied.

The w/c ratio of the concrete mixes were chosen according to the requirements in prEN 206-1. The cement content was kept constant (320 kg/m<sup>3</sup>) for all concrete mixes, because there is only a minor influence on the carbonation process. The material resistance was determined under laboratory conditions. The length of the curing period also has a strong influence on carbonation. In the calculations the curing time was assumed to be 2 days for CEM I and 3 days for CEM III/B. The climatic conditions were determined according to statistical data from local weather stations. All calculations were performed for European locations with moderate and hot climate to show the influence of temperature.

**4.3.2.1 Environmental class XC2**

In the following, durability design calculations for nominal covers of 30 and 35 mm, for different climates and for different cements (CEM I and for CEM III/B) are performed. In Figure 4.2 the results of the calculations are shown.

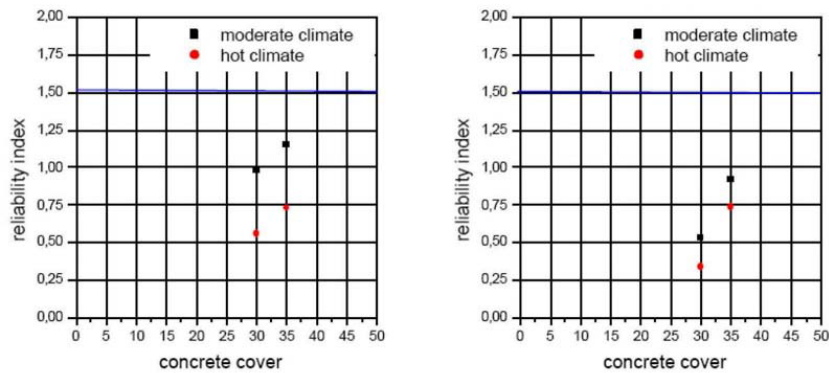


**Figure 4.2:** Reliability index versus concrete cover for environmental class XC2 (w/c=0,6, service life 50 years) a) for CEM I 42,5 R (curing 2 days) b) for CEM III/B 42,5 NW HS NA (curing 3 days)

It can be seen that the reliability index for the calculated values depends on the concrete cover, the location and the type of cement. Especially in the case of a CEM III/B, the reduction of the concrete cover by 5 mm results in a decrease of the reliability index of almost 50 %. This means a reduction of life time of more than 15 years.

It is interesting to see that the choice of a different type of cement has a bigger influence than the reduction of the concrete cover. However it needs to be taken into account that part of the effect depending by the type of cement can be counteracted by prolonged curing.

**4.3.2.2 Environmental class XC3**

For environmental class XC3 the same concrete covers are required as for XC2, but the required w/c ratio for class XC2 is higher. It can be seen, that this improvement of the concrete quality (porosity) also has an important effect on the carbonation (compare Figures 4.2 and 4.3).

Apart from this the same trends can be observed. The reduction of the nominal concrete cover from 35 to 30 mm has a big influence on the reliability index, even more pronounced than for concretes with a w/c ratio according to the requirements for XC2.

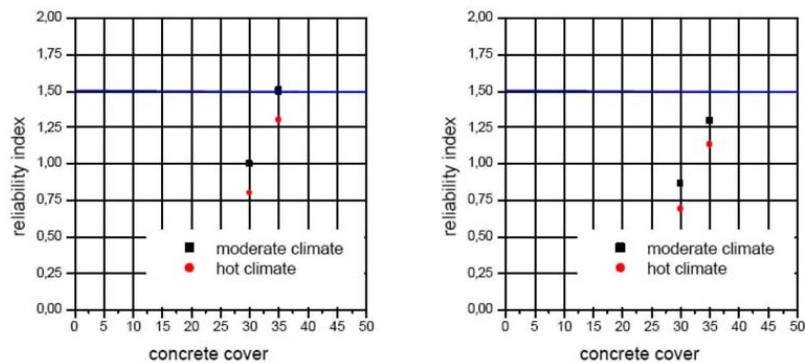


**Figure 4.3:** Reliability index versus concrete cover for environmental class XC3 (w/c=0,55, service life 50 years) a) for CEM I 42,5 R (curing 2 days) b) for CEM III/B 42,5 NW HS NA (curing 3 days)

**4.3.2.3 Environmental class XC4**

For environmental class XC4, the w/c-value is reduced to 0,5 and compared to the environmental classes XC2 and XC3 the concrete cover is increased by 5 mm. This has a considerable effect on the reliability index (compare Figures 4.1a, 4.2a and 4.3a). Although the required reliability index according to Table 4.1 is increased to 2,0 for XC4 all concrete covers are still above the value for



CEM I.

However when using a CEM III/B type of cement, (see Figure 4.3b), the reliability index is reduced by 50% and is far below the reliability index proposed for this environmental class. An additional reduction of the concrete cover means a further reduction of the reliability index.

The considerable difference in reliability index as a consequence of using two types of cements shows that the currently existing requirements for the determination of the concrete cover do not include all important parameters and are therefore not very exact. For a nominal concrete cover of 40 mm, the model seems to put in evidence that the deviation of the proposed reliability index is still acceptable, whereas a nominal concrete cover of 35 mm leads to an unacceptable decrease of total life time.

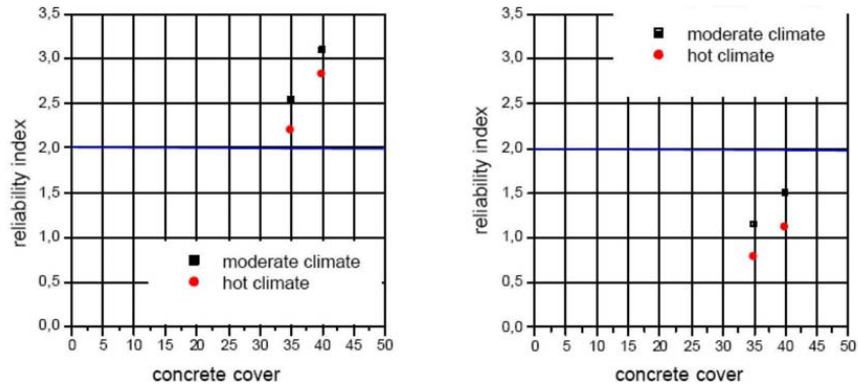


Figure 4.4 - Reliability index versus concrete cover for environmental class XC4(w/c=0,50)  
 a) for CEM I 42,5 R      b) for CEM III/B 42,5 NW HS NA

4.3.3 Chloride penetration

Chlorides are transported in the concrete by the pore water. Processes of diffusion and conveyance by water transport take place which lead to a certain chloride content in the concrete. The time before attainment of a critical chloride content depends mainly on the porosity of the concrete, which may be influenced for example by the w/c ratio and the type of cement. In general, the use of Portland cements leads to a higher permeability of the concrete for chlorides than the use of blastfurnace cements or cements with fly ash.

In this study only environmental class XS3 with nominal concrete covers of 50 and 55 mm was studied. The w/c ratio of the corresponding concrete mix was determined according to EN 206-1 (w/c = 0,45) and the cement content was 320 kg/m<sup>3</sup>. The climatic conditions (relative humidity and temperature) were determined according to statistical data of local weather stations and the calculations were performed for two European locations close to the sea in moderate and hot climate.

The calculations were performed with two different types of cement [1]: the results for a CEM I with fly ash are shown in Figure 4.4. Alternatively the calculation was performed with CEM I without fly ash [1]. The reliability index for a lifetime of 50 years was below 0, that means that corrosion probability is higher than 50%. Examples have shown that the use of Portland cements in tidal environments (e.g. harbours) has already led to deterioration (cracking) as a result of chloride induced corrosion after 10 years.

The calculation with Portland cement plus fly ash has shown similar trends as in the case of carbonation. Figure 4.5 shows that hot climates result in faster chloride ingress than moderate climates. It can also be seen, that the proposed reliability index is not reached for environmental class XS4.

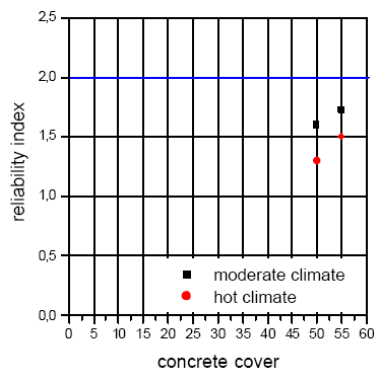


Figure 4.5: Reliability index versus concrete cover for environmental class XS3 (w/c=0,45)  
 a) for CEM I with fly ash

The results of chapters 3.2 and 3.3 have shown that lower values for the nominal concrete cover result in a significant reduction of the reliability index, leading to a decrease of the safety against reinforcement corrosion. It can be concluded that the nominal concrete cover should not be decreased as a consequence of the reduction of allowance in design for tolerance.

#### **4.4 Conclusions**

The calculations have shown the dependence of the rate of deterioration on the service life, the thickness of the concrete cover and the environmental class. It is shown that the provisions as given in EC-2 recognize the most important influencing factors. Further influences, which have not yet been regarded in detail in EN 1992-1-1 are the type of cement and the temperature.

The comparisons show that, theoretically, the prescribed reliability indexes are not always met. It should be realized, however, that there are many uncertainties in the input values of the calculations. Further to the influence of the type of cement and the temperature there is the variation in climatic conditions (wet - dry cycles, local differences due to different orientation with regard to solar radiation and wind).

The recommendations in the code are the result of theoretical considerations and engineering experience. In some respects the deterioration models give valuable information. It is shown for instance that prolonging the service life of a structure from 50 to 100 years requires globally an increase of the concrete cover between 8 and 12 mm. The advised increase of 10mm is therefore a good average value, regarding the many unknown factors. Moreover, research is necessary to close the gap between scientific models and practical observations.

**See example n. 4.1, 4.2, 4.3, 4.4.**

#### **Reference**

- [1] DuraCrete – Probabilistic Performance Based Durability Design of Concrete Structures: Statistical Quantification of the Variables in the Limit State Functions. Report No.: BE 95-1347, pp. 62-63, 2000.
- [2] FIB Bulletin n. 34 Model Code for Service Life Design, June 2006, ISBN 978-2-88394-074-1

**SECTION 5 STRUCTURAL ANALYSIS**

**5.1 General**

**SECTION 5. STRUCTURAL ANALYSIS**

**C5.1 General**

Structural analysis is the process of determination of the effects of actions (forces, impressed strain) in terms of tensional states or strain on a geometrically and mechanically defined structure.

The analysis implies a preliminary idealisation of the structure, based on more or less refined assumptions of behaviour. There are four types of idealisations:

- linear elastic behaviour that assumes, for analysis, uncracked cross sections and perfect elasticity. The design procedures for linear analysis are given in [5.4-EC2];
- linear elastic behaviour with limited redistribution [5.5-EC2]. It is a design (not analysis) procedure based on mixed assumptions, derived from both the linear and non-linear analysis.
- plastic behaviour. Its kinematic approach [5.6-EC2], assumes at ultimate limit state the transformation of the structure in a mechanism through the formation of plastic hinges; in its static approach, the structure is represented by compressed and tensioned elements (strut and tie model);
- non linear behaviour, that takes into account, for increasing actions, cracking, plastification of reinforcement steel beyond yielding, and plasticization of compressed concrete. The design procedures for non-linear analysis are given in [5.7-EC2];

The rules in the EN are technically rather similar to those in the ENV. However, the discontinuities mentioned above have been removed, and the rules have been coordinated between EC2, EC3 and EC4, see 5.2.5. The EN rules are not repeated here.

**5.2 Geometric imperfections**

**C5.2. Geometric imperfection**

**5.2.1 Symbols**

Parameter	Symbol		Comment
	ENV	EN	
Basic value of inclination	$\nu$	$\theta$	$\nu$ is both Poisson's ratio and a reduction factor for the concrete compression strength; $\theta =$ angle in general, here with subscript $i$ for inclination
Mean value of inclination	$(\alpha_n \cdot ?) \nu$	$\theta_i \cdot \alpha_n \cdot \alpha_m$	it is not always clear whether $\nu$ is basic or reduced value; with the new symbols there should be no ambiguity
Number of members	$n$	$m$	$n$ is used in the EN for relative axial force (instead of $\nu$ ), therefore $m$ is used for number of <b>m</b> embers
Axial forces	$N_{bc}, N_{ba}$	$N_a, N_b$	axial forces <b>a</b> bove and <b>b</b> elow the floor considered
Horizontal force	$H_{fd}$	$H_i$	subscript <b>i</b> for <b>i</b> mperfection
Eccentricity	$e_a$	$e_i$	subscript <b>i</b> for <b>i</b> mperfection

**5.2.2 Imperfections and tolerances**

The minimum value of the basic inclination is now 1/300 instead of 1/200 and 1/400 (with and without 2<sup>nd</sup> order effects respectively). A good reason for having *one* value, independent of the importance of 2<sup>nd</sup> order effects, is to avoid the accumulation of discontinuities. The present value is also well correlated with the tolerances given for class 1 in EN 13670, see figure 1. An upper limit 1/200 for the basic value has also been added.

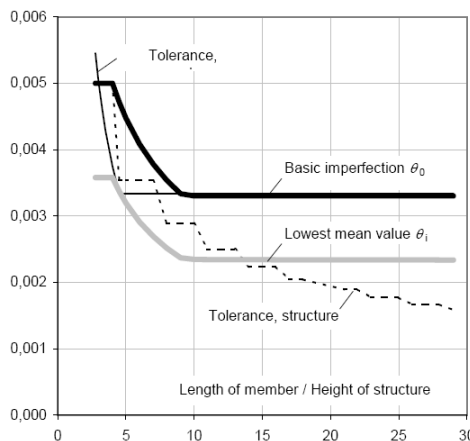


**Figure 5.1.** Comparison between imperfection and tolerances. The thick lines represent imperfections, the black line represents basic imperfection  $\theta_0$  according to expression 5.1 in EN1992-1-1, whereas the grey line represents the lower limit of the mean value  $\theta$  for a structure ( $m = \infty$ ).

The thin lines represent the tolerance according to EN13670; the solid line represents a member in one storey, the dashed line the total inclination of a structure.

For the total inclination of a column or wall in a structure, the tolerance continues to decrease below the minimum value 1/300 when the number of storeys exceeds 8. The mean value of the imperfection will also decrease in a structure where a number of individual members contribute to the total effect; the lower limit of the mean value (for  $m = \infty$ ) is shown in figure 5.1.

The fact that the mean imperfection  $\theta_i$  is sometimes less than the structural tolerance does not

mean that the imperfection is on the “unsafe side”. The tolerance has to be checked for *individual* columns and walls, whereas  $\alpha_{im}$  represents the *average inclination* of all vertical members contributing to a certain effect.

### 5.2.3 Equivalent eccentricity or horizontal force

For isolated members, like in the ENV, the inclination can be transformed to either an equivalent eccentricity (or initial deflection)  $e_i$  or a horizontal force  $H_i$ . This is important for e.g. a pin-ended column, where an inclination has no effect on the column itself. The eccentricity can then represent either an uncertainty in the position of the axial load, or an initial deflection (out-of-straightness). The equivalent eccentricity is linked to the effective length, and the horizontal force should give the same bending moment as the eccentricity (see figure 5.1 in EN chapter 5.2):

Equivalent eccentricity:  $e_i = \theta_i \cdot l_0/2$  ( $l_0$  is the effective length)

$$\text{Cantilever: } e_i = \theta_i \cdot l \quad M_i = N \cdot e_i = N \cdot \theta_i \cdot l = H_i \cdot l \rightarrow \quad H_i = \theta_i \cdot N$$

$$\text{Pin-ended: } e_i = \theta_i \cdot l/2 \quad M_i = N \cdot e_i = N \cdot \theta_i \cdot l/2 = H_i \cdot l/4 \rightarrow \quad H_i = 2\theta_i \cdot N$$

### 5.2.4 Dealing with first order effects

Imperfections can be treated as first order effects, or be added as separate safety elements without any physical meaning, “outside” the second order analysis. With a method like the “curvature method” (“model column” method in ENV), which gives a fixed second order moment independent of the first order moment, there is no difference between the two approaches. In other methods, however, the second order effects depend on the first order effects, and then it *does* make a difference whether imperfections are treated as first order effects, or added separately.

In 4.3.5.4 P(1) in the ENV, the imperfection is associated with “uncertainties in the prediction of second order effects”, which indicates that it is not regarded as a first order effect. The definition of the first order eccentricity in 4.3.5.6.2 further underlines this. On the other hand, formulations in 2.5.1.3 describe the imperfection rather as a first order effect. Thus, the ENV is ambiguous and unclear in this respect.

In the EN it is stated once and for all that imperfections are to be treated as *first order effects*; see the definition in 5.8.1. This corresponds to a physical interpretation of the imperfection as a deviation in the form of an inclination, an eccentricity or an initial deflection. This is logical, since there is a link between imperfections and tolerances. It is essential to have a clear definition in this respect for the overall analysis of structures, but also for isolated members, when other methods than the curvature method are used; see 5.8.6 and 5.8.7.

## 5.3 Idealisation of the structure

### 5.3.1 Structural models for overall analysis

## C5.3 Structural models

### C5.3.1 Classification of structural elements

For buildings, as a convention, the following provisions apply:

5. a beam is a linear element, for which the span is not less than 3 times the overall section depth. Otherwise it should be considered as a deep beam.
6. a slab is a bidimensional member for which the minimum panel dimension is not less than 5 times the overall slab thickness. Moreover: a slab subjected to dominantly uniformly distributed loads may be considered to be one-way spanning if either (Fig. 4.2):
  - it possesses two free (unsupported) and sensibly parallel edges, or
  - it is the central part of a sensibly rectangular slab supported on four edges with a ratio of the longer to shorter span greater than 2.
7. ribbed or waffle slabs need not be treated as discrete elements for the purposes of analysis, provided that the flange or structural topping and transverse ribs have sufficient torsional stiffness. This may be assumed provided that (Fig. 4.2):
  - the rib spacing does not exceed 1500 mm
  - the depth of the rib below the flange does not exceed 4 times its width
  - the depth of the flange is at least 1/10 of the clear distance between ribs or 50 mm, whichever is the greater
  - transverse ribs are provided at a clear spacing not exceeding 10 times the overall depth of the slab.

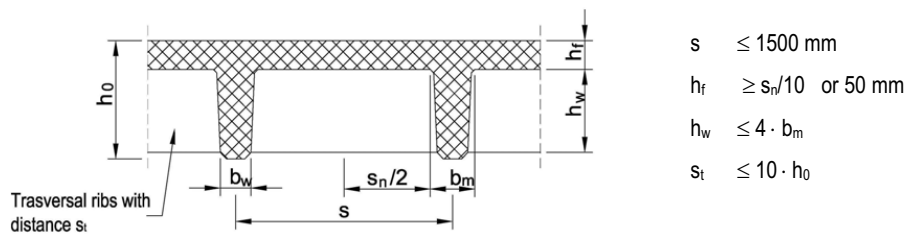


Figure 5.2. Geometric parameters for slabs

The minimum flange thickness of 50 mm may be reduced to 40 mm where permanent blocks are incorporated between the ribs. This exception applies for slabs with clay blocks only. It does not apply for expanded polystyrene blocks.

An exception to this rule is given at [10.9.3(11)-EC2] in relation to prefabricated slabs without topping, which may be analysed as solid slabs provided that the in situ transverse ribs are provided with continuous reinforcement through the precast longitudinal ribs and at a spacing according to Table [10.1) - EC2].

A column is a member for which the section depth does not exceed 4 times its width and the height is at least 3 times the section depth. Otherwise it should be considered as a wall.

**5.3.2 Geometric data**  
**5.3.2.1 Effective width of flanges (all limit states)**

**C5.3.2 Geometric data**

**C5.3.2.1 Effective width of flanges of T beams (valid for all limit states)**

If a T beam with a relatively wide flange is subjected to bending moment, the width of flange that effectively works with the rib in absorbing the compressive force (effective width) should be assessed.

An exact calculation shows that the actual distribution of compressive stresses has a higher concentration in the part of flange which is close to the rib, and a progressive reduction in the further parts. This implies that the conservation of plane sections is not respected and that the neutral axis is not rectilinear, but is higher on both sides of the rib.

In order to simplify calculations, the actual distribution of stresses is usually replaced by a conventional block, extended to the effective width. This allows the application of the usual design rules, and in particular the assumption that plane sections remain plane.

Effective width is defined at [5.3.2.1-EC2] as a function of the cross section geometry (b, distance between adjacent ribs; bw, width of ribs) and of the distance lo between points of zero moment. Note that the flange depth is not relevant, even if it is expressly cited in (1)P, and that the distance between points of zero moment depends, for continuous beams, on the type of loading Fig. 5.2-EC2 is an example of a continuous beam (subjected to a uniform load distribution) where the lo distance for spans and for parts on supports is identified.

Hence different sections have different effective width. Point (4) makes clear that a constant width may be assumed over the whole span. The value applicable to the span section should be adopted.

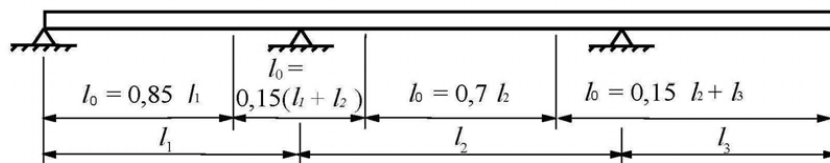


Figure 5.3. Definition of lo for calculation of the effective flange width [Fig. 5.2 – EC2].

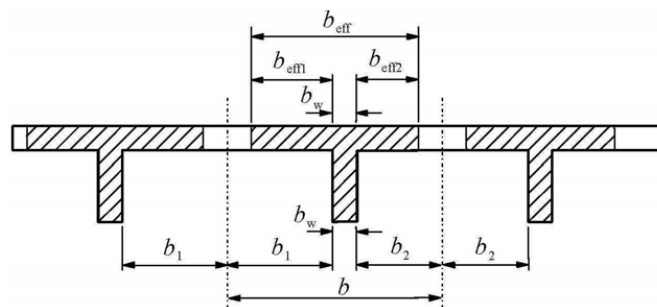


Figure 5.4. Parameters to determine effective flange width [fig. 5.3 – EC2]

### 5.3.2.2 Effective span of beams and slabs in buildings

#### C5.3.2.2 Effective span of beams and slabs in buildings

This paragraph defines the effective span length mainly for member analysis, taking into account the different types of support. Two important points must be noted:

- Where a beam or slab is monolithic with its supports, the critical design moment at the support may be taken as that at the face of the support. That moment should not be less than 65% that of the full fixed end moment.
- The design moment and reaction transferred to the supporting element should be taken as the greater of the elastic or redistributed values.
- Regardless of the method of analysis used, where a beam or slab is continuous over a support which may be considered to provide no restraint to rotation, the design support moment, calculated on the basis of a span equal to the centre-to-centre distance between supports, may be reduced by:

$$\Delta M_{Ed} = F_{Ed,sup} t / 8$$

where  $F_{Ed,sup}$  is the design support reaction  
 $t$  is the breadth of the support.

This formula derives by assuming an uniform distribution of the design support reaction  $F_{Ed,sup}$  over the breadth of the support

$$\Delta M_{Ed} = \left( \frac{F_{Ed,sup}}{t} \right) \cdot \frac{t}{2} \cdot \frac{t}{4} = \frac{F_{Ed,sup} \cdot t}{8}$$

### 5.4 Linear elastic analysis

#### C5.4 Linear elastic analysis

For the determination of load effects, linear analysis may be used assuming:

- uncracked cross sections,
- linear stress-strain relationships and
- mean value of the modulus of elasticity.

With these assumptions, stresses are proportional to loads and therefore the superposition principle applies. For thermal deformation, settlement and shrinkage effects at the ultimate limit state (ULS), a reduced stiffness corresponding to the cracked sections, neglecting tension stiffening but including the effects of creep, may be assumed in accordance with [5.4(3)-EC2]. For the serviceability limit state (SLS) a gradual evolution of cracking should be considered.

Comments.

- In the previous explanation the expression 'For the determination of load effects' was used, whereas [5.4(3)-EC2] admits "For the determination of *action* effects", therefore of all actions, including thermal deformation, settlement and shrinkage for which [5.4(3)-EC2] admits different assumptions, without which the effects of impressed deformations would be devastating and quantitatively incorrect.
- the fact that no limits were set to  $(x_u/d)$  for the application of the linear analysis method at the ultimate limit states, does not mean that any value of  $(x_u/d)$  may be used in design: it's opportune to observe a limit consistent with the method of linear elastic analysis with limited redistribution, for which  $x_u/d \leq 0,45$ . It must be remembered that increasing values of  $x_u/d$  the model uncertainty also increases and higher safety factors should be assumed for precaution.

### 5.5 Linear analysis with limited redistribution

#### C5.5 Linear elastic analysis with limited redistribution [5.5 - EC2]

At ultimate limit state plastic rotations occur at the most stressed sections. These rotations transfer to other zones the effect of further load increase, thus allowing to take, for the design of reinforcement, a reduced bending moment  $\delta M$ , smaller than the moment  $M$  resulting from elastic linear design, provided that in the other parts of the structure the corresponding variations of load effects (viz. shear), necessary to ensure equilibrium, are considered.

Despite being named "Linear analysis with limited redistribution", this is a design method.

In clause [5.5(4)-EC2], in relation with continuous beams and slabs with ratio between adjacent spans in the range [0,5 – 2] expressions are given for the redistribution factor  $\delta$  in function of the concrete class, the type of steel and the  $x_u/d$  ratio after redistribution. For instance, for concrete up to C50 and reinforcing steel of type B and C, respectively of average and high ductility, the expression is:

$$\delta \geq 0,44 + 1,25 (x_u/d) \quad ; \quad \delta \geq 0,70 \quad [5.10a - EC2] \quad (4.8)$$

where:

- $\delta$  is the ratio of the redistributed moment to the elastic bending moment
- $x_u$  is the depth of the neutral axis at the ultimate limit state after redistribution
- $d$  is the effective depth of the section



The limits of this formula are:

$$\delta = 0,70 \quad \text{per } (x_u/d) = 0,208 \quad \text{and}$$

$$\delta = 1 \quad \text{per } (x_u/d) = 0,45$$

It must be considered that a redistribution carried out in observance of the ductility rules only ensures equilibrium at the ultimate limit state. Specific verifications are needed for the serviceability limit states. Very high redistributions, which may be of advantage at the ultimate limit states, very often must be lowered in order to meet the requirements of serviceability limit states. For the design of columns the elastic moments from frame action should be used without any redistribution.

## 5.6 Plastic analysis

### C5.6 Plastic analysis

Plastic analysis should be based either on the lower bound (static) method or on the upper bound (kinematic) method for the check at ULS only.

#### 5.6.1 Static method

It is based on the static theorem of the theory of plasticity, which states: "whichever load  $Q$ , to which a statically admissible tension field corresponds, is lower or equal to the ultimate load  $Q_u$ ". The expression "statically admissible" indicates a field that meets both the conditions of equilibrium and the boundary condition without exceeding the plastic resistance.

An important application of this method is the strut-and-tie scheme [5.6.4 – EC2]. Other applications are the management of shear by the method of varying  $\theta$  and the analysis of slabs by the equivalent frame analysis method [Annex I – EC2].

#### 5.6.2 Kinematic method

In this method, the structure at ultimate limit states becomes a mechanism of rigid elements connected by yield hinges. The method is based on the kinematic theorem, which states: "every load  $Q$ , to which corresponds a kinematically admissible mechanism of collapse, is higher or equal to the ultimate load  $Q_u$ ".

The method is applied for continuous beams, frames and slabs (in this last case with the theory of yield lines).

For beams, clause [5.6.2)-EC2] states that the formation of plastic hinges is guaranteed provided that the following are fulfilled:

- i) the area of tensile reinforcement is limited such that, at any section
 
$$(x_u/d) \leq 0,25 \text{ for concrete strength classes } \leq C50/60$$

$$(x_u/d) \leq 0,15 \text{ for concrete strength classes } \geq C55/67$$
- ii) reinforcing steel is either Class B or C
- iii) the ratio of the moments at intermediate supports to the moments in the span shall be between 0,5 and 2.

If not all the conditions above are fulfilled, the rotation capacity must be verified, by checking the required rotations against those allowed in accordance with [Fig. 5.6N-EC2].

It should be remembered that the plastic analysis methods shall only be used for checking ultimate limit states. Serviceability limit states requirements should be checked by specific verifications.

## 5.7 Non-linear analysis

### C5.7 Non-linear analysis

Non-linear analysis is a procedure for calculation of action effects, based on idealisations of the non-linear behaviour of materials [non-linear constitutive laws: for concrete cf. Eurocode 2, 3.1.5(1) expression (3.14) and Fig. 3.2; for steel 3.2.7(1) Fig. 3.8], of the elements and of the structure (cracking, second order effects), suitable for the nature of the structure and for the ultimate limit state under consideration.

It requires that the section geometry and reinforcement are defined, because it is a process of analysis. Resulting stresses are not proportional to the applied actions.

The process is developed by computer-aided calculations, by verifying equilibrium and compatibility at every load increase. Compatibility conditions are normally expressed by assigning to each section its moment – curvature law, and integrating the curvatures along the axis of the elements. Inelastic rotations are generally concentrated in the critical sections. Deformations due to shear are generally neglected, those in relation with axial load are taken into account only in case have significant influence on the solution. As the superposition principle does not apply because of the non-linearity, the calculations must be developed for each load condition: for each one it is conventionally assumed that the ultimate limit state is reached through a single proportional increase of the applied load.

In the case of elements mainly subjected to bending, trilinear idealizations of the moment / rotations

law of each critical section can be adopted as in Fig. 4.6, representing the three following states:

- first state (elastic and linear): characterized by EI rigidity of the entirely reacting sections; it ends when the tensional strength of concrete is reached (cracking moment)
- second state (cracked): from the cracking moment to the moment corresponding to steel yielding, moment increases are related to the curvature increases on the basis of rigidity  $E_s A_s z(d-x)$ , where  $A_s$  is the cross section of the tensioned reinforcement,  $z$  the lever arm,  $x$  the depth of the neutral axis. The rigidity can be increased by taking into account the contribution of concrete in tension between cracks ("tension stiffening"), but with caution in case of load cycles .
- third state (plastic): a third linear line can be idealized from the steel yielding clause to the point of failure moment. The line corresponds to a  $\theta_{pl}$  plastic rotation at the critical section, with a value that can be deducted from the diagram in Fig 5.6N of Eurocode 2 in function of the relative depth of the neutral axis. Following the evolution of response to actions, it is possible to verify the conditions for the serviceability limit states and for the ultimate limit state.

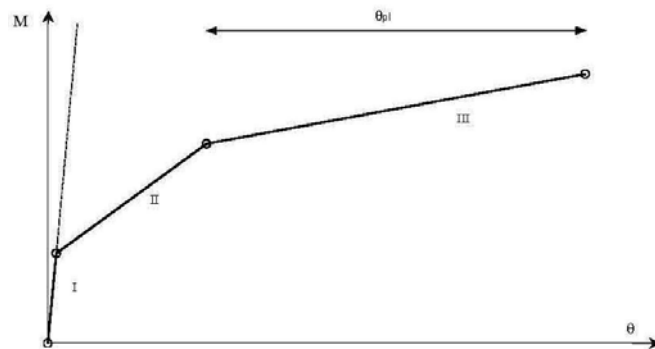


Figure 5.5. Trilinear Moment – Rotation relation for element mainly subjected to bending

**5.8 Analysis of second order effects with axial load**  
**5.8.1 Definitions**

**C5.8 Second order effects with axial load**

**C5.8.1. Definitions**

Definitions specific to chapter 5.8 are listed in 5.8.1. Some comments are given below.

**Braced – bracing**

The distinction *braced – bracing* is simple: units or systems that are assumed to contribute to the stabilization of the structure are *bracing elements*, the others are *braced*. Bracing units/systems should be designed so that they, all together, have the necessary stiffness and resistance to develop stabilization forces. The braced ones, by definition, do not need to resist such forces.

**Buckling**

The word buckling has been reserved for the "pure", hypothetical buckling of an initially straight member or structure, without load eccentricities or transverse loading. It is pointed out in a note that pure buckling is not a relevant limit state in real structures, due to the presence of imperfections, eccentricities and/or transverse loads. This is also a reason why the word "buckling" is avoided in the title of 5.8. In the text, buckling is mentioned only when a nominal buckling load is used as a parameter in certain calculation methods.

**First order effects**

First order effects are defined to include the effect of imperfections, interpreted as physical deviations in the form of inclinations or eccentricities. The ENV is ambiguous in this respect; see also clause C5.2.

**Nominal second order moment**

The nominal second order moment is used in certain simplified methods, to obtain a total moment used for design of cross sections to their ultimate moment resistance. It can be defined as the difference between the ultimate moment resistance and the first order moment, see 6.3. If the ultimate load is governed by instability before reaching the cross section resistance, then the nominal second order moment is greater than the true one; this is the reason for using the word "nominal".

**Sway – non-sway and global second order effects**

The terms sway – non-sway have been omitted in the final draft, after many comments for or against. The words in themselves are misleading, since all structures are more or less "sway"; a



structure that would be classified as “sway” could be just as stiff as one classified as “non-sway”. These terms are now replaced by *unbraced – braced*. In the ENV the concept of sway – non-sway was linked to the criterion for neglecting global second order effects in structures. The classification of structures from this point of view remains in the EN, but without using the “sway” - “non-sway” terminology. A stiffness criterion like the one in ENV-A.3.2 was avoided in earlier drafts of the EN, since it was considered as too crude, and in some cases misleading. However, during the conversion process there were many requests to include some simple criterion for evaluating the significance of global second order effects, without the need for calculating them. This led to the present rules in 5.8.3.3 and Informative Annex H, which are more general than those in ENV-A.3.2. The details are given in clause 3.3.

**5.8.2 General**

**C5.8.2. Basic criteria for neglecting second order effects**

Two basic criteria for ignoring second order effects have been discussed during the conversion process, namely:

- 1)  $\leq 10\%$  increase of the corresponding first order effect,
- 2)  $\leq 10\%$  reduction of the load capacity, assuming a constant eccentricity of the axial force.

The first criterion is the one stated in 5.8.2 (6), and in the ENV, 4.3.5.1 (5). The second one has been claimed by some to be the “true”, hidden criterion behind the ENV-rules.

Figure 5.6 illustrates the consequences of these two criteria in an interaction diagram for axial force and bending moment. Their effects on the slenderness limit are discussed in chapter 3.

In a column or a structure it is the *bending moment* that is influenced by second order effects. The axial force is governed by vertical loads, and is not significantly affected by second order effects. Most design methods are based on calculating a bending moment, including a second order moment if it is significant. From this point of view, criterion 1 is the most logical and natural one.

The basic criterion is further discussed in chapter 3 in connection with slenderness limits.

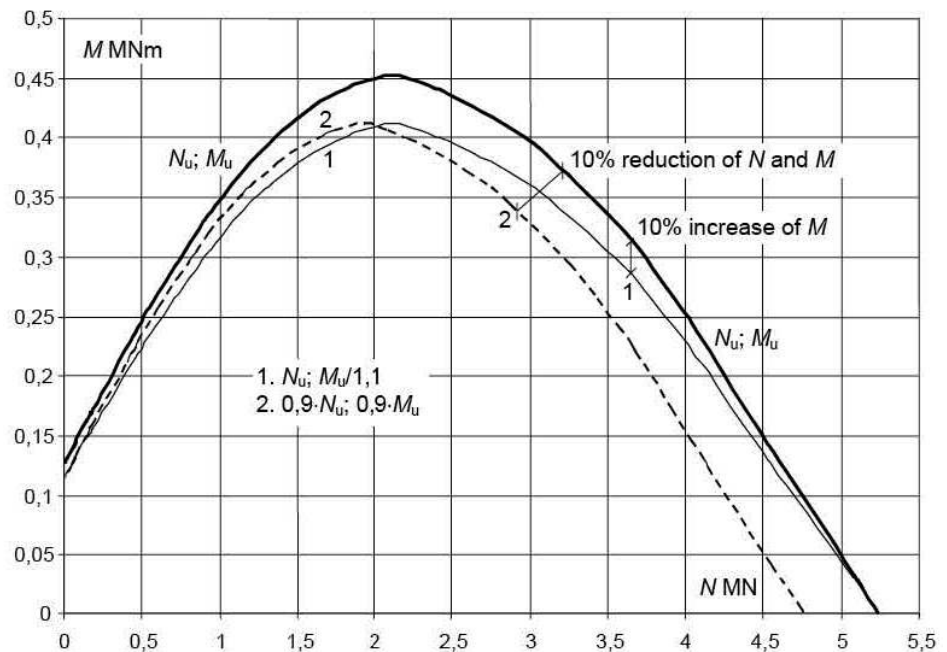


**Figure 5.6.** Two different ways of defining the basic 10%-criterion for ignoring second order effects, see text above. (The interaction diagram was calculated for rectangular cross section 400 x 600 mm, concrete C35,  $\omega = 0,1$  (total mechanical reinforcement ratio), edge distance of reinforcement 60 mm.)

**5.8.3 Simplified criteria for second order effects**  
**5.8.3.1 Slenderness criterion for isolated members**

**C5.8.3. Simplified criteria for ignoring 2nd order effects**

**C5.8.3.1 Slenderness limit for isolated members**  
**5.8.3.1.1 General**

The load bearing capacity of a member in compression for low slenderness ratios is illustrated in figure 3-1 by means of interaction curves, calculated according to the general method in 5.8.6.

(See chapter 6 in this report for more details about interaction curves and the general method.)

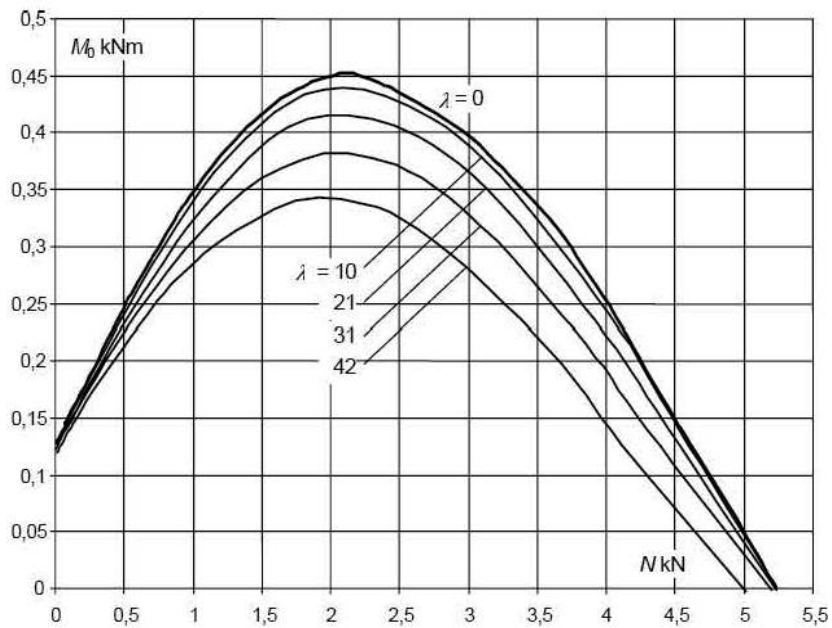


**Figure 5.7.** Interaction curves for low slenderness ratios, calculated for a pin-ended column with cross section as for figure 2-1 and subjected to a constant first order moment. Effective creep ratio  $\varphi_{ef} = 0$ . Equal first order end moments  $M_{01} = M_{02} = M_0$ .

By combining figures 5.7 and 5.6, one can find the slenderness ratios for which the basic 10%-criterion is fulfilled; see figure 5.8.

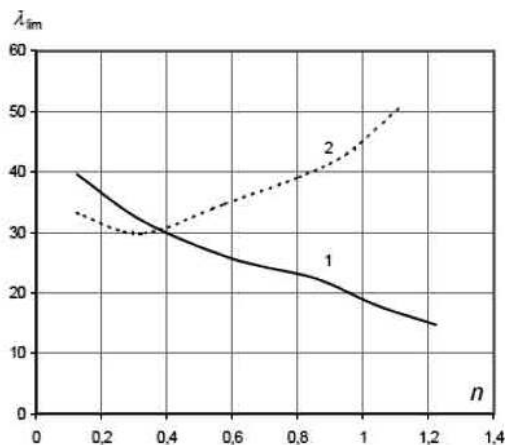


**Figure 5.8** Effect of normal force (here  $n = N/fcdAc$ ) on slenderness limit, depending on the interpretation of the 10 % criterion:

- 1.  $\leq 10\%$  increase of bending moments for a given normal force
  - 2.  $\leq 10\%$  reduction of load capacity for a constant eccentricity
- ( $\omega = 0,3, \varphi_{ef} = 0, M_{01}/M_{02} = 1$ )

Depending on which of the two basic criteria is chosen, see chapter 2, increasing the axial force will either decrease (1) or increase (2) the slenderness limit as shown in figure 3-2. Criterion 1 will be more severe for high axial loads, when there is little room for bending moments.

Criterion 2, on the other hand, will allow very high slenderness ratios for high axial loads.

In earlier drafts, including the October 2001 “final draft”, a slenderness limit independent of the axial force was chosen as a compromise between the two basic criteria; for  $\omega = 0,1$  the criterion was then identical to expression (4.62) in the ENV.

In a comment to the “final draft” it was pointed out that a limit independent of the axial force could be much on the unsafe side in certain cases (see next chapter). Therefore, a new model was developed. The following is quoted from 5.8.3.1:

- (1) As an alternative to 5.8.2 (6), second order effects may be ignored if the slenderness  $\lambda$  is below a certain value  $\lambda_{lim}$ . The following may be used:

$$\lambda_{lim} = 20 \cdot A \cdot B \cdot C \tag{5.13}$$

where:

$\lambda$  slenderness ratio as defined in 5.8.3.2

$$A = 1 / (1 + 0,2\varphi_{ef})$$

$$B = (1 + 2\omega) / n$$

$$C = 1,7 - r_m$$

$\varphi_{ef}$  effective creep ratio; see 5.8.4;

if  $\varphi_{ef}$  is not known,  $A = 0,7$  may be used

$\omega = A_s f_{yd} / (A_c f_{cd})$ ; mechanical reinforcement ratio; if  $\omega$  is not known,  $B = 1,2 / n$  may be used

$A_s$  total area of longitudinal reinforcement

$n = N_{Ed} / (A_c f_{cd})$ ; relative normal force

$r_m = M_{01} / M_{02}$ ; moment ratio

$M_{01}, M_{02}$  first order end moments,  $|M_{02}| \geq |M_{01}|$

- (2) If the end moments  $M_{01}$  and  $M_{02}$  give tension on the same side,  $r_m$  should be taken positive (i.e.  $C < 1,7$ ), otherwise negative (i.e.  $C > 1,7$ ).

In the following cases,  $r_m$  should be taken as 1,0 (i.e.  $C = 0,7$ ):

- for braced members with first order moments only or predominantly due to imperfections or transverse loading
- for unbraced members in general

The background to the new criteria is presented in the following.

### 5.8.3.1.2 History of the slenderness limit in prEN 1992

At an early stage of the conversion process (spring 1999), a slenderness limit was proposed in which the effective creep ratio  $\varphi_{ef}$  and the relative normal force  $n$  were included as parameters.

The reinforcement ratio was not included then, since it was considered impractical.

Most people also considered it impractical and unnecessary to include creep; there was a widespread opinion that creep would have little effect at these low slenderness ratios.

There was also a lot of discussion about the interpretation of the basic 10% criterion for ignoring second order effects, with the two main alternatives (see chapter 2):

1.  $\leq 10\%$  increase of bending moments due to second order effects
2.  $\leq 10\%$  reduction of the load capacity for a given eccentricity

It was then demonstrated that the effect of the normal force on the slenderness limit was different depending on which alternative was used, see figure 5.8.

However, there was no agreement as to which alternative to base the slenderness limit on, and therefore the ENV criterion (4.62), independent of the normal force, was used in draft 1.

An addition was made in draft 2, allowing the constant 25 to be increased to 35 if the reinforcement ratio  $\omega$  is at least 0,5. In the "final" draft October 2001 an interpolation was introduced to avoid discontinuity (expression (5.13)).

In November 2001, shortly after the draft had been distributed, comments and examples were presented by Prof. J. Hellesland, showing that (5.13) might be extremely unsafe in some cases, e.g. a column bent in double curvature (end moments of different directions, figure 5.9), combined with a high effect of creep and a moderate or high normal force.

Comments on earlier versions of prEN 1992-1-1, together with a general treatment of the slenderness limit, are given in [8].

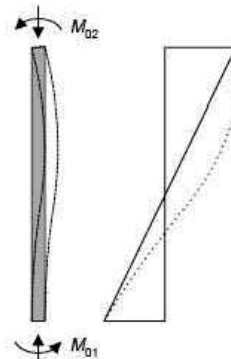


Figure 5.9. Column bent in double curvature

### 5.8.3.1.3 Background to the new proposal

After receiving the above-mentioned comments and examples from Prof Hellesland, a systematic investigation of the slenderness limit was made, with focus on the effects of *reinforcement, normal force, creep and moment ratio* (different end moments).

Figure 5.10 shows examples of the effect of a rather moderate effective creep ratio,  $\varphi_{ef} = 1$ .

Curves according to both basic 10% criteria are shown. Table 5.1 shows some values taken from the figures.

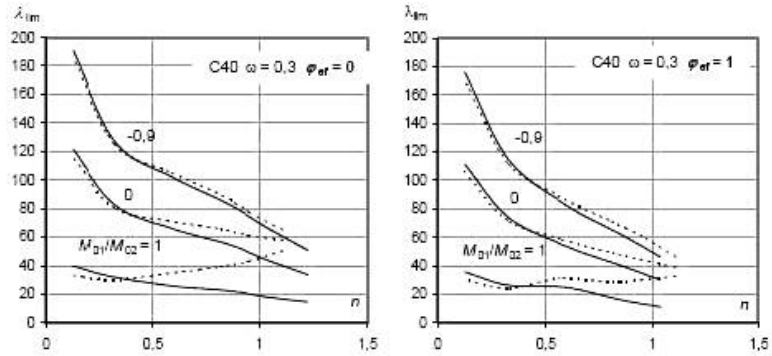


Figure 5.10. Slenderness limit as a function of the relative normal force and the moment distribution. Concrete C40,  $\omega = 0,3$ . (Solid lines = 10%-criterion alt. 1, dashed = alt. 2.)

Table 5.1. Values of slenderness limit taken from figure 5.10, alternative 1 ( $\omega = 0,3$ ).

n	M <sub>01</sub> /M <sub>02</sub>	λ <sub>lim</sub>		Average reduction due to creep, %
		φ <sub>ef</sub> = 0	φ <sub>ef</sub> = 1	
0,5	1,0	30	25	16
	0	70	60	
	-0,9	110	90	
1,0	1,0	20	10	37
	0	45	30	
	-0,9	70	50	

For  $n = 1,0$ , the average reduction due to creep is considerable, having in mind that  $\phi_{ef} = 1$  represents a rather moderate effect of creep. With a higher value of  $\phi_{ef}$  the reduction is more severe (most of the comparisons were made with  $\phi_{ef} = 0$  and 2 respectively, see Appendix 1).

The effect of  $\omega$  is considerable, as can be seen from both figure 5.11 and table 5.2. Without  $\omega$  as a parameter, the slenderness limit would have to be either very conservative for high to moderate values of  $\omega$ , or on the unsafe side for low values. However, since the reinforcement is normally not known when the slenderness criterion is checked, a default value based on a low value of  $\omega$  has also been given. This can be used for a conservative estimation, or as a starting value in an iterative process.

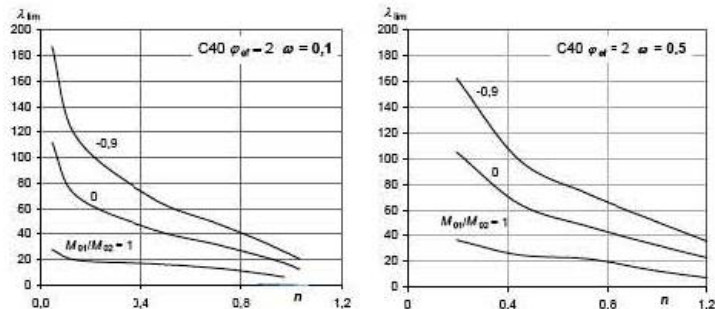


Figure 5.11. Effect of reinforcement ratio on slenderness limit (only criterion 1 is shown here).

Table 5.2. Values of slenderness limit taken from figure 5.11. ( $\phi_{ef} = 2$ )

n	M <sub>01</sub> /M <sub>02</sub>	λ <sub>lim</sub>		Average increase from $\omega = 0,1$ to $\omega = 0,5$ %
		ω = 0,1	ω = 0,5	
0,4	1,0	17	27	16
	0	47	70	
	-0,9	74	107	
0,8	1,0	11	20	37
	0	27	43	
	-0,9	41	66	

There have been national comments proposing to include the effect of  $n$  in the slenderness limit. These proposals were rejected until and including the October 2001 draft, referring to figure 5.8 and the disagreement concerning the 10%-criterion. However, as can be seen from figures 5.10 and 5.11, with different end moments there is a strong reduction of the slenderness limit with increasing normal force, and that is true for both 10%-criteria. The only exception is when criterion 2 is applied to columns with equal end moments, see figure 5.10.

**5.8.3.1.4 Comparisons with previous model for slenderness limit**

In tables 5.3 and 5.4, values from tables 5.1 and 5.2 are compared with values according to the slenderness criterion in the October 2001 draft (expression 5.13):

$$\lambda_{lim} = 25 \cdot (\omega + 0,9) \cdot (2 - M_{01}/M_{02})$$

In both cases the 10 % criterion is according to alternative 1.

**Table 5.3. Slenderness limit in draft Oct. 2001 compared to values from table 5.1 ( $\omega = 0,3$ )**

n	M <sub>01</sub> /M <sub>02</sub>	$\lambda_{lim}$		Draft Oct. 2001
		10% criterion (alt.1)		
		$\varphi_{ef} = 0$	$\varphi_{ef} = 1$	
0,4	1,0	30	25	30
	0	70	60	60
	-0,9	110	90	87
0,8	1,0	20	10	30
	0	45	30	60
	-0,9	70	50	87

For  $n = 0,5$  and  $\varphi_{ef} = 0$  the values according to draft October 2001 are reasonable (table 5.3).

For  $n = 1,0$ , however, they overestimate the slenderness limit, particularly for  $\varphi_{ef} = 1$  and most particularly for  $M_{01}/M_{02} = 1$ , where it gives a 3 times too high value.

**Table 5.4. Slenderness limit in draft Oct. 2001 compared to values from table 5.2 ( $\varphi_{ef} = 2$ )**

n	M <sub>01</sub> /M <sub>02</sub>	$\lambda_{lim}$		Average increase from $\omega = 0,1$ to $\omega = 0,5$ %
		$\omega = 0,1$	$\omega = 0,5$	
		0,4	1,0	
0	47		70	
-0,9	74		107	
0,8	1,0	11	20	37
	0	27	43	
	-0,9	41	66	

Draft October 2001 gives a fairly correct influence for  $\omega$ , but it severely overestimates the slenderness limit for a high normal force combined with a high creep effect, see table 5.4 (here the values are based on  $\varphi_{ef} = 2$ ). The omission of the effects of both normal force and creep are the main disadvantages of this model.

**5.8.3.1.5 Comparisons with new model**

In tables 5.5 and 5.6 the new model (see p. 4) is compared to the same data as in tables 5.1 and 5.2 respectively.

**Table 5.5. Slenderness limit according to new model compared with table 3-1 ( $\omega = 0,3$ )**

n	M <sub>01</sub> /M <sub>02</sub>	$\lambda_{lim}$			
		$\varphi_{ef} = 0$		$\varphi_{ef} = 1$	
		10%-criterion	New model	10%-criterion	New model
0,5	1,0	30	26	25	21
	0	70	63	60	52
	-0,9	110	96	90	80
1,0	1,0	20	18	10	15
	0	45	44	30	37
	-0,9	70	68	50	56

**Table 5.6. Slenderness limit according to new model compared with table 5.2 ( $\varphi_{ef} = 2$ )**

n	M <sub>01</sub> /M <sub>02</sub>	$\lambda_{lim}$			
		$\omega = 0,1$		$\omega = 0,5$	
		10%-criterion	New model	10%-criterion	New model
0,4	1,0	17	17	27	24
	0	47	42	70	58
	-0,9	74	65	107	88
0,8	1,0	11	12	20	17
	0	27	30	43	41
	-0,9	41	46	66	62

**5.8.3.1.6 Discussion**

On the whole, the new model gives good agreement with the 10%-criterion (alt. 1), and the main parameters are taken well into account. There is a slight overestimation of the slenderness limit for  $n = 1,0$  and  $\varphi_{ef} = 1$ , table 5.5, also for  $\omega = 0,1$  and  $n = 0,8$ , table 5.6. However, the overestimations are small compared to the old model (see 3.1.4) and in both cases the values are conservative compared to 10%-criterion alt. 2.

A complete verification of the new model is given in Appendix 1. A more sophisticated model could of course give even better agreement, e.g. by also including the concrete grade, but the present model is considered to be good enough. Concrete grade is indirectly taken into account in the  $n$  value.

The importance of considering creep in the slenderness limit is further substantiated in 4.3.3.

**5.8.3.2 Slenderness and effective length of isolated members**

**C5.8.3.2 Effective length**

New expressions (5.15) and (5.16) for the effective length of isolated members in frames, were introduced in the second draft. Derived to give accurate estimation, based on the definition of effective length in 5.8.1, they replace figure 4.27 in the ENV as well as expressions (5.22) and (5.23) in draft 1 of the prEN, December 1999.

The expressions in draft 1 were taken from UK proposals, included in comments on the ENV and on earlier EN drafts. It was found that they are very conservative in some cases, giving up to 40 % overestimation of the effective length for braced members and on the unsafe side in other cases, giving up to 20 % underestimation of the effective length for unbraced members.

It has been claimed that the conservativeness was deliberate, in order to cover certain unfavourable non-linear effects. However, the effective length is by definition based on linear behaviour, and the present models are aimed at giving an accurate estimation according to this, without including some hidden allowance for possible unfavourable effects. Such effects are instead explicitly addressed in 5.8.3.2 (5) and in 5.8.7.2 (4). The new expressions also avoid unsafe estimations, as in the case of unbraced members with the previous expressions.

Figure 5.12a and b show comparison between an accurate numerical calculation of the effective length and estimations according to draft 1 (a) and final draft (b) respectively.

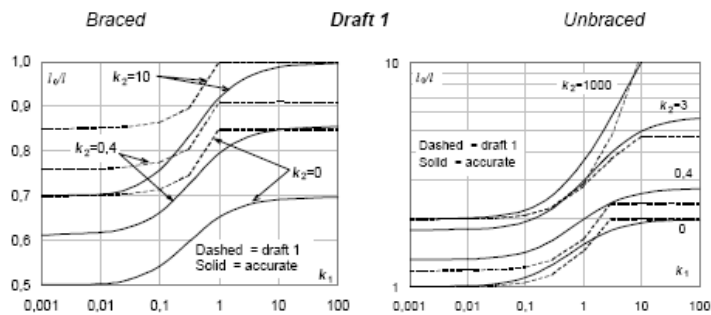


Figure 5.12a. Effective length according to accurate and simplified calculations, draft 1

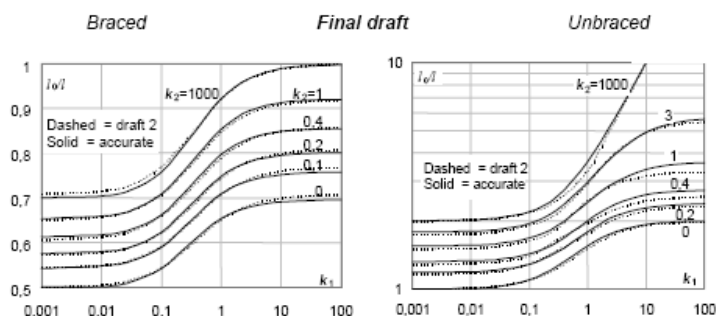
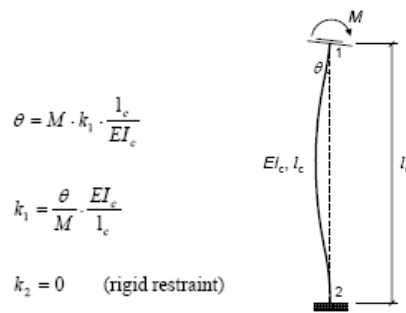


Figure 5.12b. Effective length according to accurate and simplified calculations, final version

The present  $k$ -factors are defined differently compared to the corresponding factors in draft 1 and ENV, and are called  $k_1$  and  $k_2$  to avoid confusion with the previous factors  $k_a$  and  $k_b$ . The present  $k$ -factors express the relative flexibility of the restraint according to the definitions in figures 5.13 and 5.14. They are applicable to different types of flexible moment restraint, such as beams with different boundary conditions, flexible foundations etc.



$$\theta = M \cdot k_1 \cdot \frac{l_c}{EI_c}$$

$$k_1 = \frac{\theta}{M} \cdot \frac{EI_c}{l_c}$$

$$k_2 = 0 \quad (\text{rigid restraint})$$

Figure 5.13. Flexibility of restraint, example of definition.

	Draft 1 (and ENV)	Final draft
	$k_a = \frac{EI_c/l_c}{EI_b/l_b}$ $k_b = 0$	$k_1 = \frac{EI_c/l_c}{4EI_b/l_b}$ $k_2 = 0$
	$k_a = \frac{EI_c/l_c}{EI_b/l_b}$ $k_b = \infty$	$k_1 = \frac{EI_c/l_c}{3EI_b/l_b}$ $k_2 = \infty$

Figure 5.14. Comparison between different definitions of k-factors; examples.

5.8.3.2 (4) addresses the question whether an adjacent column (in a storey above or below) in a node should be considered as *using* the same restraint as the column considered, or as *contributing* to the restraint. This will depend on the magnitude of the axial force in the adjacent column. If both columns connected to the node reach their respective buckling load at the same time (under proportional increase of loads), they will both have to *share* the restraint provided by other connected members (beams), and *k* should then be defined as

$$k = \frac{\theta}{M} \cdot \left[ \frac{EI_a}{l_a} + \frac{EI_c}{l_c} \right] \tag{3-1}$$

Here subscripts *a* and *c* refer respectively to the adjacent column and to the one considered see Figure 5.15.

In the opposite case, when the adjacent column has a relatively low axial load, it can be included among the members which *resist* the moment *M*, i.e. it will *contribute* to the restraint.

A reasonable model for the transition between the two limiting cases gives by the following:

$$k = \frac{\theta}{M_1 + M_2 + \dots + (1 - \alpha)M_a} \cdot \left( \alpha \frac{EI_a}{l_a} + \frac{EI_c}{l_c} \right) \tag{3-2}$$

where  $M_1, M_2, \dots$  restraining moments in members 1, 2, ..., see Figure 5.15

$M_a$  restraining moment in the adjacent column, see Figure 5.15, calculated without taking into account the axial force  $N_a$

$\alpha = N_a/N_{Ba}$

$N_a$  axial force on the adjacent column

$N_{Ba}$  buckling load of the adjacent column (can be estimated approximately, e.g. taking into account only the horizontal members adjacent to its nodes)



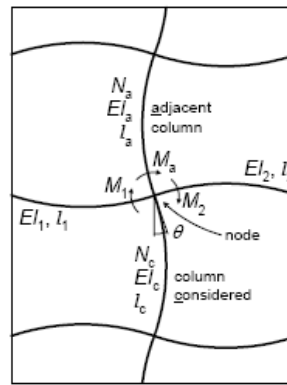


Figure 5.15. Illustration of node with adjacent members.

**5.8.3.3 Global second order effects in buildings**

**C5.8.3.3 Global second order effects in structures**

**5.8.3.3.1 Background**

**a) Model in ENV, A.3.2**

According to the ENV, global second order effects may be ignored, and the structure may be considered as “non-sway”, if

$$L = \sqrt{F_V / E_{cm} I_c} \leq \alpha \tag{3-3}$$

- Where
- $L$  total height of building ( $h_{tot}$  in the ENV)
  - $F_V$  total vertical load ( $F_V$  in the ENV)
  - $E_{cm} I_c$  sum of bending stiffnesses of bracing members
  - $\alpha$   $0,2 + 0,1n_s \leq 0,6$  (in the ENV, no particular symbol is used for this parameter)
  - $n_s$  number of storeys ( $n$  in the ENV)

This criterion is valid only on certain conditions (not stated in the ENV):

1. No significant rotation at the base (rigid restraint / stiff foundation)
2. No significant global shear deformations (e.g. no significant openings in shear walls)

These conditions are not fulfilled for e.g. a bracing system including frames, shear walls with large openings and/or flexible foundations.

The criterion also explicitly requires that bracing members are *uncracked*. In practice, bracing members are often more or less cracked in ULS, due to high lateral and low vertical loadings (most of the vertical load is often carried by the *braced* members).

For the above reasons, ENV A.3.2 has a very limited field of application. Since the limitations of the applicability are not stated, and no information is given for the cracked stage, there is a also risk that it is used outside the scope, giving unsafe results.

**b) New proposals**

Due to the above shortcomings, the ENV criterion was not included in earlier drafts of the EN. After many requests to include something similar, two alternative proposals were presented to CEN TC250/SC2 (Berlin, May 2000), a “mini-version” and a “full version”:

- **“Mini-version”**: same scope as in ENV-A.3.2, and a criterion given in a similar closed form. However, the conditions and restrictions are clearly stated, and the criterion is improved to be less conservative and to take into account cracking in a simple way.
- **“Full version”**: formulated in a more general and transparent way. Detailed information is given only for regular cases, but the formulation opens for general cases. A simple extension is given to cover the effect of global shear deformations.

In the final draft a somewhat extended “mini-version” is given in the main text, and further extension to the “full version” are given in Annex H.

**5.8.3.3.2 No significant shear deformations, rigid moment restraint**

The basic criterion “second order effects  $\leq 10\%$  of first order effects” gives, together with the simplified magnification factor for bending moment in 5.8.7.3 (3):

$$M_{Ed} \approx \frac{M_{0Ed}}{1 - F_{V,Ed} / F_{V,BB}} \leq 1,1 \cdot M_{0Ed} \tag{3-4}$$

This gives the following criterion for the vertical load, cf. expression (H.1):

$$F_{V,Ed} \leq F_{V,BB} \cdot 0,1 / 1,1 \approx 0,1 F_{V,BB} \tag{3-5}$$

Here  $F_{V,Ed}$  total vertical load



- $F_{V,BB}$  nominal buckling load for global bending (no shear deformations)
- $M_{0Ed}$  first order moment
- $M_{Ed}$  design moment

The global buckling load for bending can be written

$$F_{V,BB} = \xi_0 \cdot \frac{\sum EI}{L^2} \tag{3-6}$$

- where  $\xi_0$  coefficient depending on number of storeys, distribution of vertical load etc.
- $\sum EI$  total bending stiffness of bracing members; to account for cracking in a simplified way  $\sum EI$  is based on  $0,4 \cdot E_{cd} I_c$ ; and for uncracked section 0,8 may be used instead of 0,4
- $L$  total height

Note  $F_{V,BB}$  is a *nominal* buckling load, calculated for a secant stiffness representing the relevant ULS conditions (including lateral loading). It is not a load for which "pure" buckling (without eccentricities or lateral loading) would occur.

The coefficient 0,4 (or 0,8) for estimating the stiffness (see H.1.2 (3)) can be compared to  $0,3/(1+\varphi_{ef})$  in expression (5.26). Expression (5.26) is valid for *isolated members*, where all the vertical load considered acts on the member itself. Then there effects not only of cracking, but also of non-linearity in compression are considered. The last effect can be strong, particularly in cases where the section is uncracked, usually associated with high vertical load. For the same reason, a higher stiffness value for uncracked section is *not* given in 5.8.7.2. In a structure, on the other hand, most of the vertical load is normally on the *braced* units, which means that there is less effect of compression non-linearity on the *bracing* units, in which case a particular value for uncracked section (0,8) is justified<sup>1</sup>. A further difference is that the bending moment normally has a more favourable distribution in a bracing unit than in isolated members, which gives less overall effect of cracking. These circumstances together justify the use of 0,4/0,8 instead of  $0,3/(1+\varphi_{ef})$ . Creep is not included in the criterion for neglecting second order effects in structures (as it is for isolated members). The reason is that for global second order effects in structures, the dominating first order effect is wind. In this circumstance, there is little effect of creep, and consequently, the effective creep ratio according to 5.8.4 will be low.

The coefficient  $\xi_0$  in expression (3-6) depends on various parameters. For constant stiffness, equal load increment per storey and rigid moment restraint at the base,  $\xi_0$  will depend on the number of storeys and (to some extent) on the distribution of vertical load between braced and bracing members according to Figure 5.16 (the buckling load has been calculated numerically by Vianello's method, and  $\xi_0$  has then been evaluated according to expression (3-6)).

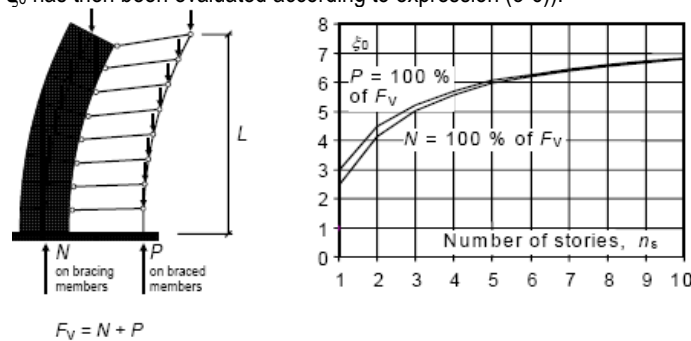


**Figure 5.16.** Global buckling due to bending and coefficient for buckling load. Constant stiffness and equal increment of vertical load per storey.

The coefficient  $\xi_0$  according to the upper curve in Figure 5.16 can be approximated by

$$\xi_0 \approx 7,8 \cdot \frac{n_s}{n_s + 1,6}$$

where  $n_s$  = number of storeys

Combining expressions (3-4) to (3-6) gives

$$F_V \leq 0,1 \cdot \xi_0 \cdot \frac{0,4 \cdot E_{cd} \cdot I_c}{L^2} = 0,312 \cdot \frac{n_s}{n_s + 1,6} \cdot \frac{E_{cd} \cdot I_c}{L^2} = \beta \cdot \frac{E_{cd} \cdot I_c}{L^2} \tag{3-8}$$

where  $0,312 = 7,8 \cdot 0,1 \cdot 0,4$  and  $\beta = 0,312 \cdot n_s / (n_s + 1,6)$

<sup>1</sup>The ratio 0,5 between the stiffnesses for cracked and uncracked sections is of course a rough simplification. The ratio should depend on the reinforcement and the normal force, and with a normal force there is a more or less smooth transition between the two stages. However, since this is about cases where second order effects are more or less negligible, a simple rule is acceptable.

This is the background to expression (5.18). Compare the ENV formulation (see 3.3.1 above):

$$L = \sqrt{F_V / E_{cm} I_c} \leq \alpha \tag{3-10}$$

Expression (5.18) can be formulated in the same way (substituting  $E_{cd}$  with  $E_{cm}$  and explicitly including partial factor  $\gamma_{cE} = 1,2$  on the right hand side):

$$L = \sqrt{F_V / E_{cm} I_c} \leq \sqrt{\beta / 1,2} \tag{3-11}$$

In Figure 5.17 the two corresponding parameters  $\beta/1,2$  (EN) and  $\alpha^2$  (ENV) are compared.

For the EN, curves for both cracked and uncracked sections are shown. The ENV gives no values for cracked section, therefore there is no comparison for this case.

The comparison shows that for uncracked section, the two models give rather similar results, although the ENV is often much more conservative.

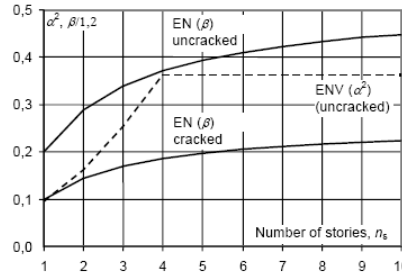


Figure 5.17. Comparison between EN and ENV criteria

**5.8.3.3 Effect of flexible moment restraint**

Flexible moment restraint at the base will reduce the buckling load. This effect can be directly included in the  $\xi$ -factor for the buckling load. (For isolated members this effect is normally taken into account by increasing the effective length. In the global analysis of structures, however, a direct reduction of the buckling load is more convenient, since the effective length is not a practical parameter for bracing members and systems having varying axial load).

For bracing units with two or more storeys, reasonably equal increment of the vertical load per storey and constant cross section, the isolated effect of flexible end restraint can be accurately modelled by the factor

$$\xi_1 \approx \frac{1}{1 + 0,7k} \tag{3-12}$$

where  $k = \frac{\theta/M}{L/EI}$  (same definition as for isolated members, see 3.2)

$\theta$  = rotation for bending moment M (compare figure 5.13)

The factor  $\xi_1$  is an approximation, which has been derived by calibration against accurate numerical calculation for different numbers of storeys, see figure 5.18. The product  $\xi_0 \xi_1$  corresponds to  $\xi$  in expression (H.2) in EN annex H.

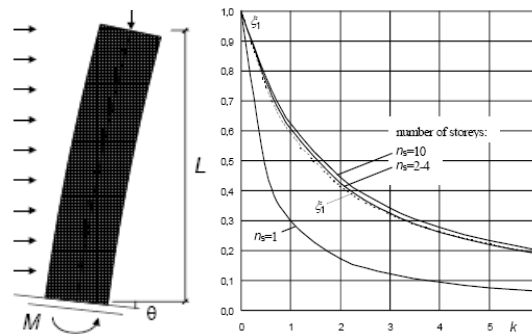


Figure 5.18. Effect of flexibility of end restraint for bracing units. Solid curves represent the "exact" solution, dashed curve the approximation according to expression (3-12)

The effect of flexible moment restraint is not covered in the ENV, therefore no comparison can be made.

**Effect of global shear deformations**

a) Shear deformations only (see Figure 5.19):

The (hypothetical) buckling load for shear deformations only is:

$$F_{V,BS} = S \text{ (or } \Sigma S \text{ for more than one bracing unit)} \tag{3-13}$$

Here S is the shear stiffness (= shear force giving a shear angle = 1; see figure H-1 in the EN).

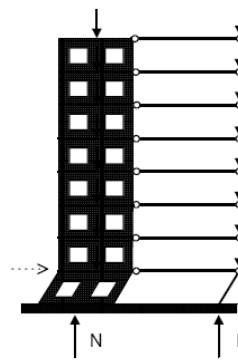


Figure 5.19. Hypothetical buckling due to global shear deformations only

b) Combined bending and shear:

The combined buckling load, taking into account bending *and* shear deformations, can be expressed as

$$F_{VB} \approx \frac{1}{1/F_{V,BB} + 1/F_{V,BS}} = \frac{F_{V,BB}}{1 + F_{V,BB}/F_{V,BS}} = \frac{F_{V,BB}}{1 + F_{V,BB}/\sum S} \tag{3-14}$$

Expression (3-14) can be derived analytically for simple cases like isolated members with constant normal force. By numerical calculations, it can be verified also for bracing units with vertically increasing axial load and significant global shear deformations (e.g. shear walls with large openings).

The basic criterion for neglecting second order effects is the same as before:

$$F_V \leq 0,1 \cdot F_{V,B} \tag{3-15}$$

which leads to expression (H.6) in Annex H.

This case is not covered in the ENV, therefore no comparison can be made.

5.8.4 Creep

C5.8.4. Effective creep ratio

5.8.4.1 General

The ENV stated *that* creep should be considered in connection with second order effects, but gave no information on *how*. In the EN, on the other hand, practical models for taking into account creep are given, based on the so called “effective creep ratio”.

A general approach would be to first calculate creep deformations under long-term load, then to analyse the structure for the additional load up to design load. With the effective creep ratio, the analysis can instead be made directly for the design load in one step.

Figure 5.20 illustrates a hypothetical load history and the corresponding deformations. The total load is assumed to consist of one Long-term part  $Q_L$  (corresponding to the quasi-permanent combination) and one additional short-term part up to the Design load  $Q_D$ , applied after a “long time”.<sup>2</sup> The total load history can then be divided into three parts:

1. AB - long-term load  $Q_L$  giving an elastic deformation
2. BC - constant load  $Q_L$  giving a creep deformation based on full creep coefficient  $\varphi$
3. CD - additional load ( $Q_D - Q_L$ ) giving an additional elastic deformation

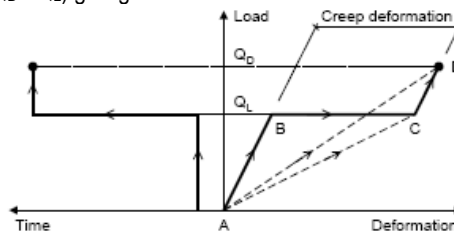


Figure 5.20. Illustration of load history and deformations

The *total deformation under long-term load* can also be calculated directly using an equivalent E-modulus<sup>3</sup> for the concrete,  $E_e = E_c/(1+\varphi)$ . This corresponds to line AC in figure 5.20.<sup>4</sup>

The *total deformation under design load* can be calculated in a similar way if an *effective creep ratio*  $\varphi_{ef}$  is used, line AD in figure 5.20. The “effective equivalent concrete modulus” would then be  $E_{ef} = E_c/(1 + \varphi_{ef})$  where  $\varphi_{ef}$  is the effective creep ratio.

5.8.4.2 Effect of creep in cross sections

In the following, three examples are used to derive and illustrate the effective creep ratio  $\varphi_{ef}$ . The examples deal with bending moment and curvature in the following cases, assuming linear elastic material behaviour:

- a) uncracked unreinforced cross section (5.8.4.2.1)
- b) uncracked reinforced section (5.8.4.2.2)
- c) cracked reinforced section (5.8.4.2.3)

#### 5.8.4.2.1 Uncracked unreinforced cross section

This is the simplest case for demonstrating the idea behind the effective creep ratio. The total curvature under a long-term bending moment  $M_L$  is (cf. line AC in figure 5.20):

$$\left(\frac{1}{r}\right)_L = \frac{M_L}{E_c I_c} (1 + \varphi) \quad (4-1)$$

The part caused by creep can be separated:

$$\left(\frac{1}{r}\right)_C = \varphi \frac{M_L}{E_c I_c} \quad (4-2)$$

Under design load with total bending moment  $M_D$ , part of which is a long-term moment  $M_L$  with a load history according to figure 5.20, the total curvature will be

$$\left(\frac{1}{r}\right)_D = \frac{M_D}{E_c I_c} + \left(\frac{1}{r}\right)_C = \frac{M_D}{E_c I_c} + \varphi \frac{M_L}{E_c I_c} = \frac{M_D}{E_c I_c} \left(1 + \varphi \frac{M_L}{M_D}\right) = \frac{M_D}{E_c I_c} (1 + \varphi_{ef}) \quad (4-3)$$

Thus, the effective creep ratio is (cf. expression (5.19), with different notation):

$$\varphi_{ef} = \varphi \frac{M_L}{M_D} \quad (4-4)$$

#### 5.8.4.2.2 Uncracked reinforced cross section

The total curvature under long-term bending moment  $M_L$  can be expressed in the following simplified way, using an equivalent E-modulus for concrete (see second footnote in 5.20):

$$\left(\frac{1}{r}\right)_L = \frac{M_L}{EI} = \frac{M_L}{\frac{E_c I_c}{1 + \varphi} + E_s I_s} \quad (4-5)$$

The part of this curvature caused by creep can be separated:

$$\left(\frac{1}{r}\right)_C = \frac{M_L}{EI} - \frac{M_L}{E_c I_c + E_s I_s} \quad (4-6)$$

Introducing the following parameters:

$$\beta = \alpha \rho (i_s/i_c)^2$$

$$\alpha \rho = (E_s/E_c)(A_s/A_c)$$

$i_c$  = radius of gyration of concrete area

$i_s$  = radius of gyration of reinforcement area

curvatures can be expressed in the following way:

$$\left(\frac{1}{r}\right)_L = \frac{M_L}{E_c I_c} \cdot \frac{1 + \varphi}{1 + (1 + \varphi)\beta} \quad (4-7)$$

$$\left(\frac{1}{r}\right)_C = \frac{M_L}{E_c I_c} \cdot \left( \frac{1 + \varphi}{1 + (1 + \varphi)\beta} - \frac{1}{1 + \beta} \right) \quad (4-8)$$

Under design load and total bending moment  $M_D$  the total curvature will be, including creep due to a long-term bending moment  $M_L$ :

$$\left(\frac{1}{r}\right)_D = \frac{M_D}{E_c I_c} \cdot \frac{1}{1 + \beta} + \left(\frac{1}{r}\right)_C = \frac{M_D}{E_c I_c} \cdot \frac{1}{1 + \beta} + \frac{M_L}{E_c I_c} \cdot \left( \frac{1 + \varphi}{1 + (1 + \varphi)\beta} - \frac{1}{1 + \beta} \right) \quad (4-9)$$

The same curvature expressed with the effective creep ratio would be, see expression (4-7):

$$\left(\frac{1}{r}\right)_D = \frac{M_D}{E_c I_c} \cdot \frac{1 + \varphi_{ef}}{1 + (1 + \varphi_{ef})\beta} \quad (4-10)$$

Combining expressions (4-9) and (4-10), after simplification:

$$\frac{1 + \varphi_{ef}}{1 + (1 + \varphi_{ef})\beta_{ef}} = \frac{1}{1 + \beta} + \frac{M_L}{M_D} \cdot \left( \frac{1 + \varphi}{1 + (1 + \varphi)\beta} - \frac{1}{1 + \beta} \right) \quad (4-11)$$

From this the effective creep ratio can be solved:

$$\varphi_{ef} = \frac{A(1 + \alpha\rho) - 1}{1 - A\alpha\rho} \quad (4-12)$$

<sup>2</sup> Subscripts L and D are used in this chapter for simplicity; they correspond to  $E_{cp}$  and  $E_d$  in 5.8.4.

<sup>3</sup> Non-linear effect will be dealt with later, see clause 4.3.

<sup>4</sup> Theoretically this is not fully correct, since concrete stresses will decrease and reinforcement stresses increase with time. However, it is a reasonable approximation in most cases.

where

$$A = \frac{1}{1+\beta} + \frac{M_L}{M_D} \cdot \left( \frac{1+\varphi}{1+(1+\varphi)\beta} - \frac{1}{1+\beta} \right)$$

Figure 5.21 shows the relationship between  $\varphi_{ef}$  and  $M_L/M_D$  for  $\varphi = 3$  and different values of  $\rho$  for the uncracked reinforced cross section.

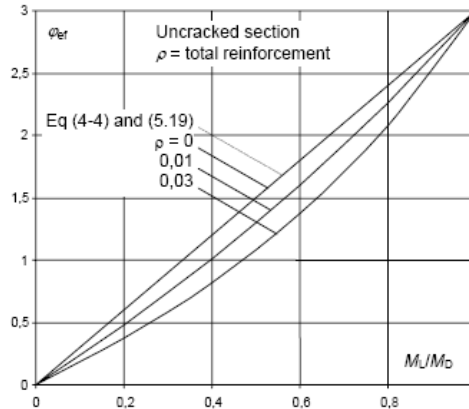


**Figure 5.21.** Effective creep ratio as a function of the ratio  $M_L/M_D$  for  $\varphi = 3$ , uncracked rectangular cross section with symmetric reinforcement, edge distance  $t = 0,1h$  and  $\alpha = E_s/E_c = 6$

The straight line for  $\rho = 0$  is identical with expressions (4-4) and (5.19). With reinforcement, i.e.  $\rho > 0$ , expression (5.19) becomes more or less conservative.

**5.8.4.2.3 Cracked reinforced cross section**

The cracked cross section can be treated analogously, although it is a little more complicated. As the simplest case, consider a rectangular cross section with bending moment only and tensile reinforcement only. The flexural stiffness in the cracked stage (ignoring any contributions from concrete in tension) can then be expressed as

$$EI = E_s A_s d^2 (1 - \xi)(1 - \xi/3) \tag{4-13}$$

- where  $A_s$  = area of reinforcement
- $d$  = effective depth
- $\xi = x/d$
- $x$  = depth of compression zone

The relative depth of compression zone for a certain creep coefficient  $\varphi$  can be obtained from

$$\xi_\varphi = (1 + \varphi) \alpha \rho \left( \sqrt{1 + \frac{2}{(1 + \varphi) \alpha \rho}} - 1 \right) \tag{4-14}$$

where  $\alpha \rho = (E_s/E_c)(A_s/A_c)$

To simplify expressions, introduce the symbol

$$B_\varphi = \frac{1}{(1 - \xi_\varphi)(1 - \xi_\varphi/3)} \tag{4-15}$$

The total curvature under design load can then be written:

$$\left( \frac{1}{r} \right)_D = \frac{M_D}{E_s A_s d^2} \cdot B_0 + \frac{M_L}{E_s A_s d^2} \cdot (B_\varphi - B_0) = \frac{M_D}{E_s A_s d^2} \cdot B_{\varphi_{ef}} \tag{4-16}$$

where  $B_0$  is parameter according to expression (4-15) for  $\varphi = 0$  and  $B_{\varphi_{ef}}$  is the same for  $\varphi = \varphi_{ef}$ . Values of  $\varphi_{ef}$  for which expression (4-16) is satisfied can be found by iteration (direct solution is not possible in this case). Figure 5.22 shows the result for  $\varphi = 3$ .

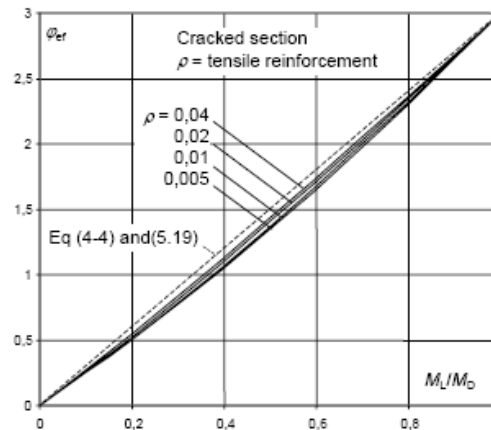


Figure 5.22. Effective creep ratio as a function of ratio  $M_t/M_D$  for a cracked rectangular cross section with tensile reinforcement only, based on  $d = 0,9h$  and  $\alpha = 6$ . Basic creep coefficient  $\varphi = 3$

In this case the curves will approach the straight line according to expression (5.19) the higher the reinforcement ratio is. However, curves for low and moderate ratios are also quite close.

**5.8.4.2.4 Conclusions concerning cross sections**

The idea behind the effective creep ratio in 5.8.4 is illustrated in figure 5.20 and demonstrated in three examples. The simple linear relationship according to expression (5.19) is always more or less conservative, but deviations are generally small. Furthermore, in a reinforced section the overall effect of creep on stiffness is reduced with increasing reinforcement, since creep only affects the concrete contribution to the stiffness. Therefore, the effect of deviations on the stiffness will not be as high as it may appear from the above figures.

**5.8.4.3 Effect of creep in slender columns**

**5.8.4.3.1 General**

The above conclusion concern only cross sections and are based on linear material behaviour. In this point the relevance of the effective creep ratio for slender columns are examined. A slender column behaves in a non-linear way, due to both material and geometrical non-linearity. A non-linear behaviour similar to the linear one in figure 5.20 is outlined in figure 5.23.

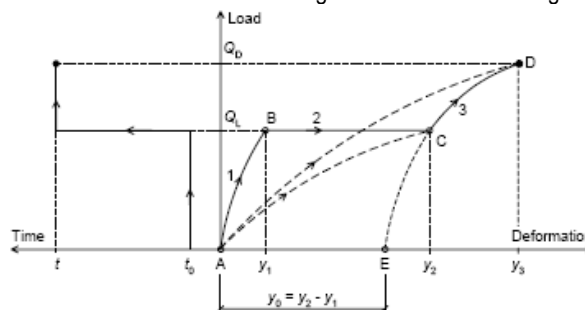


Figure 5.23. Illustration of load history and deformations with nonlinear behaviour

The load history can be divided into three steps:

1. Application of long-term load  $Q_L$ , immediate deformation  $y_1$ , calculated for  $\varphi_{ef} = 0$
2. Long-term load  $Q_L$  during time  $t - t_0$ , total deformation  $y_2$ , calculated for  $\varphi_{ef} = \varphi$
3. Load increase up to design load  $Q_D$ , additional deformation  $y_3 - y_2$ , calculated for  $\varphi_{ef} = 0$

A realistic calculation representing this load history should involve these three steps, including the relevant first order moments or eccentricities for each step. As a simplification, steps 1 and 2 can be combined into one, using a stress-strain diagram with the strains multiplied by  $(1 + \varphi)$ , see 6.4. This corresponds to line AC, and the calculation is then reduced to two steps.

The last step can be calculated in two alternative ways:

- a. After calculating point C, the additional load  $Q_D - Q_L$  is added, with deformation starting from  $y_2$ . See line CD in figure 5.23.
- b. After calculating point C, the total load  $Q_D$  is applied "from scratch", but with  $y_0 = y_2 - y_1$  as an initial deflection added to other first order effects. See line ED in figure 5.23.

Alternative b. will be used in two-step calculations in the following way. The distribution of  $y_0$  along the column should in principle be the same as the distribution of  $y_2 - y_1$ . For a pin-ended column,

however, a sine-shaped or parabolic distribution will be adopted as a simplification.

A further simplification is a *one-step calculation*, using an *effective creep ratio*  $\varphi_{ef}$ , (line AD in the figure). For the definition of  $\varphi_{ef}$  there are two main options:

- based on first order moments  $M_{0L}$  and  $M_{0D}$ , i.e.  $\varphi_{ef} = \varphi \cdot M_{0L} / M_{0D}$
- based on total moments  $M_L$  and  $M_D$ , including 2nd order moments, i.e.  $\varphi_{ef} = \varphi \cdot M_L / M_D$

The relevant deformation parameter in second order analysis is *curvature*, which depends primarily on bending moment. Therefore, the axial load should not be included in the definition of effective creep ratio.

Alternative b) is the most realistic one, since creep deformations will mainly be governed by total moments. With this alternative, however, iteration is inevitable since second order moments depend on stiffness, which depends on effective creep ratio, which depends on total moments etc. Therefore, alternative a) will be the normal choice in practical design.

Alternative a. is always more or less on the safe side. The reason is that the second order moment is a non-linear function of the axial load. Therefore, the moment increase due to second order effects will be greater under design load than under long-term load, and the ratio  $M_L/M_D$  will be lower if second order moments are included. This is easy to verify with a magnification factor based on linear material behaviour (see chapter 5.8.7); this tendency will be even stronger in a non-linear analysis.<sup>5</sup>

#### 5.8.4.3.2 Comparison between one- and two-step calculations

An example will be used to compare the one-step calculation, using the effective creep ratio, with the more realistic two-step calculation. A high slenderness ratio has been chosen, in order to emphasize the effects considered. All calculations below have been done with the *general method*. (for a general description and discussion of this method, see chapter 5.8.6). Geometric assumption are:

- Concrete C40
- Reinforcement S500
- Rectangular cross section with reinforcement concentrated to opposite sides
- Mechanical reinforcement ratio  $\omega = 0,15$  (total reinforcement)
- Edge distance of reinforcement  $0,1h$
- Eccentricity  $e_0 = 0,08h$  (same for long-term and design load; no other first order effect)
- Slenderness  $l/h = 40$  ( $\lambda = 139$ )
- Basic creep coefficient  $\varphi = 3$

In the following, all axial loads and bending moments are expressed in relative terms, i.e.  $n = N / A_{cfcd}$  and  $m = M / hA_{cfcd}$ . Therefore, no absolute dimensions are used.

**a):  $n_L = 0,100$**  (long-term axial load)

- immediate deformation, calculated with  $\varphi = 0$ :  $y_1/h = 0,0173$
- total deformation, calculated with  $\varphi = 3$ :  $y_2/h = 0,0819$
- creep deformation:  $y_0/h = 0,0819 - 0,0173 = 0,0646$

$y_0$  is taken as an initial deflection with parabolic distribution, and is added to the constant first order eccentricity  $e_0$  given above. The load capacity under this total first order effect and no creep ( $\varphi = 0$ ) is calculated. The result is  **$n_{Rd} = 0,235$**

**b):  $n_L = 0,125$**

- $y_1/h = 0,023$  ( $\varphi = 0$ )
- $y_2/h = 0,134$  ( $\varphi = 3$ )
- $y_0/h = 0,134 - 0,023 = 0,111$  (creep deformation)

The load capacity calculated with  $e_0 + y_0$  and with  $\varphi = 0$  is  **$n_{Rd} = 0,189$**

These values are compared to the result of a one-step calculation, using an effective creep ratio based on *first order moments*.

**a)  $n_L = 0,100$**

$$\varphi_{ef} = \varphi \cdot M_{0L} / M_{0D} = \varphi \cdot n_L \cdot e_0 / (n_D \cdot e_0) = \varphi \cdot n_L / n_D = 3 \cdot 0,100 / 0,235 = 1,28^6$$

The load capacity with  $\varphi_{ef} = 1,28$  is  **$n_{Rd} = 0,198$**

Cf. 0,235 in two-step calculation; thus the result is 16% conservative

<sup>5</sup> A "curvature method", giving a fixed 2nd order moment, would lead to the wrong conclusion here.

<sup>6</sup> In this particular example the first order moment is proportional to the axial load, therefore the effective creep ratio can be based on axial loads as well as moments. In the general case only moments should be used.



**b)  $n_L = 0,125$**

$\varphi_{ef} = 3 \cdot 0,125/0,189 = 1,98 \rightarrow n_{Rd} = 0,166$

Cf. 0,189 in two-step calculation; thus the result is 12 % conservative

These results are somewhat conservative, as could be expected (the reason is explained above).

Next is a one-step calculation with  $\varphi_{ef}$  based on *total moments*.

**a)  $n_L = 0,100$**

Total moment under  $n_L$  is  $m_L = n_L \cdot (e_0 + y_2) = 0,100 \cdot (0,08 + 0,0819) = 0,0162$

After iteration the following values are found:

Total moment under design load  $m_D = 0,0618$

Effective creep ratio  $\varphi_{ef} = \varphi \cdot m_L / m_D = 3 \cdot 0,0162/0,0618 = 0,786$

Load capacity with  $\varphi_{ef} = 0,786$  is  $n_{Rd} = 0,224$  (total moment for this load is  $m_D = 0,0618$ )

This is within 5 % of the two-step calculation (which gave  $n_{Rd} = 0,235$ )

**b)  $n_L = 0,125$**

Total moment under  $n_L$  is  $m_L = n_L \cdot (e_0 + y_2) = 0,125 \cdot (0,08 + 0,134) = 0,0267$

After iteration:  $m_D = 0,0531$ ,  $\varphi_{ef} = \varphi \cdot m_L / m_D = 3 \cdot 0,0267/0,0531 = 1,51$ ,  $n_{Rd} = 0,183$

This is within 3 % of the two-step calculation ( $n_{Rd} = 0,189$ )

**5.8.4.3 Conclusions**

It is conservative to use an effective creep ratio based on *first order* moments; *total* moments will give more accurate results. In practical design, however, total moments are much more complicated to use, however, since iteration will be necessary. Therefore, the normal procedure will be to use first order moments. This is further discussed below.

**5.8.4.4 The effect of creep on slenderness limit**

The effect of creep on slenderness limit will be further studied here, comparing the one-step and two-steps methods according to 4.3.1 and 4.3.2. It is thus a complement to clause 3.1, dealing with the slenderness limit in general. It is also a complement to 4.3.2, dealing with creep combined with a high slenderness, since this clause deals with low slenderness ratios.

Table 5.7 shows the results of calculations, based on a slenderness corresponding to the limit for which second order effects may be neglected with  $\varphi_{ef} = 0$ , see 3.1. The basic parameters are the same as for the example in 4.3.2, except those for which different values are given.

**Table 5.7.** The effect of creep for columns with a low slenderness.

C	$\omega$	$e_{02}/h$	$e_{01}/e_{02}$	$l_0/h$	$n_{u0}$	$n_L/n_{u0}$	$\varphi_{ef}$	$n_{u1}$	$n_{u2}$	$n_{u1}/n_{u0}$	$n_{u2}/n_{u0}$	$n_{u1}/n_{u2}$		
20	0,1	0,32	1,0	7,3	0,446	0,5	1,5	0,418	0,426	0,94	0,95	0,98		
			0,0	19,2				0,362	0,363	0,81	0,81	1,00		
	0,5	0,32	-0,9	31,2	0,725	0,67	2,0	0,325	0,348	0,73	0,78	0,93		
			1,0	8,1				0,702	0,697	0,97	0,96	1,01		
40	0,3	0,32	0,0	20,0	0,592	0,67	2,0	0,619	0,616	0,85	0,85	1,00		
			-0,9	30,5				0,596	0,593	0,82	0,82	1,01		
			1,0	7,4				0,579	0,563	0,98	0,95	1,03		
	0,5	0,32	0,0	19,0	1,033	0,67	2,0	0,463	0,455	0,78	0,77	1,02		
			-0,9	29,4				0,453	0,498	0,77	0,84	0,91		
			0,08	12,9				0,849	0,949	0,82	0,92	0,89		
80	0,1	0,32	0,0	34,7	0,122	0,67	2,0	0,111	0,095	0,91	0,78	1,17		
			-0,9	26,8				0,393	0,404	0,91	0,94	0,97		
			1,0	6,8				0,314	0,304	0,73	0,70	1,03		
	0,5	0,32	0,0	17,2	0,432	0,5	1,5	0,33	1,0	0,313	0,367	0,73	0,85	0,85
			-0,9	26,8				0,647	0,645	0,94	0,93	1,00		
			1,0	8,6				0,520	0,522	0,75	0,76	1,00		
0,5	0,32	0,0	19,4	0,690	0,67	2,0	0,518	0,604	0,75	0,88	0,86			
		-0,9	29,4				0,518	0,604	0,75	0,88	0,86			
										<b>0,83</b>	<b>0,85</b>	<b>0,98</b>		

Symbols in table:

- $e_{02}$  the greater of the two first order eccentricities
- $e_{01}$  the lesser eccentricity
- $l_0/h$  slenderness corresponding to the limit for 10 % moment increase at  $\varphi = 0$
- $n$  relative normal force  $N/A_c f_{cd}$
- $n_{u0}$  load capacity for the current slenderness and  $\varphi = 0$
- $n_L$  long-term load
- $\varphi_{ef}$  effective creep ratio =  $\varphi \cdot n_L / n_0$ ; here  $\varphi = 3$  has been assumed



- $n_{u1}$  load capacity including the effect of creep according to 1- step method  
 $n_{u2}$  load capacity including the effect of creep according to 2- step method

### Comments

The agreement between the 1-step and 2-steps methods is in most cases good. For  $e_{01}/e_{02} = -0,9$  (double curvature bending) the 1-step method is generally slightly conservative compared to the 2-steps method. There are also a few cases where the opposite is true, but in these cases the long-term load is close to the limit where instability would occur with  $\varphi_{ef} = \varphi$ , and then the 2-steps method becomes uncertain. In these cases, the result would have been more representative with a somewhat lower long-term load.

The use of an extended stress-strain diagram in the 2-steps method can be discussed. In principle it means that creep deformations will correspond to the stresses in the final stage. In a more accurate calculation they should be integrated from 0 to  $\varphi$ , with increasing second order moment. However, the error will be small, since the stresses are normally not very high under long-term load, and since second order moments are small at these low slenderness ratios.

In most cases a first order eccentricity  $e_{02}/h = 0,32$  has been used, with the aim of having a moderate normal force. For the sake of completeness, one case with a high normal force is also included ( $n_{u0} = 1,022$ ,  $e_{02}/h = 0,08$ ) and one with a low normal force ( $n_{u0} = 0,122$ ,  $e_{02}/h = 1,28$ ). Even with the low normal force, there is a significant effect of creep. (The 2-steps method in this case seems to give more effect of creep for low than for high normal force. This is misleading, however; it is a consequence of the long-term load being close to the instability load for  $\varphi_{ef} = \varphi$ , see discussion in the first paragraph above.)

### Conclusion concerning the effect of creep on the slenderness limit

In these examples, creep reduces the load capacity by 5 to 30% (average 15%). If second order moments are neglected, which is allowable at these slenderness ratios, the result is in principle already 10% on the unsafe side. If creep would also be neglected, the results would be another 5 to 30% on the unsafe side.

The conclusion is that *creep can not be neglected in the slenderness limit*.

#### 5.8.4.5 Safety under long-term load only

The effective creep ratio is based on moments under quasi-permanent load which, according to its definition in EN 1990, is an SLS load with no load factors (except  $\psi_2 < 1$  for variable loads). Thus, in the extreme case of permanent load only, assuming first order moments proportional to the load as in the above examples, the highest possible effective creep ratio is

$$\varphi_{ef} = \varphi \cdot M_{0L}/M_{0D} = \varphi \cdot 1,0/1,35 = 0,74\varphi$$

The following question now arises:

Can load  $N_L$  together with  $\varphi_{ef} = \varphi$  be more severe than  $N_D = 1,35 \cdot N_L$  with  $\varphi_{ef} = 0,74\varphi$  ?

The example in 4.3.2 is used again. The load capacity for  $\varphi_{ef} = 0,74\varphi = 2,22$  is found to be  $n_{Rd} = 0,159$ . The corresponding long-term load is  $n_L = 0,159 / 1,35 = 0,118$ . The load capacity for full creep,  $\varphi_{ef} = \varphi = 3$ , is found to be  $n_{RdL} = 0,141$ . This is higher than the current long term load, and the "safety factor" is

$$\gamma_L = 0,141/0,118 = 1,19$$

This safety factor may be considered somewhat low, although it should be observed that it is not the whole safety factor as the normal material safety factors are already included in the calculated capacities. A reasonable lower limit for the load safety factor could be 1,35.

As shown above, it is conservative to use an effective creep ratio based on first order moments.

The "extra" safety can be estimated by comparison with more accurate calculations, e.g. a two-step calculation or a one-step calculation with  $\varphi_{ef}$  based on total moments.

A two-step calculation according to the above scheme is done with different values of  $n_L$ , until a value is found for which  $n_{Rd} = 0,159$ . This happens for  $n_L = 0,134$ . Thus, one could say that the additional "built-in" safety is  $0,134/0,118 = 1,14$ , and the total safety against creep failure would be

$$\gamma_L = 1,14 \cdot 1,19 = 1,36$$

This is considered to be sufficient, and it can be shown that this factor will be higher for lower values of slenderness, higher first order moments and higher amounts of reinforcement. In this respect, the current example is rather extreme, in the unfavourable direction.

Furthermore, long-term load = 74 % of design load is the worst possible case for consideration of the effect of creep. In normal cases there is always some variable load. The percentage of longterm

load then decreases, since variable loads are included in  $Q_L$  with  $\psi_2 \cdot Q_k$ , where  $\psi_2 < 1^8$ , whereas in  $Q_D$  they are included with  $\gamma_Q \cdot Q_k$ , where  $\gamma_Q > 1$ . Therefore, the more variable the load, the higher the safety against "creep failure" will be.

The conclusion is that a one-step calculation, using an *effective creep ratio based on first order moments*, will give sufficient safety against failure under quasi-permanent load with full creep. Therefore, this case need not be checked separately, and it is *not necessary to include any safety factor on  $M_{0L}$  in the definition of  $\varphi_{ef}$* .

In 5.8.4 (3) the alternative of using *total moments* in the definition of effective creep ratio is given. This is less conservative, however, and most of the extra safety against "creep failure" is then lost. Therefore, 5.8.4 (3) states that a *separate check should then be made for 1,35  $Q_L$  and with  $\varphi_{ef} = \varphi$* . This may become the governing factor in cases where the percentage of long-term moment is moderate or high, more precisely when first order moment ratio  $M_{0L} / M_{0D} > 0,5$ .

## 5.8.5 Methods of analysis

### C5.8.5. Methods of analysis

Three basic methods are described in 5.8.5. Of the simplified methods, (b) is basically the "model column method" in the ENV, with some modifications. The old name is not used here, since it tells nothing about the method (all methods are based on models). A more suitable name is "curvature method", since the method is based on the estimation of a curvature.

This name will be used here, together with "stiffness method" for method (a), which is based on the estimation of stiffness.

There are simplified methods other than those mentioned in EC2. One such method, combining analysis and cross section design in one step, will be shortly described here as an example (it is currently used in the Swedish code).

It can be used for isolated columns with formally centric load, i.e. no other first order effect than the prescribed imperfection. The load bearing capacity is given as

$$N_{Rd} = k_c f_{cd} A_c + k_s f_{yd} A_s \quad (5-1)$$

where  $k_c$  and  $k_s$  are coefficients depending on slenderness ratio, imperfection, concrete grade, effective creep ratio etc, calibrated against calculations with the general method.

A method of this type works ideally if the imperfection, an eccentricity or an initial deflection, is proportional to the buckling length of the column. This is the case in some codes, but not in the Eurocodes. If the imperfection is proportional to the effective length, the coefficients can be given in one simple table or diagram with slenderness as the basic parameter.

If the imperfection is *not* proportional to the effective length, then the absolute value of this length must be added as a separate parameter, which complicates the presentation (for example, one diagram or table would only be valid for one length). However, with some simplifications this type of method could be useful also under EN 1992, particularly for storey high pin-ended columns, which are common as interior columns in buildings.

If there are first order moments other than that due to the imperfection, a separate design for normal force and (magnified) moment must be made. A special moment magnification factor is included in the method for such cases, but the simplicity is lost and the method no longer has any particular advantages over the "stiffness" or "curvature" methods in EC2.

In the following chapters, the general method and the simplified methods (a) and (b) are described.

## 5.8.6 General method

### C5.8.6. General method

#### 5.8.6.1 General

The most accurate of the methods described in 5.8.5 is the "general method". It is based on non-linear analysis, including both *material* and *geometric* non-linearity (second order effects).

"General" here refers to the fact that the method can be used for any type of cross section, any variation of cross section, axial load and first order moment, any boundary conditions, any stress-strain relations, uniaxial or biaxial bending etc. The limiting factor is the capability of the available computer program. The method rests on a few simple assumptions:

- linear strain distribution
- equal strains in reinforcement and concrete at the same level
- stress-strain relationships for concrete and steel

<sup>8</sup> EN 1990 gives values for  $\psi_2$ . For some loads, e.g. wind,  $\psi_2 = 0$ . A common value is 0,3 (office and residential areas). The highest value given is 0,8, can be based on axial loads as well as moments. In the general case only moments should be used.

Conditions of equilibrium and deformation compatibility are satisfied in a number of cross sections, and the deflection is calculated by double integration of the curvature, having an assumed variation between the selected sections. This may be self-evident, but it is mentioned in 5.8.6 (6) as a reference for a simplified version, in which only *one* cross section (or certain critical sections) is studied, and the curvature is pre-assumed to have a certain variation in other parts of the member. This gives simpler computer programs and faster calculation, but less accuracy. See figure 5.24.

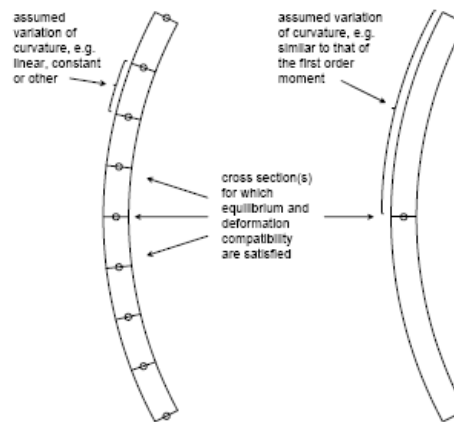


**Figure 5.24.** Illustration of accurate (left) and simplified (right) versions of the general method

Any stress-strain relations can be used. A continuous curve with a descending branch is considered to be the most realistic alternative for the concrete; it is also convenient for computational reasons. Creep can be considered in different ways; the simplest way is to multiply all concrete strains by  $(1+\varphi_{ef})$ , see clause 6.4.

Tension stiffening (i.e. the contribution from concrete in tension between cracks) can easily be taken into account in the general method, e.g. by using a descending branch of the concrete stress-strain curve in tension, by modifying the stress-strain curve of the reinforcement or by any other suitable model. In the calculations presented in this report, however, all contributions from concrete in tension have been ignored; this is always more or less conservative.

### 5.8.6.2 Safety format

The safety format in non-linear analysis has been much debated, and different models have been proposed. The safety format is particularly important in second order analysis, where the *absolute magnitude of deformations* has a direct influence on the ultimate load.<sup>9</sup>

The safety format should satisfy two basic criteria.

1. It should be possible to use the same set of material parameters in all parts of the member, in order to avoid discontinuities and computational problems.

The model in ENV 1992-1-1 (Appendix 2) does not comply with this, since it assumes mean values of material parameters for the calculation of deformations and design values for the check of resistance in critical sections. This also means that there will be *no "material safety" at all* in the calculated resistance, in cases where failure occurs before reaching the design cross section resistance (stability failure) – *unless* "critical section" is substituted by some "critical length" (which then remains to be defined, however).

2. The safety format should be compatible with the general design format based on partial safety factors.

The model in ENV 1992-2 (Appendix B) does not comply with this, since it uses mean values for the analysis and a global safety factor  $\gamma_R = 1,3$  to reduce the ultimate load resulting from the analysis. This gives the same results as using design values  $f_{cm}/1,3$ ,  $f_{yk}/1,3$ ,  $E_{cm}/1,3$  and  $E_{sm}/1,3$ . Thus, it makes no difference whether the ultimate load is governed by concrete or steel, resistance or stiffness. The reduction of the reinforcement strength is too severe, as is also the reduction of the material stiffness parameters, particularly for reinforcement ( $E_{sm}/1,3$ ). A non-linear analysis using this safety format will be conservative, and the potential benefits of using a refined method are lost.

The safety format defined in 5.8.6, based on using *design values* in the analysis, satisfies both criteria. A design value of the ultimate load will be obtained as a direct result of the analysis, and the problems associated with the above-mentioned safety formats are avoided. Since the E-moduli vary less than the corresponding strengths, the partial safety factors given for *E* should be lower than for *f*.

<sup>9</sup> The absolute magnitude can be of importance also in e.g. continuous beams, but only in the check of rotation capacity, and it would normally not have the same direct influence on the ultimate load as in 2nd order analysis.

<sup>10</sup> This diagram is taken from [1], which primarily deals with high strength concrete according to Swedish rules, but this makes no difference for what the diagram is intended to show.

For *concrete*,  $\gamma_c = 1,5$  for strength takes into account not only strength variation, but also geometrical deviations in the cross section. Assuming a factor 1,1 for these deviations, and considering the relationship between strength and E-modulus, a reasonable value of the factor for  $E_c$  is  $\gamma_{cE} = 1,1 \cdot (1,5/1,1)^{1/3} \approx 1,2$ .

For *steel*,  $\gamma_s = 1,15$  includes a factor of about 1,05 for geometrical deviations. Thus, a design value  $E_{sd} = E_{sm}/1,05$  would be logical, considering the fact that variations in the E-modulus are negligible. However, a factor 1,0 has been chosen as a simplification, and in order not to deviate from 3.2.3; differences in terms of calculated result are negligible.

**5.8.6.3 Interaction diagrams**

The resistance of slender columns resulting from a general analysis can be shown in a practical form with interaction curves, figure 5.25. One such curve shows the *maximum first order moment*  $M_0$  (or eccentricity  $e_0 = M_0/N$ ) for a certain axial load  $N$ .

The thin curves in figure 5.25 show the total moment  $M$  as a function of  $N$  for a given  $e_0$ . The higher the slenderness, the more the total moment  $M$  increases over the first order moment  $M_0$ . (Note that the diagram gives axial load and moment in relative terms  $n$  and  $m$ .) One point on the interaction curve for a given slenderness is obtained by plotting the maximum value of  $n$  on the line representing  $m_0$  or  $e_0$ . This is demonstrated in figure 5.25 for one relative eccentricity  $e_0/h = 0,1$  and different slenderness values  $\lambda = 35, 70, 105$  and  $140$ .

The difference  $M_u - M_0$  between the cross section resistance (curve  $\lambda = 0$ ) and the first order moment at maximum load represents the *second order moment*. However, in some cases there is a stability failure before any cross section reaches its ultimate moment, and then the "true" second order moment is less than  $M_u - M_0$ . This occurs for  $\lambda = 105$  and  $140$  in figure 5.25.

This *nominal second order moment*  $M_u - M_0$  is useful as a basis for simplified methods; see clause 6.5 and chapters 7 and 8.

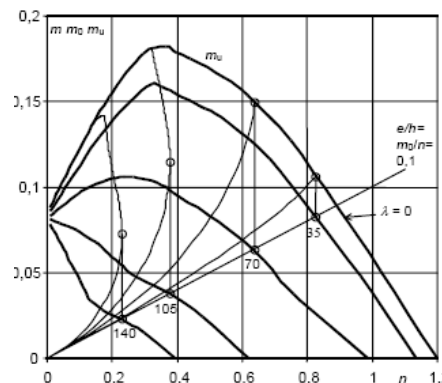


**Figure 5.25.** Interaction curves for columns of different slenderness, calculated with the general method. Rectangular cross section.  $n$  and  $m_0$  are relative axial force and first order moment respectively, i.e.  $n = N / bh^2f_{cd}$ ,  $m_0 = M_0/bh^2f_{cd}$ . All curves are based on  $\omega = 0,2$  and  $\varphi_{ef} = 0$ . Concrete grade is C80.<sup>10</sup> First order moment is constant, e.g. caused by equal end eccentricities

**5.8.6.4 The effect of creep**

Creep can be taken into account in different ways. The most accurate model would be to increase load and time in steps, for each step taking the stresses, strains (and corresponding deflections) from the previous step as starting values for the next increment. For each step, strains would be calculated taking into account their time-dependence.

A simplified model is to multiply all strain values in the concrete stress-strain function with the factor  $(1+\varphi_{ef})$ , see figure 5.26, where  $\varphi_{ef}$  is an effective creep ratio relevant for the load considered. With this model, the analysis can be made either in steps for loads of different duration, or directly for the design load combination in *one* step, see chapter 4.

For creep in slender members in particular, see clause 4.3.

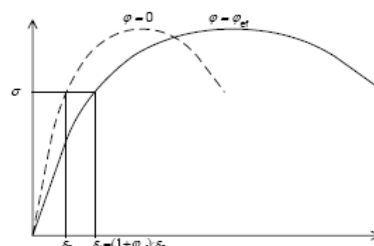


**Figure 5.26.** Simple way of taking into account creep in general method

Figure 5.27 is calculated in this way, using  $\varphi_{ef} = 2,0$  and other parameters the same as in figure 5.25. Curves according to figure 5.25 are also included (dashed), showing the reduction of the load capacity resulting from creep. The relative reduction increases with slenderness.

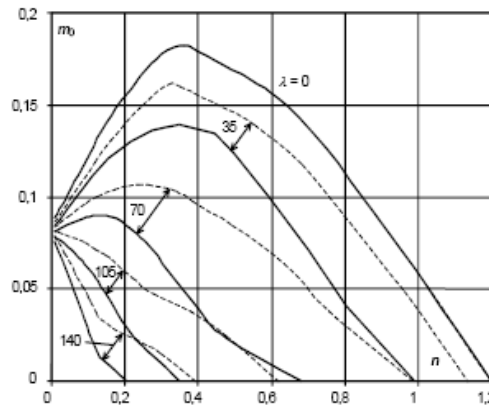


**Figure 5.27.** Interaction curves for  $\varphi_{ef} = 2$ . Other parameters are the same as in figure 5.25  
 Dashed curves are the corresponding curves from figure 6-2, i.e. for  $\varphi_{ef} = 0$ .  
 The difference represents the effect of creep

Another question is whether one and the same effective creep ratio should be used along a compression member (or in different parts of a structure), or if it should vary as the ratio  $M_{Ecp}/M_{Ed}$  may vary. The latter would be the most correct alternative, but normally it is reasonable to use one representative value of  $\varphi_{ef}$  for a member or even a whole structure.

**5.8.6.5 Simplified methods and their common basis**

In a simplified calculation method one can use the difference between cross section resistance and first order moment,  $M_u - M_0$  in figure 5.25, as a *nominal second order moment*. When this moment is added to the first order moment, a design moment is obtained for which the cross section can be designed with regard to its *ultimate resistance*. As pointed out above, this nominal second order moment is sometimes greater than the "true" second order moment.

However, it can give correct end results, even in cases where the load capacity is governed by a stability failure before reaching the cross section resistance, if given appropriate values.

For practical design, there are two principal methods to calculate this nominal second order moment:

1. estimation of the *flexural stiffness*  $EI$  to be used in a *linear second order analysis* (i.e. considering geometrical non-linearity but assuming linear material behaviour); this method is here called **stiffness method**, see chapter 5.8.7
2. estimation of the *curvature*  $1/r$  corresponding to a *second order deflection* for which the second order moment is calculated; this method is here called **curvature method**, see chapter 5.8.8.

Before entering into details of the two methods in chapters 5.8.7 and 5.8.8, their common basis will be shortly described.

The total moment including second order moment for a simple isolated member is:

$$M = M_0 + M_2 = M_0 + N \cdot y = M_0 + N \cdot \frac{1}{r} \cdot \frac{l^2}{c} \tag{6-1}$$

where (see figure 5.28)

- $M$  = total moment
- $M_0$  = first order moment
- $M_2$  = second order moment
- $N$  = axial force
- $y$  = deflection corresponding to  $1/r$
- $1/r$  = curvature corresponding to  $y$
- $l$  = length
- $c$  = factor for curvature distribution

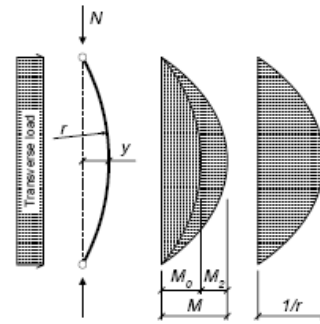


**Figure 5.28.** Illustration of deformations and moments in a pin-ended column. (In the figure, first order moment is exemplified as the effect of a transverse load. First order moment could also be given by eccentricity of the axial load.)

The difference between the two methods lies in the formulation of the curvature  $1/r$ .

In the *stiffness method*  $1/r$  is expressed in terms of an estimated nominal flexural stiffness  $EI$ :

$$\frac{1}{r} = \frac{M}{EI} \tag{6-2}$$

The stiffness  $EI$  should be defined in such a way that ULS cross section design for the total moment  $M$  will give an acceptable end result in comparison with the general method. This includes, among other things, taking account of cracking, creep and non-linear material properties.

In the *curvature method*, the curvature  $1/r$  is estimated directly, on the basis of assuming yield strain in tensile and compressive reinforcement:

$$\frac{1}{r} = \frac{2\varepsilon_{yd}}{0,9d} \tag{6-3}$$

This model overestimates the curvature in those cases where yielding is not reached, giving a too conservative end result. The typical example is where the ultimate load is governed by stability failure, before reaching the cross section resistance. The model may also underestimate the curvature in some cases, since it does not take into account creep. However, various corrections can be introduced to improve the result.

In the following chapters the two simplified methods will be described and compared to the general method.

**5.8.7 Method based on nominal stiffness**

**5.8.7.1 General**

**5.8.7.2 Nominal stiffness**

**5.8.7.3 Moment magnification factor**

**C5.8.7. Method based on stiffness**

**5.8.7.1 Basic equations**

A simple isolated column is considered, e.g. pin-ended with a length  $l = l_0$ ; see figure 5.28. The second order moment can be expressed in the following way, cf. equation (6-1) and fig. 5.28:

$$M_2 = N \cdot y = N \cdot \frac{1}{r} \cdot \frac{l^2}{c} = N \cdot \frac{M}{EI} \cdot \frac{l_0^2}{c} \cdot \left( \frac{M_0}{c_0} + \frac{M_2}{c_2} \right) \tag{7-1}$$

With  $c_0$  and  $c_2$  it is possible to consider different distributions of first and second order moments (primarily the corresponding curvatures). Solving for  $M_2$  gives

$$M_2 = M_0 \frac{N \frac{l_0^2}{c_0 EI}}{1 - N \frac{l_0^2}{c_0 EI}} = M_0 \frac{c_2/c_0}{c_2 EI / l_0^2 N - 1} \tag{7-2}$$

In many cases it is reasonable to assume that the second order moment has a sine shaped distribution. This corresponds to  $c_2 = \pi^2$ , and  $M_2$  can then be written

$$M_2 = M_0 \cdot \frac{\pi^2 / c_0}{(\pi^2 EI / l_0^2) - 1} = M_0 \cdot \frac{\beta}{N_B / N - 1} \tag{7-3}$$

where  $N_B =$  nominal buckling load (based on nominal stiffness).

$\beta = \pi^2/c_0$ , parameter taking into account the distribution of first order moment

The total moment will be

$$M = M_0 \cdot \left( 1 + \frac{\beta}{N_B / N - 1} \right) \tag{7-4}$$

which corresponds to equation (5.28) in 5.8.7.



**5.8.7.2 Moment distribution**

In some cases the value of  $c_0$  is known, as in the examples mentioned in 5.8.7.3 (2).

The case of differing end moments will be examined more closely. A reference is made to 5.8.8.2 (2), with the well-known formula for an equivalent constant first order moment:

$$M_{0e} = 0,6 M_{02} + 0,4 M_{01} \geq 0,4 M_{02} \tag{7-5}$$

This is illustrated in figure 5.29.

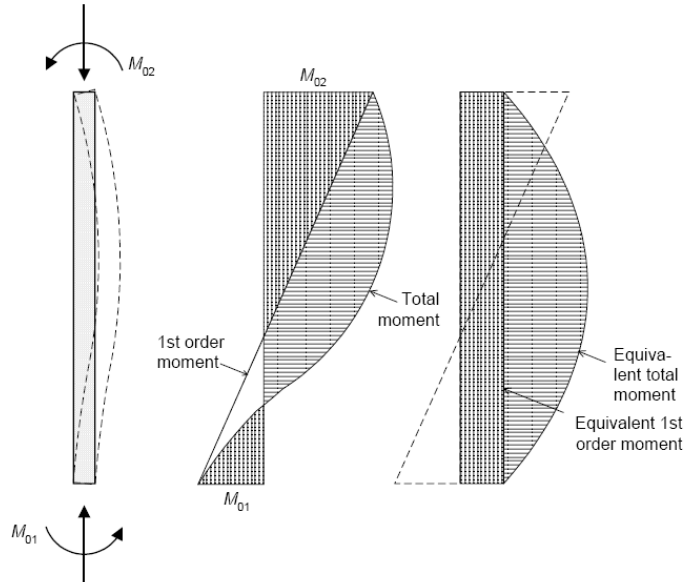


Figure 5.29. Illustration of equivalent moments in case of differing end moments

Equation (7-4) can be used with the equivalent first order moment according to (7-5) also. An example of the result is shown in figure 7-2, where two different  $c_0$  values were used: 8 and 10 respectively.

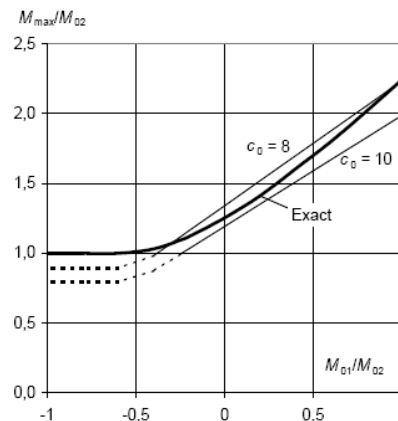


Figure 5.30. Slender member with differing end moments according to figure 7-1 with  $e_{02}/h = M_{02}/Nh = 0,1$  and  $N_B/N = 2$ : Comparison between maximum moment according to exact solution and equivalent first order moment (7-5) with magnification factor (7-4).

Thick line = exact solution.  
 Upper thin line = equivalent moment with  $c_0 = 8$   
 Lower thin line = equivalent moment with  $c_0 = 10$

Figure 5.30 shows good agreement with the exact solution for  $c_0 = 8$ , whereas for  $c_0 = 10$  slightly unsafe results may arise. Therefore  $c_0 = 8$  is recommended in 5.8.7.3 (2); this is also consistent with the assumption of a constant equivalent first order moment. The example is based on a comparatively high second order effect ( $N/N_B = 0,5$ ), which enhances the differences.

In many cases it is reasonable to assume that first and second order moments have similar distributions, in which case  $\beta \approx 1$ . Equation (7-4) can then be simplified to

$$M = \frac{M_0}{N_B / N - 1} \tag{7-6}$$

This corresponds to equation (5.30) in 5.8.7.3. It can be shown that this expression can be used also for structures, provided a global buckling load can be defined. See 5.8.7.4 for global analysis of structures.

### 5.8.7.3 Estimation of stiffness

The maximum first order moment  $M_0$  for different axial forces, slenderness ratios, and reinforcement ratios can be determined using the general method, see chapter 5.8.6.

The values thus obtained can be considered the “correct” ones. With the “stiffness” method, on the other hand, the maximum first order moment can be expressed on the basis of equation (7-4), assuming that the total moment is equal to the ultimate moment resistance  $M_u$  for the normal force  $N$ :

$$M_0 = \frac{M_u}{1 + \frac{\beta}{N_B/N - 1}} = \frac{M_u}{1 + \frac{\beta}{\pi^2 EI/l^2 N - 1}} \quad (7-7)$$

The following is a simple model for the stiffness, expressed as the sum of separate contributions from concrete and reinforcement:

$$EI = K_c E_c I_c + K_s E_s I_s \quad (7-8)$$

where  $E_c, E_s$  = concrete and steel E-moduli respectively

$I_c, I_s$  = moment of inertia of concrete and steel area

The correction factors  $K_c$  and  $K_s$  can be calibrated using more or less sophisticated models, to give the required agreement between expression (7-7) and the general method. In 5.8.7.2 (2) basically two alternative models are given: a) (expr (5.22)) is a more accurate alternative, valid for reinforcement ratios down to  $\rho = 0,002$ . b) (expr (5.26)) is a simplified alternative, valid only for reinforcement ratios  $\rho \geq 0,01$ . Thus, for  $\rho < 0,01$  only a) may be used, for  $\rho \geq 0,01$  either method may be used.

$$\begin{aligned} \text{a) if } \rho \geq 0,002 \quad & K_s = 1 \\ & K_c = k_1 k_2 / (1 + \varphi_{ef}) \end{aligned} \quad (7-9)$$

$$\begin{aligned} \text{b) if } \rho \geq 0,01 \quad & K_s = 1 \\ & K_c = 0,3 / (1 + 0,5\varphi_{ef}) \end{aligned} \quad (7-10)$$

where

$\rho$  is the geometrical reinforcement ratio,  $A_s/A_c$

$\varphi_{ef}$  is the effective creep ratio, see chapter 4

$k_1$  depends on concrete strength class, see (7-11)

$k_2$  depends on axial force and slenderness, see (7-12)

$$k_1 = \sqrt{f_{ck} / 20} \quad (7-11)$$

$$k_2 = n \cdot \frac{\lambda}{170} \leq 0,20 \quad (7-12)$$

where

$n$  is the relative axial force,  $N_{Ed} / (A_c f_{cd})$

$A_c$  is the area of concrete cross section

$\lambda$  is the slenderness ratio,  $l_0/l$

For cases where  $\lambda$  is not defined, a simplified alternative to (7-12) is also given (5.25):

$$k_2 = n \cdot 0,30 \leq 0,20 \quad (7-13)$$

More sophisticated models for estimating the stiffness can be found in [2] and [3]. Background, see [1].

The results of calculations with stiffness evaluated according to expressions (7-9) to (7-12) are presented in Appendix 2 of this report, in the form of comparison with calculations done using the general method. The Appendix also compares the curvature method; see chapter 8.

### 5.8.7.4 Linear analysis of structures

Clause 5.8.7 opens the possibility of using linear second order analysis for structures, using reduced stiffness(es) taking into account the effect of cracking, creep and material nonlinearity in a simplified way. Without this possibility, the only alternative for second order analysis of structures would be non-linear analysis.

When global second order effects are significant, the effects of cracking etc. may be as important as for isolated members. It should also be kept in mind that second order effects may be significant in a structure, even if the geometrical slenderness of individual bracing units is small, in case the *braced units* carry a comparatively high vertical load.

The paragraphs applicable to structures are 5.8.3.3 (criterion for ignoring global second order effects), 5.8.7.3 (3) and Annex H. Two different approaches can be distinguished, one based on a magnification factor for bending moments, 5.8.7.3 (3), and the other one based on a similar factor for horizontal forces, H.2.



The two approaches are basically the same, but the one based on moments is suitable mainly for structures with bracing units consisting of shear walls without significant global shear deformations, or structures braced by simple cantilever columns, see examples in figure 5.31.

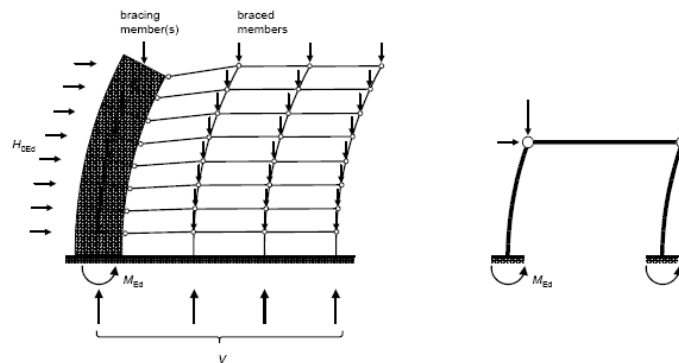


Figure 5.31. Example of structures where a magnification factor can be applied directly to bending moment(s) in bracing unit(s)

The approach based on magnification of horizontal forces, on the other hand, can be used for all kinds of structures, and it should be used for frames, shear walls with large openings etc. If properly used, it gives the correct second order effects in structural systems like frames, shear walls with or without openings etc; see the schematic example in figure 5.32.

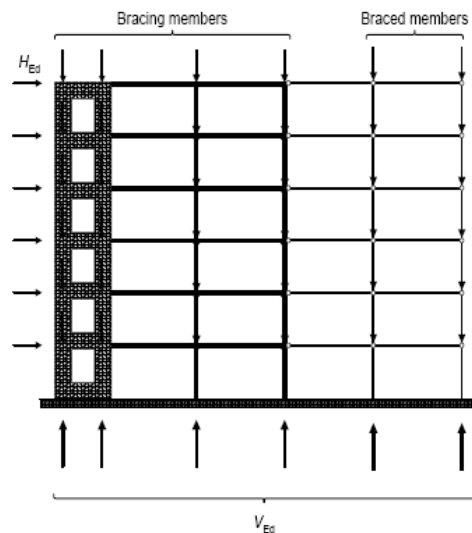


Figure 5.32. Example of a structure where the magnification factor should be applied to horizontal forces rather than to bending moments. (No deformation is shown in this case, second order effects are instead assumed to be included in the fictitious, magnified horizontal force  $H_{Ed}$ .)

Expressions (5.30) and (H.7) are useful if the global buckling load can be defined without difficulty, like in certain regular structures, see e.g. 5.8.3.3 and H.1. In other cases second order effects may be calculated step-wise as indicated for a simple frame in figure 5.33.

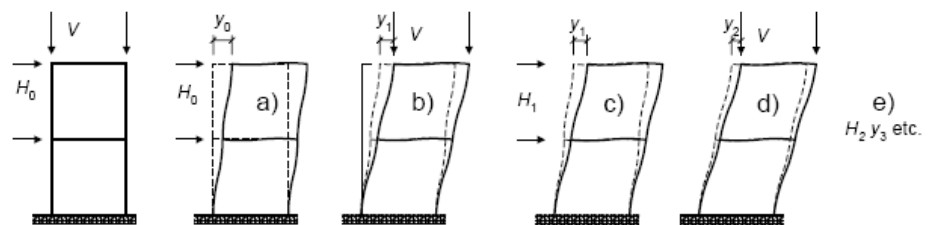


Figure 5.33. Illustration of step-wise calculation of second order effects.

- a) Horizontal load  $H_0$  (without vertical load) gives deformation  $y_0$ .
- b) Vertical load  $V$  on deformed structure gives additional deformation  $y_1$ .
- c)  $H_1$  is an equivalent horizontal load that would give the same deformation  $y_1$ .
- d) Vertical load  $V$  and deformation  $y_1$  give additional deformation  $y_2$ .
- e)  $H_2$  is equivalent horizontal load giving the same deformation  $y_2$  etc ....

The total equivalent horizontal force is

$$H = H_0 + H_1 + H_2 + H_3 + \dots \tag{7-14}$$

If  $k_i = H_i/H_{i-1} < 1$ , then the sum  $H$  will be finite (i.e. the structure is stable). With increasing number

of steps, in a linear analysis, the ratio  $k_i$  will sooner or later become constant. In other words, the following terms will form a geometric series.

The simplest alternative is to assume that *all* terms, including  $H_0$ , will form a geometric series.

The total equivalent horizontal force is then obtained as

$$H = \frac{H_0}{1 - k_1} = \frac{H_0}{1 - H_1/H_0} \tag{7-15}$$

which is equivalent to expression (H.8).

Note. Expression (7-15), including the definition of  $k$ , can also be expressed in terms of  $y$  or a relevant  $M$ .

It can also be shown that the final value of  $k$  is equal to the ratio  $V/V_B$ , where  $V$  is the total vertical load and  $V_B$  is the global buckling load. Thus, the method of stepwise calculation can be seen as just a different formulation or derivation of the method based on a magnification factor.

If the distribution of  $H_1$  is significantly different from that of  $H_0$ , the accuracy can be improved by including one or more steps:

$$H = H_0 + \frac{H_1}{1 - H_2/H_1}, \quad H = H_0 + H_1 + \frac{H_2}{1 - H_3/H_2} \dots etc. \tag{7-16}$$

The simple alternative (7-15)/(H.8) is sufficiently accurate in most cases, compared to other uncertainties like the effect of stiffness variations within and between members due to cracking etc. It should be observed that variation in the degree of cracking between first and following steps does *not* have to be considered, *if* reduced stiffness values according to 5.8.7.2 are used; these values are intended to be valid for the *final stage* of deformation. However, if values for uncracked section are used in early steps, although cracking might occur in later steps, then more steps have to be included in the analysis, like in expression (7-16);  $k$ -values for early steps would otherwise be too low for later steps. This would apply generally when a more refined analysis is used, where gradual cracking is taken into account.

When the structure is analysed for the equivalent horizontal force  $H_{Ed}$ , the relevant second order effects can be obtained everywhere in the structure.

To magnify all moments with the same factor, as in expression (7-6)/(5.30), would not be correct in for instance a frame or a shear wall with large openings.

**5.8.8 Method based on nominal curvature**

**C5.8.8. Method based on curvature**

**Basic relationships**

This method is basically the same as the previously so-called “model column” method in the ENV. The second order moment is expressed in the following way, cf. equation (6-1):

$$M_2 = N \cdot y = N \cdot \frac{1}{r} \cdot \frac{l_0^2}{c} \tag{8-1}$$

As mentioned in 6.5,  $1/r$  is estimated on the basis of reaching yield strain in tensile and compressive reinforcement. Here correction factors  $K_r$  and  $K_\varphi$  are included:

$$\frac{1}{r} = K_r \cdot K_\varphi \cdot \frac{1}{r_0} = K_r \cdot K_\varphi \cdot \frac{2\varepsilon_{yd}}{0,9d} \tag{8-2}$$

In chapter 5.8.5 an extended definition of the effective depth  $d$  has been introduced, in order to cover cases where there is no unambiguous definition of  $d$ ; see figure 5.34 where  $i_s$  is the radius of gyration of the total reinforcement area

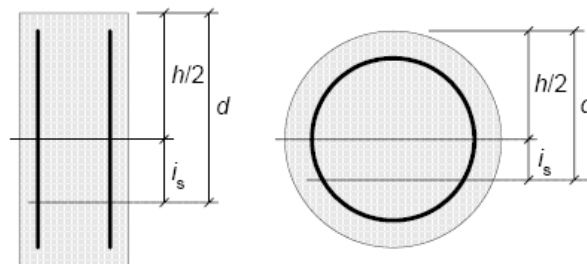


**Figure 5.34.** Effective depth in cross sections with reinforcement distributed in direction of bending

In order to reduce the curvature in cases where yielding is not reached in the tensile reinforcement, a factor  $K_r$  is introduced (same as  $K_2$  in ENV 1992-1-1, 4.3.5.6.3):

$$K_r = (n_u - n) / (n_u - n_{bal}) \leq 1 \tag{8-3}$$

where  $n = N_{Ed} / (A_c f_{cd})$ , relative normal force ( $v$  in the ENV)  
 $N_{Ed}$  is design value of normal force  
 $n_u = 1 + \omega$   
 $n_{bal}$  is value of  $n$  at maximum moment resistance; the value 0,4 may be used  
 $\omega = A_s f_{yd} / (A_c f_{cd})$   
 $A_s$  is total area of reinforcement  
 $A_c$  is area of concrete cross section

There is another factor  $K_1$  in ENV 1992-1-1, 4.3.5.6.3 (2), which reduces the curvature for values of  $\lambda$  between 15 and 35. The purpose of this factor was presumably to avoid discontinuity in cases where second order effects may be ignored. However, second order effects will often be ignored for  $\lambda$  between 25 and 35 (see 5.8.3.2), so discontinuities will still occur.

Furthermore, independent of method, there is always a basic discontinuity following from the rule that second order effects may be ignored if they are below a certain limit. For these reasons, the factor  $K_1$  has not been included in 5.8.8.

The ENV gives no indication of how to take into account creep in the “model column” method. Comparisons with the general method indicate that in certain cases the method can give unsafe results if allowance for creep is not considered, and the factor  $K_\phi$  has been introduced for this purpose. It has been calibrated against calculations with the general method.

More sophisticated models for estimating the curvature can be found in [2] and [3]. Their background is presented in [1].

**Comparison with general method and stiffness method**

The result of calculations with curvature according to expressions (8-1) to (8-3) is presented in Appendix 2, in comparison with calculations based on the general method. In the same Appendix calculations with the stiffness method (chapter 7) are also presented and compared.

**Using the curvature method for structures**

In 5.8.5 there is an indication that the curvature method can be used also for structures, “with proper assumptions concerning the distribution of curvature”. This statement is based on [4], where a method is given by which the curvature method can be used also for second order analysis and design of unbraced frames. For details, see [4].

**5.8.9 Biaxial bending**

**C5.8.9. Biaxial bending**

The general method is suitable for biaxial bending also. The same principles as in uniaxial bending apply, although the complexity of the problem increases.

Simplified methods like the stiffness or curvature method can also be used. They are then used separately for each direction, and if the resulting bending moments fulfil a certain criterion, given in expression (5.38), no further action is necessary.

The criterion in (5.38) is similar to expressions (4.74) and (4.75) in the ENV, 4.3.5.6.4, but there is one important difference: the ENV check concerns only *first order* eccentricities, whereas in 5.8.9 it concerns *total* eccentricities including second order effects. The reason for including the second order effects is illustrated in figure 5.35:

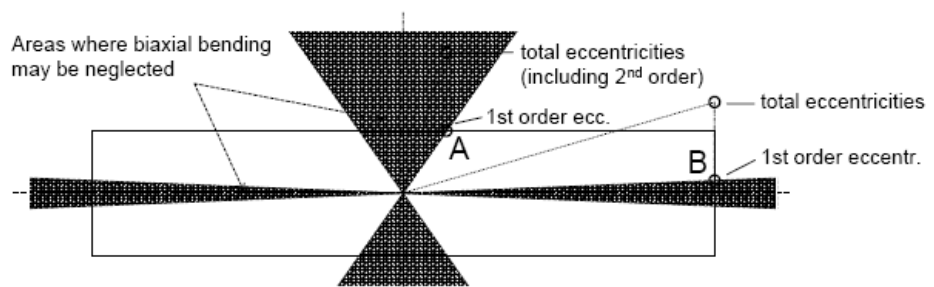


Figure 5.35. Example of member with different slenderness in the two directions

Assume for example  $\lambda = 100$  in one direction and  $\lambda = 20$  in the other. Second order effects will then be significant in one direction but negligible in the other. **A** and **B** are two examples of the position of the axial load, both fulfilling the criterion for separate checks according to the ENV, based on *first order* eccentricities. This would be acceptable for case **A**, since the second order effect will make the total eccentricities even “less biaxial”. It is *not acceptable* for case **B**, however, since the second order effect will now give total eccentricities outside the “permissible” area. Thus, a first order criterion can be misleading and unsafe.

If criterion (5.38) is *not* fulfilled, the cross section should be designed for biaxial bending. A simple

model for this, “in the absence of an accurate cross section analysis”, is given in 6.1:

$$\left(\frac{M_x}{M_{Rx}}\right)^a + \left(\frac{M_y}{M_{Ry}}\right)^a \leq 1 \tag{9-1}$$

where  $M_{x/y}$  design moment in the respective direction, including nominal 2nd order moment  
 $M_{Rx/y}$  corresponding moment resistance of cross section  
 $a$  exponent

The values of the exponent  $a$  are taken from a UK proposal based on [5]. The exponent has been slightly adjusted according to [6]. These values can be used in the absence of more accurate values.

**5.9 Lateral instability of slender beams**

**C5.9. Lateral instability of slender beams**

Compared to the ENV, the following changes have been made:

1. It is clearly stated that the check of lateral instability of beams is relevant in situations where lateral bracing is lacking. For beams in finished structures, lateral instability is normally prevented by lateral bracing from adjacent members (e.g. floor or roof elements).
2. A lateral deflection  $l/300$  has been introduced as an imperfection to be used in calculations concerning lateral instability and balance at supports.
3. The criterion for neglecting second order effects is different. It is explained and compared to the ENV below.

Expression (5.40) is based on a numerical study [7]. It is technically equivalent to the corresponding criterion in the new DIN 1045 [8], but it has a different mathematical formulation to show the main parameters  $l/b$  and  $h/b$  more clearly.

Figure 5.36 shows a comparison according to [7] between the numerical results and expression (5.40). The corresponding criterion according to the ENV is also shown. It is quite clear that the ENV criterion does not represent the numerical results very well; it is too conservative in many cases and unsafe in other cases. The DIN model is much better.

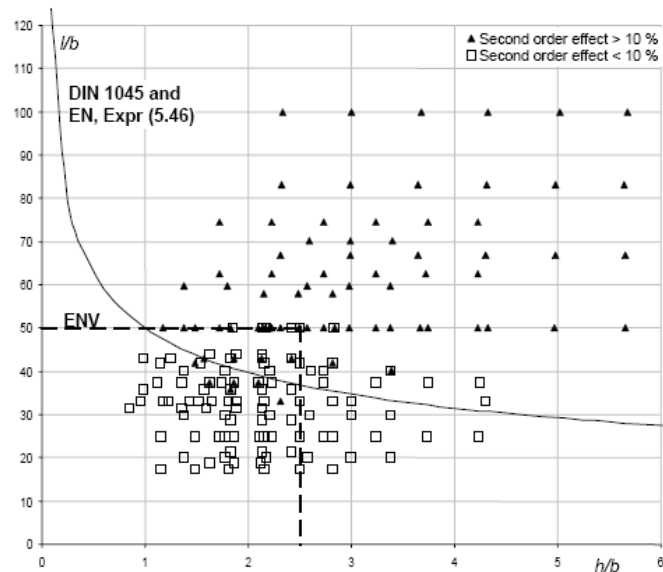


Figure 5.36. Criteria for ignoring second order effects in beams according to ENV and EN in comparison with numerical results [7]

In the final version, a distinction between persistent and transient design situations has been introduced, together with an additional criterion for  $h/b$ ; this is based on national comments.

**5.10 Prestressed members and structures**

**5.10 Prestressed members and structures**

See example 6.15

**5.11 Analysis for some particular structural members**

**5.11 Analysis for some particular structural members**

No specific comment on this part.

**Appendix 1. Verification of new model for slenderness limit**

**Variables covered:**

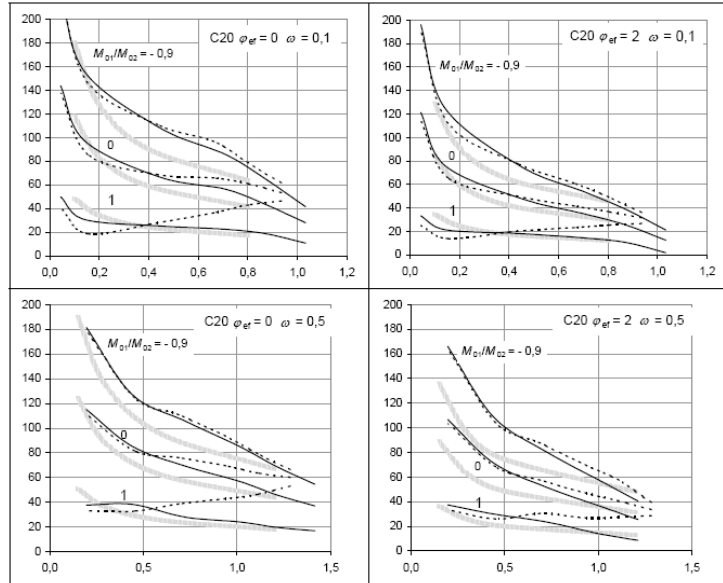
Concrete grade: C20, C40, C80

Reinforcement ratio:  $\omega = 0,1$  and  $0,5$  (for C40 also  $\omega = 0,3$ )  
 Effective creep ratio:  $\varphi_{ef} = 0$  and  $2$  (for C40 and  $\omega = 0,3$  also  $\varphi_{ef} = 1$ )

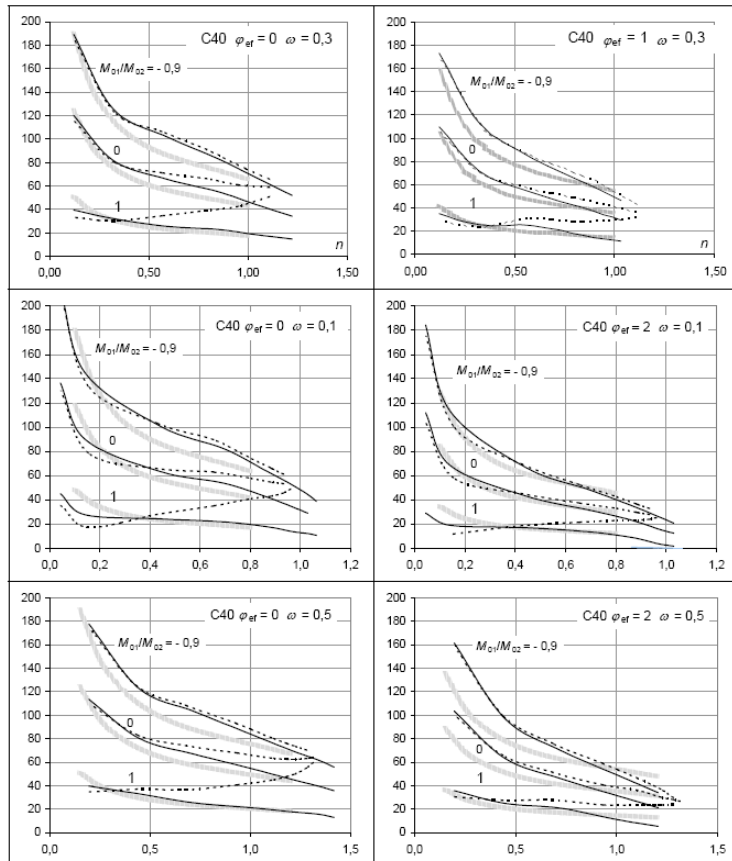
**Explanations to diagrams:**

Horizontal axis: relative normal force  $n$   
 Vertical axis: slenderness limit  $\lambda_{lim}$   
 Full curves: 10%-criterion, alternative 1  
 Dashed curves: 10%-criterion, alternative 2  
 Thick grey curves: new proposal for slenderness limit

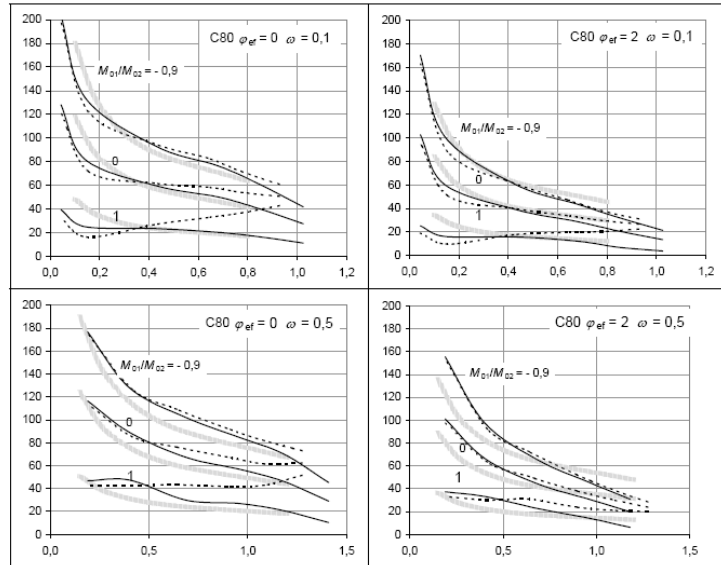
**Concrete C20**



**Concrete C40**



**Concrete C80**



**Appendix 2. Calibration of simplified methods**

**A2.1 Main calculations and results**

Calculations have been made for isolated columns with the following variables:

Cross section	Rectangular <sup>12</sup>
Reinforcement	Symmetrical, concentrated to tensile and compressive edges, edge distance 0,1h
First order moment	Constant (equal end eccentricities) <sup>5</sup>
Boundary conditions	Pin-ended
Slenderness ratio $\lambda = l_0 / i$	(0) 35 70 105 140
Relative eccentricity $e_0/h$	(0) 0,1 0,2 0,4 0,6 0,8 1,2 1,7 3,0 6,0
Reinforcement ratio $\omega = A_s f_{yk} / A_c f_{ck}$	0,1 0,2 0,4
Concrete grade $f_{ck}$	20 40 80
Effective creep ratio $\phi_{ef}$	0 1 2

The total number of individual cases is  $4 \cdot 9 \cdot 3 \cdot 3 = 972$  (not including  $\lambda = 0$  and  $e_0 = 0$ ).

For each case, calculations have been made with the general method according to 5.8.6 and with the simplified methods, i.e. the stiffness and curvature methods according to 5.8.7 and 5.8.8 respectively. The results are summarized in table A2-1 on the following two pages.

The vertical axes in the diagrams represent the ratio

$$\frac{\text{Maximum first order moment according to simplified method}}{\text{Maximum first order moment according to general method}}$$

The moment ratio is given with the mean value  $m$  and with  $m+s$  and  $m-s$  respectively, where  $s$  is standard deviation. The mean value (and standard deviation) for a certain value of the independent variable includes all the values for the other variables. Thus, for one value of e.g. the slenderness, the mean value and standard deviation of the moment ratio represent  $972/4 = 243$  individual values; for one value of the eccentricity  $972/9 = 108$  values etc.

The horizontal axes represent the main variables: slenderness  $\lambda$ , eccentricity  $e_0/h$ , reinforcement ratio (both  $\omega$  and  $\rho$ ), concrete strength  $f_{ck}$  and effective creep ratio  $\phi_{ef}$ .

Interaction diagrams have also been prepared, covering all the above-mentioned cases and including the different methods and alternatives. However, to present all these diagrams would require too much space, and it would be difficult to obtain an overall view of the results.

Therefore, only two such diagrams will be shown to illustrate certain aspects.

<sup>12</sup> In [1] the simplified methods are compared with the general method also for columns with circular cross section and with a different distribution of the first order moment. Although [1] deals with more refined versions of the stiffness and curvature methods, the main conclusion is that the same models, as for rectangular section and constant moment, can be used also for other cross sections and variations of the first order moment.

**Table 5.A2-1. Summary of comparisons between simplified methods and general method**

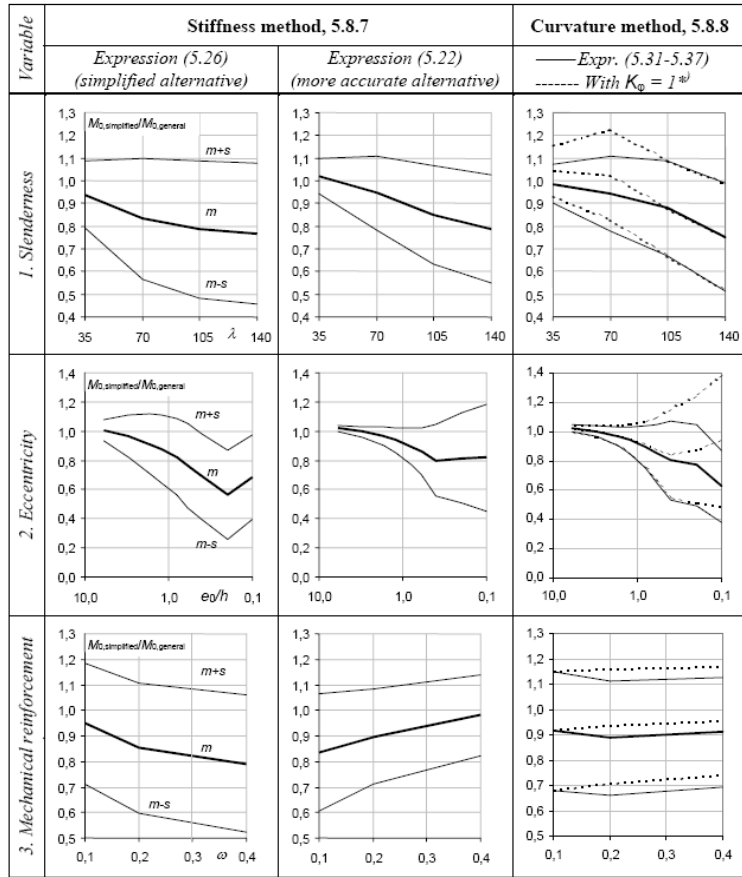
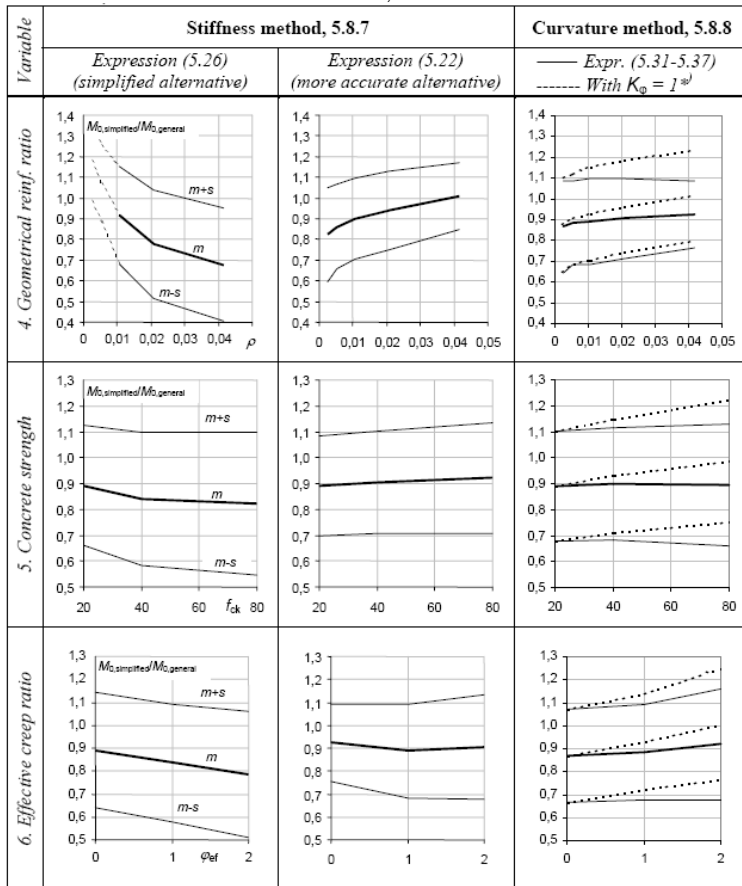


**Table 5.A2-1, continued**





**A2.2 Discussion**

All the simplified methods show a rather wide scatter when compared to the general method.

This is inevitable; a method giving close agreement with the general method over a wide range of parameter values would no longer be simple.

An illustration is given in figure A2-1. The “curvature method” gives reasonable results for low to moderate slenderness, but becomes extremely conservative for high slenderness ratios.

This is because the factor  $K_r$  ( $K_2$  in ENV) gives no reduction of the curvature at all when  $n < 0,4$ , and for high  $\lambda$  values  $n$  is practically always  $< 0,4$ . The same is true for the simplest version of the stiffness method (expr. 5.26). With correction of the stiffness for normal force and slenderness, expression (5.22) to (5.24), the result is much improved.

It is difficult to calibrate a simple method so that it accurately follows the general method, particularly for high slenderness ratios and small eccentricities. This is true for all methods, see the first and second rows of diagrams in table A2-1.

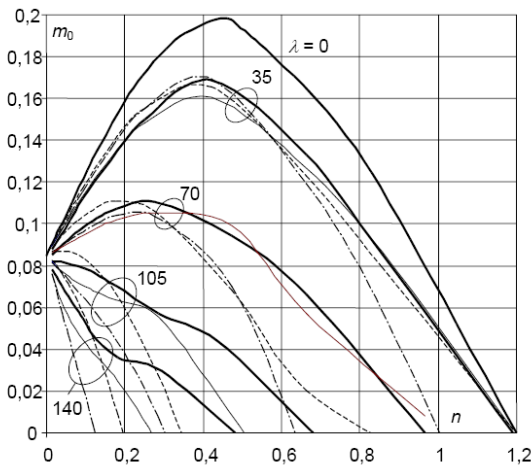


Figure A2-1. Example of interaction curves.  $f_{ck} = 40$ ,  $\omega = 0,2$ ,  $\varphi_{ef} = 0$ .  
 — general method  
 - - - stiffness method, expressions (5.22)-(5.24)  
 . . . stiffness method, expression (5.26)  
 - · - curvature method, expressions (5.31)-(5.37)

In figure A2-1 there is no effect of creep ( $\varphi_{ef} = 0$ ). Figure A2-2 shows the corresponding curves for  $\varphi_{ef} = 2$  (a comparatively high value). Two sets of curves are given for the curvature method. The upper curves are based on  $K_\varphi = 1$ , corresponding to the method in ENV 1992-1-1, 4.3.5.6.3, where there is no effect of creep. The lower curves are based on  $K_\varphi$  according to expression (5.37).

Without effect of creep (= ENV), the curvature method is consistently unsafe for low and moderate slenderness. This can be seen also in the third column of diagrams in table A2-1.

With  $K_\varphi$  according to expression (5.37), creep is well taken into account.

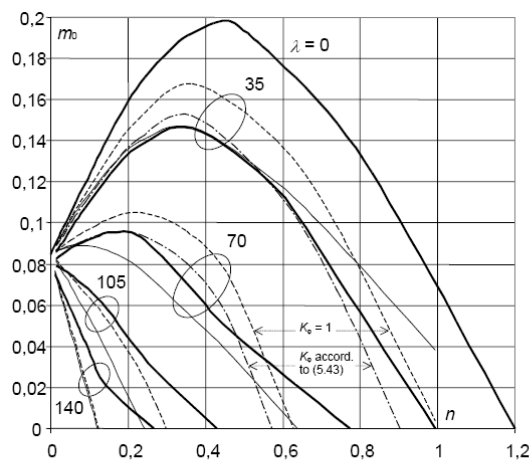


Figure A2-2. Example of interaction curves.  $f_{ck} = 40$ ,  $\omega = 0,2$ ,  $\varphi_{ef} = 2$ .  
 — general method  
 - - - stiffness method, expressions (5.22)-(5.24)  
 - · - curvature method, expressions (5.31)-(5.36) (upper curve,  $K_\varphi = 1$ )  
 · · · curvature method, expressions (5.31)-(5.37) (lower curve,  $K_\varphi$  according to (5.43))<sup>\*)</sup>  
<sup>\*)</sup> For  $\lambda = 105$  and  $140$ , (5.43) gives  $K_\varphi = 1$ , therefore there is only one curve in these cases.



**References**

- [1] Westerberg, B: *Design Methods for Slender Concrete Columns*. Tyréns Technical Report 1997:1. Stockholm, September 1997.
- [2] FIP Recommendations, *Practical Design of Structural Concrete*. fib (CEB-FIP), September 1999.
- [3] *Design Handbook for High Performance Concrete Structures*. Handbook published in Sweden, 1999.
- [4] Beeby, A W and Narayanan, R S: *Designers' Handbook to Eurocode 2, Part 1.1*. Thomas Telford, London, 1995.
- [5] Bresler, B: *Design Criteria for Reinforced Columns under Axial Load and Biaxial Bending*. ACI Journal, November 1960.
- [6] Whittle, R T and Lawson, R: *Biaxial bending with axial compression. An investigation into the use of Bresler coefficients for determining the capacity of reinforced concrete sections under combined axial compression and biaxial bending*. March 2000
- [7] König, G and Pauli, W: *Nachweis der Kippstabilität von schlanken Fertigteilträgern aus Stahlbeton und Spannbeton*. Beton- und Stahlbetonbau 87 (1992)
- [8] Hellesland, J: *On column slenderness limits*. Mechanics Division, University of Oslo, 1999-05-28



**SECTION 6 ULTIMATE LIMIT STATES (ULS)**

**6.1 Bending with or without axial force**

**SECTION 6 ULTIMATE LIMIT STATES (ULS)**

**C6.1 Bending with or without axial force**

**6.1.1 Determining the compression resultant and its position compared to the edge of maximum deformation in case of rectangular section**

Two cases should be distinguished:

- e) real neutral axis ( $x \leq h$ )
- f) virtual neutral axis ( $x > h$ )

– Real neutral axis

a1) Diagram parabola – exponential – rectangle

The resultant C of the block of compressive forces related to a rectangle of width b and depth x is expressed by

$$C = \beta_1 \cdot f_{cd} \cdot b \cdot x$$

and its position, measured starting from the edge where the strain is  $\epsilon_{cu2}$ , is defined by  $\beta_2 x$ .

The formulae of  $\beta_1$  and  $\beta_2$ , in function of strain  $\epsilon_c$ , are:

$$\beta_1(\epsilon_{cu2}) = \frac{\int_0^{\epsilon_{cu2}} \sigma_c \cdot d\epsilon}{f_{cd} \cdot \epsilon_{cu2}}$$

$$\beta_2(\epsilon_{cu2}) = 1 - \frac{\int_0^{\epsilon_{cu2}} \sigma_c(\epsilon) \cdot \epsilon \cdot d\epsilon}{\epsilon_{cu2} \cdot \int_0^{\epsilon_{cu2}} \sigma_c(\epsilon) \cdot d\epsilon}$$

The numeric values of  $\beta_1$  and  $\beta_2$  are shown in function of  $f_{ck}$  in Table 6.1.

In all tables limit the number of decimals to 3 maximum e.g. 0,80952 = 0,810 etc.

**Table 6.1. Values of  $\beta_1$  and  $\beta_2$**

$f_{ck}$ (N/mm <sup>2</sup> )	up to 50	55	60	70	80	90
$\beta_1$	0,80952	0,74194	0,69496	0,63719	0,59936	0,58333
$\beta_2$	0,41597	0,39191	0,37723	0,36201	0,35482	0,35294

a2) Rectangular diagram

With the combined effect of the  $\lambda$  and  $\eta$  factors recalled in Chapt. 3.1.7, the following values result:

$$\beta_1 = \lambda \cdot \eta$$

$$\beta_2 = \lambda / 2$$

the values are shown in Table 6.2.

**Table 6.2. Values of  $\beta_1$  and  $\beta_2$  for rectangular diagram**

$f_{ck}$ (N/mm <sup>2</sup> )	up to 50	55	60	70	80	90
$\beta_1$	0,80000	0,76781	0,73625	0,67500	0,61625	0,56000
$\beta_2$	0,40000	0,39375	0,38750	0,37500	0,36250	0,35000

b) Virtual neutral axis

b1) Parabola – exponential – rectangle diagram

With reference to Fig. 6.1, where

$$\xi' = x/h$$

the maximum and minimum strain at the section, respectively  $\epsilon_t$  and  $\epsilon_b$  (top and bottom) are given by the formulae

$$\epsilon_t = \frac{\xi' \cdot \epsilon_{e2}}{\frac{\epsilon_{e2}}{\epsilon_{cu2}} + \xi' - 1}$$

$$\epsilon_b = \left(1 - \frac{1}{\xi'}\right) \cdot \epsilon_t$$

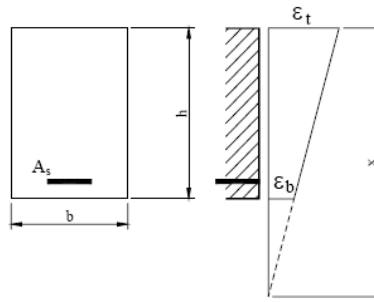


Figure 6.1. Rectangular section with virtual neutral axis

Indicating respectively by  $\beta_{1t}$  and  $\beta_{2t}$  the resultant and its position about the whole length  $x$  and by  $\beta_{1b}$  and  $\beta_{2b}$  the similar quantities about the  $x$ - $h$  part, the resultant  $\beta_3$  and its position  $\beta_4$  compared to the most compressed edge and in relation with depth  $h$  are given by:

$$\beta_3 = \xi' \cdot \beta_{1t} - (\xi' - 1) \cdot \beta_{1b}$$

$$\beta_4 = \frac{\xi'^2 \cdot \beta_{1t} \cdot \beta_{2t} - (\xi' - 1) \cdot \beta_{1b} \cdot ((\xi' - 1) \cdot \beta_{2b} + 1)}{\beta_3}$$

The  $\beta_3$  and  $\beta_4$  values for a number of  $x/h$  ratios are given in Table 6.3.

Table 6.3.  $\beta_3$  and  $\beta_4$  values

$x/h$	parabola – rectangle constitutive law											
	$f_{ck} = 50 \text{ N/mm}^2$		$f_{ck} = 55 \text{ N/mm}^2$		$f_{ck} = 60 \text{ N/mm}^2$		$f_{ck} = 70 \text{ N/mm}^2$		$f_{ck} = 80 \text{ N/mm}^2$		$f_{ck} = 90 \text{ N/mm}^2$	
	$\beta_3$	$\beta_4$	$\beta_3$	$\beta_4$	$\beta_3$	$\beta_4$	$\beta_3$	$\beta_4$	$\beta_3$	$\beta_4$	$\beta_3$	$\beta_4$
1,00	0,80952	0,41597	0,74194	0,39191	0,69496	0,37723	0,63719	0,36201	0,59936	0,35482	0,58333	0,35294
1,20	0,89549	0,45832	0,83288	0,43765	0,78714	0,42436	0,72968	0,41022	0,69249	0,40355	0,67720	0,40186
1,40	0,93409	0,47480	0,88197	0,45841	0,84129	0,44724	0,78831	0,43492	0,75381	0,42907	0,73986	0,42761
1,60	0,95468	0,48304	0,91168	0,46990	0,87615	0,46046	0,82826	0,44975	0,79679	0,44461	0,78422	0,44335
1,80	0,96693	0,48779	0,93113	0,47702	0,90007	0,46895	0,85695	0,45954	0,82834	0,45499	0,81702	0,45389
2,00	0,97481	0,49077	0,94460	0,48178	0,91730	0,47478	0,87838	0,46644	0,85234	0,46237	0,84211	0,46140
2,50	0,98550	0,49475	0,96464	0,48861	0,94420	0,48347	0,91348	0,47705	0,89255	0,47385	0,88448	0,47311
5,00	0,99702	0,49893	0,99060	0,49705	0,98285	0,49512	0,96937	0,49234	0,95972	0,49089	0,95622	0,49057

b2) Rectangular diagram

In this case ( $x \geq h$ ) EC2 does not give instructions. It is nevertheless possible to write a formula that gives the equivalent depth  $h^*$  in relation with  $x$ , so that it results  $h^* = \frac{x - \lambda h}{x - kh} h$  where the  $k$  a factor is

determined by imposing that for  $x = h$  is  $h^* = \lambda \cdot h$ . It results:

$$k = 2 - \frac{1}{\lambda}$$

so that the equivalent depth  $h^*$  is obtained from the expression:

$$h^* = \frac{x - \lambda \cdot h}{x - (2 - \frac{1}{\lambda}) \cdot h} \cdot h$$

Values of  $\lambda$ ,  $\eta$ ,  $k$  are given in function of  $f_{ck}$  in Table 6.4.

Table 6.4. Values of  $\lambda$ ,  $\eta$ ,  $k$

$f_{ck} \text{ (N/mm}^2\text{)}$	$\lambda$	$\eta$	$k$
$\leq 50$	0,80000	1,00000	0,75000
55	0,78750	0,97500	0,73016
60	0,77500	0,95000	0,70968
70	0,75000	0,90000	0,66667
80	0,72500	0,85000	0,62069
90	0,70000	0,80000	0,57143

As an application, the values of  $\beta_3$  and of  $\beta_4$  were calculated in analogy to that was developed for case b1). The resulting values are given in Table 6.5.

**Table 6.5.**  $\beta_3$  and  $\beta_4$  values for rectangular diagram

		Rectangular constitutive law										
$x/h$	$f_{ck} = 50 \text{ N/mm}^2$		$f_{ck} = 55 \text{ N/mm}^2$		$f_{ck} = 60 \text{ N/mm}^2$		$f_{ck} = 70 \text{ N/mm}^2$		$f_{ck} = 80 \text{ N/mm}^2$		$f_{ck} = 90 \text{ N/mm}^2$	
	$\beta_3$	$\beta_4$	$\beta_3$	$\beta_4$	$\beta_3$	$\beta_4$	$\beta_3$	$\beta_4$	$\beta_3$	$\beta_4$	$\beta_3$	$\beta_4$
1,00	0,80000	0,40000	0,76781	0,39375	0,73625	0,38750	0,67500	0,37500	0,61625	0,36250	0,56000	0,35000
1,20	0,88889	0,44444	0,85601	0,43898	0,82344	0,43339	0,75938	0,42188	0,69695	0,40997	0,63636	0,39773
1,40	0,92308	0,46154	0,89154	0,45720	0,86011	0,45269	0,79773	0,44318	0,73623	0,43308	0,67586	0,42241
1,60	0,94118	0,47059	0,91073	0,46704	0,88030	0,46332	0,81964	0,45536	0,75946	0,44674	0,70000	0,43750
1,80	0,95238	0,47619	0,92274	0,47320	0,89308	0,47004	0,83382	0,46324	0,77482	0,45577	0,71628	0,44767
2,00	0,96000	0,48000	0,93097	0,47742	0,90191	0,47469	0,84375	0,46875	0,78572	0,46219	0,72800	0,45500
2,50	0,97143	0,48571	0,94341	0,48380	0,91534	0,48176	0,85909	0,47727	0,80282	0,47225	0,74667	0,46667
5,00	0,98824	0,49412	0,96191	0,49329	0,93554	0,49239	0,88269	0,49038	0,82975	0,48809	0,77677	0,48548

**6.1.2 Calculation of strength of rectangular section**

**6.1.2.1 Determination of  $N_{Rd}$  and  $M_{Rd}$**

Given a transverse rectangular section with symmetrical geometry and reinforcement, the reinforcing bars, the materials and the line that defines the deformed configuration at ultimate limit states, the design normal force and the design bending moment are determined about the centroidal axis.

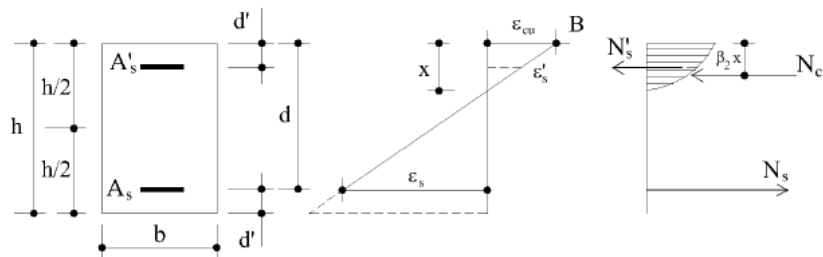


**Figure 6.2.** Rectangular section at ultimate limit state

On the hypothesis that straight sections remain straight, deformation are as in fig. 6.2. On the basis of their level from the stress-strain diagrams of concrete and steel, the corresponding stresses are calculated.

In order to determine  $N_{Rd}$  and  $M_{Rd}$  two equations of equilibrium (horizontal shift and rotation) are written.

Equilibrium to shift: if  $N_c$  is the resultant of compressive stresses applied to concrete,  $N_s'$  the resultant of stresses applied to the compressed reinforcing bars  $A_s'$  and  $N_s$  the resultant of traction in the reinforcing bars  $A_s$ ,

$$N_{Rd} = N_c + N_s' - N_s$$

The single terms can be developed as:

$$N_c = b \cdot \beta_1 \cdot x \cdot f_{cd}$$

$$N_s' = -\sigma_s' \cdot A_s'$$

$$N_s = \sigma_s \cdot A_s$$

In particular

$$\sigma_s' = \varepsilon_s' \cdot E_s \quad \text{if } \varepsilon_s' < \frac{f_{yd}}{E_s}$$

where

$$\varepsilon_s' = \varepsilon_{cu} \left( 1 - \frac{d'}{x} \right) \tag{6.1}$$

$$\sigma_s' = f_{yd} \quad \text{if } \varepsilon_s' \geq \frac{f_{yd}}{E_s}$$

likewise

$$\sigma_s = \varepsilon_s \cdot E_s \quad \text{if } \varepsilon_s < \frac{f_{yd}}{E_s}$$

where

$$\varepsilon_s = \varepsilon_{cu} \left( \frac{d}{x} - 1 \right) \tag{6.2}$$

$$\sigma_s = f_{yd} \quad \text{if } \varepsilon_s \geq \frac{f_{yd}}{E_s}$$

The design bending moment about the centroidal axis is expressed as

$$M_{Rd} = N_c \left( \frac{h}{2} - \beta_2 x \right) + A'_s \sigma'_s \left( \frac{h}{2} - d' \right) + A_s \sigma_s \left( \frac{h}{2} - d' \right).$$

In case both the reinforcing bars are yielded ( $\sigma_s = \sigma'_s = f_{yd}$ ),:

$$\begin{aligned} N_{Rd} &= -b \cdot \beta_1 \cdot x \cdot f_{cd} - A'_s \cdot f_{yd} + A_s \cdot f_{yd} \\ M_{Rd} &= \beta_1 x b f_{cd} \left( \frac{h}{2} - \beta_2 x \right) + (A_s - A'_s) f_{yd} (d - d') \end{aligned} \tag{6.3}$$

$\beta_1$  and  $\beta_2$  are factors given in Tables 6.1 or 6.2.

**6.1.3. Design of reinforcing bars in case of bending without axial force and in case of bending with great eccentricity axial force**

Let's take a transversal section with axis of symmetry  $y$  (Fig. 6.3) and load effects in the plane of symmetry. Given the design load effects at ultimate limit state  $M_{Ed}$  and  $N_{Ed}$ , the bending moment about the tension reinforcement is calculated:

$$M_{Esd} = M_{Ed} - N_{Ed} \cdot y_s$$

and the reinforcement area  $A_s$  required by  $M_{Esd}$  is calculated like in the case of simple bending moment. The axial force  $N_{Ed}$  is taken into account subsequently, by correcting of an equivalent quantity the resistance of the tensioned reinforcement steel. In such cases, the applied axial force must be taken into account with its sign: if  $N_{Ed}$  is a compression force, it will reduce the area of tensioned steel.

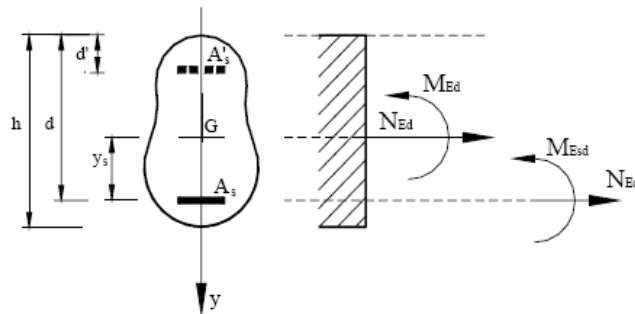


Figure 6.3. Simple bending moment and composite bending moment with great eccentricity

A general rule is adopted: only the tensioned steel ( $A_s$ ) is provided, and only in case the tensioned steel is not sufficient, some compressed steel ( $A'_s$ ) is added. In order to ensure that the structure has a ductile behaviour, the strain  $\epsilon_s$  of the tensioned steel must be greater than the strain corresponding to the limit of elasticity, that is  $\epsilon_s \geq \epsilon_{yd} = f_{yk}/E_s$ . This implies that the neutral axis does not exceed the depth

$$x_{lim} = \frac{\epsilon_{cu}}{\epsilon_{cu} + \epsilon_{yd}} \cdot d$$

where  $\epsilon_{cu}$  is the strain at the compressed end. This limitation is valid for isostatic members; for other cases, other limitations apply (see note).

The value of  $\epsilon_{cu}$  depends exclusively on the concrete class. The  $\epsilon_{cu2}$  (for parabola and exponential – rectangle diagram) and  $\epsilon_{cu3}$  (for bilateral and uniform) values are identical [Table 3.1-EC2]. The  $\epsilon_{yd}$  value depends on the steel design stress  $f_{yd} = f_{yk}/\gamma_s$ .

If  $M_{Esd}$  is greater than the moment  $M_{lim}$ , that corresponds to  $x_{lim}$  in presence of tensioned reinforcement only, a certain amount of compressed steel has to be put in place. The difference

$$\Delta M_{Esd} = M_{Esd} - M_{lim}$$

is to be absorbed by two sets of reinforcement, one compressed and one tensioned, of area

$$A'_s = \frac{\Delta M_{Esd}}{f_{yd} \cdot (d - d')},$$

which both work at the design limit of elasticity.

The area of reinforcement steel,  $A'_s$ , has to be added to the section  $A_s$  corresponding to the limit bending moment.

**Note**

The procedure exposed in the general guidelines follows from the principle of committing, as far as possible, compression to concrete and traction to steel.

More severe limitations of  $x$  than those above- are required in order to meet ductility requirements in the case of indeterminate structures in bending, where redistribution of moments may take place.

Moreover, both in statically indeterminate and determinate cases, the verification of serviceability tensional stresses [7.2(2)-EC2] implicitly requires that the depth of neutral axis at ultimate limit state is limited. In the design process point [9.2.1.1(1-EC2)] must also be taken into account requiring a minimal quantity of tensioned reinforcement steel to avoid that fragility situations arise side steel. In other words, it's necessary that the resisting bending moment of the reinforced section is greater than the moment that causes cracking.

### 6.1.4 Rectangular section

#### 6.1.4.1 Use of parabola-rectangle and exponential-rectangle stress-strain relations

Design is simple if the  $\beta_1$  and  $\beta_2$  values (respectively the resultant and its distance from the edge, for an element of unitary width and depth), given at point 7.2, are used.

Given the section dimensions ( $b$ ,  $h$ ,  $d$ , effective depth defined as distance of the tensioned reinforcement steel centroid from the compressed edge), materials and action effects, the bending moment (Fig. 6.3) about the tensioned reinforcement elements is calculated:

$$M_{Esd} = M_{Ed} - N_{Ed} \cdot y_s$$

In order to determine if  $A_s$  is sufficient, or if also  $A'_s$  is necessary, the following procedure is followed:

$x_{lim}$  is determined

the limit bending moment  $M_{Rd,lim}$  with tensioned reinforcement only is calculated

$$M_{Rd,lim} = F_c \cdot z_{lim}$$

where  $F_c = \beta_1 \cdot b \cdot x_{lim} \cdot f_{cd}$  is the resultant of compression stresses and  $z_{lim} = (d - \beta_2 \cdot x_{lim})$  is the inner lever arm.

a) If  $M_{Esd}$  is smaller than  $M_{Rd,lim}$ ,  $A_s$  alone is needed. In order to determine the value of  $x$  corresponding to  $M_{Esd}$  must be defined.

It results:

$$\beta_1 \cdot b \cdot x \cdot f_{cd} \cdot (d - \beta_2 \cdot x) = M_{Esd}$$

which, developed, becomes:

$$x^2 - x \frac{d}{\beta_2} + \frac{M_{Esd}}{\beta_1 \cdot \beta_2 \cdot b \cdot f_{cd}} = 0$$

Solving:

$$x = \frac{d}{2\beta_2} - \sqrt{\left(\frac{d}{2\beta_2}\right)^2 - \frac{M_{Esd}}{\beta_1 \cdot \beta_2 \cdot b \cdot f_{cd}}}$$

Remembering that  $M_{Esd} = A_s f_{yd} z$ , with  $z = (d - \beta_2 \cdot x)$ , finally

$$A_s = \frac{M_{Esd}}{f_{yd} \cdot z}$$

As  $F_c$  must be equal and contrary to  $F_t$ , the resultant of traction of the reinforcement steel  $A_s$ , it can also be determined by:

$$A_s = \beta_1 \cdot b \cdot x \cdot f_{cd} / f_{yd}$$

– If  $M_{Esd}$  is greater than  $M_{Rd,lim}$ , some reinforcement steel  $A'_s$  in compression is needed. To calculate it,  $\Delta M_{Esd} = M_{Esd} - M_{Rd,lim}$ , from which:

$$A'_s = \frac{\Delta M_{Esd}}{f_{yd} \cdot (d - d')}$$

The tensioned reinforcement is:

$$A_s = \frac{1}{f_{yd}} \cdot \left( \frac{M_{Rd,lim}}{z_{lim}} + N_{Ed} \right) + A'_s$$

In such cases  $\Delta M_{Esd}$  must be sensibly smaller than  $M_{Rd,lim}$ , viz. it must not distort the problem.

**6.1.4.2 Rectangular diagram of concrete stresses**

With reference to Fig. 6.4,  $y = \lambda \cdot x$  is the depth of the compressed zone and  $\eta \cdot f_{cd}$  is the design tensile stress. Values of the  $\lambda$  and  $\eta$  factors are given in Table 6.4. It results:

$$F_c = b \cdot y \cdot \eta \cdot f_{cd}$$

$$z = (d - y/2)$$

$$M_{Rd} = F_c \cdot z = b \cdot y \cdot \eta \cdot f_{cd} \cdot (d - y/2)$$

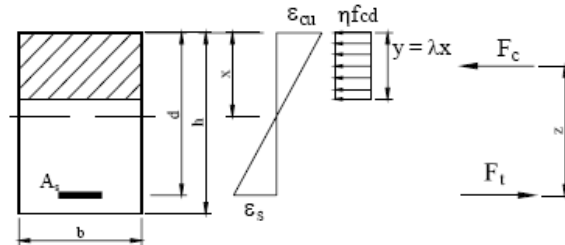


Figure 6.4. Rectangular section with rectangular concrete stress diagram

Rearranging:

$$\left(\frac{y}{d}\right)^2 - 2\left(\frac{y}{d}\right) + \frac{2M_{Ed}}{b \cdot d^2 \cdot (\eta f_{cd})} = 0$$

with the solution

$$\frac{y}{d} = 1 - \sqrt{1 - \frac{2 \cdot M_{Ed}}{b \cdot d^2 \cdot (\eta \cdot f_{cd})}}$$

Also in this case, the considerations and developments of the previous point apply.

**6.1.4.3 T-sections**

Two situations can arise in T-sections:

- the neutral axis is in the flange: no difference as if the section was rectangular;
- the neutral axis crosses the web: its determination and the subsequent developments are simple if the rectangular stress diagram provided for at paragraph [3.1.7(3)-EC2] is adopted. An approximate method is also presented.

**6.1.4.3.1 General method**

Introduction

- As very high values of resisting moments can be reached with T-sections, especially if medium/high strength concrete is used, the tensioned reinforcement steel should be laid on two layers, each one of area  $A_s$ . The upper layer will have distance  $d$  from the compressed edge so that, as this reinforcement layer will have at least strain  $\epsilon_{yd}$ , the lower layer is also surely yielded. In some cases, a lower bulb for the placement of tensioned reinforcement steel could be needed.
- The rectangular stress diagram is adopted for calculation. The block of compressive stresses is defined by a uniform value  $\eta f_{cd}$  and by the extension  $y = \lambda x$  where  $\lambda$  and  $\eta$  are two factors lower than 1 and function of  $f_{ck}$  according to the formulae [3.19 to 3.22-EC2]. Values of  $\lambda$  and  $\eta$  are given in Table 2.3.
- In case of simple bending moment, the equilibrium to rotation between external and internal moment is written with reference to the layer that corresponds to half way between the reinforcement layers  $A_s$  (steel reinforcement centroid). In this way the contributions of the two tensioned reinforcement layers do not appear in the equation. The position of the neutral axis is determined through this equation. Then, the reinforcement elements are determined by equilibrium to shifting.
- In case of bending with axial force the reference layer of bending moments  $M^*$  (sum of the given moment and of the one deriving from the shifting of the force  $N_{Ed}$ ) will still be the above-indicated one. In this case the equilibrium to shifting, that is used to determine  $A_s$ , also contain  $N_{Ed}$ .

Procedure

With reference to Fig. 6.5  $y$  is assumed as the basic parameter.  $M^*$  is the given bending moment about the  $A_s$  reinforcement centroid.  $s$  is the distance of this centroid from the concrete compressed edge. The bending moment resistance is expressed as the sum of the moments of blocks of compression, about the same layer. The equilibrium gives:



$$\eta f_{cd} \left[ b_w y \cdot \left( s - \frac{y}{2} \right) + (b - b_w) \cdot c \cdot \left( s - \frac{c}{2} \right) \right] = M^*$$

By developing, it results:

$$y^2 - 2sy + \frac{2M^*}{b_w (\eta f_{cd})} - (b - b_w) \cdot c \cdot \left( s - \frac{c}{2} \right) = 0$$

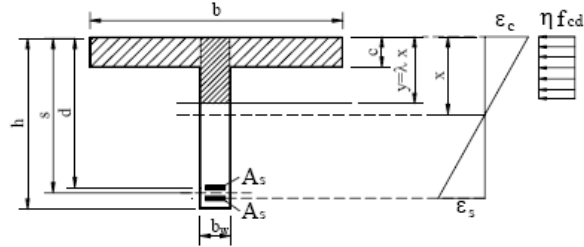


Figure 6.5. T-section treated with the rectangular stress diagram

Taking:

$$k = \frac{2}{b_w} \cdot (b - b_w) \cdot c \cdot \left( s - \frac{c}{2} \right)$$

with k function of the geometrical data only, y is given by:

$$y = s - \sqrt{s^2 - \frac{2M^*}{b_w (\eta f_{cd})} + k}$$

If  $M^*$  is lower than the limit moment, no compressed reinforcement bars are needed. The tensioned reinforcement area is given by:

$$2A_s = (F_c + N_{Ed}) / f_{yd}$$

and the resultant of compression  $F_c$  is:

$$F_c = \eta f_{cd} \cdot [b_w y + (b - b_w) \cdot c]$$

If it is not necessary to put the tensioned reinforcement bars on two layers, in the above-shown formulae is sufficient to identify  $s$  as  $d$ , while the first member of (7.13) gives the necessary area of reinforcement.

#### 6.1.4.3.2 Approximate design method

The method applies to those T-beams where the flange is able to withstand all compressive forces deriving from bending moment and axial force, without addition of compressed reinforcement bars. It's assumed that tensile stresses are uniformly distributed.

With reference to Fig. 6.6, the total bending moment  $M^*$  about the centroid of tensioned reinforcement bars is calculated:  $M^* = M_{Ed} - y^* \cdot N_{Ed}$  ( $N_{Ed}$  positive if traction).

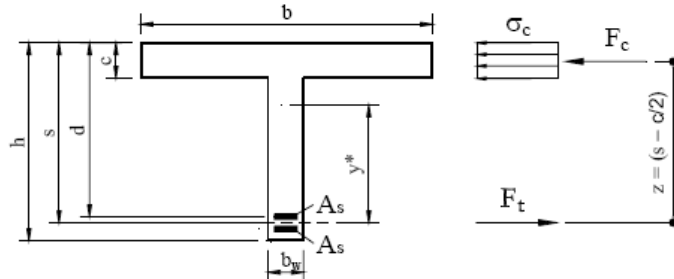


Fig.6.6. T-section. Approximate design method

The reinforcement is given by the formula

$$2A_s = \frac{1}{f_{yd}} \left[ \frac{M^*}{\left( s - \frac{c}{2} \right)} + N_{Ed} \right]$$

and it must be verified that the average compressive stress in the flange is not greater than  $f_{cd}$ :

$$\sigma_c = \frac{M^*}{b \cdot c \left( s - \frac{c}{2} \right)} \leq f_{cd}$$

**6.1.5 Bending with axial force in rectangular section with symmetric reinforcement bars**

The ultimate limit state behaviour of a rectangular section with reinforcement bars  $A_s = A'_s$  placed symmetrically at the section edges and subjected to simple bending moment with an eccentric axial force  $N_{Ed}$  is studied. The analysis is carried out through the determination of the moment resistance  $M_{Rd}$  about the centroidal axis for given values of  $N_{Ed}$  and geometric and mechanical properties of the section.

The study starts from Fig. 6.1 which is reproduced as far as it's needed in Fig. 6.7. Four deformed configurations (1-2-3-4) are taken into account. The first three, obtained by rotation around point B of the straight line that represents the plane section, are characterized by particular depths of the neutral axis  $x$ ; line 4, that configures uniform strain  $\epsilon_{c2}$ , is vertical in the representation and passes by point C.

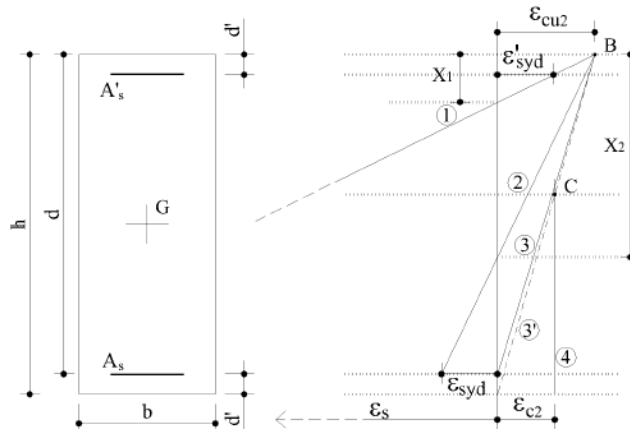


Fig.6.7. Possible strain distributions at the ultimate limit state

Relations that are recalled in the treatment:

Strain of upper reinforcement  $A'_s$  (see point 6.1.2.1):

$$\epsilon'_s = \epsilon_{cu2} \left( 1 - \frac{d'}{x} \right)$$

Strain of lower reinforcement  $A_s$  (see point 6.1.2.1):

$$\epsilon_s = \epsilon_{cu2} \left( \frac{d}{x} - 1 \right)$$

Definition of line 1

Passing by B, the straight line assumes configuration 1 characterized, at the level of the upper reinforcement layer, by strain  $\epsilon'_s = \epsilon_{synd} = \frac{f_{yk}}{\gamma_s E_s} = 0,00196$  (design limit of elasticity for B450 steel with  $t_{yk} = 450 \text{ N/mm}^2$  and  $E_s = 200 \text{ kN/mm}^2$ ). The depth of the neutral axis, calculated by (6.1) results:

$$x_1 = \left( \frac{\epsilon_{cu2}}{\epsilon_{cu2} - \epsilon_{synd}} \right) \cdot d' = k_1 d'$$

The  $k_1$  values for different concrete classes (as  $\epsilon_{cu2}$  is function of  $f_{ck}$ ), are given in Table 6.6 ( $\epsilon_{cu2}$  in absolute value).

For  $x < x_1$  the upper reinforcement layer is in elastic field; for  $x \geq x_1$  it works at stress  $f_{yd}$ . The lower reinforcement layer, for  $x \leq x_1$ , works at stress  $f_{yd}$ .

Table 6.6 values of  $k_1$  and  $k_2$

$f_{ck}$ ( $\text{N/mm}^2$ )	$\epsilon_{cu2}$	$k_1$	$k_2$
$\leq 50$	0,0035	2,27	0,64
55	0,0031	2,71	0,61
60	0,0029	3,08	0,59
70	0,0027	3,65	0,58
80	0,0026	4,06	0,57
90	0,0026	4,06	0,57

Line 2: it is defined by the strain  $\epsilon_s = \epsilon_{synd}$  of the lower layer of reinforcement. In this case the depth of the neutral axis, deduced by (6.2) results:

$$x_2 = \left( \frac{\epsilon_{cu2}}{\epsilon_{cu2} + \epsilon_{syd}} \right) \cdot d = k_2 \cdot d$$

$k_2$  values are shown in Table 6.6.

For positions of the neutral axis  $x_1 \leq x \leq x_2$ , both reinforcement layers are subjected to a stress  $\sigma_s = f_{yd}$  (compression for the upper one, traction for the lower one), with strain  $\epsilon_s \geq \epsilon_{syd}$ .

Configuration 3 is characterized by strain value  $\epsilon_s = 0$  (and therefore  $\sigma_s = 0$ ) for the lower reinforcement ( $x = d$ ). Therefore in the 3-4 range stress is  $\sigma_s = f_{yd}$  for the upper reinforcement and  $\sigma_s = \epsilon_s \cdot E_s$  for the lower.

Line 3' is defined by  $\epsilon_c = 0$  at the lower edge of section.

In configuration 4:  $\epsilon_s = \epsilon_s' = \epsilon_{c2}$  (in absolute value), which is always greater than  $\epsilon_{syd}$ . It results then  $\sigma_s = \sigma_s' = f_{yd}$ . In the transition from 3 to 4 the upper reinforcement is compressed at stress  $f_{yd}$ , the lower reinforcement at stress increasing from 0 to  $f_{yd}$ .

The following values of the axial force resistance  $N_{Rd}$  correspond to configurations 1,2,3,4:

$$N_{Rd1} = \beta_1 b x_1 f_{cd}$$

$$N_{Rd2} = \beta_1 b x_2 f_{cd}$$

In these two cases there are no contributions from the reinforcement bars because these are subjected to  $\pm f_{yd}$ , and generate two equal and opposite forces in equilibrium.

$$N_{Rd3} = \beta_1 b d f_{cd} + A_s' f_{yd}$$

$$N_{Rd4} = b h f_{cd} + 2 A_s f_{yd}$$

$\beta_1$  values are given in Table 6.1 from the parabola-exponential rectangle model and in Table 6.2 for the rectangle model.

Calculation of the moment resistance in the four above-defined sectors.

a)  $N_{Ed} < N_{Rd1}$ , that is  $x < x_1$

The position  $x$  of the neutral axis must be preliminary determined by the equation of equilibrium to shifting. Keeping in mind that the upper reinforcement  $A_s'$  is compressed in elastic field and that the lower reinforcement  $A_s$  is tensioned at stress  $f_{yd}$ , the equilibrium is written as:

$$-\sigma_s' A_s' - \beta_1 x b f_{cd} + A_s f_{yd} = -N_{Ed}$$

Taken  $\sigma_s' = E \epsilon_s'$  where  $\epsilon_s'$  is given by (6.1), it results:

$$x^2 - \left( \frac{N_{Ed} + A_s f_{yd} - \epsilon_{cu2} E_s A_s'}{\beta_1 b f_{cd}} \right) x - \left( \frac{\epsilon_{cu2} E_s A_s' d'}{\beta_1 b f_{cd}} \right) = 0$$

The equation, written in synthesis

$$x^2 - (***) x - (****) = 0$$

has the solution

$$x = + \frac{1}{2} (***) + \sqrt{\frac{1}{4} (***)^2 + (****)}$$

The  $\sigma_s'$  stress is now known and adds up to  $\sigma_s' = E_s \epsilon_{cu2} \left( 1 - \frac{d'}{x} \right)$

and the moment resistance about the centroidal level is:

$$M_{Rd} = A_s f_{yd} \left( \frac{h}{2} - d' \right) + A_s' \sigma_s' \left( \frac{h}{2} - d' \right) + \beta_1 x b f_{cd} \left( \frac{h}{2} - \beta_2 x \right)$$

b)  $N_{Rd1} \leq N_{Ed} \leq N_{Rd2}$

As both reinforcements are yielded,  $N_{Ed}$  is exclusively supported by concrete. The equilibrium equation is:

$N_{Ed} = N_{Rd} = \beta_1 b x f_{cd}$ , so that the depth of the neutral axis is:

$$x = \frac{N_{Ed}}{\beta_1 b f_{cd}}$$

With the above-determined  $x$  value, the moment resistance is:

$$M_{Rd} = A_s f_{yd} (d - d') + \beta_1 x b f_{cd} (0,5h - \beta_2 x) \tag{6.4}$$

$$c) N_{Rd2} \leq N_{Ed} \leq N_{Rd3}$$

The equation of equilibrium to shifting is:

$$-f_{yd} A_s' - \beta_1 x b f_{cd} + A_s \sigma_s = -N_{Ed} \tag{6.5}$$

As the reinforcement  $A_s$  is in elastic field,  $\sigma_s = E_s \varepsilon_s$   $\varepsilon_s$  is given by (6.2)

Replacing and developing it results:

$$x^2 - \left( \frac{N_{Ed} - A_s' f_{yd} - \varepsilon_{cu2} E_s A_s}{\beta_1 b f_{cd}} \right) x - \left( \frac{\varepsilon_{cu2} E_s A_s d}{\beta_1 b f_{cd}} \right) = 0 \tag{6.5bis}$$

Once determined  $x$  e  $\sigma_s$ , the moment resistance results:

$$M_{Rd} = A_s' f_{yd} \left( \frac{h}{2} - d' \right) + A_s \sigma_s \left( \frac{h}{2} - d' \right) + \beta_1 x b f_{cd} \left( \frac{h}{2} - \beta_2 x \right) \tag{6.6}$$

d) In the fourth field ( $N_{Rd3} \leq N_{Ed} \leq N_{Rd4}$ ) the moment resistance can be determined, with a good approximation, by the relation of proportionality indicated in fig. 6.8, which shows the final end of the interaction diagram M-N.

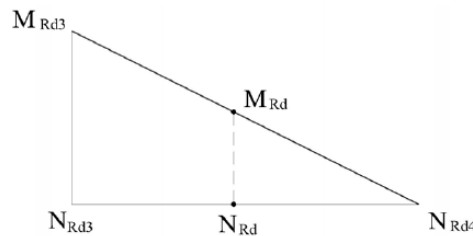


Figure 6.8. Terminal end of the interaction diagram M-N

The moment resistance reaches a maximum for  $x = x_2$  where the analytic function that expresses it has an edge point due to the discontinuity between (6.4) and (6.6). The derivative for  $x = x_2$  is positive if (6.4) is used and is negative with (6.6).

### 6.1.6 Interaction diagram $M_{Rd}$ - $N_{Rd}$

In the case of sections subjected to bending with axial force with small eccentricity, such as those of columns, the most logical solution is the one with double symmetric reinforcement. Such sections can also withstand simple bending and, if it's the case, composed bending in relation if the dimensions and placement of reinforcement.

In order to have an overview on the problem, let's consider the load capacity of a rectangular section (Fig. 6.9) with dimension  $h = 600$  mm,  $b = 400$  mm of  $f_{ck} 30$  concrete, in the four conditions:

- no reinforcement
- symmetric reinforcement ( $f_{yk} = 450$  N/mm<sup>2</sup>) at the edges in percentage 0,5 – 1,0 – 1,5 on each edge, distanced at  $d' = 50$  mm.

The calculation of the resistance of this section at the ultimate limit state is developed, for each of the four reinforcement conditions, by associating the parabola-rectangle diagrams for concrete and the bilinear diagram or steel, with 7 configurations characterized by strain values of plane section (reference to Fig. 1) given in Table 6.7. Steel B450 ( $f_{yk} = 450$  N/mm<sup>2</sup>).

Table 6.7. Deformed section configurations

$\varepsilon_c = -0,0035$ at upper end	$\varepsilon_s = +0,05000$ (bottom reinf.)
$\varepsilon_c = -0,0035$ at upper end	$\varepsilon_s = +0,02500$ (bottom reinf.)
$\varepsilon_c = -0,0035$ at upper end	$\varepsilon_s = +0,01000$ (bottom reinf.)
$\varepsilon_c = -0,0035$ at upper end	$\varepsilon_s = +0,00196$ (bottom reinf.)
$\varepsilon_c = -0,0035$ at upper end	$\varepsilon_s = 0,00000$ (bottom reinf.)
$\varepsilon_c = -0,0035$ at upper end	$\varepsilon_c = 0,00000$ at lower end
$\varepsilon_c = -0,0020$ everywhere	$\varepsilon_c = -0,0020$ everywhere

Development of the calculation in relation with the third strain condition for the reinforced section with 1% bilateral reinforcement ( $A_s = A_s' = 2400$  mm<sup>2</sup>)

Upper reinforcement:  $\varepsilon_s' = -0,0023$  and therefore  $\sigma_s' = -391$  N/mm<sup>2</sup>;  $F_s' = -939$  kN

Lower reinforcement:  $\varepsilon_s = +0,010$  and therefore  $\sigma_s = +391$  N/mm<sup>2</sup>,  $F_s = +939$  kN

Neutral axis:  $x/d = 3,5/(3,5+10)$ , and as  $d = 550$  mm,  $x = 142,6$  mm

$$F_c = \beta_1 b x_{f_{od}} = 0,8095 \cdot 400 \cdot 142,6 \cdot 17,0 = -785 \text{ kN}$$

Distance of  $F_c$  from the compressed edge:  $\beta_2 x = 59 \text{ mm}$

$$N_{Rd} = F_c + F_s + F'_s = -785 - 939 + 939 = -785 \text{ kN}$$

Moment about the concrete section centroid

$$M_{Rd} = F_c (d/2 - \beta_2 x) + F_s (d - d') = 189,1 + 469,5 = 658,6 \text{ kNm}$$

The eccentricity of  $N_{Rd}$  is  $M_{Rd} / N_{Rd} = 839 \text{ mm}$ .

Fig. 6.9 graphically shows the 29 pairs of results obtained. For each value of the percentage of reinforcement the points are joined by a straight line. The result is convex polygons.

The following observations arise from the observation of Fig. 6.9:

3. the polygons include the domains of resistance: the points of co-ordinates  $M_{Ed}$ ,  $N_{Ed}$  placed inside the polygon are in a safe zone; the points on the polygon strictly verify the ultimate limit state; external point do not meet resistance conditions at ultimate limit state
4. a straight line parallel to the  $N$  axis intersects the polygon in two points. This means that with a given reinforcement, a given bending moment can be withstood by two different values of the axial force. The limit case of a single  $N$  value happens when the straight line passes by the highest point of the polygon.
5. Only one value of  $M$  can be associated to a given value of  $N$ , as it's possible to verify by tracing a line parallel to the  $M$  axis.
6. The polygon related to the non-reinforced section denotes the possibility to withstand bending moments only if they come with an adequate axial force (provided by self weight or by prestressing).
7. The branches on the left of the  $M$  axis denote resistance to bending with positive axial force
8. The straight line of inclination  $M/N = h/30 = 20 \text{ mm}$  defines the field of use of the polygons: in fact, according to [6.1(4)-EC2] a minimal eccentricity must always be taken into account, adding up to the bigger value between  $h/30$  and  $20 \text{ mm}$ .

Such polygons as those traced below are called "M-N interaction diagrams".

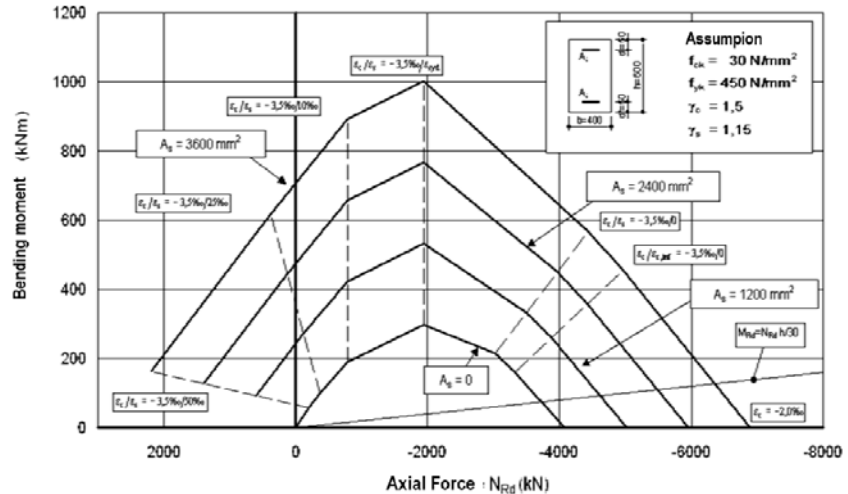


Figure 6.9. Interaction diagram for rectangular section

### 6.1.7 Biaxial bending and bending with axial force

Biaxial bending may be separated into separate uniaxial bending components under circumstances laid down in Eurocode 2 5.8.9 . For pure biaxial bending, where the bending components lay on the two centroid axis of inertia, the problem solution has computational difficulties. If a design software is not used, and calculation developed by hand, it should be processed by iterations; in such case it's convenient to adopt the rectangular stress diagram for concrete.

Given a section subjected to an axial force  $N_{Ed}$  applied on the centre of gravity, and to two bending components  $M_{Ey}$  e  $M_{Ez}$  expressed by two vectors orientated along a couple of orthogonal axis  $y$  e  $z$  with origin in the centre of gravity. In general, the existence of a stress distribution that gives place to resistance greater or equal to the action effects must be demonstrated, as well as the fact that the straight line that connects the centre of gravity of the compressed zone with the centre of gravity of the tensioned reinforcement is perpendicular to the resultant bending vector  $M_{Ed}$ . This implies that the eccentric axial force must also lay on that line.

## 6.2 Shear

### 6.2.2 Members not requiring design shear reinforcement

#### C6.2.2 Shear capacity of members without shear reinforcement

##### 6.2.2.1. Shear flexure capacity

Most shear failures occur in the region of the member cracked in flexure. It is necessary to make a distinction between shear flexure and shear tension. In this chapter only shear flexure is regarded, which can be considered as the general case.

In ENV 1992-1-1 the equation for the shear capacity of members without shear reinforcement was

$$V_{Rd1} = [\tau_{Rd} k (1.2 + 40 \rho_l) + 0.15 \sigma_{cp}] b_w d \quad (6.7)$$

Where

$\tau_{Rd}$  basic shear strength, which follows from  $\tau_{Rd} = 0.25 f_{ctk,0.05} / \gamma_c$ .

$k$  factor allowing for the size effect, equal to  $k = 1.6 - d (m) > 1$

$\rho_l$  flexural tensile reinforcement ratio,  $A_s / b_w d < 0.02$

$\sigma_{cp}$  design axial stress (if any) =  $N_{Sd} / A_c$

$b_w$  minimum web section

There are two shortcomings with regard to the use of this equation. At first the role of the concrete strength is not correct, as was demonstrated in [Walraven, 1987, pp. 68 - 71.] For lower strength concrete classes the deviations were not yet very large, but if the strength increases the deviations soon reach an unacceptable level.

The second problem is that the equation has principally been derived for beams, failing in shear flexure and is not valid for members which typically fail in shear tension. Such members are for instance prestressed hollow core slabs, which nearly always fail in shear tension, in the area where the member is not cracked in flexure. Applied to such members Eq. 6.7 would give unnecessary conservative results.

The recommendations for the determination of the shear flexure capacity of members not reinforced in shear are given in chapter 6.2.2 of prEN 1992-1-1:2001. The basic formula is given as Eq. 6.2.a in this document. This equation has been derived in the following way. The basic equation adopted, which was believed to take appropriate account of the most important influencing factors like concrete strength, longitudinal reinforcement ratio and cross-sectional height was

$$V_u = C \cdot k (100 \rho_l f_c)^{1/3} b_w d \quad (6.8)$$

where

$k$  = size factor =  $1 + (200/d)^{1/2}$

$\rho_l$  = longitudinal reinforcement ratio

$f_c$  = concrete cylinder strength (N/mm<sup>2</sup>)

$C$  = coefficient to be determined

A selection was made of a representative number of shear tests, considering a parameter variation as wide as possible and as well as possible distributed within practical limits. This was already done by König and Fischer (1995). An overview of the test parameters is given in Fig. 6.10.

Then for every test result the optimum value  $C$  was determined. If the distribution is normal, Fig. 6.11 a lower bound value for  $C$  was determined according to the level 2 method described in [Taerwe, 1993] with the equation:

$$C_{\text{lower bound}} = C_{\text{mean}} \cdot (1 - \alpha \cdot \beta \cdot v) \quad (6.9)$$

where

$\alpha$  sensitivity factor, equal to 0.8 for the case of one dominating variable (concrete strength)

$\beta$  reliability index, taken equal to 3.8 according to [Eurocode, Basis of Structural design, Draft version 2001]

$v$  standard deviation

If the distribution turns out to be log-normal, Fig. 6.11, the equation is

$$C_{\text{lower bound}} = C_{\text{mean}} \cdot \exp(\alpha \beta v - 0.5 v^2) \quad (6.10)$$

In these equations a reliability index  $\beta = 3.8$  means a probability of occurrence of 0.0072%. König and Fisher (1995) carried out this procedure for 176 shear tests.

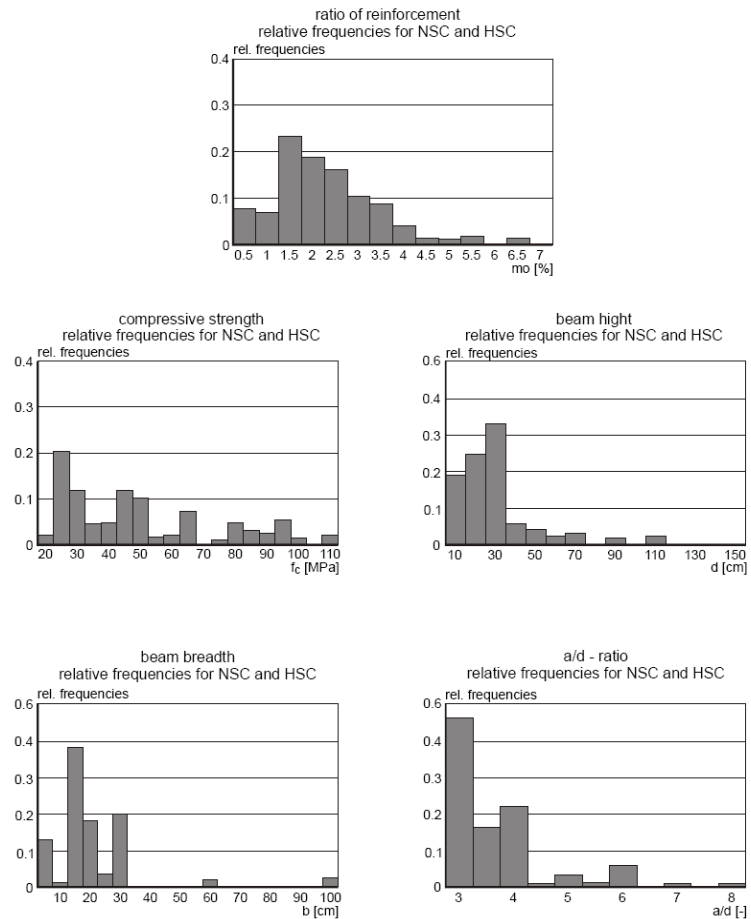


Figure 6.10. Relative frequency of parameters in test data bank used by König and Fischer (1995) in order to find a reliable lower bound equation for the shear capacity of members without shear reinforcement

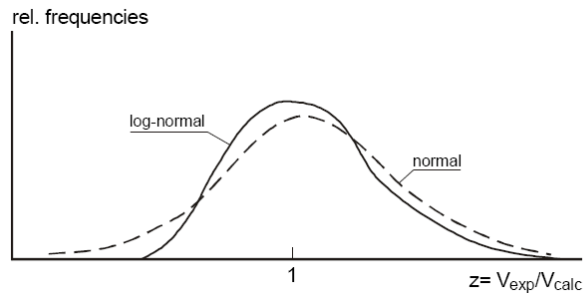


Figure 6.11. Normal and log-normal distribution

As a result of their analysis they found that a coefficient  $C = 0.12$  would be a good lower bound. In Fig. 6.12 it is shown that the prediction accuracy of this equation is substantially better than that of the old EC-1992-1-1 formula.

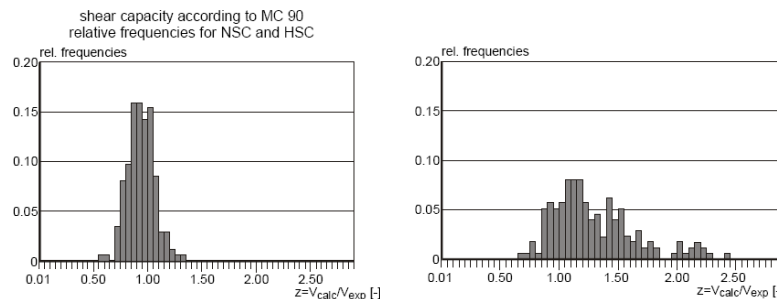


Figure 6.12. a. Shear capacity according to Eq. 6.8 (MC 90): relative frequency for NSC and HSC (König, Fischer, 1993)  
 b. Shear capacity according to Eq. 6.7 (ENV 1992-1-1): relative frequency for NSC and HSC, according to König, Fischer (1993)

As an addition Fig. 6.13 shows an evaluation carried out by Regan [Regan, 1993], which confirms the findings by König/Fischer.

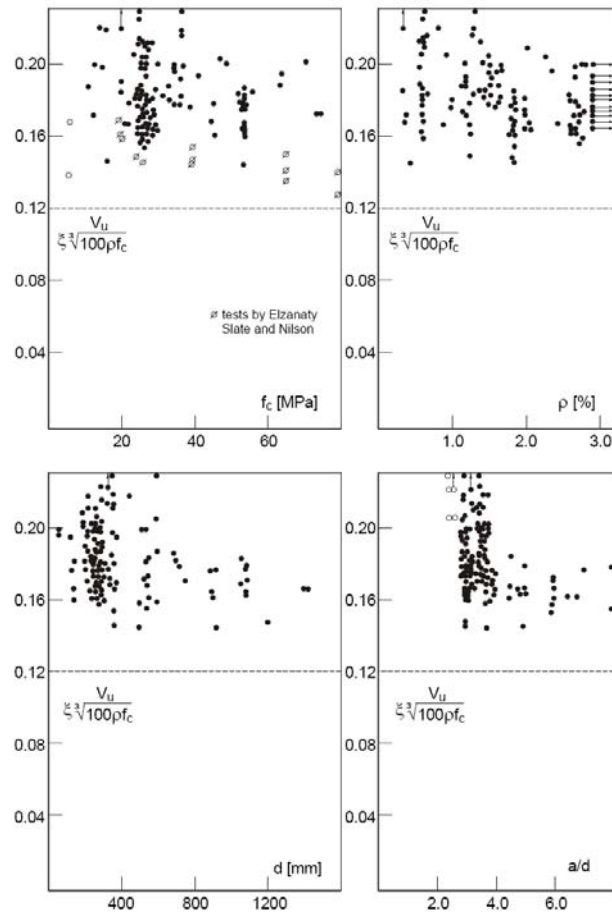


Figure 6.13. Shear strength of non-prestressed members without shear reinforcement, comparison of test results with Eq. 6.8 [Regan, 1999.]

It was however argued, that the equation

$$V_{Rd,c} = 0,12 k (100 \rho_l f_{ck})^{1/3} b_w d \tag{6.11}$$

has two disadvantages the first is that it does not distinguish between persistent & transient loading combinations and accidental loading combinations, for which different safety levels apply (prEN 1992-1-1:2001 chapter 2.4.1.4 gives  $\gamma_c = 1,5$  for persistent and transient and  $\gamma_c = 1,2$  for accidental situations). Therefore the equation was modified by introducing the concrete safety factor explicitly.

$$V_{Rd,c} = (0,18/\gamma_c) k (100 \rho_l f_{ck})^{1/3} b_w d \tag{6.12}$$

The second is that the shear capacity goes to 0 when  $\rho_l = 0$ .

Furthermore it was wished to have a simple conservative value for  $V_{Rd,c}$  for a first check of the bearing capacity. In many countries simple formulations have been used on the basis of

$$V_{Rd,c} = C f_{ctd} b_w d \tag{6.13}$$

where  $f_{ctd}$  is the design tensile strength of the concrete and C is a coefficient. Practice in the various countries however is quite different because C varies in the range from 0,3 to 0,75.

Considering the value of C it should be noted that this equation is a simplification of the rigorous one. To have general validity, even for rare but still possible cases, C should be based on the most unfavourable combination of parameters. That means that the governing case is a slab with a large cross-sectional depth d and a low longitudinal reinforcement ratio.

In his paper “Basic facts concerning shear failure”, Kani (1966) showed that shear failures are unlikely to occur for longitudinal reinforcement ratio’s smaller than 0,6%. However, his “shear valley” was based on beams with a cross-sectional effective depth of only  $d = 270$  mm. For larger depths the critical value of  $\rho_0$  decreases. Therefore a number of shear failures reported in literature have been selected with large d and small  $\rho_0$  values, see Table 6.8.



**Table 6.8. Determination of C on the basis of selected tests**

Aster, Koch (1974)

Beam	D (mm)	B (mm)	a/d	$\rho_0$ (%)	$f_{cm}$ (Mpa)	$V_{u,exp}$ (Mpa)	$f_{ck}$ (Mpa)	$f_{ctm}$ (Mpa)	$f_{ctk}$ (Mpa)	C
2	250	1000	3,7	0,64	27,5	0,88	19,5	2,17	1,52	0,58
3	250	1000	3,7	0,91	27,6	0,90	19,6	2,18	1,52	0,59
11	500	1000	3,7	0,46	28,4	0,53	20,4	2,24	1,56	0,34
12	500	1000	3,7	0,65	27,6	0,66	19,6	2,18	1,52	0,43
16	750	1000	3,7	0,42	28,3	0,53	20,3	2,23	1,56	0,34

Walraven (1978)

A1	125	200	3	0,83	27,5	1,19	19,5	2,17	1,52	0,78
A2	420	200	3	0,74	27,5	0,84	19,5	2,17	1,52	0,55
A3	720	200	3	0,79	27,5	0,70	19,5	2,17	1,52	0,46

Mathey, Watstein (1963)

Via24	403	203	3,8	0,47	26,3	0,67	18,3	2,09	1,46	0,46
Via25	403	203	3,8	0,47	25,8	0,61	17,8	2,05	1,43	0,43

The most unfavourable values for C are 0,34, found for Aster&Koch's tests Nr.11 and 16, with d = 500 and 750 mm and  $\rho_0 = 0,46$  and 0,42% respectively.

So, with some rounding off a value C = 0,35 would be appropriate for the simplified design equation. In prEN 1992-1-1:2001 a value 0,40 is used. An argument might be that the utmost part of the practical cases consists of slabs with smaller depths, subjected to uniform loading, where the maximum shear force does not coincide with the maximum moment, and the reinforcement ratio's are small enough to ensure failure by bending. The seldom case of a slab spanning in one direction, with a high cross-section, a critically low reinforcement ratio and a line load just at the most critical position from the support would then have a slightly lower safety. On the other hand formula's should always be safe enough to take account of any possible (not likely) case, which would be an argument in favour of the use of 0,35.

Some questions may be raised with regard to the definition of  $b_w$  being "the smallest width of the cross-section in the tensile area". Tests on tapered cross-sections showed that there is certainly an influence of the definition of the web width, as shown in Fig. 6.14, left (tests by Leung, Chew and Regan, 1976). Fig. 6.14, right, shows that a definition of  $b_w$  as the average width of the beam would be appropriate for this case.

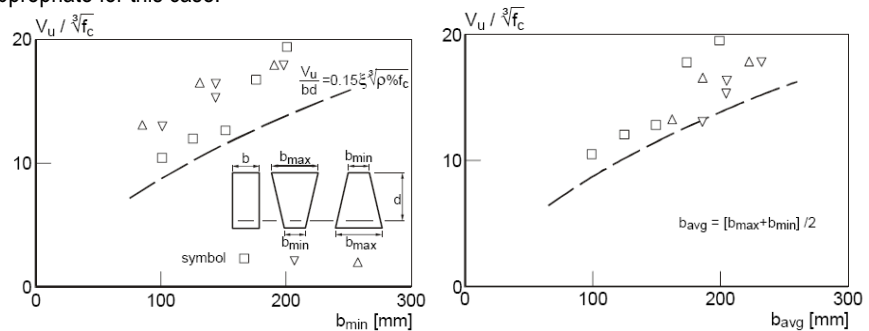


**Figure 6.14. Shear resistance of beams with tapered cross-section (Leung, Chew and Regan, 1976)**

In a more recent publication (Regan, 2000) the author opts for a definition of  $b_w = 2/3 b_{min} + 1/3 b_{max}$ , but admits at the same time that the available evidence is rather scarce. A possible compromise could be to define  $b_w$  as the average width of the part of the cross-section in tension, with a maximum of 1,25 of the minimum width.

The equations in prEN 1991-1-1:2001 contain as well a term  $0,15 \sigma_{cp}$  regarding the influence of an axial force on the shear capacity, for instance by prestressing. Basically the influence of prestressing can be taken into account as proposed by Hedman & Losberg (1978). It was argued that, with regard to the behaviour in shear, a prestressed beam can be regarded as a reinforced beam after the decompression moment has been reached. On the basis of this argument the shear resistance was formulated as

$$V_{Rd,c} = V_c + V_p$$

where  $V_c$  is the shear resistance of a similar non-prestressed beam and  $V_p$  is the contribution of the prestressing force to the shear capacity, which can be formulated as  $V_p = M_0/a$ , where  $M_0$  is the decompression moment and  $a$  is the distance from the load to the support, Fig. 6.15.

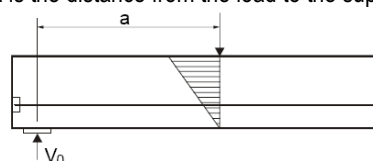


**Figure 6.15. Calculation of contribution  $V_p$  from prestressing to the shear resistance according to Hedman and Losberg (1978)**

However, this method works well for the evaluation of laboratory tests but is less suitable for real

members mostly subjected to uniformly distributed loading. A solution is to replace  $M_0/a$  by  $M_0/(M_x/V_x)$ , where  $M_x$  and  $V_x$  are the bending moment and the shear force in the section considered. However, this would complicate the shear design because then  $V_p$  would be different in any cross-section.

Another disadvantage is that  $V_p$  would go to infinity in a moment inflexion point, where  $M_x = 0$ .

It can simply be derived that for a rectangular cross-section with a width  $b$ , a height  $h$  and an eccentricity of the prestressing force  $e_p$ , the contribution  $V_p$  to the shear resistance is

$$V_p = F_p (1/6 + e_p/h) (a/h) \tag{6.14}$$

Assuming  $d = 0,85h$  this would result in;

$$V_p = 1,18 F_p (1/6 + e_p/h) (a/d) \tag{6.15}$$

In most tests on shear critical beams the ratio  $e_p/h$  is about 0,35. With  $a/d$  varying between 2,5 and 4,0, like in most shear tests, this would mean that  $V_p$  would vary between  $0,15\sigma_{cp}b d$  and  $0,25\sigma_{cp}b d$ . Evaluating test results it is therefore not amazing that the coefficient 0,15 turns out to be a safe lower bound in shear critical regions.

Nielsen (1990) compared the shear equation in ENV 1992-1-1 which gives about the same results as Eq. 6.2a in prEN 1992-1-1:2001 for moderate concrete strengths, with 287 test results and found that it was at the safe side.

The effect of longitudinal compression should, of course, not be mixed up with the effect of the cable curvature, which exerts a favourable transverse load on the member. This effect, known as the load balancing effect, is introduced as a load (load balancing principle).

For axial tension in prEN 1992-1-1 the same formula is used, with a different sign for  $0,15\sigma_{cp}$ , so that an axial tensile force gives rise to a slight reduction of the shear capacity. It should be noted that in continuous beams there is tension in both top and bottom and excessive curtailment at sections of contra flexure may lead to diagonal cracking and shear failure in such a region. This was the main cause of failure in an actual structure [Hognestad and Elstner, 1957]. If a structural member is well designed for axial tension the shear capacity of the members is hardly reduced.

This was for instance shown by Regan [Regan, 1971 and 1999] who carried out a systematic investigation into the effect of an axial tensile force on the shear capacity of both members unreinforced and reinforced for shear. Tests have been carried out according to the principle shown in Fig. 6.16. Beams with a rectangular cross-section were provided with nibs, enabling the transmission of an axial tensile force in the middle part. The axial tensile force varied between 0 and 130 kN. The force could be applied in two ways: before subjecting the member to transverse loading, or in proportion to the transverse loading. In both cases the shear capacity was hardly influenced, although the member sometimes showed wide open cracks across the total cross section in the moment inflexion region.

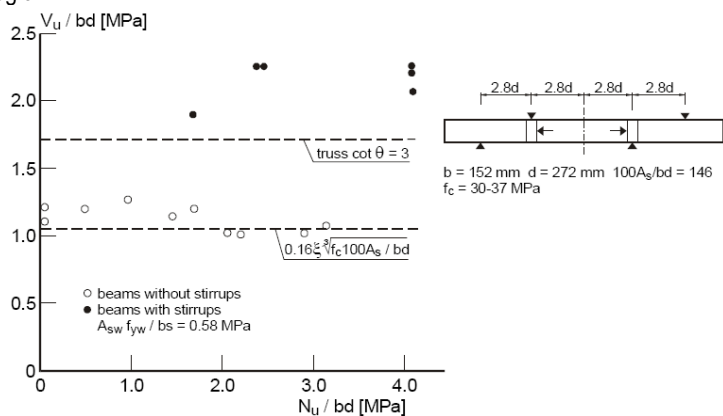


Figure 6.16. Results of tests on beams subjected to axial tension, bending and shear, and failing in shear [Regan, 1999]

For similar arguments, reference is made to [Bhide and Collins, 1989]

**6.2.2.2 Shear tension capacity**

In special cases, like for instance when pretensioned strands are used in members with reduced web widths, such as in prestressed hollow core slabs, shear tension failures can occur, Fig. 6.17.

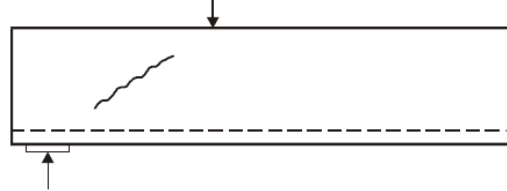


Figure 6.17. Shear tension failure

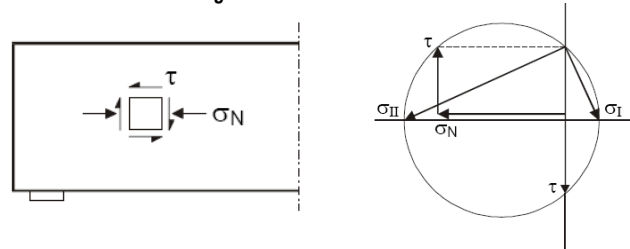


Figure 6.18. Calculation of shear tension capacity with Mohr's circle

In this case failure occurs due to the fact that the principal tensile stress in the web reaches the tensile strength of the concrete in the region uncracked in flexure. The principal tensile strength in the web calculated using Mohr's circle, Fig. 6.18, is equal to

$$\sigma_I = -\frac{1}{2}\sigma_N + \sqrt{\left(\tau^2 + \frac{1}{4}\sigma_N^2\right)} \tag{6.16}$$

substituting  $\tau = V_{Rd,ct} S/b_w l$  and  $\sigma_N = \alpha_l \sigma_{cp}$  the code's expression EC-2, Eq. 6.3

$$V_{Rd,ct} = \frac{l \cdot b_w}{S} \sqrt{\left(f_{ctd}\right)^2 - \alpha_l \sigma_{cp} f_{ctd}} \tag{6.17}$$

is obtained.

**6.2.2.3. Loads near to supports**

In 6.2.2 (5) the equation (5) or in prENV 1992-1-1:2001 the Equation 6.2.a, is extended with a factor  $(2d/x)$  in order to cope with the increased shear capacity in the case of loads applied near to supports. According to this formulation, at a distance  $0.5d < x < 2d$  the shear capacity may be increased to

$$V_{Rd,ct} = 0,12 k (100 \rho_l f_{ck})^{1/3} (2d/x) b_w d. \tag{6.18}$$

This may need some explanation, since it might be argued that loads near to supports may be treated with the rules given in EC-2, 2001 version, chapter 6.5 "Design of discontinuity regions with strut and tie models".

However, there are many arguments in favour of the formulation according to Eq. 6.18:

- According to the formulations for the strut and tie model the capacity of the concrete struts only depends on the strength of the concrete, see e.g. fig. 6.19.

Consequently, the maximum capacity is a function of the concrete strength and the width of the support area.

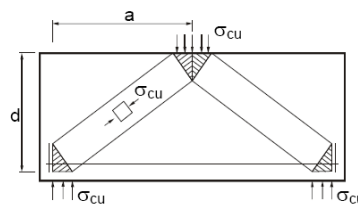


Figure 6.19. Bearing capacity of short member according to strut and tie model with defined maximum concrete stress in the struts

It can easily be seen that this is a very simplified representation of reality, since the capacity of such a member results to be independent of the slenderness ratio  $a/d$ , which is known to have a strong influence. Furthermore short members are prone to significant size effects. It was shown [Lehwalter and Walraven, 1994], that the size effect in short members is the same for short and slender members, so that here also the factor  $k = 1 + \sqrt{(200/d)}$  applies.

Lehwalter carried out tests on short members with various sizes,  $a/d$  ratio's and support widths, and compared the equivalent maximum stress in the concrete struts, Fig. 6.20. The dotted plane is valid for a maximum stress  $0,6 f_c$ . It is seen that for lower  $a/d$  ratio's the capacity is considerably higher than the one obtained with the strut and tie model. It is seen furthermore that the limit  $0.55 f_c$  as

defined in 6.4.5 5(P) for struts with transverse tension is appropriate for  $a/d < 2.0$ , members with depths until 1 m and a support width up to about 0.25d.

For a number of practical members, like in the case of corbels and pile caps, it is important to reduce the size as much as possible. A more accurate formulation than the strut and tie model is therefore useful in those cases.

- Another case is shown in Fig. 6.21. It is a part of a foundation caisson in the Storebaelt bridge, with a slab of about 1 meter and wall distances of about 5 m. A substantial part of the counterpressure of the soil is transmitted directly to the walls, so that the governing shear load is small. Without a provision like the one given in Eq. 10, unnecessary shear reinforcement would be required.

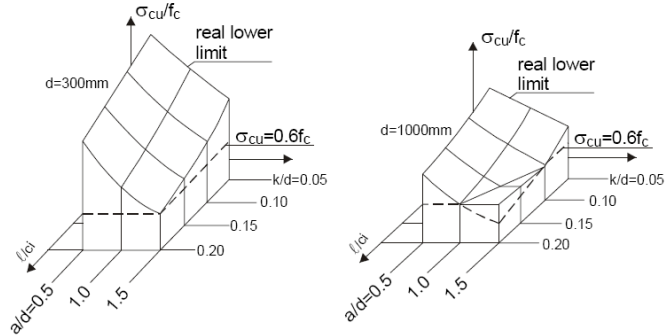


Figure 6.20. Maximum stress in concrete struts as calculated on the basis of test results (Walraven, Lehwalter, 1989)

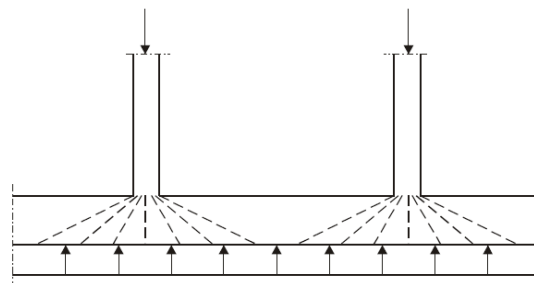


Figure 6.21. Foundation slab in Storebaelt caisson

By introducing the distance  $x$  and determining the shear capacity in every cross section, also combinations of loads (like two concentrated loads, or a uniformly distributed load and a concentrated load) can be handled.

An important question is whether the multiplication factor should be  $(3d/a, 2.5d/a$  or  $2d)$ . Regan [1998], on the basis of the analysis of many experiments, concluded that:

- For simply supported beams subjected to concentrated loads a factor  $(2.5d/a)$  is appropriate. This is confirmed in Fig. 6.22 on the basis of tests by Baldwin and Viest (1958), Clark (1951), De Cossio and Siess (1960), Küng, Lehwalter (198 ), Matthey and Watstein (1963), Morrow and Viest (1957), Regan (1971) and Rogowski and MacGregor (1983)
- For continuous beams with concentrated loads even  $(3d/a)$  gives safe results.
- For simply supported beams subjected to distributed loading only  $(2d/a)$  gives safe results. The diagram in Fig. 6.23 is based on tests by Bernaert and Siess (1956), Leonhardt and Walther (1961), Rüschi, Haugli, Mayer (1962) and Krefeld and Thurston (1966). The figure shows graphs of  $V_{test}/V_{calc}$  plotted against  $l/d$ , with  $V_{calc}$  computed assuming values of  $2d/x$  and  $2.5d/x$ . Most, but not 95% of the points lie above  $V_{test}/V_{calc} = 1$  for  $2d/x$ , but less than half do so with  $2.5d/x$ . The results which are on the unsafe side with  $2d/x$  need not to be of too much concern as Krefeld and Thurston's work includes many beams with low concrete strengths.

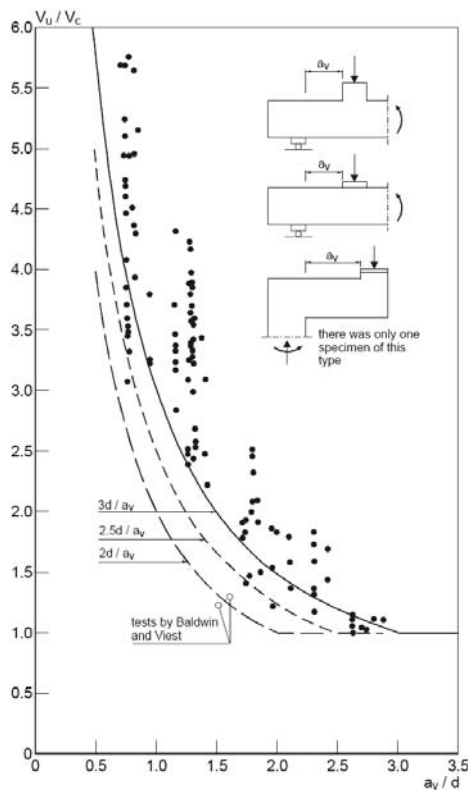


Figure 6.22. Results of tests on simply supported beams without shear reinforcement subjected to concentrated loads (Regan, 1998)

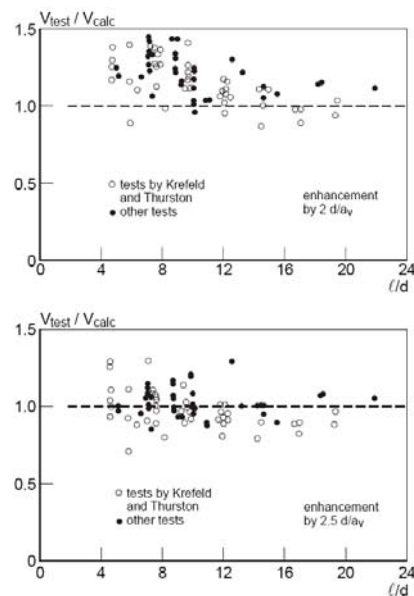


Figure 6.23. Results of tests on simply supported beams without shear reinforcement subjected to distributed loads (Regan, 1998)

**6.2.2.4. Prestressed members without shear reinforcement**

Four failure modes may be envisaged under combination of shear and bending within the extremity region for such elements:

1. Exceeding the tensile strength of concrete in regions uncracked in bending as described by expression (6.4).
2. Exceeding the shear resistance given by expression (6.2a) in presence of bending moments greater than the cracking bending moment.
3. Anchorage loss due to bending cracks within transmission length.
4. Snap back failure at cracking bending moment outside the transmission length, when the acting shear corresponding to the cracking bending moment exceeds the bearing capacity calculated with expression (6.2a).

The designer should verify all the four failure mechanisms described above with particular care to the snap back behavior.

**6.2.3 Members requiring design shear reinforcement**

**C6.2.3 Members requiring shear reinforcement.**

**6.2.3.1 Non prestressed members**

In ENV 1992-1-1 the Standard Method and the Variable Inclination Method were offered as design alternatives. The Standard Method, in spite of its acceptable accuracy, is from a physical point of view unsatisfactory, because the “concrete term” is purely empirical and hides the physical reality. This reality is, that a redistribution of forces occurs in the webs of shear reinforced concrete beams, resulting in strut inclinations smaller than 45°, Fig. 6.24.

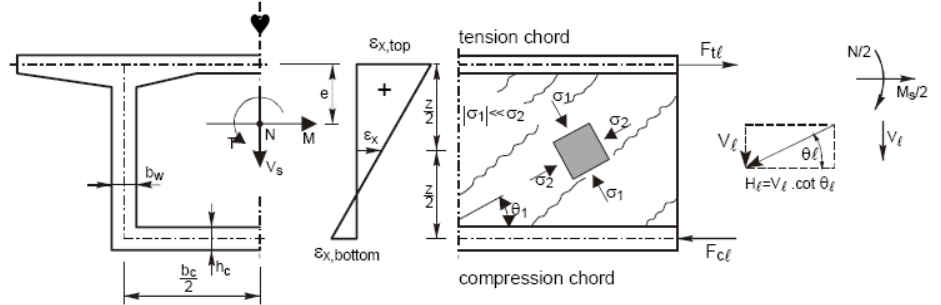


**Figure 6.24.** Redistribution of forces in a shear-loaded web by strut rotation

Because of a smaller strut inclination, a larger number of stirrups is activated, and the shear capacity is increased. A result of the smaller strut inclination is, however, that the stresses in the concrete struts are larger, so that an appropriate upper limit to the shear capacity has to be defined. This method, with strut inclinations smaller than 45° may be assumed for design, and is known as the “variable strut inclination” method. This approach is not only attractive because of its agreement with the physical reality, but also because it is a simple equilibrium method, giving a transparent view of the flow of forces in the structure.

In ENV 1992-1-1, in chapter 4.3.2.4.4, the designer is allowed to choose the strut inclination between  $0,4 < \cot \theta < 2,5$

which means that  $\theta$  may be chosen between 21,8° and 68,2°. The choice of the lowest value mostly leads to the most economic design. In this case the compression struts are supposed to rotate from an initial value of 45° to a lower value of about 22°. If the strut inclination is  $\theta$  and the (vertical) shear reinforcement yields, a shear force

$$V_{u,3} = \frac{A_{sw}}{s} \cdot z \cdot f_{yw} \cdot \cot \theta \tag{6.19}$$

is transmitted, Fig. 6.25a. If the shear reinforcement yields, the truss can, by rotation of the compression struts to a lower inclination, activate more stirrups for the transmission of the shear force and, as such, extend the zone of failure.

Due to strut rotation, the stress in the concrete struts increases. Consequently, rotation can only continue until crushing of the concrete occurs. For an ultimate compression stress  $f_{c1}$  in the concrete struts, the corresponding shear force is (Figure 6.25b).

$$V_{u,2} = \frac{b_w \cdot z \cdot f_{c1}}{\cot \theta + \tan \theta} \tag{6.20}$$

where  $f_{c1} = v f_c$

In those equations

- $b_w$  web width
- $z$  inner lever arm  $\cong 0,9d$
- $s$  stirrup distance
- $f_{yw}$  yield stress of stirrups
- $\theta$  inclination of concrete struts
- $A_{sw}$  cross-sectional area of one stirrup
- $v$  effectiveness factor, taking account of the fact that the beam web, which is transversally in tension, is not as well suited to resist the inclined compression as cylinders used to determine  $f_c$ .

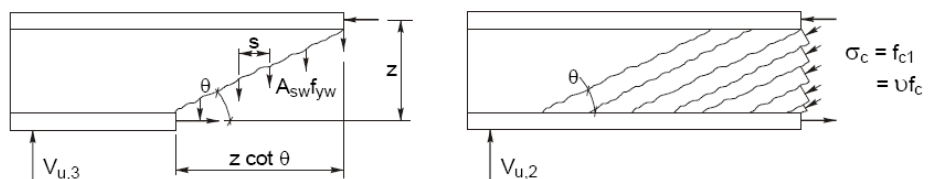


**Fig. 6.25.** a. Ultimate capacity  $V_{u,3}$  for yielding stirrups  
b. Ultimate capacity  $V_{u,2}$  for crushing of concrete struts

For  $v$  generally the expression

$$v = 0,6 (1 - f_{ck}/250) \tag{6.21}$$

is used (CEB-FIP Model Code 1990).

By equalling 6.19 and 6.20 the maximum possible shear force and the corresponding inclination  $\theta$  are found. Fig. 19 shows the development of  $V_{u,2}$  and  $V_{u,3}$  for decreasing  $\theta$ .

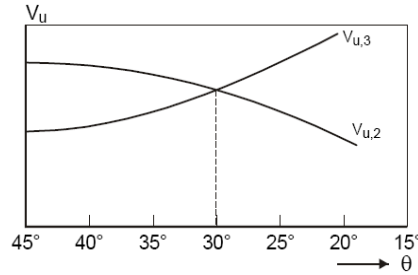


Figure 6.26. Dependence of  $V_{u,2}$  and  $V_{u,3}$  on the strut inclination  $\theta$

The expression for the ultimate nominal shear strength  $v_u$  and the corresponding value of  $\theta$  are then

$$\frac{v_u}{f_{c1}} \sqrt{\psi(1-\psi)} \tag{6.22}$$

And

$$\tan\theta = \sqrt{\frac{\psi}{1-\psi}} \tag{6.23}$$

Where

$$v_u = \frac{V_u}{(b_w \cdot 0,9d)} \tag{6.24}$$

$$\psi = \frac{\rho_{sw} f_{yw}}{f_{c1}} \tag{6.25}$$

with

$$f_{c1} = v f_c$$

and  $\rho_w$  is the shear reinforcement ratio according to  $\rho_w = A_{sw}/b_w s$ .

Eq. 6.22 represents a circle in a  $V_u/f_{c1} - \psi$  coordinate system, Fig. 6.27. It is found that when  $\psi$  runs from 0 to 0.5,  $\theta$  runs from 0 to 45°. For  $\psi > 0.5$ , the value of  $\theta$  is constant and equal to 45°. However, it was assumed that  $\cot \theta = 2,5$  is a limit. In graphical terms this is shown as the linear cut-off in Fig. 6.27.

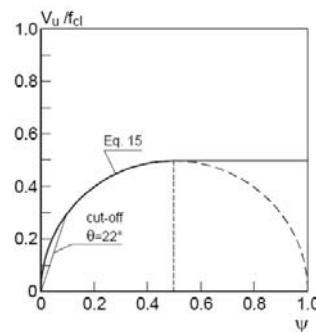


Figure 6.27. Graphical representation of Eq. 16, with cut-off for  $\cot \theta = 2,5$

Measurements of the deformation of the web in shear loaded I-beams show typically a behaviour as shown in Fig. 6.28. The diagram shows lines numbered from 1 to 4.

- Line 1 In the beginning of shear loading the beams is uncracked in shear so that the principal strain direction is 45°.
- Line 2 At the formation of inclined shear cracks the principal strain direction decreases
- Line 3 After having reached the stabilized inclined crack pattern a new type of equilibrium is obtained. The behaviour is elastic: the (constant) principal strain direction depends on the "stiffness ratio" in the cracked state.
- Line 4 When the stirrups start yielding the web searches for a new state of equilibrium. By rotating down to a lower inclination the beam activates more stirrups to carry the load. In the mean time the compressive stress in the concrete increases. When the crushing strength of the struts is reached the beam fails in shear.

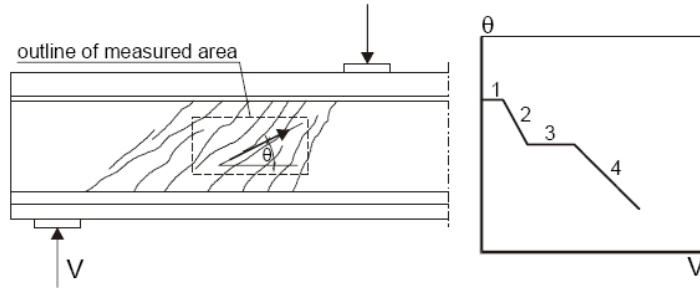


Figure 6.28. Rotation of the concrete struts as measured on the web of beams with shear reinforcement, schematically represented (Walraven, 1995 and 1999)

Fig. 6.29a shows the strut rotation as measured in three beams with different shear reinforcement ratio's (L = low, M = medium and H = High). It can be seen that for M and H the beams fail before the stirrups have yielded. Fig. 6.29b shows a similar diagram for a series of high strength concrete beams ( $f_c \approx 90 \text{ N/mm}^2$ ).

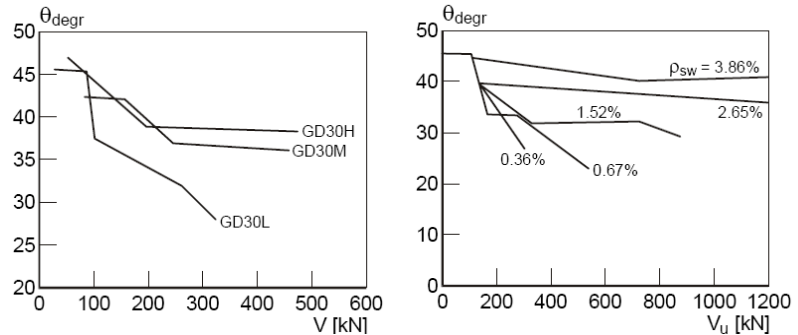


Figure 6.29. a. Strut rotation as measured in beams with normal strength concrete (Walraven, 1995)  
 b. Strut rotation as measured in beams made of high strength concrete (Walraven, 1999)

Fig. 6.30 shows a verification of the combination of Eq. 6.19 and Eq. 6.20 with the limit  $\cot \theta = 2.5$  with test results from Sørensen (1974), Regan and Rezai-Jorabi (1987), Placas and Regan (1971), Leonhardt and Walther (1961), Kahn and Regan (1971), Moayer and Regan (1971), Hamadi and Regan (1980), Muhidin and Regan (1977), Levi and Marro (1993) and Walraven (1999).

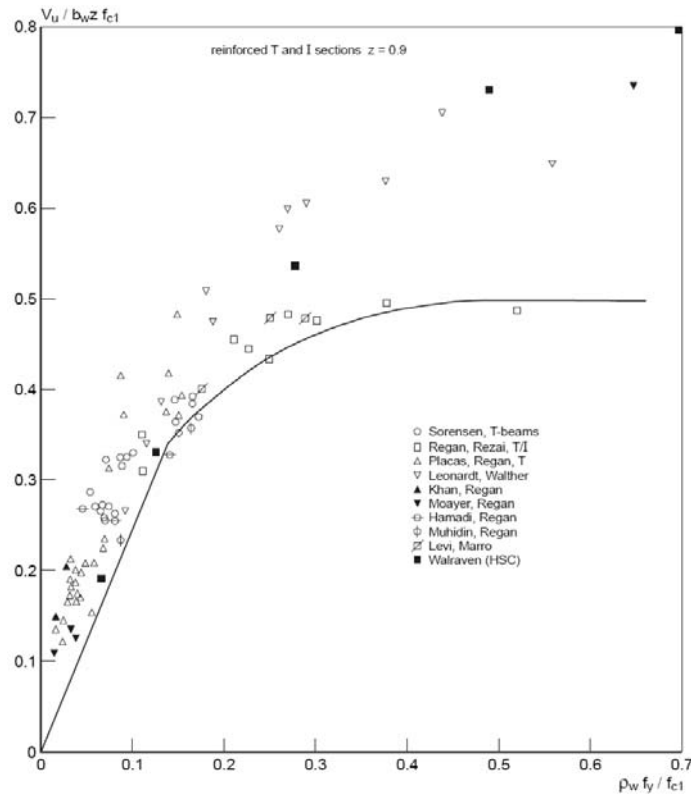
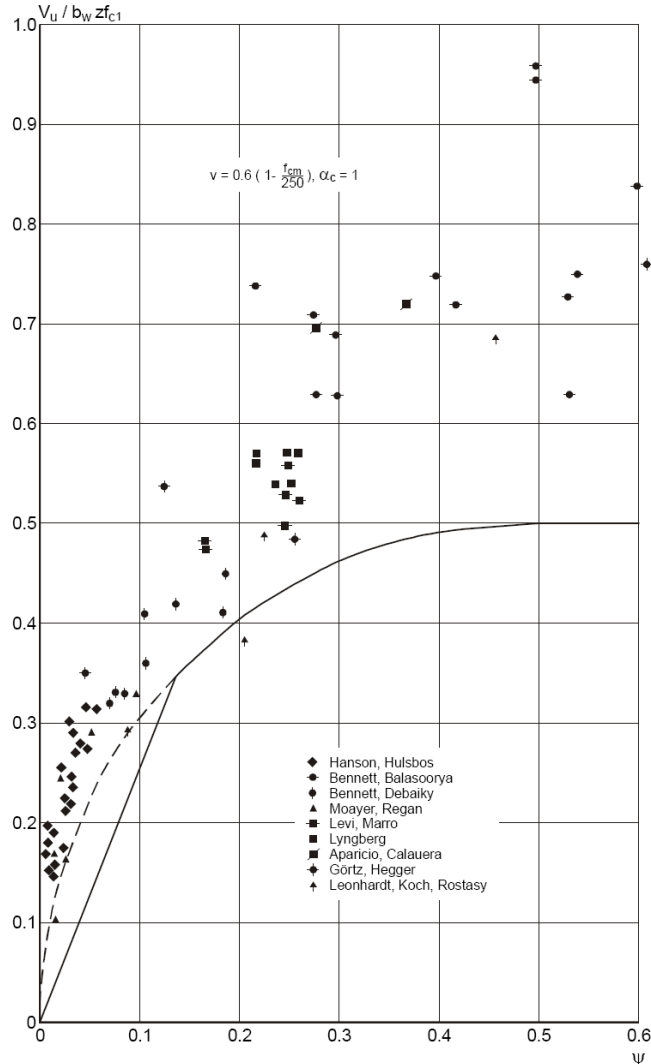


Figure 6.30. Non prestressed beams with vertical stirrups – relationship between shear strength and stirrup reinforcement



**6.2.3.2. Prestressed members with shear reinforcement**

If the same rules are applied to prestressed members with shear reinforcement, like in ENV 1992-1-1 and MC'90, it can be seen that there is apparently an increase of both safety and scatter, Fig. 6.30. The test used for this figure are from Hanson and Hulsbos (1964), Bennett and Debaiky (1974), Moayer and Regan (1974), Levi and Marro (1993), Lyngberg (1976), Aparicio and Calavera (2000), Görtz and Hegger (1999), Leonhardt, Koch and Rostasy (1974). Many of the test results are collected in a databank, described in (Walraven, 1987).



**Figure 6.31.** Experimental results of shear tests on prestressed beams with shear reinforcement, in comparison with the calculated results according to the variable strut inclination method (no special web crushing criterion for prestressed concrete)

In ENV-1992-1-1 the effect of prestressing on the upper limit of the shear capacity  $V_{Rd,i}$  is partially neutral and partially negative. In 4.3.2.2 (4). The following statement is found:

“In the absence of more rigorous analysis, at no section in any element should the design shear force exceed  $V_{Rd,2}$ . Where the member is subjected to an applied axial compression,  $V_{Rd,2}$  should be in accordance with the following equation:

$$V_{Rd,red} = 1.67 V_{Rd,2} (1 - \sigma_{cp,eff}/f_{cd}) < V_{Rd,2} \tag{6.26}$$

Fig. 6.32 shows the dependence of the upper limit for the shear capacity on the level of prestressing.

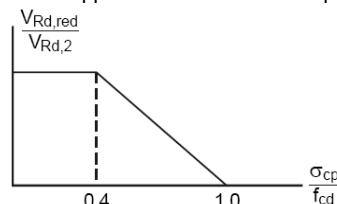


**Figure 6.32.** Reduction of maximum shear capacity by axial compressive stress according to ENV 1992-1-1, Clause 4.3.2.2 (4)

In his "Commentaries on Shear and Torsion", Nielsen (1990) states that prestressing has a positive influence on the shear capacity of beams with shear reinforcement. He proposed to multiply  $v$  (which was then equal to  $v = 0.7 - f_{ck}/200 > 0.5$ ) with a factor

$$\alpha_c = 1 + 2.0 \sigma_{cp,eff} / f_c \quad \text{with } \sigma_{cp,eff} / f_c < 0,5 \quad (6.27)$$

A comparison with 93 tests results shows, however, that the expression is not sufficiently conservative, to serve as a safe lower bound over the whole region of test results, Fig. 6.33. It should furthermore be noted that all test results, used in the comparison, have ratio's of  $\sigma_{cp}/f_c$  lower than 0,4 and that the multiplication factor is obviously applicable only for this region.

Another proposal for taking the influence of prestressing into account in the  $v$ -value was given by Fouré (2000):

- for small compression, with  $0 < \sigma_{cp} < 0,4f_{cd}$

$$\alpha_c = (1 - 0,67 \sigma_{cp}/f_{ctm}) \quad (6.28)$$

- for large compression, with  $0,4f_{cd} < \sigma_{cp} < f_{cd}$

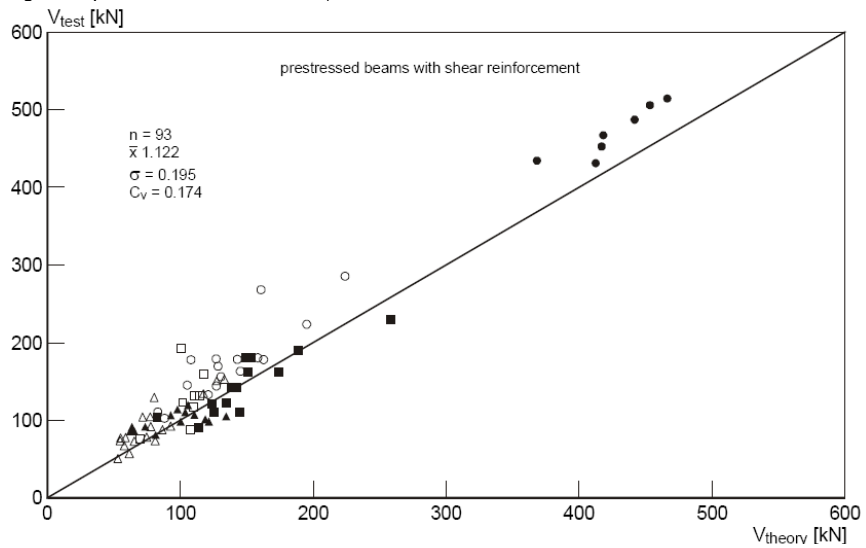


Figure 6.33. Comparison of results of shear tests with variable inclination truss analogy with effectivity factor  $v = (0,7 - f_c/200)(1 + \sigma_{cp}/f_c)$ , according to Nielsen (1990)

$$\alpha_c = \{1,2 (1 - \sigma_{cp}/f_{cd}) (1 + \sigma_{cp}/f_{cd})\}^{0,5} \quad (6.29)$$

However, for the region of low compressive stresses this expression gives about the same results as Eq. 6.27

A more moderate expression, taking into account the influence of prestressing, is

$$\alpha_c = (1 + \sigma_{cp}/f_c) \quad \text{for } 0 < \sigma_{cp}/f_c < 0.25 f_c$$

$$\alpha_c = 1.25 \quad \text{for } 0.25f_c < \sigma_{cp} < 0.5f_c$$

$$\alpha_c = 2.5 (1 - \sigma_{cp}/f_c) \quad \text{for } 0.5f_c < \sigma_{cp} < 1.0f_c$$

In Fig. 6.35 the same data as used in Fig. 6.31 are evaluated using Eq. 6.29. It appears that the safety margin and the scatter are reduced (the details of the calculation are found in Appendix 1). The new proposal is compared with the other ones in Fig. 6.34.

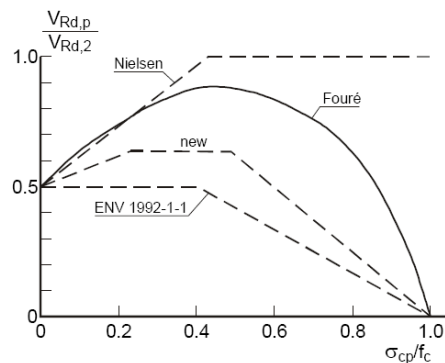


Figure 6.34. Comparison of new proposal (Eq. 6.29) with original formulation in ENV- 1992-1-1 (without influence of prestressing) and proposals by Nielsen (1990) and Fouré (2000) for  $f_{ck}$

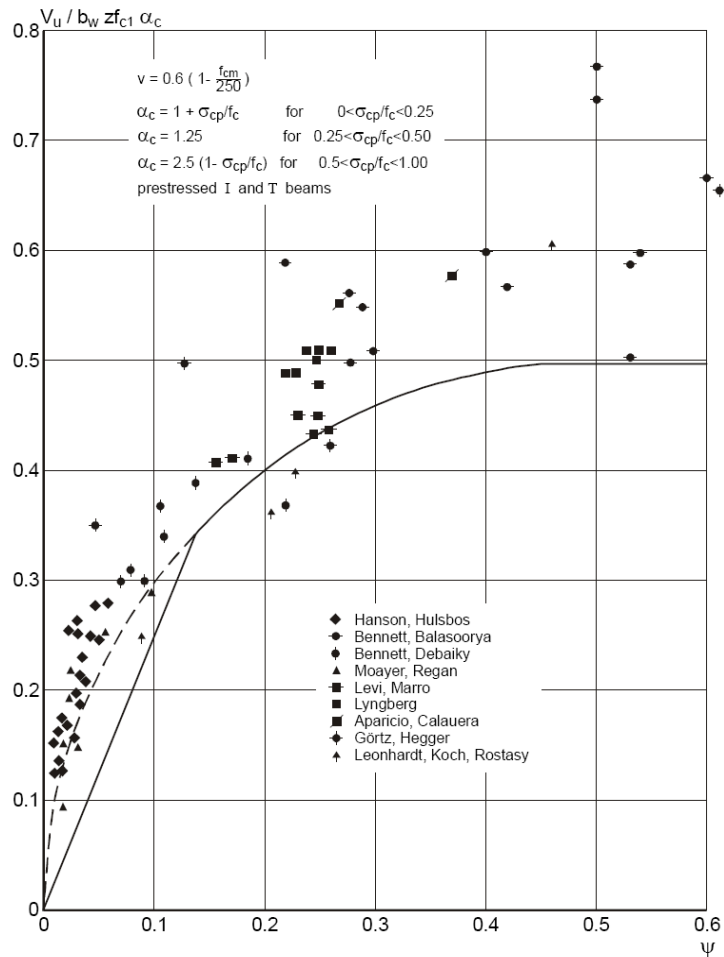


Figure 6.35. Experimental results of shear tests on prestressed beams with shear reinforcement, in comparison with the calculated results according to the variable strut inclination method, with extension according to Eq. 6.29

**6.2.3.3. Members reinforced in shear with loads near to supports**

Similar to members without shear reinforcement, in members with shear reinforcement the load bearing capacity is increased for loads near to supports. In the Standard Method, as formulated in ENV 1992-1-1 this was taken into account by multiplying the “concrete term”, with a factor (2d/x). However, the Variable Inclination Method not containing a concrete term, it was introduced here for  $x/d < 2$ . The formulation for this case is then

$$V_{Rd} = V_{Rd,ct} + A_{sw} \cdot f_{ywd} \sin \alpha \tag{6.30}$$

The transmission of forces occurs according to Figure 6.36.

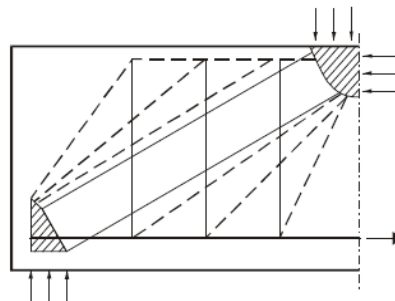


Figure 6.36. Combination of truss and strut and tie

Measurements on shear reinforcement showed that the stirrups just adjacent to the load- and support area do not reach the yield stress, (Asin, 2000). Therefore the shear reinforcement is considered to be effective only within the central 0,75 area between load and support.

**6.3 Torsion**

See example 6.6 and 6.7

6.4 Punching

C6.4. Basic equation for symmetrical punching at interior columns

6.4.1. Punching shear capacity of non-prestressed slabs without punching reinforcement

In ENV 1992-1-1 a nominal shear stress was defined as the load divided by the product the slab's effective depth and the length of the control perimeter, which was defined to located at (1.5d) from the edge of the column. The design punching shear capacity was

$$V_{Rd1} = \tau_{Rd1} \cdot u \tag{6.31a}$$

Where u is the length of the critical perimeter, taken at a distance 1.5d from the loaded area, the design shear resistance per unit length  $\tau_{Rd1}$  followed from

$$\tau_{Rd1} = \tau_{Rd} k (1.2 + 40\rho_l) d \tag{6.31b}$$

- where  $\tau_{Rd}$  basic shear strength =  $0.25 f_{ctk} / \gamma_c$
- k size factor =  $1.6 - d [m] > 1.0$
- d effective depth of slab =  $(d_x + d_y) / 2$
- $\rho_l$  flexural reinforcement ratio =  $(\rho_x + \rho_y) / 2$

It was already shown in 1980 [1], that in the derivation of this equation an error was committed, which leads to unconservative results for higher concrete strengths. Therefore it was decided adopt the formulation for the punching shear capacity given in Model Code 1990. when the design punching shear capacity is given by

$$V_{Rdc} = \tau_{Rdc} \cdot u \cdot d \tag{6.32a}$$

where

- u = length of the critical perimeter, taken at a 2d distance from the loaded area
- d = mean effective slab depth =  $(d_x + d_y) / 2$

and where the design punching shear stress for non-prestressed slabs value is

$$\tau_{Rdc} = 0.12 k (100 \rho_l f_{ck})^{1/3} \tag{6.32b}$$

with

- k = size factor =  $1 + \sqrt{200/d} \leq 2.0$  d in mm
- $\rho_l = \sqrt{(\rho_{lx} \cdot \rho_{ly})} \leq 0.02$
- $f_{ck}$  = characteristic cylinder strength of concrete

In the new definition, according to MC'90, the control perimeter is moved from a distance 1.5d from the column, to a distance of 2d, see Fig. 6.37. There are two reasons to adopt the distance 2d. First it makes the limiting shear stress much more uniform for different column sizes. Second now for punching the same formulation can be used as for normal shear in members without shear reinforcement, where also Eq. 6.32b is applied.

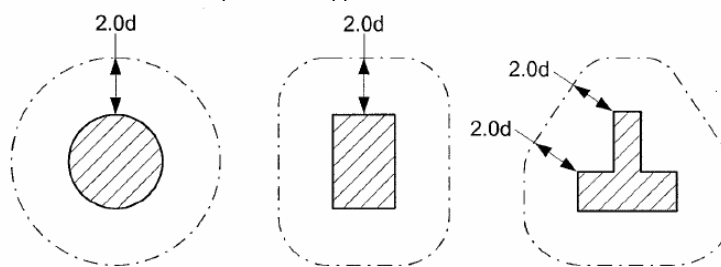


Figure 6.37. Basic control perimeters around loaded areas

Often questions are raised with regard to the coefficient 0.12 in Eq. 6.32b. Therefore at first an evaluation is carried out in order to verify this value. Altogether 112 test results have been considered, taken from [2-12]. 78 of those results refer to tests on specimens with cylinder strength ranging from 15 to 60 MPa, whereas 32 refer to tests on high strength concrete specimens with concrete cylinder strengths ranging from 60 to 120 MPa. This enables a good evaluation of the validity of the punching shear formula (Eq. 6.32a and 6.32b) for higher concrete strengths.

The tests cover the interval of individual parameters given in Table 6.9.

Table 6.9. Range of parameters in tests used for evaluation

Compressive strength on cylinders	14 - 120 Mpa
Effective slab depth	100 - 275 mm
Reinforcement ratio for bending	0.4 - 2.5%
Column diameter/effective slab thickness	1.2 - 2.5

Fig. 6.38 shows a diagram in which the values  $V_{exp} / V_{calc}$  are shown as a function of the concrete strength. The tests of Base fall somewhat outside of the scope probably due to the very small maximum particle diameter ( $D_{max} = 4,2$  mm). Those tests therefore have to be regarded with some reservation.

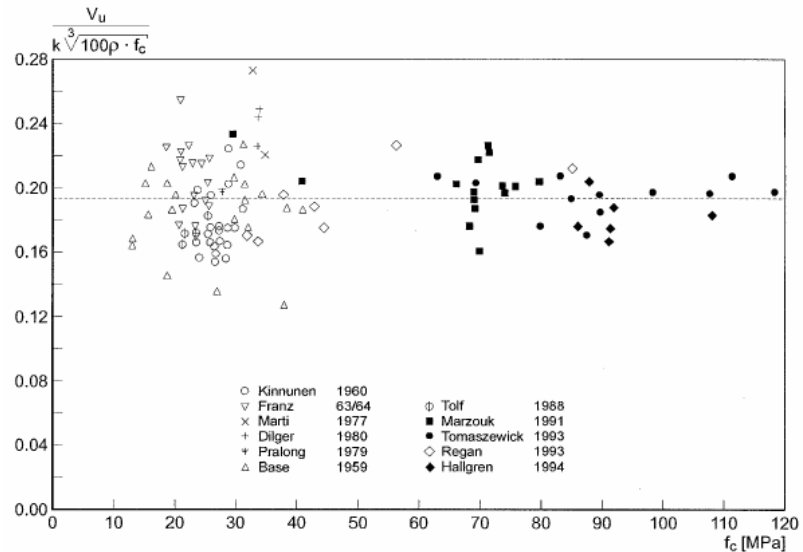


Figure 6.38. Punching strength of slabs without shear reinforcement: comparison of test results v/s eq. 6.32

Fig. 6.39 shows the frequencies of the relative punching shear capacities (ratio experimental to calculated values) for the data considered.

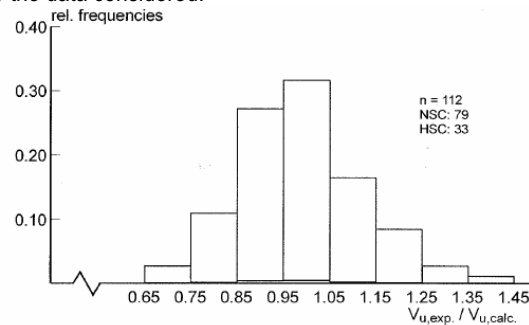


Figure 6.39. Frequencies of relative punching shear carrying capacity

Assuming a normal distribution, a mean value of 0.191 is obtained with a standard deviation of  $\delta = 0.0247$ , and a coefficient of variation  $v = 0.13$ . Strictly speaking this would mean a characteristic lower bound value of  $0.191 - 0.164 \cdot 0.0247 = 0.15$ . assuming a safety factor of 1.5 this would result in a coefficient of 0.10 in stead of 0.12 in the equation of the design punching shear stress (Eq. 6.32b). However, although the variation of the concrete strength (for which a material safety factor 1.5 applies) is the dominating factor with regard to the scatter of results in punching shear tests, the punching shear capacity is not linearly proportional to the concrete compressive strength (the  $f_{ck}$  value has an exponent 1/3 in Eq. 6.32b), so that simply applying a material safety factor 1.5 as well for the derivation of the punching shear capacity would be inappropriate.

Therefore a more sophisticated approach was necessary in order to unambiguously derive a design equation with the required level of reliability. For such a case the classical "level 2 method", as described in EC-I Basis of Design is suitable. The way how to deal with this method has been described and illustrated by Taerwe [13]. The same method was applied by König and Fischer for investigating the reliability of existing formulations for the shear capacity of members without shear reinforcement [14].

According to the level 2 method, a reliable design equation can be derived from test results with the general formulation

$$B_{Rd} = \mu_{BR} (1 - \alpha_{BR} \beta \delta_{BR}) \tag{6.33}$$

where

- $B_{Rd}$  design value
- $\mu_{BR}$  mean value of test results
- $\alpha_{BR}$  sensitivity factor for  $B_R$ , normally taken as 0.8 in the case of one dominating parameter
- $\beta$  target safety index, taken 3.8
- $\delta_{BR}$  coefficient of variation

with  $\mu_{BR} = 0.191$ ,  $\alpha_{BR} = 0.8$  and  $\delta_{BR} = 0.130$  a value for the design coefficient in Eq. 6.32b of 0.116

was obtained. In this derivation, however, the *mean* concrete cylinder compressive strength has been used, whereas in the code expression the *5%-lower value*  $f_{ck}$  is used. In the Model Code the relation

$$f_{ck} = f_{cm} - 8 \text{ (MPa)} \tag{6.34}$$

is given. This means a coefficient of variation for a concrete C25 of  $v = 0.15$  and for a concrete C90 of  $v = 0.05$ . In combination with  $B_R = 0.13$  for the punching tests this would mean an increase of the coefficient 0.116 of about 6.8 % for C25 and 3.6 % for C90 (see [14, p. 91]). This would then result in a coefficient 0.124 for a concrete class C25 to 0.120 for a concrete class C90. It can therefore be concluded that equation 6.32a,b is correct.

A disadvantage of Eq. 6.32.a,b is that they go to 0 if  $\rho$  goes to 0. This could give unrealistically low punching shear capacities for low reinforcement ratio's, that may for instance occur in prestressed slabs. Furthermore designers like to have a simple lower bound formulation for a first check.

Therefore a lower bound was added, solely depending on the concrete tensile strength, according to the relation  $v_u > C \cdot f_{ctd}$ , where  $f_{ctd} = f_{ctk} / \gamma_c$ . Evaluating the same results as shown in Fig. 6.38 with the equation  $v_u = C \cdot f_{ctk}$ , it was found that for normal strength concrete (<C50/60) a 5% lower value  $C = 0,57$  applied and for high strength concrete (>C50/60) a value equal to  $C = 0,42$ . It should however be noted that the collection of tests does not contain slabs with cross-sectional depths larger than 275 mm. In order to cope with larger slab depths used in practice the coefficient C 5% should therefore be further reduced. The value 0,35, used as a lower limit for shear as well, seems to be quite reasonable. Taking into account this lower li the design equation for non-prestressed slabs should therefore be:

$$V_{Rd,c} = (0,18/\gamma_c) k (100\rho_l f_{ck})^{1/3} > 0,35f_{ctd} \tag{6.35}$$

**6.4.2.2 Punching shear resistance of prestressed slabs without shear reinforcement.**

For shear loaded members the influence of a normal compression force is taken into account a separate contribution of  $0,15\sigma_{cp}$  to the ultimate shear stress  $v_{Rd,c}$  (prENV 1992-1-1:2001 6.2a), see also the report for shear. It is logic that also with regard to punching the effect of prestressing will be positive. It is however not expected that the same term as for shear can be used, because the contribution of prestressing to the punching resistance depends also decisively on the definition of the control perimeter.

In order to find the contribution prestressing a selection of test results has been made: Andersson [40], Gerber & Bums [41], Stahlton [42], Pralong, Brändli, Thürlimann [43] and Kordina, Nölting [44]. A comparison of the test results with the design equation:

$$V_{Rd,c} = (0,18/\gamma_c) k (100\rho_l f_{ck})^{1/3} - 0,08\sigma_{cp} > 0,35 f_{ctk} / \gamma_c - 0,08\sigma_{cp} \tag{6.36}$$

The mean value of  $v_{exp}/v_{Rd,c}$  is 1,58 and the standard variation is  $s = 0,20$ . According to Eq. 6.33, with  $\alpha = 0,8$  and  $\beta = 3,8$  the design value should be  $(1,58 - 0,8 \cdot 3,8 \cdot 0,20) v_{Rd,c} = 0,972 v_{Rd,c}$ . Actually this means that Eq. 6.36, giving values which are only slightly (2,8%) too high, is acceptable as a design equation.

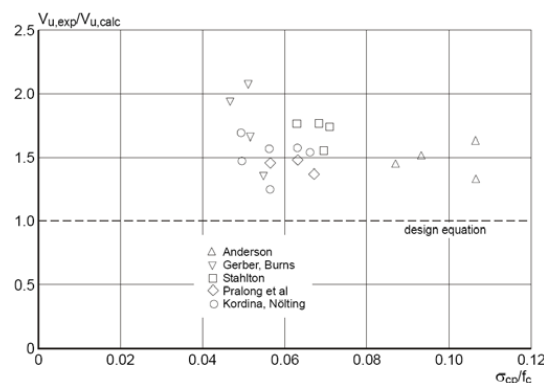


Fig 6.40. Verification of Eq. 6 with test results

**6.4.2.3 Punching shear resistance of labs with punching shear reinforcement**

In ENV 1992-1-1, Eq. 6.34, it was assumed that the contribution of punching shear reinforcement to the total shear capacity can be accounted for by

$$\Sigma A_{sw} f_{yd} \sin \alpha \tag{6.37}$$

Adding this contribution to the punching shear capacity of a similar slab without shear capacity,

according to Eq. 6.31, would give the total punching shear resistance.

A first important question is if the summation principle of a concrete component and a punching reinforcement component is valid anyhow. In the descriptive model of Kinnunen and Nylander [15] for slabs without punching reinforcement the tangential compressive strain at the bottom face of the slab is the design criterion. A punching shear reinforcement would then only be able to limit the rotation of the kinematic punching shear mechanism and as such reduce the compressive strain in the critical area, so that the failure load is increased. A further argument against the taking into account in full of the reinforcement according to Eq. 6.34 is that it is hard to find adequately anchored punching shear reinforcement at both sides of a critical crack. Therefore the punching shear reinforcement is not yet yielding when the concrete contribution is at its maximum. One can also say that due to the vertical movement of the punching cone, concrete contribution has already a reduced value at the moment that yielding of the shear reinforcement has been reached.

In literature two types of proposals are distinguished in order to cope with this phenomenon. One group of researchers, such as Moe [15], Pranz [6], Herzog [16], Petcu [17], Kordina, Nölting [18] propose efficiency factors for the contribution of the shear reinforcement ranging from 0.80 down to even 0.25. Others, like Elstner/Hognestadt [19], and Regan [20], propose to use the summation principle, however with a reduced concrete contribution (efficiency factors ranging from 0.6 to 0.8).

Fig. 6.41 shows a comparison of test results (punching failures) from Gomcs [22, 23], Yitzakhi [25] and Regan [24] with the formulation

$$V_u = 0.75V_c + V_s \tag{6.38}$$

where  $V_c$  is the concrete contribution (punching shear capacity of similar slab without shear reinforcement) and  $V_s$  is the contribution of the *yielding* steel.

In the prENV 1992-1-1:2001, the formulation according to MC'90 has been chosen, but with effective design strength of the shear reinforcement which depends on the slab depth, in order to account for the anchorage efficiency. This means that

$$V_{Rd,cs} = 0,75 v_{Rd,c} \cdot u_d + \Sigma A_{sw} f_{ywd,eff} \sin \alpha \tag{6.39}$$

where

- $v_{Rd,c}$  according to Eq. 6.32b
- $\alpha$  inclination of the shear reinforcement
- $f_{ywd,eff}$  design strength of shear reinforcement, according to  $f_{ywd,eff} = 250 + 0,25d < f_{ywd}$  (Mpa).
- $\Sigma A_{sw}$  shear reinforcement within the perimeter considered.

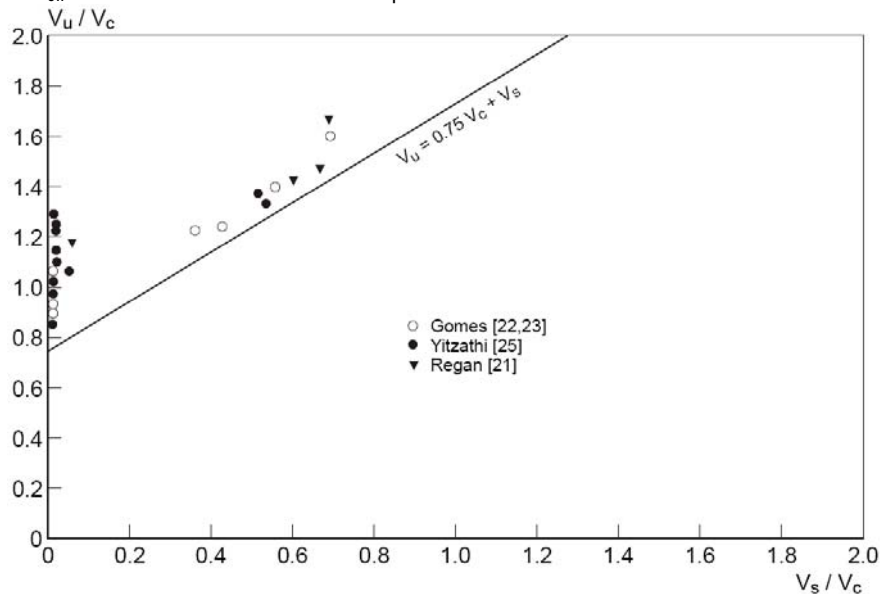


Figure 6.41. Punching capacities related to resistance of the shear reinforcement (Regan [24])

The increase of the punching shear capacity by shear reinforcement is limited to a bound. In the version of EC-2 of 1988 the upper bound was formulated as  $V_{Rd,max} = 1.4 v_{Rd1}$ , where  $v_{Rd1}$  follows from Eq. 6.31b. In a redraft in 1991 this value was increased to  $1.6 v_{Rd1}$ . This upper limit will, however, hardly be reached in practical situations, where normal punching shear reinforcement is used. However, using shear heads and shear studs, which can be more efficient than stirrups as shear reinforcement, higher values of the upper punching capacity than  $1.6v_{Rd1}$  can be reached. Therefore a

modified upper limit has been defined according to MC'90, according to

$$V_{Rd,max} = 0.5v f_{cd} u_0 d \tag{6.40}$$

where  $u_0$  is the length of the column periphery, and  $v$  is equal to

$$v = 0.60 (1-f_{ck} / 250) \tag{6.41}$$

The distance from the column to the inner shear reinforcement should not be larger than  $0.5d$ , nor should it be less than  $0.3d$ , since steel closer than this will not be well anchored in the compression zone if intersected by cracks at lower inclinations (Regan [24]). The distance between the layers of shear reinforcement in radial direction should not be larger than  $0.75d$ .

It should be verified that no punching failure occurs outside the outermost layer of shear reinforcement. Therefore an additional perimeter  $u_n$  is defined at a distance of  $1.5d$  from the outermost shear reinforcement. It should be shown that here

$$v_{Ed} < 0.12 k (100\rho_l f_{ck})^{1/3} - 0.08\sigma_{cp} \tag{6.42}$$

where  $v_{Ed}$  is the design calculated of the ultimate shear stress on the perimeter  $u_n$ , see fig. 6.42

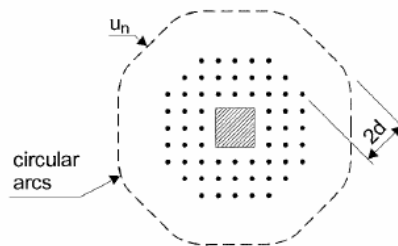


Figure 6.42. Control perimeter  $u_n$  at interior column

Practically the design of the shear reinforcement is quite simple. At first at the perimeter with distance  $2d$  from the loaded area the punching capacity is checked and the eventual shear reinforcement is calculated. Then the perimeter is determined for which  $v_{Ed} < v_{Rd,c}$ . Finally the shear reinforcement (with the same cross section per unit area) is extended to a distance  $1.5d$  from the outer perimeter.

**6.4.3. Basic equation for eccentric punching**

In the draft of 1988 only a very general approach as in combination with a bending moment. The design punching shear stress  $v_{Ed}$  was formulated as

$$v_{Ed} = (\beta V_{Ed}) / (u \cdot d) \tag{6.43}$$

where

- $V_{Ed}$  design value of the punching shear
- $\beta$  factor taking account of the expected effect of eccentricity, "in the absence of a more rigorous analysis". No further indication on what this "more rigorous analysis" means was given. In Fig. 6.43 the values for the eccentricity factor  $\beta$  are given.

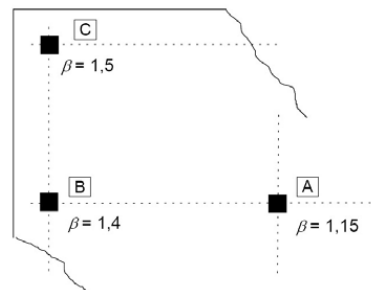


Figure 6.43. Approximate values for eccentricity factor  $\beta$  in new draft

Complementary to this simplified approach the more accurate method, given in MC'90 has been adopted in prENV 1992-1-1:2001. This method takes the effect of an unbalanced moment into account with the formulation:

$$v_{Ed} = V_{Ed} / (u_1 d) + (KM_{Ed}) / (W_1 d) \tag{6.44}$$

where  $W_1$  is a function of the control perimeter  $u_1$ :  $W_1 = \int_0^{u_1} |e| d\ell$

The property  $W_1$  corresponds to a type of "plastic" distribution of the shear stresses as illustrated in



Fig. 6.44. An analysis by Mast [34,35] on the basis of an elastic analysis of the distribution of shear stresses in a slab in the vicinity of a column showed that those stresses approach the distribution shown in Fig. 6.45 quite well. For a rectangular column  $W_1$  follows from

$$W_1 = c_1^2 + c_1 c_{12} + 4c_2 d + 17.8d^2 + 2\pi dc_1 \tag{6.45}$$

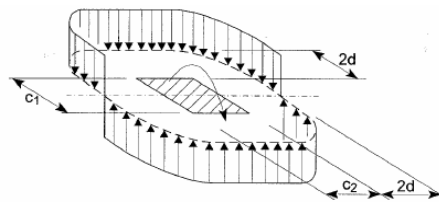


Figure 6.44. Shear distribution due to an unbalanced moment at a slab internal column connection

$K$  is a factor taking into consideration that a bending moment in the slab, is only sustained by bending in the column but also by bending and torsion in the slab itself.  $K$  follows from the table below

$c_1/c_2$	0.5	1.0	2.0	3.0
$K$	0.45	0.60	0.70	0.80

For round columns  $c_1/c_2 = 1$  so  $K = 0.6$ .

With this approach the shear capacity depends on the column size and the value of the unbalanced moment and is therefore much more accurate than from Eq. 6.40.

Fig. 6.45 shows Eq. 6.41 in comparison with tests results. The diagram is a combination of two figures, from Regan [24,36].

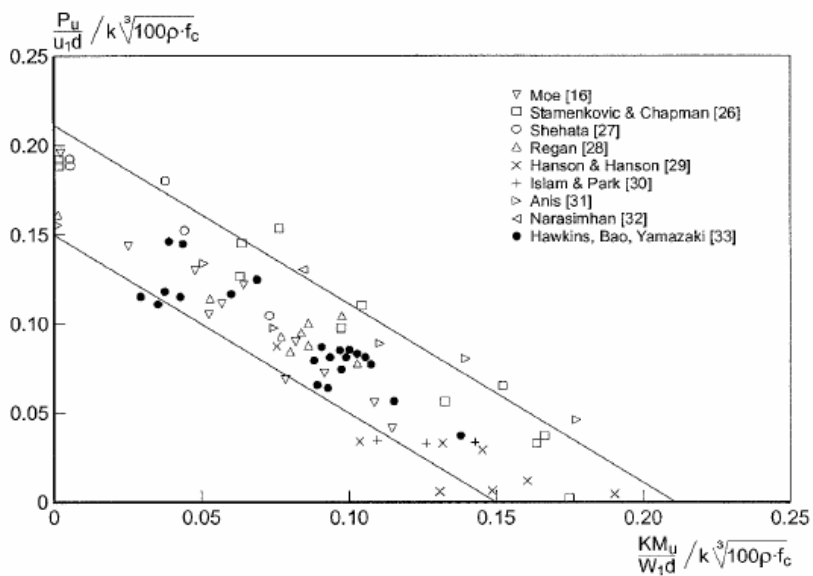


Fig 6.45. Comparison of Eq. 11 with test on interior column – slab connections

The method can be as well applied to edge and corner columns. However, in those cases the ultimate punching shear stress can as well be calculated in a simplified way assuming uniform shear on the reduced perimeter shown in Fig. 6.46.

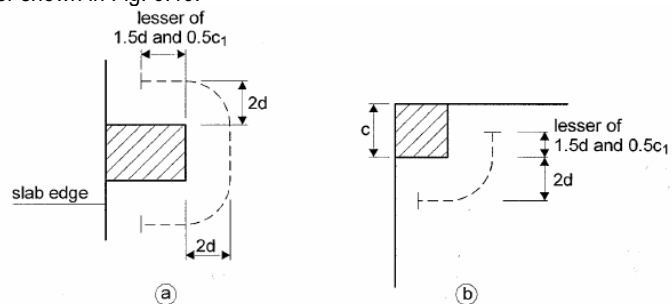


Figure 6.46. Reduced perimeters for assumed uniform shear for edge and corner columns

**6.4.3.1 Punching shear in column bases**

The most important difference between punching of a slab around a column and punching of column base supporting a column is the presence of a significant counter pressure from the soil. A second difference is that the distance from columns to the edges of their bases are commonly much smaller than those to sections of radial contra flexure in suspended slabs [38].

Due to the influence of the vertical soil pressure, the inclination of the punching cone in column bases may well be steeper than in suspended slabs, which gives rise to uncertainty with regard to the critical perimeter to be checked. This was not regarded in the EC-2 version of 1988. The CE Model Code 1990 gives an alternative, in which the position of the control perimeter is treated as a variable and the unit punching resistance, is taken to vary with the distance from the column to the control perimeter, i.e. with the inclination of the failure surface.

For concentric loading the design punching force is

$$V_{Ed,red} = V_{Ed} - \Delta V_{Ed} \tag{6.46}$$

where

$V_{Ed}$  column load

$\Delta V_{Ed}$  the upward force within the control perimeter considered i.e. upward pressure from soil minus self weight of base

$$V_{Ed} = V_{Ed,red}/u \tag{6.47}$$

where  $u$  is the control perimeter taking a value  $a < 2d$  instead of  $2d$  into account (see also fig. 6.37).

The nominal ultimate shear stress at the perimeter is

$$v_{Rdc} = 0,12 k(100\rho f_{ck})^{1/3} 2d/a < 0.5v_{fd} \tag{6.48}$$

where

$a$  distance from the periphery of the control perimeter considered

$$v = 0.60 (1 - f_{ck}/250) \tag{6.49}$$

Fig. 6.47 shows a result of a parameter study, carried out with the previous equations. For many combinations of base width to column width  $l/c$  and column width to effective slab depth  $c/d$  the critical ratio  $a_{crit}/d$  has been determined, for which the lowest column load is obtained. The results are shown in Fig. 6.47. It turns out that the ultimate column load is a function of the based to column width  $l/c$  but is independent of the ratio  $c/d$ . In the lower diagram of fig. 6.47 the design column load  $V_{Ed}$  can immediately be determined as a function of the ratio  $l/c$ . The corresponding value of the critical control perimeter  $a_{crit}/d$  is read in the upper diagram. It can be seen that in the utmost number of cases the value of  $a_{crit}$  is smaller than  $2d$ , which means indeed that the inclination of the punching cone is much steeper than in suspended slabs.

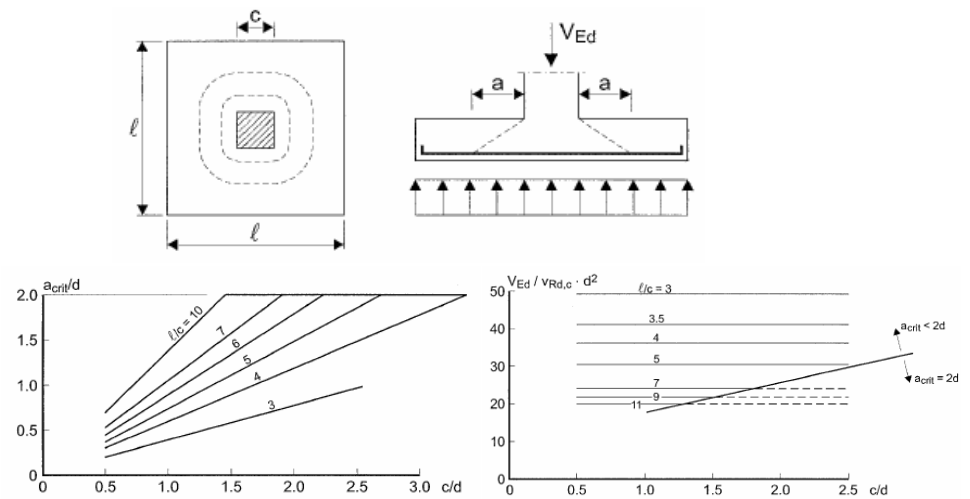


Figure 6.47. Shear capacity of column bases

**6.5 Design with strut and tie models**

See example n. 6.8 to 6.14

**6.6 Anchorages and laps**

See example n. 6.15

**6.7 Partially loaded areas**

No comments

**6.8 Fatigue**

No comments

**REFERENCES****Shear**

- Aparicio, A., Calavera, J., del Pozo, F.J., (2000) "Testing strut compression shear failure in beams", Polytechnic University of Barcelona.
- Asin, M. (2000), "The behaviour of reinforced concrete deep beams", PhD-Thesis, Delft University of Technology, The Netherlands.
- Aster, H., Koch, R. (1974), "Schubtragfähigkeit dicker Stahlbetonplatten", Beton- und Stahlbetonbau, 11/1974
- Baldwin, J.W., Viest, I.M. (1958), "Effect of axial compression in shear strength of reinforced concrete frame members", ACI-Journal, Vol. 30, No. 4, Nov. 1958, pp. 635-654.
- Bennett, E.W., Balasooriya, B.M.A. (1971), "Shear strength of prestressed beams with thin webs failing in inclined compression", ACI-Journal, March 1971.
- Bennett, E.W., Debaiky, S.Y. (1974), "High strength steel as shear reinforcement in prestressed concrete beams", ACI Special Publication 42, Vol. I, pp. 231-248, 1974.
- Bernaert, S., and Siess, O. (1956), "Strength of shear in reinforced concrete beams under uniform loading", University of Illinois, June 1956.
- Bhide, S.B., Collins, M.P., (1989) "Influence of Axial Tension on the Shear Capacity of Reinforced Concrete Members", ACI Journal Sept.-Oct. 1989, pp. 570-581.
- Chen Ganwei (1988), "Plastic Analysis of Shear in Beams, Deep Beams and Corbels", Department of Structural Engineering, Technical University of Denmark, Serie R, No. 237, 1988.
- Clark, A.P. (1951), "Diagonal tension in reinforced concrete beams", ACI Journal Vol. 32, No. 2, October 1951, pp. 145-156.
- De Cossio, R.D., Siess, C.P. (1960), "Behavior and strength in shear of beams and frames without web reinforcement", ACI-Journal, Feb. 1960, pp. 695-735.
- Fouré, B. (2000), "Proposal for rewriting item 6.2.4 in section 6.2 (Ultimate Limit State – Shear)", Note to Project Team for EC-2, May 2000 (unpublished).
- Görtz, S., Hegger, J. (1999), "Shear Capacity of Prestressed Concrete Beams of HSC Elements", Symposium Utilization of High Strength/ High performance Concrete, Sandefjord, Norway, 20-24 June 1999, proceedings, Vol. 1, pp. 312-321.
- Hamadi, Y.D. and Regan, P.E. (1980), "Behavior of normal and lightweight aggregate beams with shear cracks", The Structural Engineer, Vol. 58B No. 4, December 1980, pp. 71-79.
- Hanson, J.M., Hulsbos, C.L. (1964), "Ultimate shear tests on prestressed concrete beams under concentrated and uniform loading", PCI-Journal, June 1964, pp. 15-28
- Hedman, O., Losberg, A. (1978), "Design of concrete structures with regard to shear forces", CEB Bulletin d'Information No. 126, pp. 184-209, 1978.
- Hognestadt, E., Elstner, R.C. (1957), "Laboratory investigation of rigid frame failure", ACI Journal, V. 53 No. 1, Jan 1957, pp. 637-668.
- Kani, G.N.J. (1966), "Basic Facts Concerning Shear Failure", ACI-Journal 64, (1966), No. 6, pp. 675 – 692.
- König, G., Fischer, J. (1995), "Model Uncertainties concerning Design Equations for the Shear Capacity of Concrete Members without Shear Reinforcement", CEB Bulletin 224, July 1995, pp. 49-100.
- Krefeld, W.J., and Thurston, C.W. (1966), "Studies of the shear and diagonal tension strength of simply supported reinforced concrete beams", ACI Journal, Vol. 63, No. 4, April 1966, pp. 451-476.
- Küng, R., "Ein Beitrag zur Schubsicherung im Stahlbetonbau", Betonstahl in Entwicklung, Heft 33, Tor-Esteg Steel Corporation, Luxemborg.
- Lehwalter, N. (1988), "The bearing capacity of concrete struts in strut and tie models exemplified for the case of short beams", PhD-Thesis, Darmstadt University of Technology, Germany (in German).
- Leonhardt, F., Walther, R. (1961), "The Stuttgart shear tests 1961", Series of papers in Beton- und Stahlbetonbau,
- Leonhardt, F., Koch, R., Rostsy, F., (1973), "Schubversuche an Spannbetonträgern", Deutscher Ausschuss für Stahlbeton, Heft 227, Berlin.
- Levi, F., Marro, P. (1993), "Shear tests on HSC prestressed beams – proposals of new interpretative models", Conference on High Strength Concrete 1993, Lillehammer 20- 24 June, Proceedings, pp. 293-305.

- Leung, Y.W., Chew, C.B. and Regan, P.E. (1976), "Shear strength of various shapes of concrete beams without shear reinforcement", Polytechnic of Central London, 1976.
- Lyngberg, B.S., (1976), "Ultimate shear resistance of partially prestressed concrete lbeams", ACI-Journl, April 1976, pp. 214-221.
- Mathey, R.G., Watstein, D. (1963), "Shear strength of beams without web reinforcement containing deformed bars of different yield strengths", ACI Journal Vol. 60., No. 2, Feb. 1963, pp. 183-207.
- Moayer, H. and Regan, P.E., (1974) "Shear strength of prestressed and reinforced concrete T-beams", ACI Special Publication 42, Vol 1, pp. 183-221, 1974.
- Morrow, J., Viest, .M. (1957), "Shear strength of reinforced concrete beams, ACI Journal, Vol. 28, No. 9, March 1957, pp. 833-869.
- Muhidin, N.A. and Regan, P.E. (1977), "Chopped steel fibres as shear reinforcement in concrete beams", Fibre reinforced materials – design and engineering applications, Proceedings of a conference, Institution of Civil Engineers, London 1977, pp. 135 - 149.
- Nielsen, M.P. (1990), "Commentaries on Shear and Torsion", Eurocode 2 editorial Group – 1st draft – October 1990.
- PrEN 1990, Eurocode: Basis of Structural Design, Stage 34, Draft version Dec. 2001.
- Regan, P.E. (1971), "Shear in reinforced concrete – an experimental study", Technical Note 45, CIRIA, London.
- Regan, P.E. (1999), "Ultimate Limit State Principles: Basic design for moment, shear and torsion", in *fib* Text Book on Structural Concrete, Vol. 2, pp. 141-223.
- Regan, P.E., Reza-Jorabi, H. (1987), "The shear resistance of reinforced concrete lbeams", Studi e Ricerche, Politecnico di Milano, Vol 19, 1987, pp. 305-321.
- Regan, P.E. (1998), "Enhancement of shear resistance in short shear spans of reinforced concrete", an evaluation of UK recommendations and particularly of BD- 44/95, University of Westminster, London, 1998 (14 pages).
- Regan, P.E. (2000), "Aspects of diagonal tension in reinforced concrete", Structural Concrete, Journal of fib, No. 13, 2000, Sept. 119-132.
- Rogowski, D.M., MacGregor, J.G. (1983), "Shear strength of deep reinforced concrete continuous beams", Structural Engineering Report, No. 11., University of Alberta, Nov. 1983.
- Rüsch, H., Haugli, F.R., Mayer, H. (1962), "Shear tests on rectangular reinforced concrete beams with uniformly distributed loads", Deutscher Ausschuss für Stahlbeton, Berlin, Heft 145 (in German).
- Sörensen, H.C. (1974). "Shear tests on 12 reinforced concrete T-beams", report R60, Structural research Laboratory, Technical University of Denmark, 1974.
- Taerwe, L.R. (1993), "Toward a consistent treatment of model uncertainties in reliability formats for concrete structures", CEB Bulletin d'Information 219, "Safety and Performance Concepts", pp. 5-35.
- Walraven, J.C. (1978), "The influence of member depth on the shear strength of normal and lightweight concrete beams without shear reinforcement", Stevin Report 5-78-4, Delft University of Technology, 1978.
- Walraven, J.C. (1987), "Shear in prestressed concrete", CEB-Bulletin d'Information Nr. 180, 144 pages.
- Walraven, J.C., Lehwalther, N. (1989), "The bearing capacity of concrete struts in strut and tie models exemplified for the case of short beams", Beton-und Stahlbetonbau, Heft 4, April '89, pp. 81-87 (in German).
- Walraven, J.C., Lehwalther, N. (1994), "Size effects in short beams loaded in shear", AC\_ - Structural Journal, Vol. 91., No. 5., Sept.-Oct. 1994, pp. 585-593.
- Walraven, J.C., Al-Zubi, N. (1995), "Shear capacity of lightweight concrete beams with shear reinforcement", Proceedings Symposium on Lightweight Aggregate Concrete, Sandefjord, Norway, Vol. 1, pp. 91-104
- Walraven, J.C., Stroband, J. (1999), "Shear capacity of high strength concrete beams with shear reinforcement", Symposium on High Strength Concrete, Sandefjord, Norway, 20-24 June 1999, Proceedings Vol. 1. pp. 693-700.

### Punching

1. Walraven, J.C.; CEB-Bulletin d'Information 180, "Shear in Prestressed Concrete" pp.68-71.
2. Kinnunen, S., H. Nylander; "Punching of concrete slabs without shear reinforcement", Transactions of the Royal Institute of Technology, Stockholm, Civil Engineering 3, Nr. 158, 1960.
3. Marti, P., J. Pralong, B. Thurlimann; "Schubversuche an Stahlbetonplatten", Institut für Baustatik und Konstruktion, ETH Zurich, Bericht Nr. 7305-2, Birkhäuser Verlag Basel, September 1977.
4. Seible, F., A. Ghali, W.H. Digger; "Preassembled shear reinforcing units for flat plates", ACI-Journal, Jan-Feb. 1980, pp. 28-35
5. Pralong, J., w. Briindli, B. Thurlimann; "Durchstanzversuche an Stahlbeton- und Spannbetonplatten", Institut für Baustatik und Konstruktion, EHT ZURICH, Bericht Nr. 7305-3, Birkhäuser Verlag Basel, December 1979.
6. Franz, G.; "Versuche an Stahlbetonkörper der Flachdecke im Stützenbereich-Versuchsreihen I en II, Institut für Beton- und Stahlbetonbau," TH Karlsruhe, 1963 und 1964.
7. Base, G.D.; CEB-Bulletin Nr.57, 1968, pp.68-82
8. Tolf, P.; "Effect of slab thickness on punching shear strength of concrete slabs. Tests on circular slabs", Bulletin 146, Dept. of Structural Mechanics and Engineering, Royal Institute of Technology, Stockholm (in Swedish with summary in English).
9. Marzouk, H., A. Hussein; "Experimental investigation on the behavior of high strength concrete slabs" ACI-Structural Journal, Vol. 88, No.6, American Concrete Institute, Detroit, pp. 701-713.
10. Tomaszewicz, A.; "High-Strength .SP2 -Plates and Shells, Report 2.3 "Punching shear capacity of reinforced concrete slabs", Report No. STF70 A93082, SINTEF Structures and Concrete, Trondheim, 36 pp.
11. Regan P.F., A. Al-Hussaini, K.E. Ramdane, H.Y. Xue; "Behavior of high strength concrete slabs", Proceedings of the international conference *Concrete 2000*, Sept. 7-9, 1993, Vol. 1, pp. 761-773.
12. Hallgren, M; "Punching shear tests on reinforced high strength concrete slabs", KTH Stockholm, Technical Report 1994, No.14. Structural Mechanics.
13. Taerwe, L.R.; "Towards a consistent treatment of model uncertainties in reliability formats for concrete structures", CEB-Bulletin d'Information 219, "Safety and Performance Concepts", p 5-35.
14. König, G., Fischer, J., "Model Uncertainties concerning Design Equations for the Shear Capacity of Concrete Members without Shear Reinforcement", in CEB Bulletin 224, Model Uncertainties, July 1995, pp. 49-100.
15. Kinnunen, S., Nylander, H., "Punching of Concrete Slabs without Shear Reinforcement" Meddelande N. 38, Institutionen for Byggnadstatik, Kungilga Tekniska Hogskolan, Stockholm 1960.
16. Moe, J ., "Shearing strength of reinforced concrete slabs and footings under concentrated loads" Development Department Bulletin d47, Portland Cement Association, April 1961.
17. Herzog, M., "Der Durchstandswiderstand von Stahlbetonplatten nach neu ausgewerteten Versuchen", Österreichische Ingenieurzeitschrift, Vol. 14, 1971, Nr. 6, pp. 186-192, Nr. 7. Pp.216-219.
18. Petcu, V., Stanculescu, G., Pancaldi, U., "Punching strength predictions for two-way reinforced concrete slabs", Revue Romaine des Sciences Techniques: serie de la mecanique applique, No 2, March/April 1979, Rumania.
19. Kordina, K., Nolting, D., "Shear capacity of reinforced concrete slabs subjected to punching", Deutscher Ausschuss für Stahlbeton, Nr. 371, Berlin, 1986 (in German)
20. Elstner, R.C., Hognestad, E., "Shearing strength of reinforced concrete slabs", ACI Journal, Vol. 53, July 1956, pp. 29-58.
21. Regan, P.E., "Single legged stirrups as shear reinforcement in reinforced concrete flat slabs", Structures Research Group, Polytechnic of Central London, 1980
22. Gomes, R.B., "Punching resistance of reinforced concrete flat slabs", PhD-Thesis, Polytechnic of Central London, 1991
23. Gomes, R.B., Andrade, M.A.S., "Punching in reinforced concrete flat slabs with holes", Developments in Computer Aided Design and Modeling for Structural Engineering, Civil- Comp Press, , Edingburgh, pp. 185-193.
24. Regan, P.E., "Ultimate Limit State Principles", Model Code Text Book, Part 7.4 Punching, in fib-

- Bulletin 2, Structural Concrete, July, 1999, Vol. 2, pp. 202-223.
25. Yitzhaki, R., "Punching strength of reinforced concrete slabs", ACI Journal Vol. 63, Nr. 5, Mau 1966, pp. 527-542.
  26. Stamencovic, A., Chapman, J.C., "Local strength of flat slabs at column heads",
  27. Report Nr. 39, Construction Industry Research and Information Association, London, 1972.
  28. Shehata, L.A.E., "Puncionamento assimetrico em lajes de concreto, COPPE/UFRJ, Rio de Janeiro, 1987
  29. Regan, P .E., "Behaviour of reinforced concrete flat slabs", Report No.89, Construction Industry Research and Information Association, London 1980.
  30. Hanson, N.W., Hanson, J.M., "Shear and moment transfer between concrete slabs and columns", Portland Cement Association, Development Bulletin D129, Jan 196B.
  31. Islam, S., Park, R., "Tests on slab-column connections with shear and unbalanced flexure, Journal of the Structural Division, Proceedings, ASCE, Vol. 1002 No ST3, March 1976, pp. 549-568.
  32. Anis, N.N., "Shear strength of reinforced concrete flat PhD slabs without shear reinforcement", Thesis Imperial College, London, 1970.
  33. Narasimhan, N., "Shear reinforcement in reinforced concrete column heads", PhD Thesis, Imperial College, London 1971
  34. Hawkins, N.M., Bao, A., Yamazaki, J., "Moment transfer from concrete slabs to columns", ACI Structural Journal, v. 86, No.6, Nov-Dec. 1998, pp. 705-716.
  35. Mast, P.E., "Stresses in flat plates near columns", ACI Journal, Oct. 1970, pp. 761- 768.
  36. Mast, P.E., "Plate stresses at columns near to free edges", ACI Journal, Nov. 1970, pp. 899- 902.
  37. Regan, P .E., "Explanatory notes on proposed Model Code (MC'90)", Note to CEB Commission IV, May 8th 1990.
  38. Regan. P.E., Braestrup. M.W., "Punching shear in reinforced concrete", CEB-Bulletin d'Information No.168, Jan.1985.
  39. Lucio, V.J.G., Appleton, J.A.S., Almeida, J.P., "Ultimate limit state of punching in the (fib) FIP Recommendations for the design of post-tensioned slabs and foundations", Structural Concrete, Journal of fib, 2000, 1, No.3, Sept. 143-149.
  40. Andersson, J.L., "Genomstansning ay lift slabs (Punching of lift slabs)", Nordisk Betong, Year 7,1963, H.3, pp. 229-252.
  41. Gerber, L.L., Burns, N.H., "Ultimate strength tests of post-tensioned flat plates", PCI Journal, Nov/Dec. 1971, pp. 40-58.
  42. Stahlton, A.G., "Flat slabs with Stahlton column strip prestressing", unpublished Report of Stahlton AG, Zurich, 1974/75 (in German).
  43. Pralong, J., Brandli, W., Thurimann, B., "Punching tests on reinforced and prestressed slabs", Institute for Building Statics and Structural Design", ETH Zurich, Report Nr.7305-3, Birkhiuser Verlag Basel, December 1979 (in German).
  44. Kordina, K., Nolting, D., "Tests on shear in slabs, prestressed with unbonded tendons", Report of the Institute for Materials, Concrete Structures and Fire, TU Braunschweig, September 1984 (in German).

**SECTION 7. SERVICEABILITY LIMIT STATES (SLS)**

**7.1 General**

**7.2 Stress limitation**

**7.3 Crack control**

**7.3.1 General considerations**

**7.3.2 Minimum reinforcement areas**

**SECTION 7. SERVICEABILITY LIMIT STATES**

See example n. 7.1

See example n. 7.3

**C7.3.2 Formula for minimum reinforcement**

Formula 7.1 of prEN can be partially deduced by expressing the condition that the minimum reinforcement should be able to withstand the cracking moment working at a certain stress  $\sigma_s \leq f_{yk}$ .

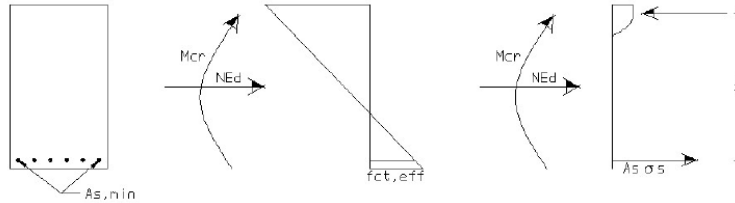


**Figure 7.1** Minimum reinforcement concept

For a rectangular cross section subject to combined bending and axial force, the cracking moment can be determined by:

$$M_{cr} = \frac{1}{3} f_{ct,eff} A_{ct} h + \frac{N_{Ed}}{3} \left( \frac{h}{2} + h_{cr} \right) \tag{7.1}$$

After cracking this same bending moment, together with the axial force, must be taken by the cracked cross section:

$$\frac{1}{3} f_{ct,eff} A_{ct} h - \frac{N_{Ed}}{3} \left( \frac{h}{2} + h_{cr} \right) = A_s \sigma_s z - N_{Ed} \left( \frac{h}{2} - (0,9h - z) \right) \tag{7.2}$$

The lever arm  $z$ , may be taken as a certain fraction  $\alpha$  of  $h$  (around  $0.8h$  for pure bending). Introducing the following notation:

$$A_{ct} = b h_{cr} \quad \sigma_c = \frac{N_{Ed} \cdot z}{b h} = \alpha h$$

Equation above can be rewritten as:

$$f_{ct,eff} A_{ct} \frac{1}{3\alpha} \left( 1 - \frac{\sigma_c}{f_{ct,eff}} \left[ 1 + \left[ 3(0,9 - \alpha) - 1 \right] \frac{h}{h_{cr}} \right] \right) = A_s \sigma_s \tag{7.3}$$

$$f_{ct,eff} A_{ct} k_c = A_s \sigma_s \tag{7.4}$$

The above value of  $k_c$  is valid only if  $\alpha > 0$ , since the deduction assumes that there is a part of the cross section which is in compression. In order to approximate  $k_c$  in the following figure the value of  $\alpha = z/h$  is plotted against the adimensional axial force  $v = \frac{N_{Ed}}{b h f_{ct}}$  within a range of +0.03 to -0.22. Over

0.03, there is no compression block and under -0.22 there is no need to provide minimum reinforcement according to the principle established above.

Factor  $\alpha = z/h$  as a function of adimensional axial force

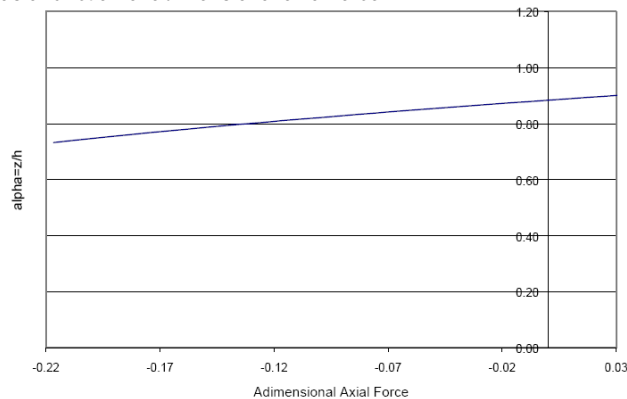


**Figure 7.2** Value of  $\alpha$  as a function of the axial force

It can be seen from the above figure that it is reasonable to assume a value of 0.8 for parameter  $\alpha$ . With this assumption and for compression force or moderate tensile force, the values of  $k_c$  may be estimated as:

$$k_c = 0,4 \left( 1 - \frac{\sigma_c}{f_{ct,eff}} \left( 1 - 0,7 \frac{h}{h_{cr}} \right) \right) \tag{7.5}$$

$h_{cr}$  can be computed as a function of the axial compression and the tensile strength of concrete.



The cracking moment is given by the following condition:

$$f_{ct,eff} = \frac{N_{Ed}}{bh} + \frac{M_{cr}}{bh^2} \times 6 = \sigma_c + \frac{M_{cr}}{bh^2} \times 6 \Rightarrow M_{cr} = (f_{ct,eff} - \sigma_c) \frac{bh^2}{6} \tag{7.6}$$

The depth of the tensile zone prior to cracking, relative to the centre of gravity of the cross section, is given by the condition that the stress be nil when the existing axial force is applied together with the cracking moment:

$$0 = \sigma_c + \frac{M_{cr}}{bh^3} \cdot 12x \Rightarrow x = -\frac{\sigma_c}{(f_{ct,eff} - \sigma_c)} \frac{h}{2} \tag{7.7}$$

Therefore,  $h_{cr}$  can be calculated as:

$$h_{cr} = \frac{h}{2} - x = \frac{h}{2} \left( 1 + \frac{\sigma_c}{(f_{ct,eff} - \sigma_c)} \right) \Rightarrow \frac{h_{cr}}{h} = 2 \left( \frac{(f_{ct,eff} - \sigma_c)}{f_{ct,eff}} \right) \tag{7.8}$$

Introducing equation (7.8) in (7.5), the expression of  $k_c$  becomes:

$$k_c = 0,4 \left[ 1 - \frac{\sigma_c}{f_{ct,eff}} \left( 1 - 1,4 \left( \frac{f_{ct,eff} - \sigma_c}{f_{ct,eff}} \right) \right) \right] \tag{7.9}$$

In the following figure the value of  $k_c$  is plotted against  $\sigma_c$  for a value of  $f_{ct,eff}$  of 2.9 Mpa according to both the above formulation and the equation of prEN.

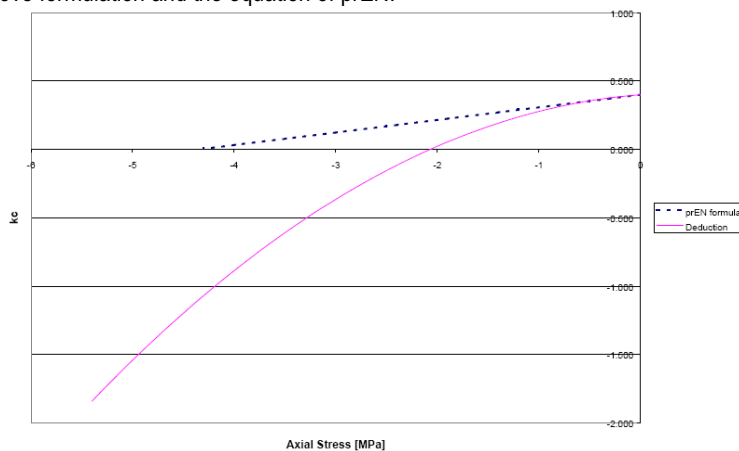


Figure 7.3. Value of  $k_c$  as a function of the axial force

In the next figure the minimum reinforcement for a section subject to a compressive force (expressed in terms of a reduced axial force) is shown calculated according to 4 different methods:

- Proposal of prEN
- Compensation of tension block. This procedure is on the safe side since it neglects the increase of the lever arm which occurs after cracking.
- Direct calculation (exact determination of  $\alpha$ )
- Procedure explained above in which  $\alpha$  is taken as a constant equal to 0.8.

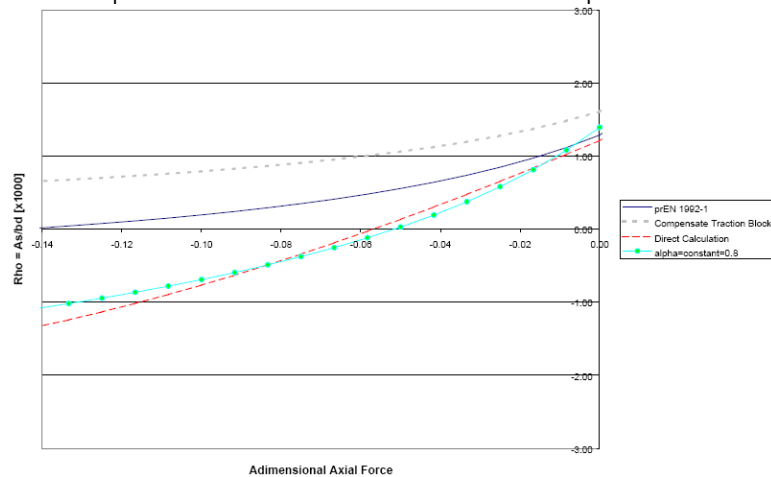


Figure 7.4. Comparison of different approximate expressions for the calculation of the minimum reinforcement

It can be seen that the 2 last methods give almost the same results. It can also be seen that the formula of prEN is mostly on the safe side.



**7.3.3 Control of cracking without direct calculation**

**C7.3.3. Formula for maximum bar diameter**

In this paragraph the formula for the maximum bar diameter is deduced for three crack width formulations: MC-90 [3], EC2 [4] and prEN. This deduction, as will be seen, requires the introduction of simplifications and the assumption that the steel ratio, for which a certain stress  $\sigma_s$  is achieved corresponds to the minimum steel ratio given by prEN equation 7.1. This assumption is on the safe side. A more exact formulation could be obtained if  $\rho_{eff}$  were to remain a variable.

**C7.3.3.1 Deduction of formula**

Using the MC-90 formulation, the crack width is given by:

$$w_k = 2l_t (\varepsilon_{sm} - \varepsilon_{cm}) = \frac{\phi}{3,6\rho_{eff}} \frac{\sigma_s}{E_s} \left( 1 - k_t \frac{\sigma_{sr}}{\sigma_s} \right) \tag{7.10}$$

$\sigma_{sr}$  is the stress calculated for the fully cracked cross section for the cracking moment.  $\sigma_{sr}$  may be calculated by:

$$\sigma_{sr} = \frac{f_{ct,eff} A_{ct} k_c k}{A_s} = \frac{f_{ct,eff} k_c k}{\rho_{s,eff}} \frac{h_{cr}}{2,5k'(h-d)} \tag{7.11}$$

In the above expression,  $k'$  is a factor which is equal to 1 for bending and equal to 2 for tension. Introducing the expression of  $\sigma_{sr}$  into equation (7.10), and rearranging:

$$\phi = \frac{3,6 \cdot w_k \rho_{eff}}{\left( 1 - k_t \frac{f_{ct,eff} k_c}{\rho_{s,eff} \sigma_s} \frac{h_{cr}}{2,5k'(h-d)} \right)} \tag{7.12}$$

In order to obtain numerical values from this expression, it is necessary to assume values for those coefficients which are not considered as variables in table 7.1. The following values have been assumed to derive table 7.1:

$$\begin{aligned} k &= 1,0 \leftarrow h \leq 0,3 \text{ (assumption on safe side)} \\ k_c &= 0,4; \quad k' = 1 \text{ (pure bending)} \\ k_t &= 0,38 \\ \frac{h_{cr}}{h-d} &\approx \frac{h}{2} \frac{10}{h} = 5 \\ f_{ct,eff} &= 2,9 \text{ N/mm}^2 \\ w_k &= 0,3 \text{ mm} \end{aligned} \tag{7.13}$$

With the above values equation (7.12) can be written as:

$$\phi = \frac{720000 \cdot w_k \rho_{eff}}{\left( 1 - 0,88 \frac{1}{\rho_{s,eff} \sigma_s} \right)} \sigma_s \tag{7.14}$$

The above expression, which is valid only for  $\sigma_s > \sigma_{sr}$ , is a function of 3 parameters. Therefore some assumption regarding  $\rho_{eff}$  must be made in order to obtain table 7.2. The assumption which will be made is that  $\rho_{eff} = \rho_{eff,min}$  (i.e.  $\sigma_s = \sigma_{sr}$ ). This assumption is justified because lower values of  $\sigma_s$  will not produce cracking and because if cracking does occur, then formula (7.14) will give smaller bar diameters if the smallest the value of  $\rho_{eff}$  is used. The value of  $\rho_{eff}$  can therefore be taken from the following equation:

$$\rho_{eff} = \rho_{eff,min} = \frac{f_{ct,eff} k_c k}{\sigma_s} \frac{h_{cr}}{2,5k'(h-d)} \tag{7.15}$$

If the above value of  $\rho_{eff}$  is substituted into Eq. (7.12), this equation can be simplified into:

$$\phi = \frac{3,6 \cdot w_k f_{ct,eff} k_c k E_s}{(1 - k_t) \sigma_s^2} \frac{h_{cr}}{2,5k'(h-d)} \approx \frac{808258}{\sigma_s^2} \tag{7.16}$$

In Table 1 the minimum reinforcement ratio which can to be used in equation (7.14) is given for each stress level. In the same table, the maximum bar diameter obtained using equation (7.14) for  $w_k=0.3$  mm and that included in MC-90 Table 7.4.3 are also given.

$\sigma_s$	$\rho_{eff,min}$ valid	$w_k=0.3$ mm	
		$\phi_{max,Eq. (7.14)}$	$\phi_{max,MC-90}$
160	14.5	32	-
200	11.6	20	25
240	9.7	14	20
280	8.3	10	14
320	7.3	8	10
360	6.4	6	8
400	5.8	5	6
450	5.2	4	5

**Table 7.1. MC-90 - Minimum reinforcement ratio for a given value of  $\sigma_s$  which fulfils the condition  $\sigma_s > \sigma_{sr}$ . Value of corresponding  $\phi_{max}$**

These results are plotted in the following figure.

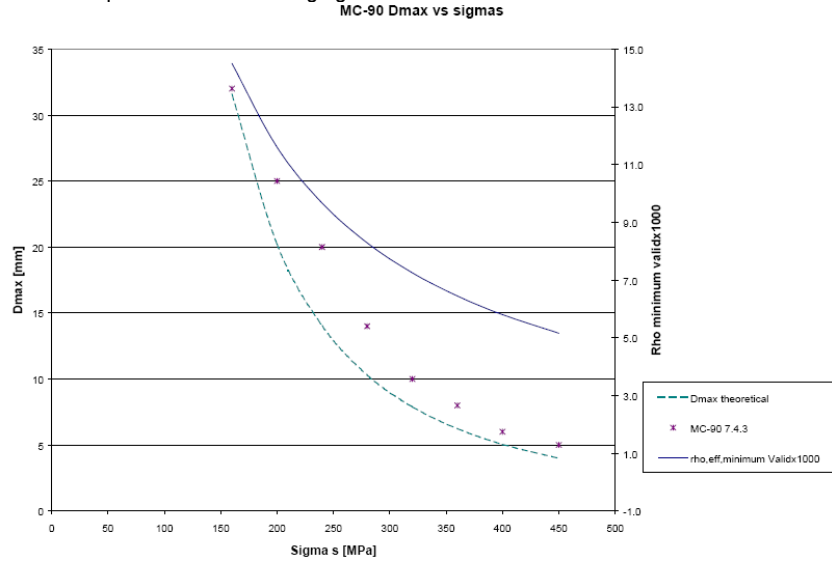


Figure 7.5. Theoretical and actual values of  $D_{max}$ , according to MC-90

Using the EC2 formulation, the crack width is given by:

$$w_k = 1,7s_{sm} (\epsilon_{sm} - \epsilon_{cm}) = 1,7 \left( 50 + 0,25k_1k_2 \frac{\phi}{\rho_{eff}} \right) \frac{\sigma_s}{E_s} \left( 1 - \beta_1\beta_2 \left( \frac{\sigma_{sr}}{\sigma_s} \right)^2 \right) \quad (7.17)$$

$\sigma_{sr}$  is the stress calculated for the fully cracked cross section for the cracking moment.  $\sigma_{sr}$  may be calculated by:

$$\sigma_{sr} = \frac{f_{ct,eff} A_{ct} k_c k}{A_s} = \frac{f_{ct,eff} k_c k}{\rho_{s,eff}} \frac{h_{cr}}{2,5k'(h-d)} \quad (7.18)$$

Introducing the expression of  $\sigma_{sr}$  into equation (7.10), and rearranging:

$$\phi = \left\{ \frac{w_k}{\left( 1 - \beta_1\beta_2 \left( \frac{f_{ct,eff} k_c}{\rho_{s,eff} \sigma_s} \frac{h_{cr}}{2,5k'(h-d)} \right)^2 \right)} \frac{E_s}{1,7\sigma_s} - 50 \right\} \frac{\rho_{eff}}{0,25k_1k_2} \quad (7.19)$$

In order to obtain numerical values from this expression, it is necessary to assume values for those coefficients which are not considered as variables in table 7.2. The following values have been assumed to derive table 7.2:

$$\begin{aligned} k &= 1,0 \leftarrow h \leq 0,3 \text{ (assumption on safe side)} \\ k_c &= 0,4; \quad k' = 1 \text{ (pure bending)} \\ \frac{h_{cr}}{h-d} &\approx \frac{h}{2h} = 0,5 \\ f_{ct,eff} &= 2,5 \text{ N/mm}^2 \\ \beta_1\beta_2 &= 0,50 \\ 0,25 k_1k_2 &= 0,10 \end{aligned} \quad (7.20)$$

With the above values equation (7.19) can be written as:

$$\phi = \left\{ \frac{117647}{\left( 1 - \left( \frac{1,414}{\rho_{s,eff} \sigma_s} \right)^2 \right)} \frac{w_k}{\sigma_s} - 50 \right\} 10\rho_{eff} \quad (7.21)$$

Similarly, a value must be given to  $\rho_{eff}$  in order to obtain values from this expression. As stated before, it is on the safe side to assume for this purpose that  $\sigma_s = \sigma_{sr}$  and that therefore the value of  $\rho_{eff}$  can be determined using equation (7.15). With this assumption, equation (7.19) can be rewritten as:

$$\phi = \left\{ \frac{w_k}{(1 - \beta_1\beta_2)} \frac{E_s}{1,7\sigma_s} - 50 \right\} \frac{f_{ct,eff} k_c k}{0,25k_1k_2} \frac{h_{cr}}{2,5k'(h-d)} \approx \left\{ \frac{70588}{\sigma_s} - 50 \right\} \frac{20}{\sigma_s} \quad (7.22)$$

In the following table, the results obtained by application of the above formula and the values of  $\phi_{max}$  according to EC2 are compared.

$\sigma_s$	$\rho_{eff,min}$ valid	$w_k=0.3$ mm	
		$\phi_{max,eq(7.22)}$	$\phi_{max,EC-2}$ Table 4.11
160	12.5	49	32
200	10.0	30	25
240	8.3	20	20
280	7.1	14	16
320	6.3	11	12
360	5.6	8	10
400	5.0	6	8
450	4.4	5	6

**Table 7.2** EC2 - Minimum reinforcement ratio for a given value of  $\sigma_s$  which fulfils the condition  $\sigma_s > \sigma_{sr}$ . Value of corresponding  $\phi_{max}$

In the following graph, the above results are plotted.

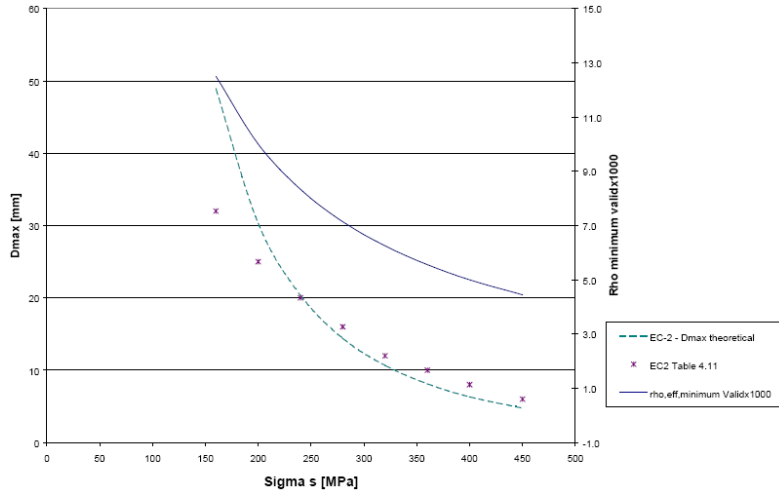


**Fig 7.6.** Theoretical and actual values of  $D_{max}$ , according to EC2

Using the prEN formulation, the crack width is given by:

$$w_k = 1,7s_{rm} (\varepsilon_{sm} - \varepsilon_{cm}) = \left( 3,4c + 0,425k_1k_2 \frac{\phi}{\rho_{eff}} \right) \frac{\sigma_s}{E_s} \left( 1 - k_t \left( \frac{\sigma_{sr}}{\sigma_s} \right) \right) \tag{7.23}$$

$\sigma_{sr}$  is the stress calculated for the fully cracked cross section for the cracking moment.  $\sigma_{sr}$  may be calculated by:

$$\sigma_{sr} = \frac{f_{ct,eff} A_{ct} k_c k}{A_s} = \frac{f_{ct,eff} k_c k}{\rho_{s,eff}} \frac{h_{cr}}{2,5k'(h-d)} \tag{7.24}$$

Introducing the expression of  $\sigma_{sr}$  into equation (7.23), and rearranging:

$$\phi = \left\{ \frac{w_k}{\left( 1 - k_t \left( \frac{f_{ct,eff} k_c}{\rho_{s,eff} \sigma_s} \frac{h_{cr}}{2,5k'(h-d)} \right)^2 \right) \sigma_s} - 3,4c \right\} \frac{E_s}{0,425k_1k_2} \rho_{eff} \tag{7.25}$$

In order to obtain numerical values from this expression, it is necessary to assume values for those coefficients which are not considered as variables in table 7.2. The following values have been assumed to derive table 7.2:

$$\begin{aligned} k &= 1,0 & h \leq 0,3 \text{ (assumption on safe side)} \\ k_c &= 0,4; & k' = 1 \text{ (pure bending)} \\ \frac{h_{cr}}{h-d} &\approx \frac{h}{2} = 5 \\ f_{ct,eff} &= 2,9 \text{ N/mm}^2 \\ k_t &= 0,40 \\ 0,425 k_1 k_2 &= 0,17 \\ C &= 25 \text{ mm} \end{aligned} \tag{7.26}$$

With the above values equation (7.25) can be written as:

$$\phi = \left\{ \frac{200000}{\left( 1 - \left( \frac{0,928}{\rho_{s,eff} \sigma_s} \right) \right)} \frac{w_k}{\sigma_s} - 85 \right\} 5,88 \rho_{eff} \tag{7.27}$$

The above expression is a function of 3 parameters and again can be simplified with the assumptions explained above, into:

$$\phi = \left\{ \frac{w_k}{(1-k_t)} \frac{E_s}{\sigma_s} - 3,4c \right\} \frac{f_{ct,eff} k_c k}{\sigma_s 0,425 k_2} \frac{h_{cr}}{2,5k'(h-d)} \approx \left\{ \frac{100000}{\sigma_s} - 85 \right\} \frac{13,65}{\sigma_s} \tag{7.28}$$

This curve is represented in the following figure and given in numerical form in table 7.3. It can be seen that good agreement is obtained between theory and prEN table. The small differences observed are due to the need to use commercial bar diameters in table 7.3.

w <sub>k</sub> =0.3 mm			
σ <sub>s</sub>	ρ <sub>eff,min</sub> valid	φ <sub>max</sub> Eq. (7.14)	φ <sub>max</sub> prENV
160	14.5	46	32
200	11.6	28	25
240	9.7	19	16
280	8.3	13	12
320	7.3	10	10
360	6.4	7	8
400	5.8	6	6
450	5.2	4	5

**Table 7.3** prENV - Minimum reinforcement ratio for a given value of σ<sub>s</sub> which fulfils the condition σ<sub>s</sub> > σ<sub>sr</sub>. Value of corresponding φ<sub>max</sub>

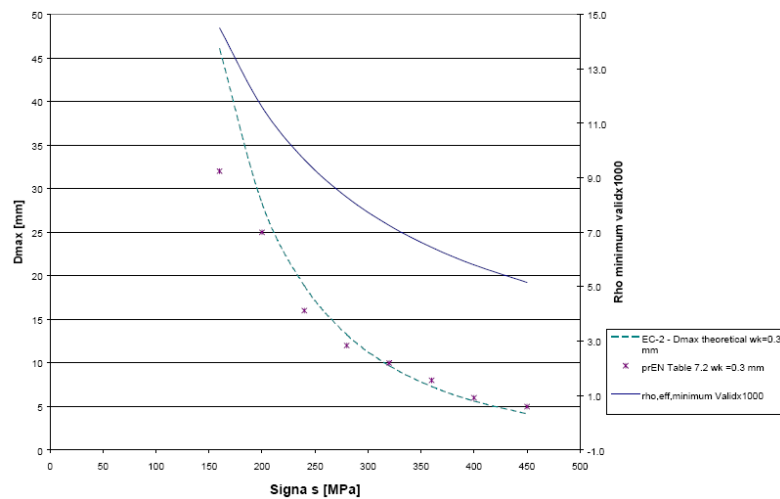


**Figure 7.7.** Theoretical and actual values of D<sub>max</sub>, according to prEN

The three formulas analyzed are compared in the following graph. It can be seen that the theoretical results for EC-2 and prEN are very similar while the MC-90 equation is somewhat more conservative. The values included in the tables of the codes do not always match the theoretical equation but are generally conservative for EC2 and prEN. The MC90 table values are somewhat above the theoretical curve as already shown before.

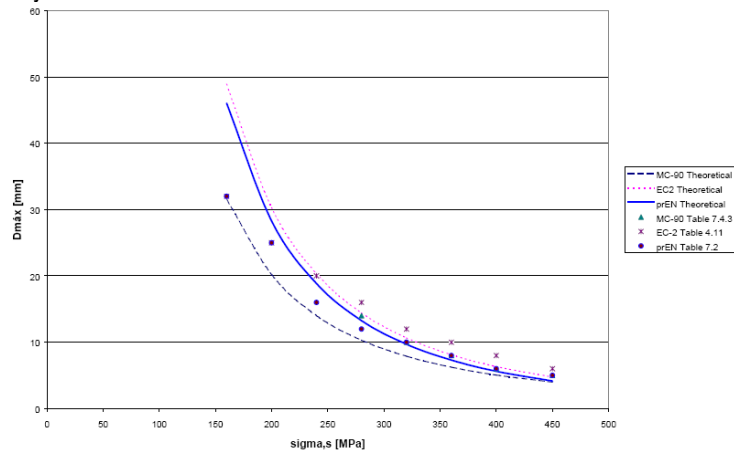


**Figure 7.8** Theoretical and actual values of D<sub>max</sub>. Comparison of the 3 models considered

**7.3.3.2 Correction for cover**

In the above expressions it has been assumed that  $h - d \approx 0,1h$  and also that a problem of pure bending is being analysed and therefore,  $h_{cr} = 0.5h$ ,  $k_c = 0.4$  and  $k'=1$ . Furthermore, the tensile strength of concrete has been assumed to be  $2.9 \text{ N/mm}^2$  ( $2.5$  in case of EC2). If different values are assumed for these parameters, then the value obtained from the tables must be corrected by the following factor:

Part of cross section compressed: 
$$\frac{f_{ct,eff}}{2,9} \frac{k_c}{0,4} \frac{h_{cr}}{0,5h} \frac{0,1h}{(h-d)} \frac{k'}{1} = \frac{f_{ct,eff}}{2,9} \frac{k_c h_{cr}}{2(h-d)} \frac{1}{1} \tag{7.29}$$

Cross section in tension: 
$$\frac{f_{ct,eff}}{2,9} \frac{k_c}{0,4} \frac{h_{cr}}{0,5h} \frac{0,1h}{(h-d)} \frac{1}{k'} = \frac{f_{ct,eff}}{2,9} \frac{k_c h_{cr}}{2(h-d)} \frac{1}{2} \tag{7.30}$$

It can therefore be written that:

$$\phi_s = \phi_s' \frac{f_{ct,eff}}{2,9} \frac{k_c h_{cr}}{2(h-d)} \text{ part of section compressed} \tag{7.31a}$$

$$\phi_s = \phi_s' \frac{f_{ct,eff}}{2,9} \frac{k_c h_{cr}}{4(h-d)} \text{ all section in tension} \tag{7.31b}$$

**7.3.4 Calculation of crack widths**

**C7.3.4. Formula for crack width**

**7.3.4.1 Introduction**

The formula proposed for crack width is a mixture of EC2 and MC90.

In order to evaluate the accuracy of this formula, it has been tested against an experimental data base including results from the researchers Rehm & Rüsçh [11-13], Krips [9], Falkner [6], Elighausen [5], Hartl [7], Beeby [1,2] and Jaccoud [8].

The data base has been drafted specifically for this document and is detailed in appendix A. The criteria for the selection of the experimental results are clearly explained below. It is the intention of the authors to avoid ambiguity and provide a self explaining instrument which can be used by other researchers in the future so that the work carried out here need not be repeated. A detailed presentation of this data base is therefore given.

After a review of the proposed model, the results of the comparison between model and experimental data are presented. The performance of the new prEN formula is also compared to that of MC-90 and EC2. The results show small differences between the 3 models.

The analysis, however, shows that for all 3 models, the error margin grows as the crack width grows and that all models tend to underestimate the crack width when it is large. This fact is unfortunate since the control of cracking in normal structures is most important when cracks are large. This fact suggests that in future editions of EC2, some correction might be needed to allow for this situation.

**7.3.4.2 Proposed formulation**

According to the prEN proposal, the design crack width can be determined using the following expression:

$$w_k = s_{rm} (\epsilon_{sm} - \epsilon_{cm})$$

where

$w_k$  design crack width

$s_{rmax}$  maximum crack spacing

$\epsilon_{sm}$  mean strain in the reinforcement, under the relevant combination of loads, taking into account the effects of tension stiffening, etc.

$\epsilon_{cm}$  mean strain in concrete between cracks

The strain difference ( $\epsilon_{sm} - \epsilon_{cm}$ ) may be calculated from the expression:

$$(\epsilon_{sm} - \epsilon_{cm}) = \frac{\sigma_s}{E_s} - k_t \epsilon_{sr} = \frac{\sigma_s - k_t \frac{f_{ctm}}{\rho_{eff}} (1 + \alpha \rho_{eff})}{E_s} \geq 0,6 \frac{\sigma_s}{E_s} \tag{7.32}$$

where

$\sigma_s$  stress in the tension reinforcement assuming a cracked section.

$$\epsilon_{sr} = \frac{\sigma_{sr}}{E_s} \approx \frac{\frac{f_{ctm}}{\rho_{eff}} (1 - \alpha \rho_{eff})}{E_s}$$

This is a simplification which is exact for pure tension but not for bending. However, this simplification makes it easier to apply the model in practical cases and does not imply any significant loss of accuracy as is shown below.

$\alpha_e$  ratio  $E_s/E_c$

$$\rho_{p,eff} = \frac{A_s}{A_c}$$

$A_{c,eff}$  effective tension area.  $A_{c,eff}$  is the area of concrete surrounding the tension reinforcement of depth,  $h_{c,ef}$ , where  $h_{c,ef}$  is the lesser of  $2,5(h-d)$ ,  $(h-x)/3$  or  $h/2$  (see figure).

$k_t$  factor dependent on the duration of the load  
 $k_t = 0,6$  for short term loading  
 $k_t = 0,4$  for long term loading

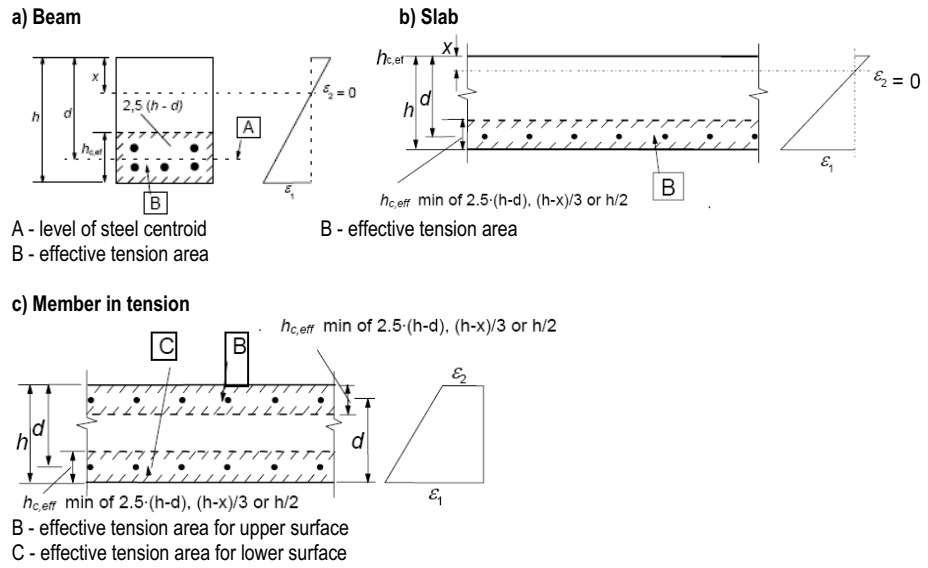


Figure 7.9 Definition of the effective tension area

In situations, where bonded reinforcement is fixed at reasonably close spacing within the tension zone (spacing  $\leq 5(c+\phi/2)$ ), the maximum final crack spacing can be calculated from the expression:

$$s_{max} = 3,4c + 0,425k_1k_2 \frac{\phi}{\rho_{eff}} \tag{7.33}$$

where

- $\phi$  bar diameter.
  - $c$  cover to the reinforcement
  - $k_1$  coefficient which takes account of the bond properties of the bonded reinforcement;  
 $k_1 = 0.8$  for high bond bars  
 $k_1 = 1.6$  for bars with an effectively plain surface
  - $k_2$  coefficient which takes account of the distribution of strain;  
 $k_2 = 0.5$  for bending  
 $k_2 = 1.0$  for pure tension
- For cases of eccentric tension or for local areas, intermediate values of  $k_2$  should be used which can be calculated from the relation:

$$k_2 = \frac{(\epsilon_1 + \epsilon_2)}{2\epsilon_1} \tag{7.34}$$

Where  $\epsilon_1$  is the greater and  $\epsilon_2$  is the lesser tensile strain at the boundaries of the section considered, assessed on the basis of a cracked section.

As can be seen, with regard to crack spacing, the cover,  $c$ , is introduced explicitly into the expression of the crack width as suggested by A. Beeby. This suggestion is backed up by the following figure, taken from reference [1], which clearly shows the dependence of the crack spacing on this parameter. In EC2,  $c$  is implicitly taken as 25 mm.

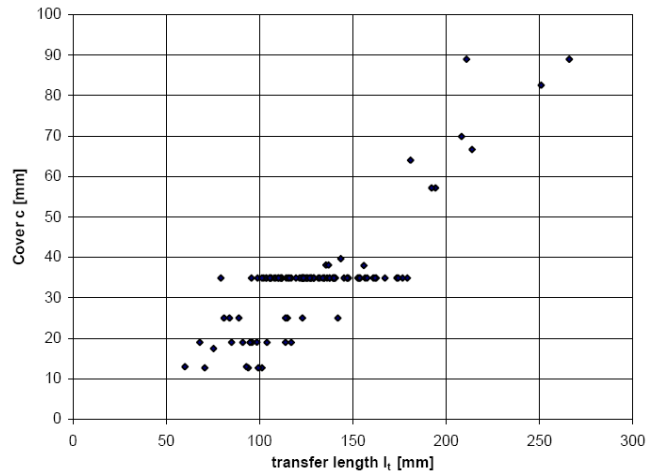


Fig.7.10 Influence of cover on the transfer length according to Beeby [1]

Also, on a formal level, the formula of prEN gives  $s_{max}$  instead of  $s_m$ .  $s_{max}$  is obtained as 1.7 times  $s_m$ . Thus,

$$1,7 \cdot 2 \cdot 25 + 0,25k_1k_2 \frac{\phi}{\rho_{p,eff}} \tag{7.35}$$

of EC2 becomes

$$3,4c + 0,425k_1k_2 \frac{\phi}{\rho_{p,eff}} \tag{7.36}$$

of prEN.

In the case in which 2 different bar diameters are used, an equivalent diameter  $\phi_{eq}$  has to be determined in order to apply the above formulation.

In EC2 [4] it is recommended to use the average diameter  $\phi_m$ .

MC90[3] and prEN [10] suggest for this case the equivalent diameter  $\phi_{eq}$ , although MC90 provides no definition of  $\phi_{eq}$ . The definition of  $\phi_{eq}$  depends on the definition of  $\rho_{eff}$ . To show the difference, first  $\phi_m$  will be applied to the equilibrium equation (7.33) to derive  $\phi_{eq}$  and then  $\phi_{eq}$  will be derived by considering 2 diameters in the determination of the steel area (7.35).

$$f_{ctm} A_{ctm} = \tau \cdot \pi \cdot n \cdot \phi \cdot l_t \tag{7.37}$$

(7.33) changes in case of the use of 2 different diameters into (7.34).

$$f_{ctm} A_{ctm} = \tau \pi (n\phi_1 + n\phi_2) l_t \tag{7.38}$$

Hence:

$$l_t = \frac{f_{ctm} A_{ctm}}{\tau \pi (n\phi_1 + n\phi_2)} \tag{7.39}$$

since  $s_{max} = 2l_t$  and  $s_{max} = \phi/3.6\rho$  and, according to MC90[5]

$$\frac{f_{ctm}}{\tau} = \frac{1}{1,80}, \text{ it can be written: } s_{max} = \frac{2f_{ctm} A_{ct,eff}}{\tau \pi (n_1\phi_1 + n_2\phi_2)} = 2 \frac{A_{ct,eff} \phi_{eq}}{1,80 \times 4 \frac{\pi \phi_{eq}^2}{4}} \tag{7.40}$$

From (7.36) can be seen that the equivalent diameter is:

$$\phi_{eq} = \frac{(n_1\phi_1 + n_2\phi_2)}{n_1 + n_2} = \phi_m \tag{7.41}$$

This is correct when the steel section in  $\rho = \frac{A_s}{A_{ct,eff}}$  is defined with  $A_s = (n_1 + n_2) \frac{\pi \phi_{eq}^2}{4}$

If this is not the case, and the steel area is instead described by

$$A_s = n_1 \frac{\pi \phi_1^2}{4} + n_2 \frac{\pi \phi_2^2}{4} \text{ then, } A_{c,eff} = \frac{\pi (n_1\phi_1^2 + n_2\phi_2^2)}{4\rho} \text{ and therefore}$$

$$s_{max} = 2 \frac{f_{ctm} (n_1\phi_1^2 + n_2\phi_2^2)}{\tau \rho (n_1\phi_1 + n_2\phi_2)} \tag{7.42}$$

$$\text{From (1.38) can be derived that the equivalent diameter is: } \phi_{eq} = \frac{(n_1\phi_1^2 + n_2\phi_2^2)}{(n_1\phi_1 + n_2\phi_2)} \tag{7.43}$$

It can be seen that EC2 and MC90 could be misleading and thus should be clarified, since the code user will naturally define  $\rho_{eff}$  as  $A_s/A_{c,eff}$ . For this reason the definition of  $\phi_{eq}$  is made explicit in prEN.

**7.3.4.3 Presentation of data base**

As stated above, the data base includes data from different researchers. The data has been selected among the different tests available following a few simple rules:

- The materials used in the tests need to be similar to the materials used today in the building of structures. This rule leads to discard tests which use low bond rebars, or concrete qualities less than 20 N/mm<sup>2</sup> and steel qualities of less than 400 N/mm<sup>2</sup>.
- The stress range should be a serviceability range. For this purpose, only results within a stress range in steel from 150 to 350 N/mm<sup>2</sup> were considered for tests involving direct actions. For indirect actions, steel stresses up to the yielding stress of steel were considered, since these test can be representative of walls subject to shrinkage and temperature.
- For the determining of the crack spacing the number of cracks present at the last phase of the test is always considered since it is the closest to stabilized cracking, which is the crack spacing given in equation (7.32).

**7.3.4.4 Analysis of the experimental data**

This paragraph includes the analysis of the experimental data as well as the comparison between the values obtained from the experimental data base and the values obtained from the theoretical models. The comparison includes not only the prEN model, but also those of EC2 and MC-90, in order to verify a satisfactory performance of the new proposal.

Experimental data generally includes the values for the mean crack width and, in most cases, also for the maximum crack width.

The models are compared on the basis of the mean crack width because it is difficult to determine the experimental characteristic crack width.

However, since in many of the experimental results the maximum crack width is also available, first an analysis of the distribution function of the maximum crack width is made, since this analysis provides some interesting conclusions. For this the results of Rehm & Rüsç [11-13] are used.

**7.3.4.4.1 Probability function of the maximum crack width**

In this paragraph a first analysis of the probability distribution of the maximum crack width is made.

Figure 11 shows the crack width distribution function for all selected members within the service stress range. The distribution function of the maximum crack widths shows clearly a tendency to a normal distribution. Equation (7.44) shows the mathematical equation for the normal distribution function. This expression is also plotted in Figure 7.11 showing very close agreement with the experimental data.

$$f(x, \mu, \sigma) = \frac{1}{\sqrt{2\pi}\sigma} e^{-\frac{(x-\mu)^2}{2\sigma^2}} \tag{7.44}$$

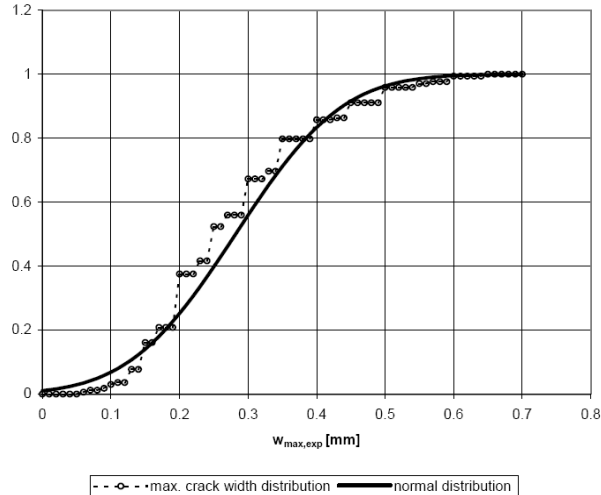


**Fig.7.11. Maximum experimental crack width distribution**

Having proven that it is reasonable to assume that the probability distribution of the maximum crack width can be assumed is a normal distribution, the distribution and the density functions were evaluated for each stress level within the service spectrum: 200 N/mm<sup>2</sup>, 250 N/mm<sup>2</sup>, 300 N/mm<sup>2</sup> and 350 N/mm<sup>2</sup>.

These functions are displayed in Figure 7.12 (distribution function) and Figure 7.13 (density function). The division of the results into different stress levels shows the evolution of the maximum crack width as a function of the stress level. Figure 7.12 shows the distribution of the crack width for the different stress levels. It can be seen that for a stress level of 200 N/mm<sup>2</sup> there is a probability of 95% that a maximum crack width smaller than 0.3 mm occurs. This is consistent with the available experience. It can be stated that for normal durability conditions, stress levels under 250 N/mm<sup>2</sup> will not pose any



serious cracking problems

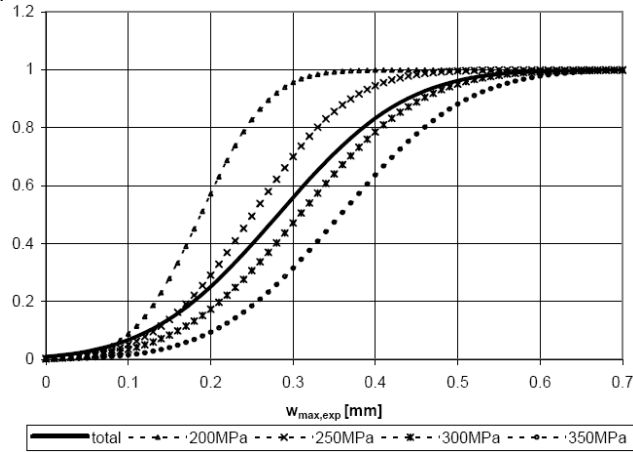


Figure 7.12. Normal distribution of the maximum crack width for different stress levels

The density curves show the concentration of the crack opening. It can be seen in Figure 7.13, which crack opening is typical for a certain stress level.

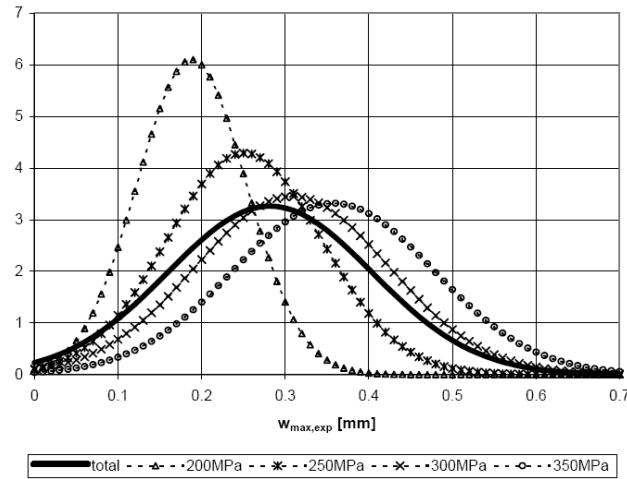


Fig.7.13. Density curves of the maximum crack width for different stress levels

This shows, that in the given data, a maximum crack width of 0.19 mm is typical for a steel stress of 200 N/mm<sup>2</sup>, 0.25 mm for 250 N/mm<sup>2</sup> and so on.

**7.3.4.5 Comparison of the standards**

In this paragraph a direct comparison between the formulae according to [3,4,10] is presented. This comparison shows the performance of the formulae, not only against each other, but also against the test results. Since prEN and MC-90 provide the characteristic crack width, the mean crack width has been estimated by dividing the value given by these codes by 1.7 and 1.5 respectively, since these are the values they assume.

In Figure 7.14, all the data obtained by the evaluation of the experimental results and all the data obtained by processing the corresponding input results according to the standards, is displayed.

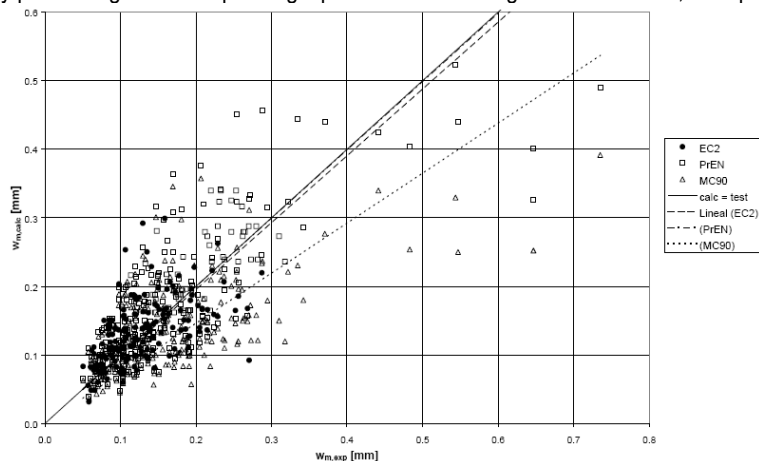


Figure 14 Comparison test-calc., acc. to EC2, MC90 and prEN

All 3 formulae perform quite closely to each other. This is shown by the corresponding trend lines. A better view of this information can be obtained by plotting the error of the estimation instead of the crack value. The error is defined as:

$$W_m - W_{m,exp} \tag{7.45}$$

This result is given in the following graph and table:

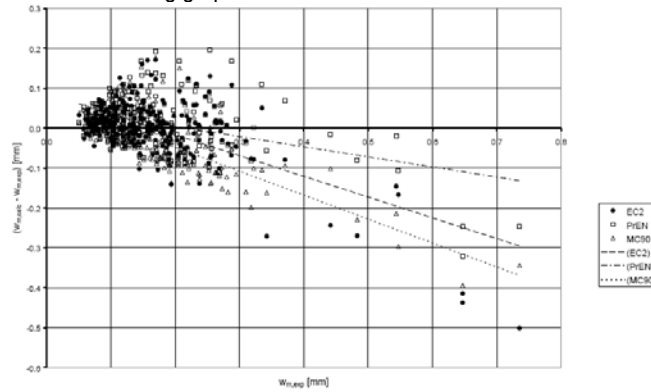


Figure 7.15 Error in crack width prediction

	EC2 error	MC90 error	PrEN error
$W_{error}$	$W_m - W_{m,exp}$ [mm]	$W_m - W_{m,exp}$ [mm]	$W_m - W_{m,exp}$ [mm]
$\mu$	0.0022	-0.0259	0.0136
$\sigma$	0.0769	0.0751	0.0628
$\mu + 1.64 \cdot \sigma$	0.1283	0.097	0.117
$\mu - 1.64 \cdot \sigma$	-0.1240	-0.149	-0.089

Table 7.4. Errors in crack width prediction

The above table shows the mean value of the error, its standard deviation and the 95% confidence intervals (assuming a normal distribution for the error) For example the mean error according to EC2 is  $W_{error} = 0.005$  mm (overestimation). With a 95% probability the underestimation will be less than -0.12 mm and the overestimation less than of 0.13 mm.

A normal distribution was assumed based on the following figure which shows the experimental error compared to normal distribution having approximately the same mean value and standard deviation (the theoretical value of the curve corresponds to EC2, but the values of the 3 models are fairly close). It can be seen that good agreement is found and that the error can effectively be assumed have a normal distribution.

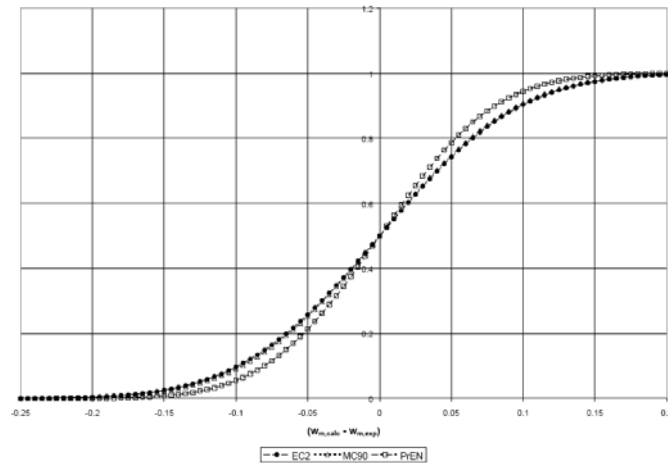


Figure 7.16 Distribution function of the error in the estimation of the mean crack width

The diagram below shows the density function of the errors of each model.

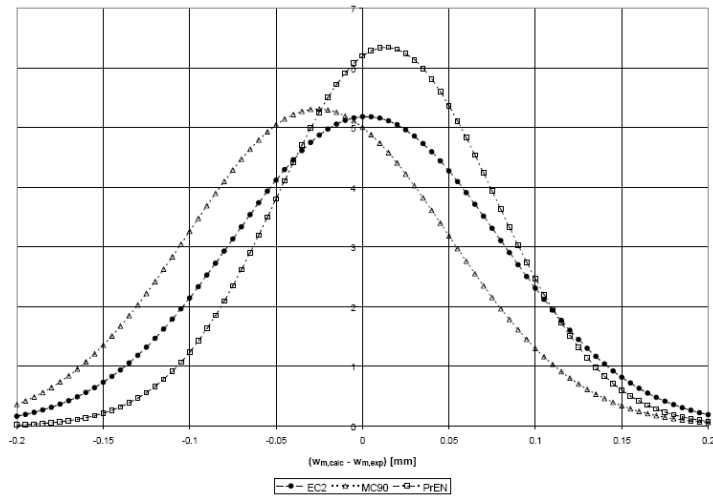


Figure 7.17 Density function of the error in the estimation of the mean crack width

**7.3.4.6 Conclusion**

With the experimental data gathered, and the selection criteria given above, the crack formulae [3,4,10] proposed for the crack prediction for the 3 different models discussed above was evaluated.

During the process of gathering and computing all the result data, three things became manifest:

- Within a steel stress limit of 250MPa the crack width does not have to be necessarily checked. This was confirmed by the statistical evaluation, which demonstrated that below 250 N/mm<sup>2</sup> the anticipated maximum crack opening will not exceed a value of 0.4 mm with a plausibility of 95%.
- The error of the formulae in the evaluation of the crack width [3,4,10] increases for larger crack openings. Also all models tend to underestimate the crack width when it is large. This is a critical point, because especially for higher steel stresses, the crack opening is expected to be critically larger and the prediction more important than for small cracks under lower steel stress. It might be interesting for future proposals of the EC2 crack prediction formula to provide an adjustment to compensate this tendency.
- Nevertheless it could be verified that the existing models, EC2 [4] and MC90 [3] and the PrEN [10], provide acceptable predictions. The mean value of the observed error is in all cases close to zero. Also the standard deviation of this error is relatively small (0.063 to 0.076 mm).

With all this information it can be said, that the PrEN has a good performance range and will be an adequate substitute for the existing EC2 formula.

**7.3.4.7.1 Exact derivation**

The EC2 cracking opening formula is:  $w_k = \frac{\sigma_s}{E_s} \left[ 1 - \frac{\sigma_{s,cr}}{\sigma_s} \right] \cdot \left[ k_3 \cdot c + k_1 k_2 k_4 \frac{\phi}{\rho_s} \lambda \right]$  (7.46)

Assuming the prescribed values  $k_3=3.4$ ,  $k_4=0.425$  and considering the bending case ( $k_2=0.5$ ) with high bond reinforcement ( $k_1=0.8$ ), it results

$$w_k = \frac{\sigma_s}{E_s} \left[ 1 - \frac{\sigma_{s,cr}}{\sigma_s} \right] \cdot \left[ 3.4 \cdot c + 0.17 \frac{\phi}{\rho_s} \lambda \right]$$
 (7.47)

which can be used as a design formula. In particular, for given  $b$ ,  $h$ ,  $d'$ ,  $b$ , and fixed  $M$ , we want to deduce the steel reinforcement amount  $A_s$  and its design tension  $\sigma_s$  in order to have a crack width  $w_k$  lower than the fixed value  $\bar{w}_k$ . The non-dimensional depth of the neutral axis is

$$-\frac{1}{2} \xi^2 - \alpha_c \cdot \rho_s (1 + \beta) \xi + \alpha_c \cdot \rho_s (\delta + \beta \cdot \delta') = 0$$
 (7.48)

The steel tension is

$$\sigma_s = \frac{\alpha_c v (\delta - \xi) f_{ctm} k_t}{2 \left[ 3n \cdot \rho_s \left[ (\delta - \xi)^2 + \beta (\delta' - \xi)^2 \right] + \xi^3 \right]}$$
 (7.49)

Assuming  $v = \frac{M}{M_{cr}^0} = \frac{M}{k_t f_{ctm} \frac{b \cdot h^2}{6}}$  we get (7.50)

$$\rho_s = \frac{\xi^2}{2\alpha_c \left[ -(1 + \beta) \xi + \delta + \beta \delta' \right]}$$
 (7.51)

$$\frac{\alpha_c v (\delta - \xi) - 2\xi^3 p}{(\delta - \xi)^2 + \beta (\delta' - \xi)^2} = \frac{3\xi^2 p}{\delta + \beta \delta' - (1 + \beta)\xi} \quad \text{where } p = \sigma_s / (k_t f_{ctm}) \quad (7.52)$$

When  $w = \bar{w}_k$ , after some calculations we deduce

$$p = \frac{\bar{w}_k^0}{3.4 \cdot c + 0.17 \frac{\phi \cdot \lambda}{\rho_s}} + \frac{\lambda}{\rho_s} + n \quad (7.53)$$

$$\text{setting } \bar{w}_{ok} = \frac{E_s \bar{w}_k}{k_t f_{ctm}}$$

Combining the above equations it results

$$\frac{\alpha_c v (\delta - \xi)}{[(\delta - \xi)^2 + \beta (\delta' - \xi)^2]} = \left[ \frac{\bar{w}_k^0 \cdot \xi^2}{3.4 \cdot c \cdot \xi^2 + 0.34 \alpha_c \cdot \phi \cdot \lambda [\delta + \beta \delta' - (1 + \beta)\xi]} + \frac{2\alpha_c \cdot \lambda}{\xi^2} [\delta + \beta \delta' - (1 + \beta)\xi] + \alpha_c \right] \times \left[ \frac{3\xi^2}{[\delta + \beta \delta' - (1 + \beta)\xi]} + \frac{2\xi^3}{[(\delta - \xi)^2 + \beta (\delta' - \xi)^2]} \right] \quad (7.54)$$

which numerically solved, gives the neutral axis position from which the reinforcement tension and its amount can be determined. If it is not the case, it is necessary to set in the  $\lambda = 2.5 \cdot (1 - \delta)$  and then re-evaluating  $\xi$ , being the value  $\lambda = 0.5$  practically impossible for bending problems.

The procedure, aimed to the determination of the reinforcement amount and its tension corresponding to fixed crack width values and stress level, requires to assume the value of the bars diameter  $\phi$ .

Alternatively, it is possible to set the tensional level  $\sigma_s$ , for example equal to the limit one, and to evaluate the corresponding reinforcement amount  $\rho_s$  and the maximal bar diameter. In this case, as the parameter  $p$  is defined, the neutral axis is calculated from (7.52),  $\rho_s$  from (7.50) and the maximal diameter can be derived solving with respect to  $\phi$ , which gives

$$\phi_{\max} = \frac{\rho_s}{\lambda} \left[ \frac{5.88 \rho_s \bar{w}_{ok}}{(p - \alpha_c) \rho_s - \lambda} - 2c \right] \quad (7.55)$$

#### 7.3.4.7.2 Approximated derivation

The procedure discussed above is quite laborious as it requires iteration. An alternative procedure, easier to be applied, is based on the assumption of a lever arm  $h_0 = 0.9d$  constant and independent from  $\xi$ . Therefore,  $\sigma_s A_s 0.9d = M$  and

$$\rho_s = 0.185 v / (p \delta) \quad (7.56)$$

The general formula for  $w = \bar{w}_k$  gives

$$\bar{w}_k = \frac{\sigma_s}{E_s} \left[ 1 - \frac{\lambda}{\rho_s \cdot p} \left( 1 + \frac{\alpha_c \cdot \rho_s}{\lambda} \right) \right] \left( 3.4c + 0.17 \frac{\phi \cdot \lambda}{\rho_s} \right) \quad (7.57)$$

For further simplification of the problem, assuming  $\delta = 0.9$ , therefore  $\lambda = 0.243$  and by definition

$$v^* = \frac{v}{1 - \frac{\delta \cdot \lambda}{0.185 v}} = \frac{v}{1 - \frac{1.18}{v}} \quad u_1 = \frac{c}{\phi} \quad u_2 = \frac{\bar{w}_{ok}}{\phi} \quad (7.58)$$

the following equation is obtained

$$p^2 + 5 \cdot v^* \left[ 3.4 u_1 \sqrt{v^*} - 0.20 \frac{\alpha_c}{v} \right] p - v^* [17 \alpha_c \cdot u_1 + 5 u_2] = 0 \quad (7.59)$$

This formula is easy to solve and leads to the desired values  $\rho_s$  and  $\sigma_s$ .

In this case too, for a given value of  $\sigma_s$ , solving for  $\phi$  we obtain

$$\phi_{\max} = \frac{[17c(vp - \alpha_c v^*) - 5v^* \bar{w}_{ok}]}{\alpha_c \sqrt{v^*} p - p^2} \quad (7.60)$$

that defines the maximal bar diameter, which satisfies the cracking limit state corresponding to a fixed value of the tension in the steel

**7.4 Deflection control**

- 7.4.1 General considerations**
- 7.4.2 Cases where calculations may be omitted**
- 7.4.3 Checking deflections by calculation**

**C7.4 Discussion of the general method followed for deflection calculation**

**7.4.1 Instantaneous deflections**

Instantaneous deflections are computed by applying the total load on a structure in which there is a reduction of the stiffness. The law to calculate the reduction of stiffness is deduced from equation 7.8 of prEN 1992-1:

$$\frac{1}{r} = \frac{M}{EI_e} = \zeta \left( \frac{1}{r} \right)_{II} + (1 - \zeta) \left( \frac{1}{r} \right)_I = \zeta \frac{M}{EI_I} + (1 - \zeta) \frac{M}{EI_{II}} \tag{7.61}$$

From this equation, the following relationship is obtained:

$$I_e = \frac{I_I I_{II}}{\zeta I_I + (1 - \zeta) I_{II}} \tag{7.62}$$

The coefficient applied to the stiffness of each section is obtained as:

$$\text{coef} = \frac{I_e}{I_I} \tag{7.63}$$

**7.4.2 Long-term deflections**

**7.4.2.1 Assumed Load History**

The load history influences the value of the deflections. In this study a realistic load history has been taken into account. A typical load history for buildings could be:

- Application of self weight at 10 days
- Application of the remaining dead load at 60 days
- Application of quasi-permanent load at 365 days.

**7.4.2.2 Deflections due to creep**

*Complex Loading History* The interpretation of prEN 1992-1 regarding deflections due to creep is not clear when the load-history is complex.

As described in paragraph 7.4.2.1, the assumed load history involves 3 dates for the application of the loads:

- Application of self weight of the structure,  $g_1$  at time  $t_1$
- Application of remaining dead load  $g_2$  at time  $t_2$
- Application of quasi-permanent live load  $\psi_{02}q$  at  $t_3$

prEN 1992-1 proposes to take into account the creep of concrete by using an effective modulus for concrete:

$$E_{c,eff} = \frac{1}{1 + \varphi} \tag{7.64}$$

The question then arises about which time should be used to compute the creep coefficient.

To solve this problem the following procedure is proposed:

- Compute  $f_{g_1,(t_1, \zeta_1)}$  with  $\varphi(t, t_1)$  and  $\zeta_1$ .
- Compute  $f_{g_1+g_2(t_2, \zeta_2)}$  with  $\varphi(t, t_2)$  and  $\zeta_2$ .
- Compute  $f_{g_1+g_2+q(t_3, \zeta_3)}$  with  $\varphi(t, t_3)$  and  $\zeta_3$ .
- Compute  $f_{q_1(t_2, \zeta_1)}$  with  $\varphi(t, t_2)$  and  $\zeta_1$ .
- Compute  $f_{g_1+g_2(t_3, \zeta_2)}$  with  $\varphi(t, t_3)$  and  $\zeta_2$
- Compute the total deformation by using the following expression:

$$f_{g_1+g_2+q,\infty} = f_{g_1,(t_1, \zeta_1)} + f_{g_1+g_2(t_2, \zeta_2)} - f_{q_1(t_2, \zeta_1)} + f_{g_1+g_2+q(t_3, \zeta_3)} - f_{g_1+g_2(t_3, \zeta_2)} \tag{7.65}$$

This complicated and time-consuming procedure is necessary due to progressive cracking of cross sections. This expression takes into account, for example, that part of the deflection due to  $g_1$  occurs at time  $t_2$  due to the reduction of stiffness produced by the application of load  $g_2$ . The creep of this extra deflection must therefore be referred to time  $t_2$ . This is what is achieved by the above expression.

In case a construction live load equivalent to the value of  $g_1+g_2+\psi_{01}q$  is assumed to be applied at time  $t_1$ , the above expression is greatly simplified, since no reduction of stiffness occurs after the application of  $g_1$ +construction load:

$$f_{g_1+g_2+q,\infty} = f_{g_1,(t_1, \zeta_3)} + f_{g_1+g_2(t_2, \zeta_3)} - f_{q_1(t_2, \zeta_3)} + f_{g_1+g_2+q(t_3, \zeta_3)} - f_{g_1+g_2(t_3, \zeta_3)} = f_{g_1,(t_1, \zeta_3)} + f_{g_2+q(t_2, \zeta_3)} + f_{q(t_3, \zeta_3)} \tag{7.66}$$

**7.4.2.3 Deflections due to shrinkage**

Deflections due to shrinkage are computed for a stiffness corresponding to the quasi-permanent load condition, taking into account an effective modulus with a creep coefficient corresponding to the start of development of shrinkage (i.e. end of curing),  $\varphi(t, t_s)$ .

Also, II and III are calculated using  $E_{c,eff}$ .

**7.4.3 Parametric study of slenderness limit**

**7.4.3.1 Introduction**

ENV 1992-1-1:1991 in table 4.14 and MC-90 in table 7.5.2 provide slenderness limits for lightly reinforced and heavily reinforced concrete elements. In both cases, for a simply supported beam the

corresponding values are, respectively,  $L/d=18$  and  $L/d=25$ . These values are given for a steel yield stress of 400 N/mm<sup>2</sup>, and are inversely proportional to the steel grade. This means, that the equivalent values for a 500 N/mm<sup>2</sup> steel would be  $L/d=14$  and  $L/d=20$ .

There have been complaints in the sense that this table is too conservative, or too general. The parametric study described in the following sections, considers a large range of variables affecting the deformation of concrete structures, in order to quantify their influence and study the possibility of including them in the calculation of the slenderness limit. The present proposal for section 7.4 of prEN 1992-1, is based on this study.

The parametric study, which has been carried out according to the procedure described above, considers the influence on the slenderness limit of the following parameters:

- Complex load history. The influence of the values of  $t_1$ ,  $t_2$  and  $t_3$  on the slenderness limit has been studied.
- Control of total deflections vs. control of deflection which produced cracking of partitions (referred to in this document as *active deflection*). Slenderness limits are calculated by limiting the total deflection to  $L/250$ . It has been investigated whether the limitation of the deflection producing cracking of partitions to  $L/500$  can be more restrictive.
- Influence of relative humidity. The relative humidity affects long term deflections through creep and shrinkage. The influence of this parameter on the slenderness limit has been studied for relative humidity varying from 50 to 80%.
- Real reinforcement vs. required reinforcement. The effect of considering a 5% to 10% increase in the real reinforcement with respect to the required reinforcement determined from U.L.S. analysis has been studied in order to take into account the round-off in detailing.
- Distribution of reinforcement. Reinforcement in real beams is not constant. The influence of the real distribution of reinforcement on the slenderness limit has been studied.
- Concrete grade
- Percentage of self weight ( $g_1$ ), additional deal load (flooring and partitions  $g_2$ ) and quasi-permanent live load ( $\psi_{02}q$ ) with respect to the total load ( $q_{tot}$ ). According to Spanish practice, typical values for these relations could be:

- For one-way slabs,

$$\frac{G_1}{Q_{tot}} = 0,45$$

$$\frac{G_2}{Q_{tot}} = 0,30$$

$$\frac{\psi_{02}Q}{Q_{tot}} = 0,30 \cdot 0,25 = 0,075$$

- For flat slabs,

$$\frac{G_1}{Q_{tot}} = 0,60$$

$$\frac{G_2}{Q_{tot}} = 0,20$$

$$\frac{\psi_{02}Q}{Q_{tot}} = 0,30 \cdot 0,20 = 0,06$$

For this study, as for prEN 1992-1, the slenderness limit is defined as the relationship between the span and the effective depth  $L/d$ .

The slenderness limit curves which are presented in the following paragraphs, are given for different reinforcement ratios. The reinforcement ratio,  $\rho$ , is defined as the ratio of tensile reinforcement  $A_s$ , to effective cross section  $bd$ .

#### 7.4.3.2 Assumptions for parametric study

The parametric study which follows has been carried out for a simply supported beam with a cross section of 100 x 30 cm<sup>2</sup>. The cover has been assumed as 1/10 of the total depth.

The reference values for which the study is formulated are the following:

- Relative humidity of 70%
- Load history:  $t_1/t_2/t_3 = 10/60/365$  days
- Permanent load vs. live load:  $g_1 = 45\%q_{tot}$ ,  $g_2 = 30\%q_{tot}$  and  $q = 25\%$  of  $q_{tot}$ .
- Quasi permanent live load is 30% of characteristic live load
- Tensile and compressive reinforcements are those strictly needed for ULS.
- Concrete Strength: 30 N/mm<sup>2</sup>
- Steel Yield Stress: 500 N/mm<sup>2</sup>
- Distribution of reinforcement is considered constant over the beam length.

For each part of the study, one of the above parameters is varied while the others remain constant.

**7.4.3.3 Method for determining the slenderness ratio**

In order to determine the slenderness ratio, the following steps were taken for each reinforcement ratio:

- A certain span length,  $L$ , is assumed.
- Calculation of the ultimate bending moment ( $M_{ULS}$ ). When compression reinforcement is needed in order to yield the tensile reinforcement, compressive reinforcement is provided and taken into account in the calculation of deflections.
- The ultimate load,  $q_{ULS}$ , is determined from the  $M_{ULS}$ , assuming a simply supported beam:

$$q_{ULS} = \frac{M_{ULS}}{L^2} \cdot 8$$

- The total service load ( $q_{tot}$ ) is determined from  $q_{ULS}$ , and the assumed ratios for  $g_1/q_{tot}$ ,  $g_2/q_{tot}$  and  $q/q_{tot}$ , according to:

$$q_{ULS} = 1.35 \cdot (g_1 + g_2) + 1.5 \cdot q = 1.35 \cdot (0.45 + 0.30) \cdot q_{tot} + 1.5 \cdot 0.25 \cdot q_{tot} = 1.38 \cdot q_{tot} \rightarrow q_{tot} = 0.72 \cdot q_{ULS}$$

- The values of  $g_1$ ,  $g_2$  and  $q$  are determined from the above ratios.
- The deflection is computed. According to the general method of prEN 1992-1. If the deflection obtained is not  $L/250$  for total deflection or  $L/500$  for active deflection, the procedure is repeated until convergence is achieved.

**7.4.3.4 Influence of the dimensions of the cross section used**

The cross section assumed for the parametric study is, as stated above, a rectangular cross section of  $b \times h = 100 \times 30 \text{ cm}^2$ . In order to insure that the particular dimensions of the cross section are not important, the slenderness limit for different reinforcement ratios has also been determined for the cross section used by Beeby in [2], all other parameters being those taken as reference (see section 3.2).

This cross section is rectangular of dimensions  $b \times h = 30 \times 50 \text{ cm}^2$ .

Figure shows the comparison between both rectangular cross sections.

As can be seen no significant difference can be observed.

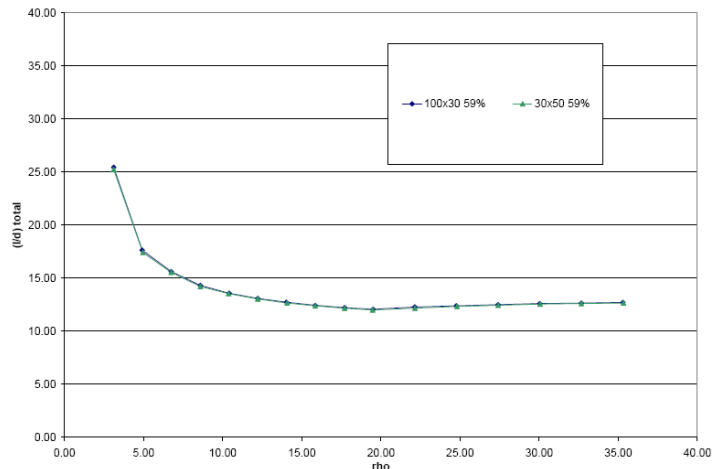


Figure 7.18. Slenderness ratio for two rectangular cross section of different dimensions

**7.4.3.5 Influence of load history**

The load history used for the parametric study is described above in 2.2.1. It is assumed that the construction live load is applied at the same time as the self weight so that the section is fully cracked from the beginning. This provides an upper bound estimation for total deflection (not so for active deflection).

The reference load history is:  $t_1/t_2/t_3=10/60/365$  days

Two other load histories are considered:  $t_1/t_2/t_3=7/14/365$  days and  $t_1/t_2/t_3=28/90/365$  days.

The calculation of the slenderness limit has been carried out in this case for two steel ratios: 0.5% and 1.5%.

The results are shown in Table 7.5. As can be seen, the influence of the load history is very limited. This suggests that simplifications are possible. One such simplification, consisting in considering a single time of loading together with an equivalent creep coefficient is described in detail in section 7.4.4.1.

	$(t_1, t_2, t_3)=(7, 14, 365)$	$(t_1, t_2, t_3)=(28, 90, 365)$
$A_s/bd=0.5\%$	-2%	+2%
$A_s/bd=1.5\%$	-3%	+3%

Table 7.5. Influence of load history on the slenderness limit.  
 $((L/d)(10, 60, 365) - (L/d)(t_1, t_2, t_3)) / (L/d)(10, 60, 365)$

**7.4.3.6 Influence of additional reinforcement**

The slenderness ratio is referred to the deflection occurring in case the strict reinforcement is placed in the beam. However, it is normal for structures to have extra reinforcement due to rounding off, on the safe side, of the required values.

The influence of this factor has been studied by comparing the deflection of a beam with different required reinforcement ratios in case an extra 5% or 10% reinforcement is provided in tension. The results are given in Fig. 7.19.

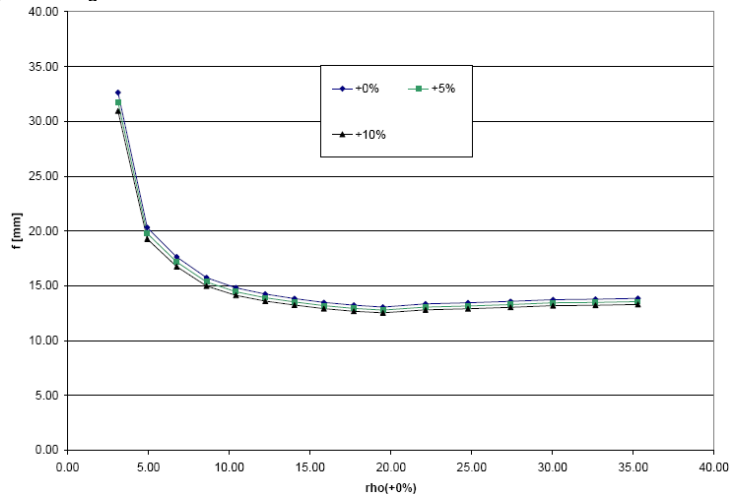


Figure 7.19. Influence of round-off extra reinforcement in the deflection of a simply supported beam

**7.4.3.7 Influence of distribution of reinforcement**

Distribution of reinforcement in beams is not constant in practice.

Normally, minimum reinforcement is placed near the points of zero bending moment (base reinforcement) and a supplementary reinforcement is placed in the areas near the maximum bending moment. The influence of the length of the additional reinforcement has been studied for two reinforcement ratios (0.5% and 1.5%) and assuming a length ( $l_s$ ) of the supplementary reinforcement of 60, 80, 90 and 100% of the span. Outside this length minimum reinforcement was considered.

The results are given in Table 7.6 by comparing the deflection for  $l_s=100\%$  to the deflection for the different values of  $l_s$ . It can be seen that for low values of the reinforcement ratio and no influence is detected. The difference becomes significant only for high reinforcement ratios and small length of additional reinforcement.

100%	Ratio $l_s/L$				
	100%	90%	80%	70%	60%
$f/f_{100\%}, \rho=0.5\%$	1.0	1.0	1.0	1.0	1.0
$f/f_{100\%}, \rho=1.5\%$	1.0	1.0	1.0	1.0	1.3

Table 7.6. Influence of the length of supplementary reinforcement on the deflection of a simply supported beam.

**7.4.3.8 Active deflection vs. total deflection**

Table 4.14 of ENV-1992-1-1:1991 as well as table 7.4 of prEN 1992-1, has been determined by limiting total deflections. However, as can be seen from figure Fig. 7.20, the limit of active deflection to a maximum value of  $L/500$  is a more strict condition. Further consideration should be given to this fact.

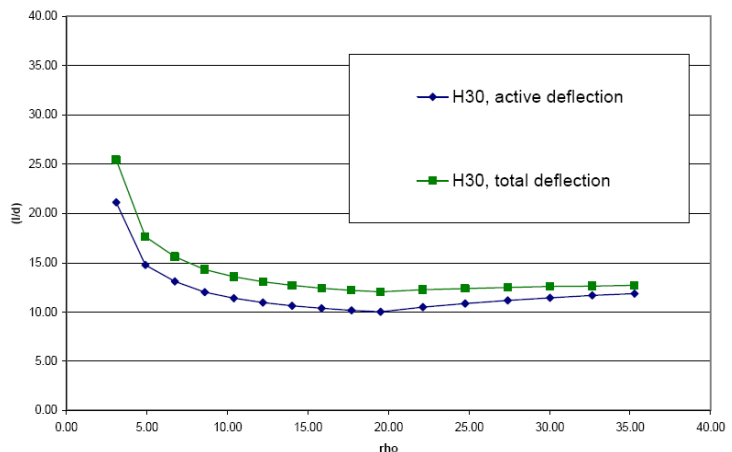
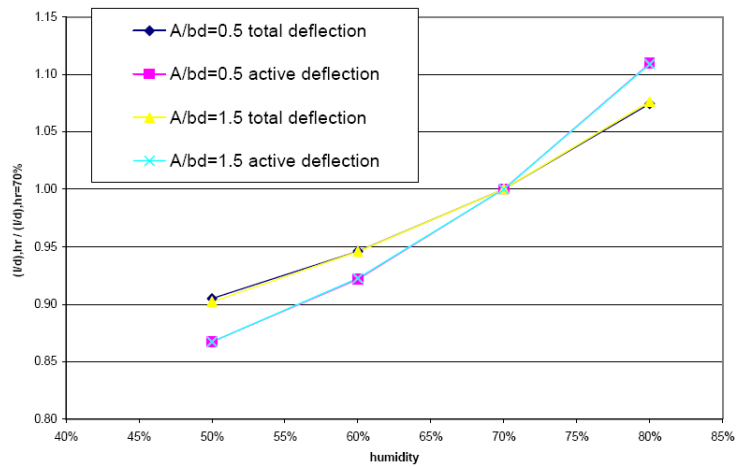


Figure 7.20 – Slenderness Limit for Total and Active Deflection



**7.4.3.9 Influence of relative humidity**

The influence of relative humidity on the slenderness limits was studied for two different steel ratios:  $\rho = 0.5\%$  and  $\rho = 1.5\%$ . The slenderness limit was determined for these two steel ratios and relative humidity of 50, 60, 70 and 80%. The results are given in Fig. 7.21.



**Figure 7.21.** Influence of relative humidity on Slenderness Limits for Total and Active Deflections (referred to 70% RH)

From Fig. 7.21 it can be seen that the influence of relative humidity on the slenderness ratio is important with a variation of  $\pm 15\%$  for the active deflection and  $\pm 10\%$  for total deflection from the reference value of 70% of relative humidity.

The figure also shows that the influence of relative humidity does not significantly depend on the steel reinforcement ratio.

**7.4.3.10 Influence of the percentage of self weight, superimposed dead load and live load with respect to total load.**

For this study, different load distributions have been assumed, including the assumption that the quasi permanent service load,  $q_{cp}$ , can be taken as 0.5 times the ultimate limit state (ULS) load. The ULS load is given by the following expression:

$$q_{ULS} = 1.35 \cdot (g_1 + g_2) + 1.5 \cdot q$$

As explained in section 7.4.3.3, the ultimate load  $q_{ULS}$  is known from the value of the reinforcement. If it is assumed that  $g_1 \approx 1.5 \cdot g_2$ , then by fixing different values for the quasi permanent service load ( $q_{cp}$ )/ultimate load ( $q_{ULS}$ ) ratio,  $g_1$ ,  $g_2$  and  $q$  may be determined for each ratio. This provides, in the end, significantly different values for the permanent to live load ratios for the quasi permanent combination. The lower the value of the permanent load, the lower will be the load considered for the verification of deflections, since only 30% of the live load is considered quasi permanent.

In Table 7.7, the different ratios of  $q_{cp}/q_{ULS}$  considered and the resulting ratios of  $g_1/q_{tot}$ ,  $g_2/q_{tot}$  and  $q/q_{tot}$  are given.

$q_{cp}/q_{ULS}$	$g_1/q_{tot}$	$g_2/q_{tot}$	$q/q_{tot}$
46%	30%	20%	50%
51%	36%	24%	40%
57%	42%	28%	30%
59%	45%	30%	25%
68%	54%	36%	10%

**Table 7.7.** Total service load/Ultimate load ratios and corresponding values of self weight, superimposed dead load and live load to total service load ratios

The comparison of the results of the slenderness limits for the different quasi permanent service load to ultimate load ratios is plotted in Fig. 7.22. As can be seen the difference is important. It is also interesting to note that the values of  $l/d = 20$  for 0.5% reinforcement ratio and  $l/d=14$  for 15% reinforcement ratio, are obtained approximately for a ratio of  $q_{cp}/q_{ULS}=0.5$ .

**Comparison Different load distribution ( $g_1/q_{tot}$ ), ( $g_2/q_{tot}$ ), ( $q/q_{tot}$ )**

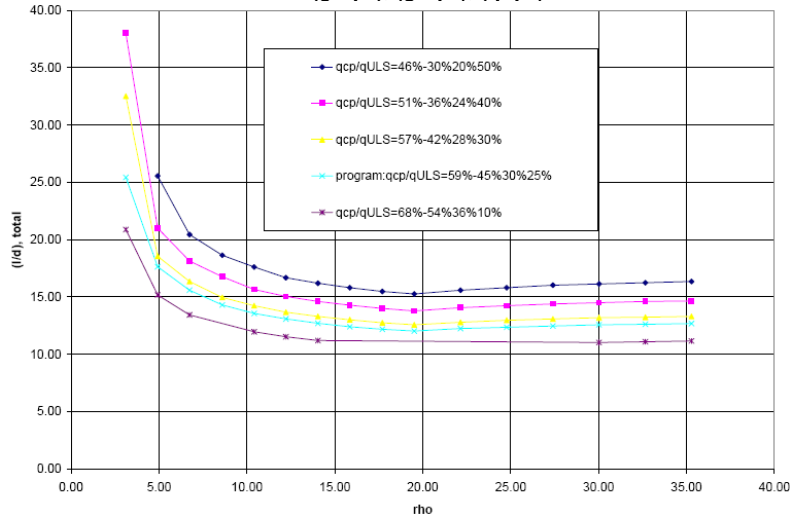


Figure 7.22. Slenderness limits for total deflection and different total service load to ultimate load ratios

**7.4.3.11 Influence of the concrete grade**

The influence of the concrete grade on the slenderness limit has been studied in a very detailed manner for many values of the reinforcement ratio. The concrete grades considered are: C30, C40, C60 and C100.

For this comparison, the relationship between total service load and ultimate load has been taken as 51%. This value, is different from the reference value, but, as explained in section 7.4.3.10, agrees well with the values of prEN 1992-1 table 4.14 which are also in accordance with the values of MC-90 and ENV-1992-1-1:1991.

Fig. 7.23 shows the results of this comparison. It can be seen that there is a very significant influence of the concrete grade on the slenderness limit. These curves, also show very well the behaviour for very low steel ratios. There is a clear discontinuity in the curves which separates the point in which cracking does not occur from the point in which the bending moment is greater than the cracking moment. The curves also show that for low steel ratios, much higher slenderness limits can be established. These curves form the basis for the formula proposed for the slenderness limit in prEN 1992-1, which is dependent on the concrete grade, and provides a continuous estimation of the slenderness limit as a function of the reinforcement ratio.

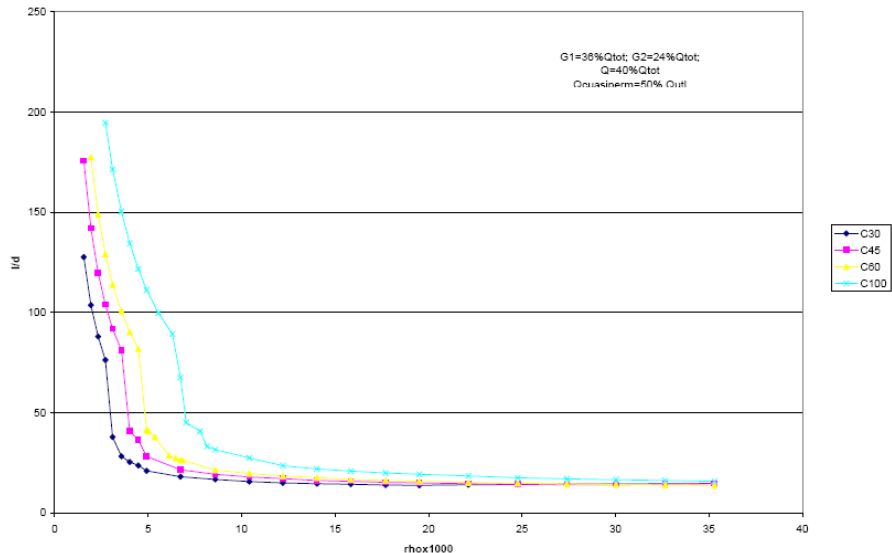


Figure 7.23. Slenderness ratio as a function of the concrete grade

**7.4.3.12 Influence of the tensile strength of concrete ( $f_{ctm}$  vs.  $f_{ctm,n}$ )**

The final version of prENV, allows the use of the flexural tensile strength of concrete instead of the mean tensile strength for the calculation of deflections. This topic was subject of much controversy and it is therefore interesting to test the differences to which this may lead. For this purpose, the slenderness limits were redetermined with the assumption that the flexural tensile stress of concrete could be used. The results are shown in Fig. 7.24.

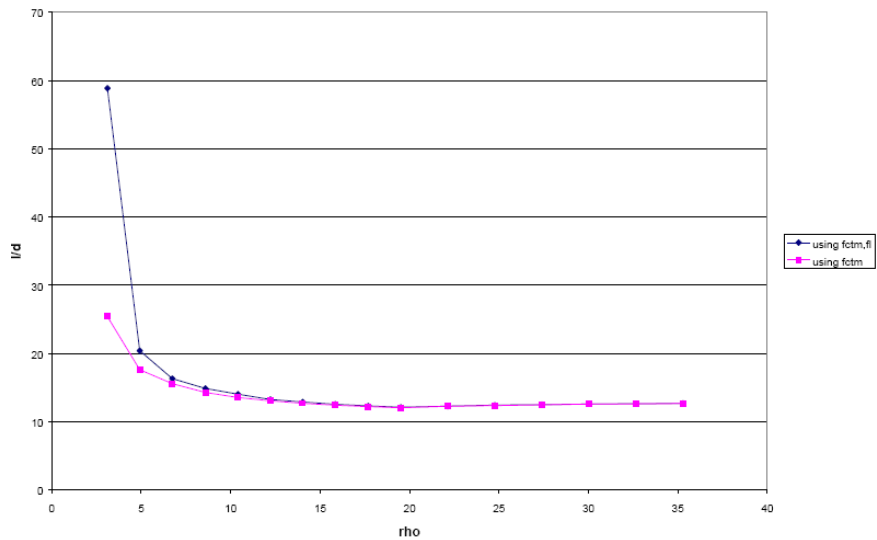


Figure 7.24. Slenderness Limit using  $f_{ctm}$  and  $f_{ctm,fl}$

As can be seen there is an important difference only for very small reinforcement ratios. For reinforcement ratios larger than 0.6%, the difference is negligible.

### 7.4.4 Simplified formulae

#### 7.4.4.1 Simplified formula of EC2

The application of the general method of prEN 1992-1 is very tedious and time consuming, since calculations have to be made for many sections. As an alternative to this procedure a simplified method consisting in calculating an equivalent moment of inertia as explained in section 2.1 for the centre span of the beam only and assuming this value for the whole beam is also recommended in the present draft for prEN 1992-1. This procedure is on the safe side, since cross sections near the point of zero bending moment will not crack.

Additionally, in this comparison and in order to keep the simplified formula simple, an equivalent creep coefficient is used. This creep coefficient which allows to take into account the load history in a simplified manner is defined as:

$$\phi_{eq} = \frac{g_1\phi(t,t_1) + g_2\phi(t,t_2) + \psi_{02}q\phi(t,t_3)}{g_1 + g_2 + \psi_{02}q} \tag{7.67}$$

The general and simplified procedure are compared for the reference values described in section 7.4.3.2, in Fig.7.25. The comparison is made in terms of the differences in the value of the slenderness limit for different reinforcement ratios. As can be seen, both procedures yield practically equivalent for steel ratios greater than 1%. For a 0.5% reinforcement ratio, the error is about 5% on the safe side. Fig. 7.26 shows a comparison of the differences obtained by plotting the ratio of  $(L/d)_{simplified}$  to  $(L/d)_{general}$  as a function of the steel ratio. In this case a maximum difference of 20% is obtained for the lowest reinforcement ratio considered.

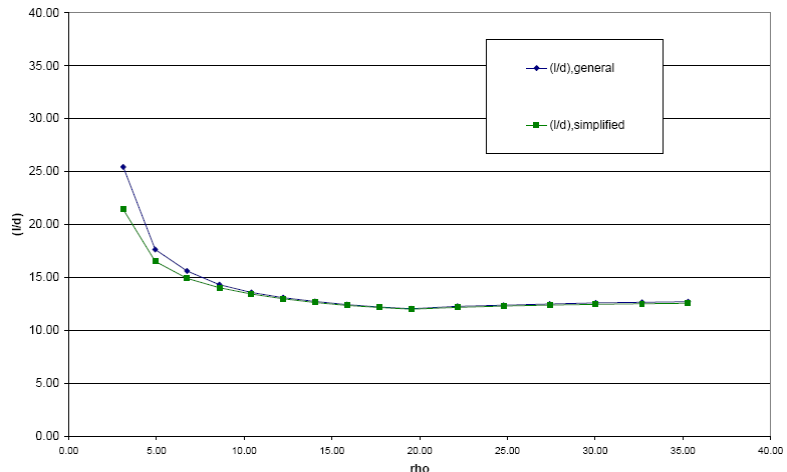


Figure 7.25. Comparison of general and simplified methods of prEN 1992-1 proposal

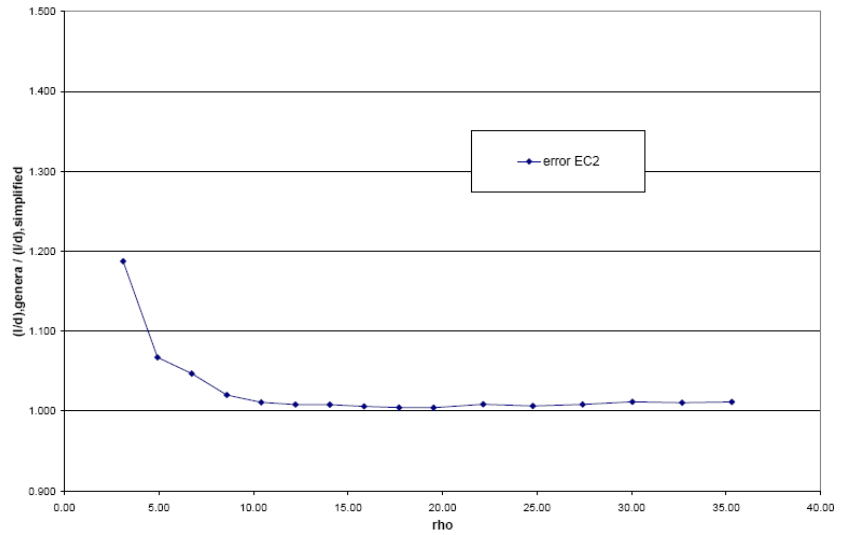


Figure 7.26. Comparison of general and simplified methods of prEN 1992-1 proposal – Evaluation of the relative error

### 7.4.5 Formula proposed for slenderness limit

In order to take into account the influence of the concrete grade on deflections, which is important, especially for low steel ratios, and in order to provide designers with a continuous relationship between the slenderness ratio and the reinforcement ratio, which is especially helpful for slab elements, the following expressions have been proposed.

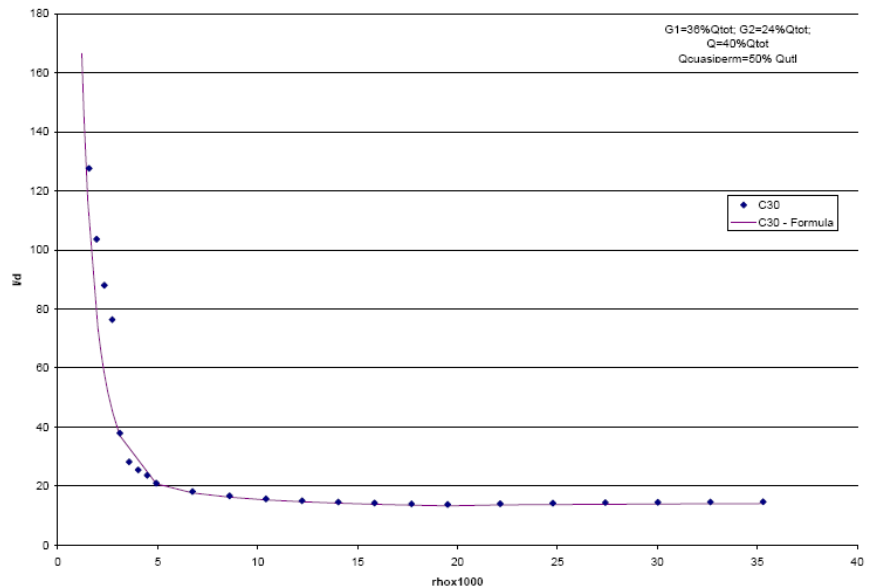
$$\rho_0 = \sqrt{f_{ck}} \cdot 10^{-3} \tag{7.68}$$

$$\frac{l}{d} = k \left[ 11 + 1.5\sqrt{f_{ck}} \frac{\rho_0}{\rho} + 3.2\sqrt{f_{ck}} \left( \frac{\rho_0}{\rho} - 1 \right)^{3/2} \right] \quad \text{if } \rho < \rho_0 \tag{7.69}$$

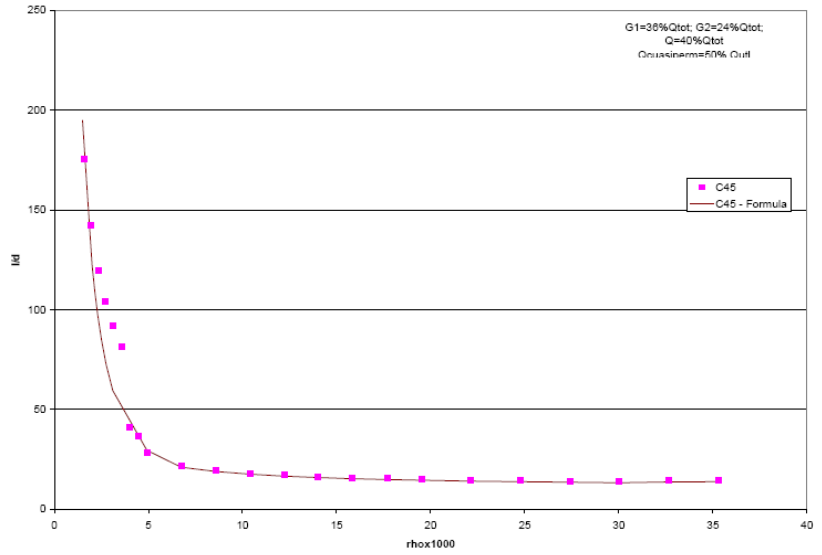
$$\frac{l}{d} = k \left[ 11 + 1.5\sqrt{f_{ck}} \frac{\rho_0}{\rho - \rho_0} + 3.2\sqrt{f_{ck}} \left( \sqrt{\frac{\rho_0}{\rho}} \right) \right] \quad \text{if } \rho \geq \rho_0 \tag{7.70}$$

These formulas are a mathematical approximation to Fig. 7.23. In Fig. 7.27, this approximation is evaluated. Four plots are presented for the four concrete grades considered in section 7.4.3.11. As can be seen the degree of coincidence between the formula and the calculated values of the slenderness limits is very good, and mostly on the safe side.

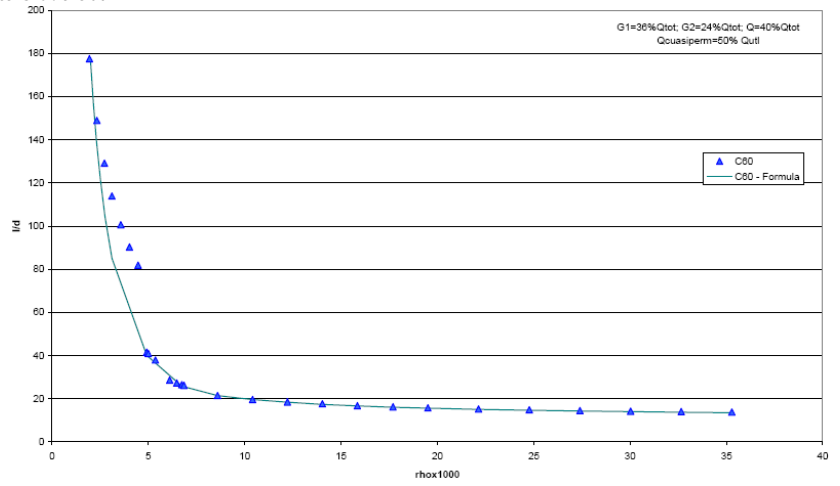
#### Concrete Grade C30



**Formula - Concrete Grade C45**



**Concrete Grade C60**



**Concrete Grade C100**

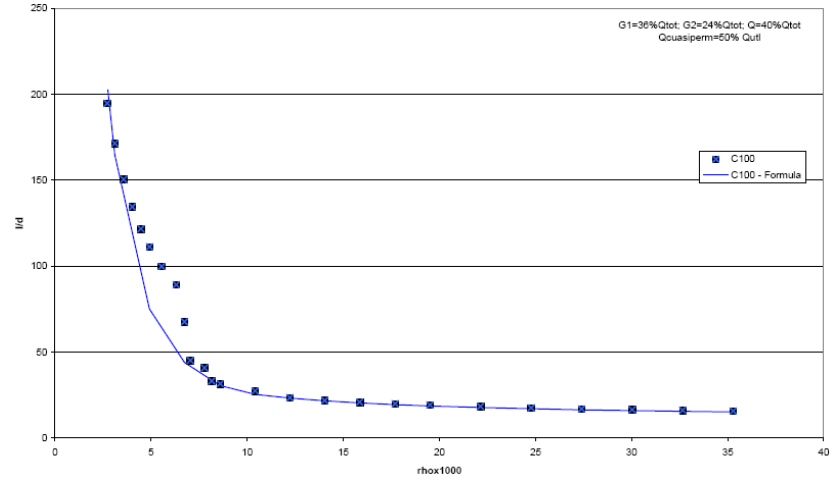


**Figure 7.27.** Comparison of General procedure with simplified formula for slenderness limit

**REFERENCES****Cracking**

- [1] A.W. Beeby, Calculation of Crack Width, PrEN 1992-1 (Final draft) Chapter 7.3.4 (2001).
- [2] A.W. Beeby, R. Favre, M. Koprna, J.P. Jaccoud, Cracking and Deformations, CEB Manual (1985).
- [3] CEB, Draft of chapter 15, Model Code 1990, (1987).
- [4] EC2, Planung von Stahlbeton- und Spannbetontragwerken, Teil 1-1 (1996).
- [5] R. Elighausen, R. Mällée, G. Rehm, Rissverhalten von Stahlbetonkörpern bei Zugbeanspruchung, Untersuchungsbericht (1976).
- [6] M. Falkner, Zur Frage der Rissbildung durch Eigen – und Zwangsspannungen in Folge Temperatur im Stahlbetonbau, Deutscher Ausschuss Für Stahlbeton Heft 208 (1969).
- [7] G. Hartl, Die Arbeitslinie eingebetteter Stähle bei Erst – und Kurzzeitbelastung, Dissertation (1977).
- [8] J.P. Jaccoud, H. Charif, Armature Minimale pour le Contrôle de la Fissuration, Publication N° 114 (1986).
- [9] M. Krips, Rissenbreitenbeschränkung im Stahlbeton und Spannbeton, TH Damstadt (1985).
- [10] PrEN, 1992-1, Serviceability Limit States, Final Draft (2001).
- [11] G. Rehm, H. Rüsç, Versuche mit Betonformstählen Teil I, Deutscher Ausschuss für Stahlbeton Heft 140 (1963).
- [12] G. Rehm, H. Rüsç, Versuche mit Betonformstählen Teil II, Deutscher Ausschuss für Stahlbeton Heft 160 (1963).
- [13] G. Rehm, H. Rüsç, Versuche mit Betonformstählen Teil III, Deutscher Ausschuss für Stahlbeton Heft 165 (1964).

**Deflection**

- [1] CEN. Eurocode 2: *Design of concrete structures – Part 1: General rules and rules for buildings. Ref. No.. prEN 1992-1:2000.* 1<sup>st</sup> Draft.
- [2] Beeby, A.W. 4.3.3 *Deformation.* fib Bulletin 2 – Structural concrete Textbook. Volume 2. July 1999
- [3] CEB-FIP. Model Code 90. Bulletin d'Information N°213/214. May 1993.
- [4] CEN. Eurocode 2: *Design of concrete structures – Part 1: General rules and rules for buildings. Ref. No.. prEN 1992-1:1991.*

**SECTION 8 DETAILING OF REINFORCEMENT AND PRESTRESSING TENDONS - GENERAL**

- 8.1 General
- 8.2 Spacing of bars
- 8.3 Permissible mandrel diameters for bent bars
- 8.4 Anchorage of longitudinal reinforcement
- 8.5 Anchorage of links and shear reinforcement
- 8.6 Anchorage by welded bars
- 8.7 Laps and mechanical couplers
- 8.8 Additional rules for large diameter bars
- 8.9 Bundled bars
- 8.10 Prestressing tendons

**SECTION 8. DETAILING OF REINFORCEMENT AND PRESTRESSING TENDONS - GENERAL**

See example 6.15

See example 6.15

See example 6.15

**C8.10.2.**

**8.10.2.1. Background**

The ENV rules for the anchorage of pre-tensioned tendons are found in 4.2.3.5.6. The basic value of the transmission length for prestress at release (transfer) is given as a multiplier  $\beta_b$  for the nominal diameter, table 8.1.

Actual concrete strength at transfer, MPa		25	30	35	40	45	50
$\beta_b$	Strands and smooth or indented wires	75	70	65	60	55	50
	Ribbed wires	55	50	45	40	35	30

*Table 8.1. Basic value of factor  $\beta_b$  for transmission length according to ENV, table 4.7*

Two design values of the transmission length are defined, 0,8 and 1,2 times the basic value, of which the more unfavourable one should be used depending on the design situation. For anchorage at the ultimate limit state, the bond is assumed to be the same as at release of prestress.

The ENV rules did not take into account the following parameters:

- a) the initial prestress in the tendons<sup>1</sup>
- b) the way of release of prestress (gradual or sudden)<sup>2</sup>
- c) the difference in bond conditions with regard to the position of tendons etc.
- d) the difference in bond conditions with regard to "push-in" and "pull-out"<sup>3</sup>
- e) the difference between strands and indented wires.

The national comments on clause 4.2.3.5.6 were mainly editorial, but the rules needed a thorough update based on MC90, which represents a more up-to-date knowledge, and takes into account all the important parameters.

The present rules in clause 8.10.2 of the EN are basically a different formulation of clause 6.9.11 in MC90. There is one difference, however. MC90 gives two design values of the transmission length, with a ratio 2,0 between the upper and lower value. The rules in 8.10.2 have been calibrated to give the same *mean value* as MC90, but with a ratio 1,2/0,8 = 1,5 between the upper and lower values, like in the ENV. Thus, the upper value will be a lower and the lower value somewhat higher according to the EN, compared to MC90.

Among the ENV rules the alternative parabolic development of prestress, given in ENV 1992-1-3 should also be mentioned. This has not been explicitly included in the EN, since a linear development is considered to be more realistic. However, an opening for "alternative build-up of prestress" is given, without details.

**8.10.2.2. Rules in MC90 and EN 1992-1-1**

**8.10.2.2.1 Summary of rules**

The rules in MC90 and EN 1992-1-1 are summarized in table 8.2. They are described and commented more in detail in the following clauses.

<sup>1</sup> It is stated in the ENV that table 4.7 (table 1 above) is valid for the maximum allowable prestress, but nothing is said about reducing the transmission length for lower values of prestress

<sup>2</sup> A "neutralized zone" for the case of sudden release is mentioned in 4.2.3.5.6 (5), but no value is given

<sup>3</sup> "Push-in" refers to the situation at release of prestress, whereas "pull-out" refers to anchorage in ULS

Parameter	MC90, 6.9.11 <i>Expression</i>	EN 1992, 8.10.2 <i>Expression</i>
<b>Basic anchorage length</b>	$l_{bp} = \frac{A_{sp} f_{pd}}{\pi \phi f_{bpd}} \quad (6.9-13)$ where $A_{sp}/\pi\phi = (1/4)\phi$ for circular tendons $= (7/36)\phi$ for 7-wire strands $f_{pd} = f_{ptk}/\gamma_s$ , design value of steel tensile str. $f_{bpd}$ is design value of bond strength	Not used as a separate parameter in 8.10.2
<b>Bond strength at release</b>	$f_{bpd} = \eta_{p1} \eta_{p2} f_{ctd}(t) \quad (6.9-12)$ where $\eta_{p1} = 1,4$ for indented or crimped wires $= 1,2$ for 7-wire strands $\eta_{p2} = 1,0$ for good bond conditions $= 0,7$ for other cases $f_{ctd}(t)$ is design value of tensile strength at release	$f_{bpt} = \eta_{p1} \eta_1 f_{ctd}(t) \quad (8.14)$ where $\eta_{p1} = 2,7$ for indented wires $= 3,2$ for 7-wire strands $\eta_1 = 1,0$ for good bond conditions acc. to 8.4.1 $= 0,7$ otherwise (unless good bond conditions can be verified)
<b>Transmission length</b>	$l_{bpt} = \alpha_8 \alpha_9 \alpha_{10} l_{bp} \frac{\sigma_{pi}}{f_{pd}} \quad (6.9-14)$ where $\alpha_8 = 1,0$ for gradual release $= 1,25$ for sudden release $\alpha_9 = 1,0$ for anchorage length ULS $= 0,5$ for stresses at release $\alpha_{10} = 0,7$ for indented or crimped wires $= 0,5$ for strands $\sigma_{pi}$ is steel stress just after release	$l_{pt} = \alpha_1 \alpha_2 \phi \sigma_{pi} / f_{bpt} \quad (8.15)$ where $\alpha_1$ is the same as $\alpha_8$ in MC90 $\alpha_2 = 0,25$ for circular tendons $= 0,19$ for 7-wire strands <b>Note.</b> MC90's $\alpha_9$ is taken into account by 0,8 and 1,2 in expressions (8.16) and (8.17), $\alpha_{10}$ by $\eta_{p1}$ .
<b>Design values of <math>l_{pt}</math></b>	See factor $\alpha_9$ above	$l_{pt1} = 0,8 l_{pt} \quad (8.16)$ $l_{pt2} = 1,2 l_{pt} \quad (8.17)$
<b>Bond at anchorage</b>	$f_{bpd} = \eta_{p1} \eta_{p2} f_{ctd} \quad (6.9-12)$ where $f_{ctd}$ is design value of tensile strength	$f_{bpd} = \eta_{p2} \eta_1 f_{ctd} \quad (8.19)$ where $\eta_{p2}$ is the same as $\eta_{p1}$ in MC90
<b>Anchorage length</b>	$l_{bpd} = l_{bpt} + l_{bp} \frac{\sigma_{pd} - \sigma_{pcs}}{f_{pd}} \quad (6.9-15)$ where $\sigma_{pd}$ is tendon stress to be anchored $\sigma_{pcs}$ is tendon stress due to prestress after losses	$l_{bpd} = l_{pt2} + \alpha_2 \phi (\sigma_{pd} - \sigma_{p\infty}) / f_{bpd} \quad (8.20)$ where $l_{pt2}$ is upper design value of transmission length $\sigma_{p\infty}$ is tendon stress due to prestress after losses

Table 8.2. Summary of rules in MC90, 6.9.11, and EN 1992, 8.10.2

**8.10.2.2.2 Rules in MC90**

**8.10.2.2.2.1 Basic anchorage length**

$$l_{bp} = \frac{A_{sp} f_{pd}}{\pi \phi f_{bpd}}$$

where

$A_{sp}/\pi\phi = \phi/4$  for circular tendons,  $(7/36)\phi$  for 7-wire strands

$f_{pd} = f_{ptk}/\gamma_s$  design value of tensile strength of tendons

$f_{bpd}$  design value of bond strength, see below

**8.10.2.2.2.2 Design value of bond strength**

$$f_{bpd} = \eta_{p1} \eta_{p2} f_{ctd}(t)$$

where

$\eta_{p1}$  takes into account the type of prestressing tendon:

$\eta_{p1} = 1,4$  for indented and crimped wires and

$\eta_{p1} = 1,2$  for 7-wire strands

$\eta_{p2}$  takes into account the position of the tendon:

$\eta_{p2} = 1,0$  for good bond condition,

$\eta_{p2} = 0,7$  for all other cases.

$f_{ctd}(t)$  is the lower design value of concrete tensile strength at time of release, or at 28 days for verifications in ULS.

**8.10.2.2.2.3 Transmission length**

$$l_{bpt} = \alpha_8 \alpha_9 \alpha_{10} l_{bp} \frac{\sigma_{pi}}{f_{pd}}$$

where

$\alpha_8$  considers the way of release:

$\alpha_8 = 1,0$  for gradual and 1,25 for sudden release

$\alpha_9$  considers the action effect to be verified:



$\alpha_9 = 1,0$  for calculation of anchorage length when moment and shear capacity in ULS is considered, and  
 $\alpha_9 = 0,5$  for verification of transverse stresses in the anchorage zone  
 $\alpha_{10}$  considers the influence of bond situation:  
 $\alpha_{10} = 0,5$  for strands and  
 $\alpha_{10} = 0,7$  for indented or crimped wires  
 $\sigma_{pi}$  is the steel stress just after release

**8.10.2.2.4 Anchorage length in ULS**

$$l_{bpd} = l_{bpt} + l_{bp} \frac{\sigma_{pd} - \sigma_{pcs}}{f_{pd}}$$

where

$\sigma_{pd}$  tendon stress under design load ( $\sigma_{pd} \leq f_{pd}$ )  
 $\sigma_{pcs}$  tendon stress due to prestress including all losses

**8.10.2.2.3 Rules in EN 1992-1-1**

The rules in 8.10.2 are summarized below and compared to those in MC90. The “basic anchorage length” used as a separate parameter in 8.10.2 is instead incorporated directly in the expressions for transmission length and anchorage length.

**8.10.2.2.3.1 Transfer of prestress**

**8.10.2.2.3.1.1 Bond strength**

The bond strength governing the transmission at release of prestress is

$$f_{bpt} = \eta_{p1} \eta_1 f_{ctd}(t)$$

where

$\eta_{p1}$  takes into account the type of tendon and the bond situation at release (“push-in”)  
 = 2,7 for indented wires (“crimped” wires are hardly used anymore, therefore not incl.)  
 = 3,2 for 7-wire strands  
 $\eta_1 = 1,0$  for good bond conditions (see 8.4.1) or = 0,7 otherwise, unless good bond conditions can be verified  
 $f_{ctd}(t) = f_{ctk,0,05}(t) / \gamma_C$ , design value of tensile strength at the time of release, related to the compressive strength at the same time according to table 3.1

The factor  $\eta_1$  is the same as in 8.4.1 (and the same as  $\eta_{p2}$  in MC90). However, a possibility to assume “good bond conditions”, even if the criteria in 8.4.1 are not met, has been added for cases where good conditions can be achieved by other means, and verified.

The factor  $\eta_{p1}$  here includes two factors, which in MC90 are applied to the transmission length instead, namely the factor  $\alpha_{10}$  and the mean value of  $\alpha_9$ ,  $(0,5 + 1,0)/2 = 0,75$ :

$$\eta_{p1,EN} = \frac{\eta_{p1,MC90}}{\alpha_{10} \alpha_{9,mean}} \quad \text{which gives} \quad \eta_{p1,EN} = \frac{1,4}{0,7 \times 0,75} = 2,7 \quad \text{for wires}$$

$$\eta_{p1,EN} = \frac{1,2}{0,5 \times 0,75} = 3,2 \quad \text{for strands}$$

Thus,  $f_{bpt}$  includes the favourable effect of “push-in” at release. This is the “bond situation” to which MC90 refers in the definition of  $\alpha_{10}$ : when the stress decreases at release there is transverse expansion of the tendons, giving a kind of “wedge” effect. Furthermore,  $f_{bpt}$  is here a mean value of the bond strength, not a lower limit as in MC90 (the upper limit corresponds to  $\alpha_9 = 0,5$  for the transmission length). See 8.10.2.2.3.1.2 for upper and lower design values.

**8.10.2.2.3.1.2 Transmission length**

The basic value of the transmission length is

$$l_{pt} = \alpha_1 \alpha_2 \phi \sigma_{pi} / f_{bpt}$$

where

$\alpha_1 = 1,0$  for gradual release, 1,25 for sudden release (same as  $\alpha_8$  in MC90)  
 $\alpha_2 = 0,25$  for circular tendons, 0,19 for 7-wire strands (cf. MC90:  $7/36 \approx 0,19$ )  
 $\sigma_{pi}$  stress in tendon just after release (same as MC90)

Normally a short transmission length gives higher transverse stresses in the concrete at release (spalling, splitting and bursting stresses in the terminology of MC90), whereas a long transmission length is more critical for ULS with regard to shear, bending moment etc. Furthermore, there is an uncertainty in the calculated value. Therefore, the more unfavourable of the following two values should be used as a design value, depending on the design situation:

$$l_{pt1} = 0,8 l_{pt}$$

$$l_{pt2} = 1,2 l_{pt}$$

The factors 0,8 and 1,2 are the same as in the ENV, 4.2.3.5.6 (4). The corresponding factor in MC90 is  $\alpha_9$  with the values 0,5 and 1,0. With the mean value of this factor included elsewhere, see 8.10.2.2.3.1, comparable values of  $\alpha_9$  would be 0,67 and 1,33.

### 8.10.2.2.3.3 Anchorage in ULS

#### 8.10.2.2.3.3.1 Bond strength

The bond strength for anchorage of stresses above prestress is

$$f_{bpd} = \eta_{p2} \eta_1 f_{ctd}$$

where

$\eta_{p2}$  takes into account the type of tendon and the bond situation at anchorage ("pull-out")

= 1,4 for indented wires

= 1,2 for 7-wire strands

$\eta_1$  same as above

$f_{ctd} = f_{ctk,0,05} / \gamma_C$ , design value of concrete tensile strength

$\eta_{p2}$  has the same values as  $\eta_{p1}$  in MC90. and there is no favourable effect of "push-in". Instead the bond situation at anchorage is characterized by "pull-out", where the tendons "shrink" in the transverse direction when the stress increases.

For  $f_{ctd}$  there is a limitation to the value valid for C55. The reason is that the linear relationship between  $f_{bpd}$  and  $f_{ctd}$  cannot be expected to be valid for higher concrete strengths. This is due to an increasing brittleness, which results in a more uneven distribution of the bond stress. The average bond strength will normally increase also above C55, although not in proportion to the tensile strength. This may be taken into account, but requires a special verification.

#### 8.10.2.2.3.3.2 Anchorage length

The anchorage length is based on the upper design value of the transmission length and the increase of stress above the remaining prestress, with bond strength according to 8.10.2.2.3.3.1:

$$l_{bpd} = l_{pt2} + \alpha_2 \phi (\sigma_{pd} - \sigma_{p\infty}) / f_{bpd}$$

where

$l_{pt2}$  the upper design value of the transmission length (see 8.10.2.2.3.2.2)

$\sigma_{pd}$  tendon stress to be anchored (same as in MC90)

$\sigma_{p\infty}$  the remaining prestress (after all losses; same as in MC90)

### 8.10.2.3. Numerical comparisons

#### 8.10.2.3.1 Transmission length

##### 8.10.2.3.1.1 Effect of concrete strength

The transmission length according to EN, MC90 and ENV is shown in figure 8.1 as a function of the concrete strength. The figure covers indented wires and strands, different bond conditions and the way of release. The lower design value of the transmission length is shown.

The straight line representing the ENV is the same in all 6 diagrams, since the ENV does not make any difference between strands and indented wires, nor does it take into account bond conditions, nor the way of release (at least does not tell how to do it). The EN and MC90, on the other hand, do take these parameters into account.

Due to this the comparison gives very different results. For example, for strands released gradually and in good bond conditions, the ENV is extremely conservative compared to the EN and MC90, whereas for indented wires released suddenly and in bad bond conditions, the ENV is by far on the unsafe side.

##### 8.10.2.3.1.2 Effect of initial prestress

Figure 2 shows the transmission length as a function of the initial prestress. The most notable difference in this case is that the ENV does not take into account the magnitude of the initial prestress at all (at least it is not explained how to do), whereas according to the EN and MC90 the transmission length is directly proportional to the prestress.

The comment to figure 8.1 in the third paragraph of 8.10.2.3.1.1 applies also to figure 8.2.

#### 8.10.2.3.2 Anchorage length

In figure 8.3 the total anchorage length in ULS is shown as a function of the stress to be anchored.

Like for the transmission length, the ENV is conservative for gradually released strands in good bond conditions, and far on the unsafe side for wires in bad bond conditions, particularly if released suddenly.

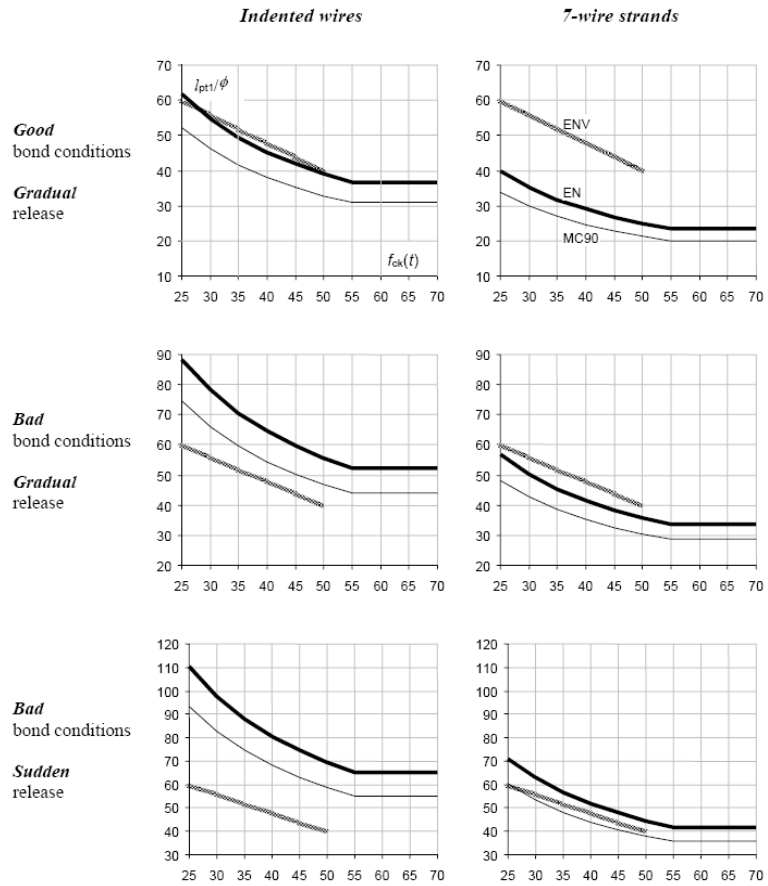


**Figure 8.1.** Transmission length (lower design value  $l_{pt1}$ ) as a function of the concrete strength  $f_{ck}(t)$  at release. Initial prestress is 1000 MPa. Thick black line = EN, thick grey line = ENV, thin black line = MC90

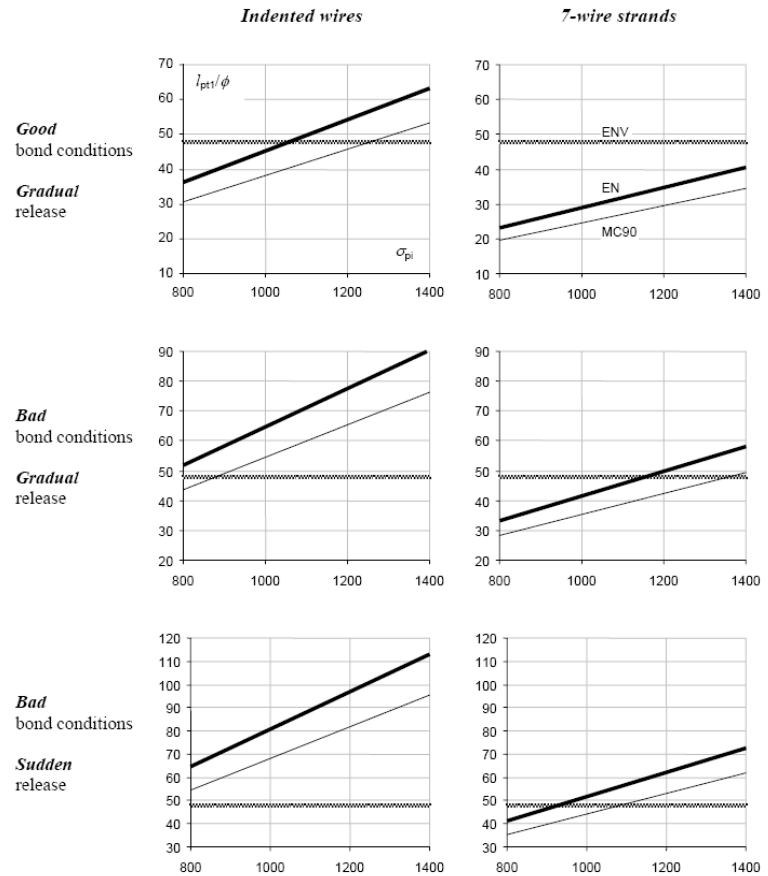


**Figure 8.2.** Transmission length (lower design value  $l_{pt1}$ ) as a function of the initial prestress  $\sigma_{pi}$ . Concrete strength at release is 40 MPa. Thick black line = EN, thick grey line = ENV, thin black line = MC90

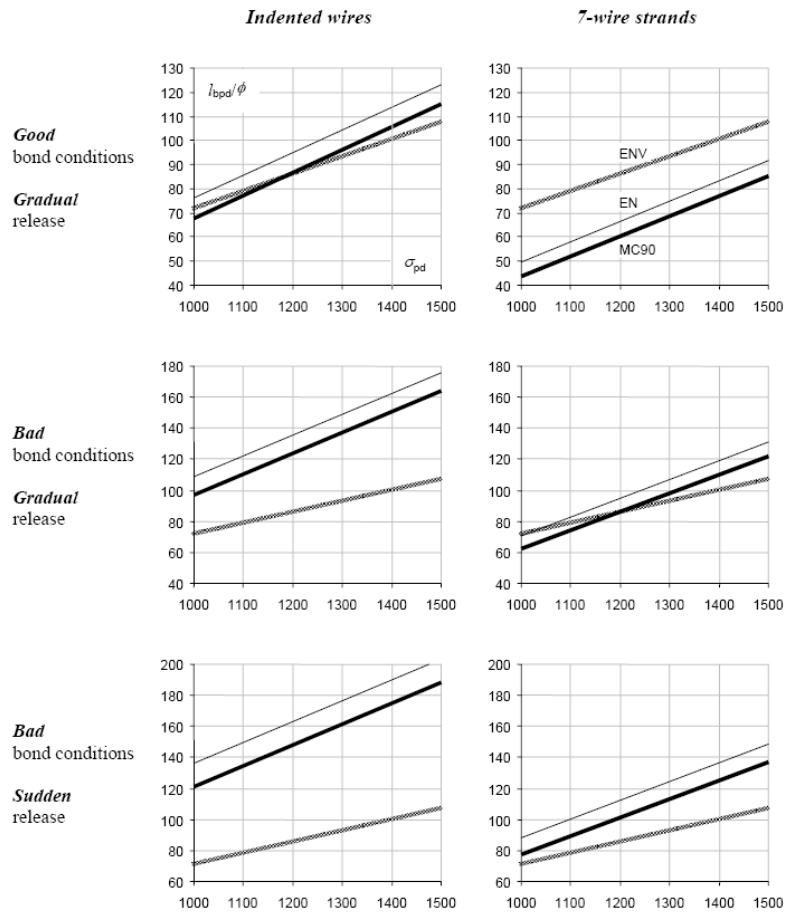


**Figure 8.3.** Anchorage length  $l_{bpd}$  as a function of the stress to be anchored,  $\sigma_{pd}$ . Concrete strength at release is 40 MPa, nominal concrete strength is C50 and initial prestress is 1000 MPa.  
 Thick black line = EN, thick grey line = ENV, thin black line = MC90

**SECTION 11 LIGHTWEIGHT CONCRETE**

**SECTION 11 LIGHTWEIGHT CONCRETE**

**11.1 General**

**C11.1 General**

A favourable circumstance for the preparation of Chapter 11 was that during the last years substantial work was conducted in updating the state-of-the-art on lightweight aggregate concrete to the most actual level. In this respect the joint CEB/FIP (now fib) Task Group 8.1 published in 1999 fib Bulletin 4 “Lightweight Aggregate Concrete: Codes and Standards”, a State-of-the-Art Report giving a good overview of common practice with regard to design practice in various countries [1]. Another report “Structural Lightweight Aggregate Concrete: Recommended Extensions to Model Code 90”, by the same Task Group, is now ready to be published [2]. Other valuable work was done within the scope of the Brite-Euram Project “EuroLightcon”. Important reports produced by the partners in this project were [3] and [4].

Chapter 10 in the new draft for EC-2 of 1/1/2000 applies to all concretes with a closed structure made with natural or artificial mineral lightweight aggregates, unless reliable experience indicates that provisions different from those given can be adopted safely.

“Lightweight aggregate concrete” is defined as a concrete having a closed structure and an oven-dry density of not more than 2200 kg/m<sup>3</sup> consisting of or containing a proportion of artificial or natural lightweight aggregates having a particle density of less than 2000 kg/m<sup>3</sup>.

**11.3 Materials**

**C11.3 Material properties**

The material properties of lightweight aggregate concrete are related to the corresponding properties of normal aggregate concrete as defined in section 3.1. The following conversion factors have been introduced in order to derive the properties of lightweight concrete from those of normal weight concrete:

- $\eta_E$  conversion factor for the calculation of the modulus of elasticity
- $\eta_1$  coefficient for the determination of the tensile strength
- $\eta_2$  coefficient for the determination of the creep coefficient
- $\eta_3$  coefficient for the determination of the drying shrinkage
- $\rho$  oven-dry density of lightweight aggregate concrete in kg/m<sup>3</sup>

*Concrete strength and stress-strain relations*

The strength classes for lightweight aggregate concrete range from LC 12/15 to LC 80/95, where the first figure stands for the characteristic cylinder strength and the second for the characteristic cube strength.

Altogether 3 stress strain relations have been defined. The first one describes the average behaviour as realistically as possible and is meant for calculating the distribution of forces and moments in a structure. The second and the third are both given, as alternatives, for the design of cross sections. The second and the third differ only in the ascending branch, the second being parabolic and the third being linear, Fig. 11.1.

Lightweight concrete is more brittle than normal density concrete of the same strength class. This is reflected in the formulation of the ultimate strain, where the factor  $\eta_1$  has been added.

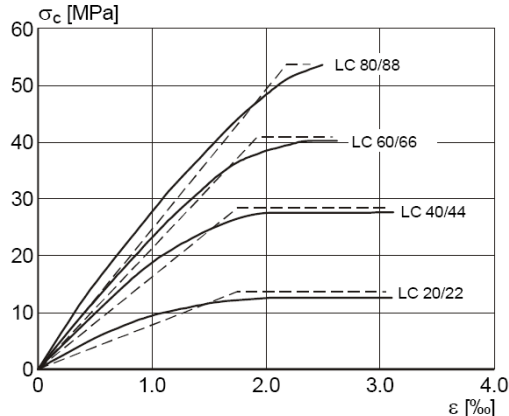


**Figure 11.1.** Design stress-strain relations for concrete in compression

The maximum stress in the diagram is obtained by multiplying the characteristic cylinder strength with a sustained loading factor of 0.85 and dividing by a material safety factor of 1.5, so that  $f_{cd} = 0.57f_{ck}$ . For normal density concrete the sustained loading factor is defined to be 1, unless

specified otherwise (Clause 3.5(1P)). The most important reason is that sustained loading effects, if occurring anyhow, will occur after a considerable time. So when loaded the concrete will be much older (maybe even years) than 28 days. The sustained loading effect is therefore with high probability compensated by the gain in strength between 28 days and actual loading of the structural member (see further the background report of chapter 3.1).

In lightweight concrete, however, the increase in strength after 28 days is smaller than in normal weight concrete [4]. Furthermore it is reported that the sustained loading effect is more pronounced than in normal aggregate concrete. Weigler [5] reported that the strength of lightweight concrete under sustained loading was only about 70-75% of the short term strength. Similar results were obtained by Smeplass [6]. The results are explained by creep of the matrix, overloading the aggregates. Consequently this phenomenon occurs when the strength of the aggregates it utilized to its maximum [4]. Since further research seems to be necessary here, this would support the idea of introducing a sustained loading factor for lightweight concrete anyhow. Therefore in 10.3.1.5  $\alpha_{loc}$  should preferably be defined as 0.85 “unless specified otherwise”.

The tensile strength of lightweight concrete can be obtained by multiplying the corresponding strength of normal density concrete of the same strength class with a factor

$$\eta_1 = 0.40 + 0.60\rho/2200 \quad (11.1)$$

where  $\rho$  is the upper limit of the oven-dry density.

Here it should be noted that the average tensile strength  $f_{ctm}$  normal density concrete follows from

$$f_{ctm} = 0.30 f_{ctk}^{2/3} \quad \text{for concretes } < C50/60 \quad (11.2a)$$

and

$$f_{ctm} = 2.12 \ln(1 + f_{cm}/10) \quad \text{for concretes } > C50/60 \quad (11.2b)$$

the characteristic (5%) value follows from

$$f_{ctk} = 0.7 f_{ctm} \quad (11.3)$$

### E-modulus

An estimate of the mean value of the secant modulus  $E_{cm}$  for LWAC can be obtained by multiplying the corresponding value for normal density concrete by the coefficient

$$\eta_E = (\rho/2200)^2 \quad (11.4)$$

In the previous part of the Eurocode, ENV 1992-1-4 “General rules for lightweight concrete with a closed structure, the equation  $\eta_E = (\rho/2200)^2$  was mentioned. For normal density concrete, according to chapter 3.1, the E-modulus is calculated from

$$E_{cm} = 9.5(f_{ck}+8)^{1/3} \quad (11.5)$$

### Creep

In the the old version ENV-1992-1-4 it is denoted that for lightweight concrete the creep coefficient  $\phi$  can be assumed equal to the value of normal density concrete multiplied by a factor  $(\rho/2300)^2$  for  $\rho > 1800 \text{ kg/m}^3$ . For  $\rho < 1500 \text{ kg/m}^3$  a factor  $1.3(\rho/2300)^2$  can be used. For intermediate values of  $\rho$  linear interpolation may be applied. Furthermore the creep strain has to be multiplied by a factor  $\eta_2 = 1.3$  for lightweight concrete classes lower than LC20/25.

There is however serious doubt on the correctness of the statement in ENV 1992-1-4 that the creep of lightweight concrete is smaller than that of normal density concrete, in spite of the fact that, according to [1] also other codes like the Norwegian Code NS 3473, the Japanese Code JSCE and the German code DIN4219 give formulations with the same tendency.

Kordina [5] states that creep is a matter of the cement paste and not of the aggregate, which would imply that similar compositions of LWAC and NDC should give the same specific creep. Neville [6] developed a two-phase model where he distinguishes the cement paste and the aggregates as two parallel load bearing components. The stiffer the aggregate, the more load will be carried by the aggregate skeleton and the more the stresses in the paste will decrease. A decrease of the stresses in the paste will result in smaller creep deformation of the paste and hence of the concrete. Since most of the lightweight aggregates have a lower stiffness, the stresses in the paste will remain higher and so the creep of LWAC [4]. Anyhow, existing information seems to confirm that there is not difference between normal density concrete and lightweight concrete with regard to the

specified creep, see f.i. Fig. 11.2 [7].

A reconsideration of the formulation for creep of LWAC, as given in ENV 1992-1-4 and provisionally adopted in the version of EC-2 of 1/1/2000 seems to be necessary. The best formulation seems to be that creep of LWAC is the same as creep of NDC and can be calculated with the same formula's.

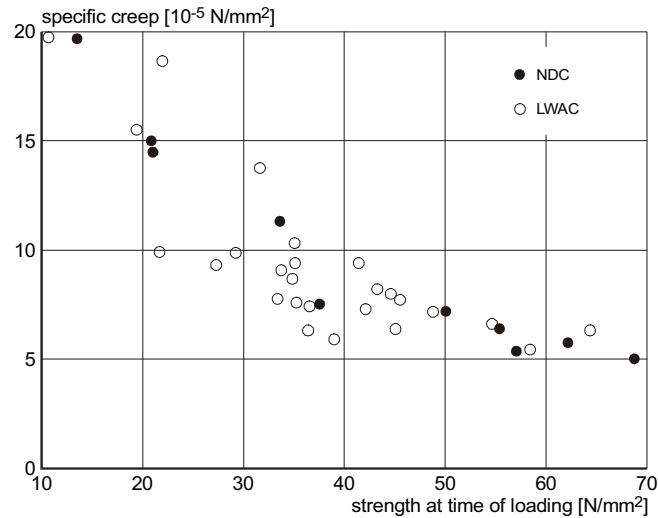


Figure 11.2. Final specific creep as a function of strength at the age of loading [7]

**Shrinkage**

For normal strength concrete the shrinkage is formulated as

$$\epsilon_{cs} = \epsilon_{cd} + \epsilon_{ca} \tag{11.6}$$

- where  $\epsilon_{cs}$  final shrinkage strain
- $\epsilon_{cd}$  drying shrinkage strain
- $\epsilon_{ca}$  autogenous shrinkage

The component  $\epsilon_{cd}$ , representing the drying shrinkage strain, is known to be higher for lightweight concrete. In [8] it is reported that the final shrinkage of LWAC is about 1-1.5 times the final shrinkage of NDC of the same strength. Hoffman and Stöckl [9] reported for LWAC's with cylinder strengths of 40-50 MPa differences of about 30% with NDC. Theissing [10] reported, on the basis of a literature survey, for concretes with a cylinder strength of 21 Mpa, values which were about 35% higher than for NDC. Probst [11] reported about shrinkage tests on three different LWAC's made with Liapor ( $f_{cc} = 65$  Mpa), Berwilit ( $f_{cc} = 43$  Mpa) and Leca ( $f_{cc} = 33$  Mpa), kept under a RH of 65%, values of 0.55% in axial direction and 0.85 % in transverse direction. This is about the same as found for NDC.

In ENV-1992-1-4 it is stated that final drying shrinkage values for lightweight concrete can be obtained by multiplying the values for normal density concrete with a factor  $\eta_3$  defined by

$$\begin{aligned} \text{LC12/15 to LC/20:} & \quad \eta_3 = 1.5 \\ \text{LC20/25 and higher} & \quad \eta_3 = 1.2 \end{aligned}$$

Since the information from literature is not fully consistent and the values given in ENV 1992-1-4 will presumably be not be too far from reality they have been maintained in the new draft of 1.1.2000.

A new element in the formulation of shrinkage is the component  $\epsilon_{ca}$  which represents autogenous shrinkage. The attention to this additional type of shrinkage contribution was drawn during the introduction of high strength normal density concretes, with low water/cement ratio's. Autogenous shrinkage is believed to be caused by "self-dissiccation", which is a result of a volume reduction of the hydration product compared to the volume of the reacting water and cement, i.e. chemical shrinkage, and goes along with a decrease of the relative humidity in the pore system. This drop in relative humidity is accompanied by a volume reduction of the matrix. This volume reduction is sometimes also denoted with the term "chemical shrinkage". [4].

For normal density concrete the component of autogenous shrinkage is formulated as:

$$\epsilon_{ca,\infty}(t) = \beta_{cc}(t) \epsilon_{ca,\infty} \tag{11.7a}$$

where

$$\varepsilon_{ca,\infty} = 2.5 (f_{ck} - 10) 10^{-3} \quad (11.7b)$$

and  $\beta_{cc}(t)$  is the hardening function.

The contribution of autogenous shrinkage decreases considerably with increasing strength of the concrete.

In lightweight aggregate concrete the conditions are quite different if the aggregate particles are saturated with water. In that case the possible supply of water from the aggregate to the drying microstructure will prevent a significant drop of the relative humidity in the paste and will thus reduce autogenous shrinkage. Therefore for LWAC the contribution of autogenous shrinkage as given by Eq. (EC-3.10/11) has to be regarded as an upper value.

#### Ultimate bearing capacity of LWAC structures

With regard to the bearing capacity of structures in the ultimate limit state specially the behaviour in shear and punching is important. This holds particularly true because cracks in lightweight concretes are supposed to be smoother than cracks in normal density concrete: in normal strength concretes of moderate strength cracks are propagating *around* the aggregate particles, whereas in lightweight concrete the crack *intersects* the aggregate particles, which have generally a much lower strength than gravel aggregate particles. This might reduce the shear friction capacity of the cracks and as such reduce the total shear carrying capacity. This difference might also limit the redistribution capacity of the concrete web (rotation of compression struts to lower angles), which is particularly important since in the draft of 1.1.2000 the standard method has not been involved anymore and only the variable inclination method is given as the basis for the calculation of the shear reinforcement. Those questions will be systematically treated.

#### Shear capacity of reinforced concrete members without shear reinforcement

In Section 6, the shear capacity of reinforced (normal density) concrete members without shear reinforcement has been formulated as:

$$V_{Rdc} = [0.12\eta_1 k (100\rho f_{ck})^{1/3} - 0.15\sigma_{cd}] b_w d \quad (11.8)$$

where

$f_{ck}$	characteristic cylinder strength of lightweight concrete
$k$	size factor = $1 + (200/d)^{1/3} \leq 2.0$
$\rho_l$	longitudinal reinforcement ratio = $A_{sl}/b_w d < 0.02$
$\sigma_{cd}$	average longitudinal prestress in the cross section
$\eta_1$	conversion term from NDC to LWAC, see Eq. 11.1.

The coefficient 0.12 has been replaced ( $0.18/\gamma_c$ ) in order to show explicitly the safety margin.

On order to see if this formulation is also suitable for lightweight concrete, the expression has been verified with 86 test results, from Ivey/Buth [12], Walraven [13], Hansson [14], Taylor/Brewer [15], Evans/Dongre [16], Torenfeld/Drangsholt [17], Thorenfeld/Stemland [18] and Aster/Koch [29]. Fig. 11.3 shows the results. A mean value of  $v_{test}/k\eta_1(\rho f_{cm})^{1/3}$  of  $x = 0.162$  with a standard deviation of 0.0235 is obtained, corresponding to a coefficient of variation of 0.145. A design value can be obtained on the basis of a statistical evaluation. For such a case the classical level-2 method, as described in EC-1 Basis of Design is suitable. The way how to deal with this method has been described and illustrated by Taerwe [20].



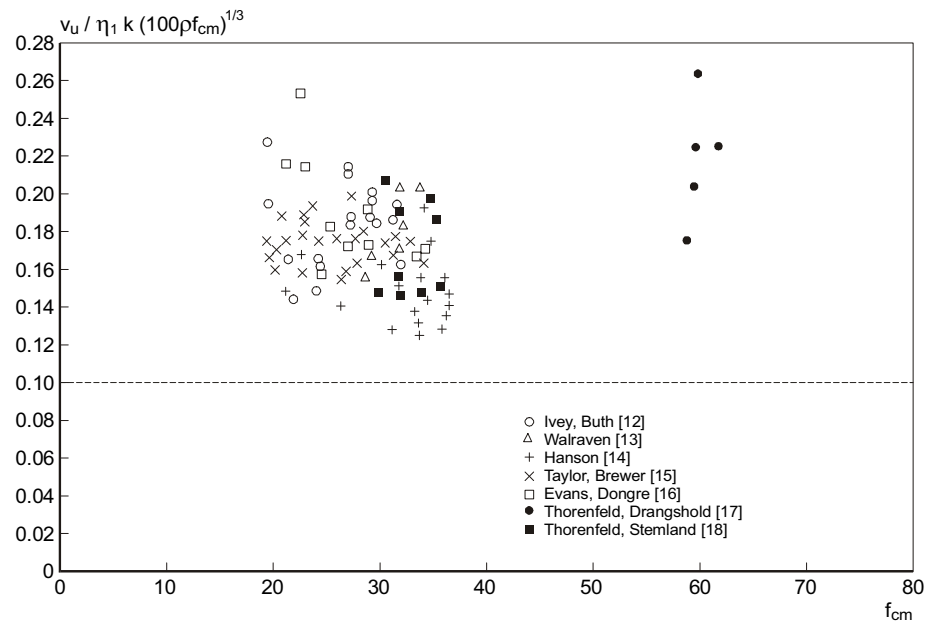


Figure 11.3. Verification of Eq. 11.8 for the shear capacity of members without shear reinforcement with test results

According to the level 2 method, a reliable design equation can be derived from test results with the general formulation

$$B_{Rd} = \mu_{BR}(1 - \alpha_{BR} \beta \delta_{BR}) \tag{11.9}$$

where

- $B_{Rd}$  design value
- $\mu_{BR}$  mean value of tests
- $\alpha_{BR}$  sensitivity factor for  $B_R$  normally taken 0.8 in the case of one dominating parameter
- $\beta$  target safety index, taken 3.8
- $\delta_{BR}$  coefficient of variation

with  $\mu_{BR} = 0.162$ ,  $\alpha_{BR} = 0.8$  and  $\delta_{BR} = 0.145$  a value for the design coefficient in Eq. 11.8 of 0.091 is obtained. In this derivation, however, the *mean* concrete cylinder compressive strength has been used, whereas in the code expression the *5%-lower value*  $f_{ck}$  is used. In the new version of EC-2, according to the Model Code, the relation

$$f_{ck} = f_{cm} - 8 \text{ (Mpa)} \tag{11.10}$$

is used. This means coefficients of variation  $\delta_f = 0.15$  for a concrete LC 25/30 and  $\delta_f = 0.055$  for a concrete LC 80/95. This would mean an increase of the coefficient 0.091 with 9% for C25 and 3% for LC 80/95. This would then result in a coefficient 0.100 for a concrete class LC25/30 and 0.095 for a concrete class of LC80/95. The conclusion is that Eq. 11.8 should be modified to

$$V_{1Rdc} = [0.10 \eta_1 k (100\rho f_{ck})^{1/3} - 0.15\sigma_{cd}] b_w d \tag{11.11}$$

This agrees with the proposal given in [2].

**Shear capacity of members with shear reinforcement**

In the new version for EC-2, contrary to ENV 1992-1-1, only one method for the design of members with shear reinforcement is given. This method is based on the variable angle truss model. For members of *normal density concrete* not subjected to axial forces, with vertical shear reinforcement, the shear capacity is the smaller value of

$$V_{Rd,sy} = \frac{A_{sw}}{s} z f_{ywd} \cot \theta \tag{11.12a}$$

where  $A_{sw}$  = cross-sectional area of one stirrup,  $s$  = stirrup distance,  $z$  = inner lever arm of the cross-section,  $f_{ywd}$  = design yield stress of shear reinforcement,  $\theta$  = inclination of compression strut, and

$$V_{Rd,max} = b_w z v f_{cd} / (\cot\theta + \tan\theta) \tag{11.12b}$$

With the additional condition

$$\frac{A_{sw}f_{ywd}}{b_w s} \leq 0.5v f_{cd} \tag{11.12c}$$

The first eq. 11.12a represents yielding of the shear reinforcement and the second equation 11.12b crushing of the inclined concrete struts. The inclination of the concrete struts can freely be chosen between 21.8° (cot θ = 2.5) and 45° (cot θ = 1).

v is an efficiency factor for the concrete crushing strength depending on the concrete strength according to:

$$v = 0.6(1 - f_{ck}/250) \geq 0.5 \tag{11.13}$$

An important question with regard to the applicability of those formulations for lightweight aggregate concrete is if the concrete struts in the web have a sufficient capacity to rotate. In normal density concrete during crack formation the strong aggregate particles do not fracture and the crack propagates around them: therefore the crack surface is very rough so that large frictional forces can be transmitted. This is a very important condition to allow a rotation of the inclined struts from 45° down to an angle of 21.8° as a minimum. In lightweight aggregate concrete the aggregate particles are intersected, so that a less rough crack surface is obtained. It is therefore questionable whether the rotation capacity of the web is sufficient to allow as well a lowest strut inclination of 21.8°, or if a higher lower limit should be defined. In order to answer this question tests have been carried out on I-shaped beams with varying shear reinforcement, Fig. 11.4, Walraven [21]. Any series consisted of three beams, which contained whether low, medium or high ratio's of shear reinforcement, whereas furthermore the beams were exactly similar. Three types of lightweight aggregates were used in the various concrete mixes: Lytag, Liapor and Aardelite. In those concretes only the coarse aggregate particles were of the lightweight type: the mixtures contained natural sand. The concrete volume weights were 2050 kg/m³ (Aardelite), 1975 kg/m³ (Lytag) and 1780 kg/m³ (Liapor). Those series were compared with a reference series with beams made of normal density concrete. On the web the state of deformation was continuously measured, so that the inclination of the principal compression strain could be monitored. Fig. 11.4 shows two diagrams, in which the inclination of the principal strain is represented. The left diagram shows the results for the gravel concrete members, with low (GD30L), medium (GD30M) and high (GD30H) shear reinforcement ratio's, the right diagram shows the corresponding curves for lightweight concrete. The tests show that the rotational behaviour of the inclined struts is similar for LWAC and NDC. In both cases the beams with the lowest shear reinforcement ratio showed the highest strut rotation capacity. Obviously the other two shear reinforcement ratio's were both too high to reach yielding of the steel, so that the final rotation remained relatively small. The unexpected result that NDC- and LWAC-beams behave similarly can be explained by the overall shape of the cracks. On a meso-level the roughness of the cracks in lightweight concrete is indeed smaller, but this was compensated by the roughness on the macro-level, caused by the overall crack undulation. In this way also in the interface contact areas occurred, with sufficient capacity to develop the necessary transmission of forces across the inclined cracks. Also Thorenfeld [22] reported a substantial decrease of the strut inclination with increasing load. For a shear reinforcement ratio of 0.5% he found a lowest strut inclination at failure of 25°. His tests were carried out on lightweight concrete with Leca aggregates, both for the coarse and the sand fractions. The volume weight of this concrete was 1500 kg/m³.

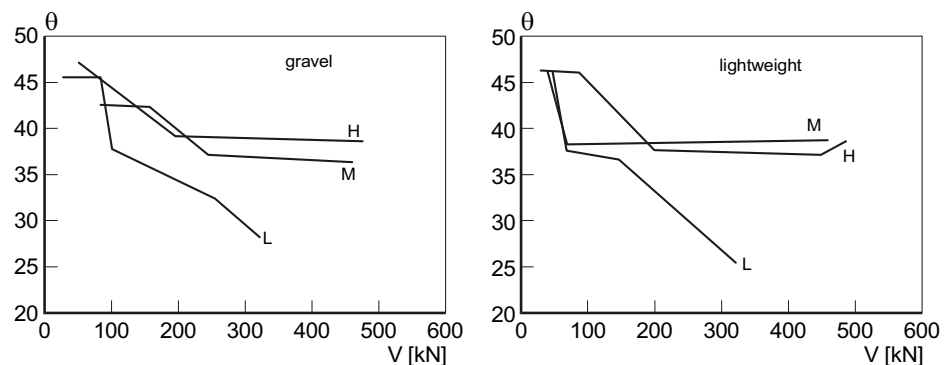


**Figure 11.4.** Principal strain directions θ in relation to the longitudinal member axis, as a function of the shear force for gravel concrete (left) and lightweight concrete (Aardelite, right), for high (H), medium (M) and low (L) shear reinforcement ratio's [21]

On the basis of those observations, for the design of members with shear reinforcement in *lightweight concrete*, the same principle as for normal density concrete was maintained in the new version for EC-2, including a lower limit for the strut inclination of 21.8° (cot θ = 2.5).

In ENV 1992-1-4, the part on lightweight aggregate concrete, the efficiency factor  $\nu$ , defining the crushing capacity of the concrete struts, was formulated as

$$\nu = 0.6 - f_{ck}/235 \geq 0.425 \tag{11.14}$$

The efficiency factor  $\nu$  is only slightly smaller than the corresponding expression for NDC in the new EC-2 version. Comparison with tests shows that the combination of the equations 11.12.a-c and 11.14 does not give an appropriate lower bound. An analysis showed that this can not be solved by restricting the strut rotation to a higher value of  $\theta_{min}$ . reducing the allowable inclined compressive stress. Implicitly this means that a reduction of the efficiency factor  $\nu$  is necessary. A better formulations is therefore

$$V_{LWAC} = 0.85 \eta_1 V_{NDC} \tag{11.15a}$$

or

$$V_{LWAC} = 0.85 \eta_1 0.6 (1 - f_{ck}/250) \geq 0.425 \eta_1 \tag{11.15b}$$

Fig. 11.5 shows the comparison of the combination of Eq. 11.12.a-c and 11.15 with test results from Walraven [21], Hamadi [22] and Thorenfeld [23].

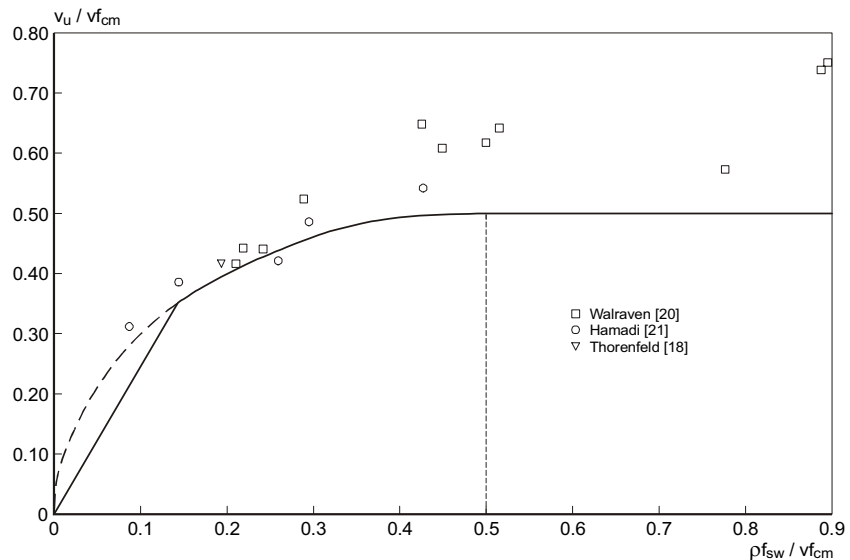


Figure 11.5. Verification of the design equation 11.12/15 for lightweight concrete members with shear reinforcement by test results

Eq.11.14 could be simplified to

$$V_{LWAC} = 0.50(1 - f_{ck}/250) \tag{11.16}$$

Punching shear capacity of lightweight concrete slabs and column bases.

In normal density concrete the punching shear capacity is calculated with the nominal design punching shear stress

$$V_{Rd,c} = 0.12\eta_1k (100 \rho_l f_{ck})^{1/3} - 0.08 \sigma_{cd} \tag{11.17}$$

which is multiplied with a basic control section at a distance of  $2d$  from the loaded area.

Since Eq. 11.17 is the same as the equation used for shear, it may be wondered whether also here, like in the case of Eq. 11.9, a factor 0.10 should be applied in stead of the factor 0.12 basically valid for NDC. Fig. 11.6 shows a comparison between Eq. 11.17 (only reinforced concrete, so  $\sigma_{cd} = 0$ ) and test results by Tomaszewicz [24], Regan [25], Hognestad [26], Corley [27] and Ivey [28]. Although the number of available tests was limited, a statistical derivation according to the level 2 method leads to the conclusion that the coefficient 0.12 is correct, so that Eq. 11.16 can be maintained (for the 22 tests a mean value of  $\mu_{Rd} = V_{test}/V_{calc} = 0.181$  is obtained, with a standard deviation of 0.0183, which means a coefficient of variation of 0.10. The level-2 method yields then a design value, including the model uncertainty, of  $x_d = 0.181 - 0.8 \cdot 3.8 \cdot 0.0183 = 0.125$ ).

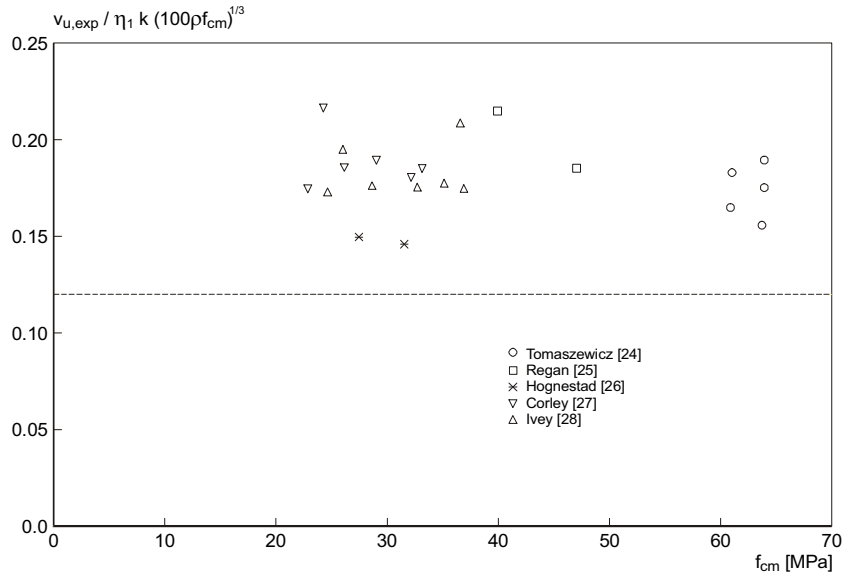


Figure 11.6. Verification of Eq. 11.16 for the punching shear capacity of slabs with test results modification

**Multiaxial states of stress**

A short review of the major points on this subject, as treated in [1] and [2], is given by Faust in [30]. The text is cited here:

Major differences between LWAC and NDC arise from differences in transversal behaviour, strength under multiaxial state of stress, local compression and efficiency of confinement. All of these aspects are connected with each other and attributed to various LWAC phenomena. First, the transversal strain of LWAC at the maximum compressive load is in part considerably lower, although Poissons ratio in the elastic region is almost the same as for NDC. This is valid in particular for LWAC with lightweight sand, because of the minimum microcracking. The second reason is the lesser resistance of LWA to lateral pressure in comparison to dense aggregates. This leads to a higher compressibility under multiaxial loads due to the porous nature of LWA. Hence, increasing effects of lateral pressure on confined concrete sections are generally reduced in LWAC, Fig. 11.7.

Finally, the lower ratio between the tensile and the compressive strengths reduces the compressive bearing capacity of locally loaded LWAC (Fig. 11.8).

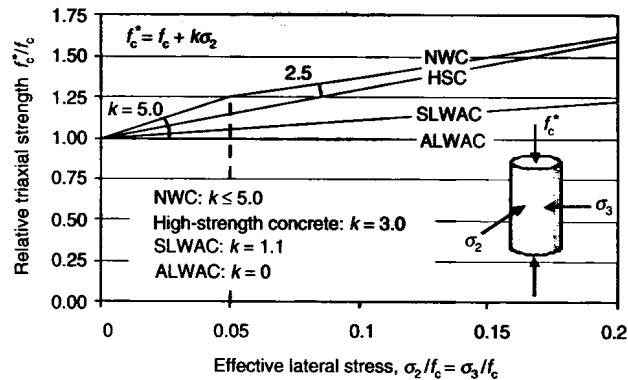


Figure 11.7. Efficiency of a confining reinforcement in different concretes according to MC'90, fib Bulletin 8 and CEB Bulletin 228

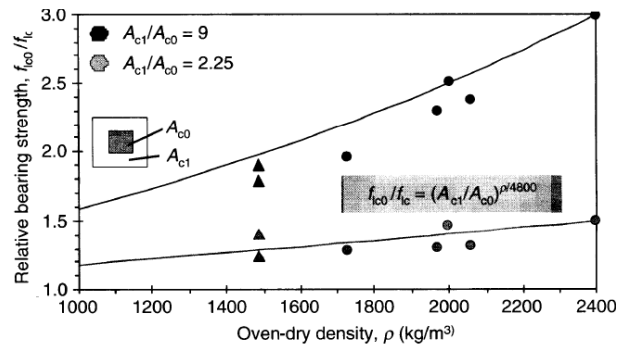


Fig. 11.8. Local compression in LWAC according to Walraven et al. [31]

**Deflection of slabs**

Since the E-modulus for LWAC is smaller than for NWAC this will influence the acceptable limits for  $l/d$ . This can be calculated as follows:

The deflection of a slab, spanning one way, and subjected to a uniformly distributed load is (assuming the cracked state)

$$\delta = \frac{5}{384} \frac{ql^4}{(EI)r}$$

with  $M_{max} = 1/8 ql^2$  this can be written as:

$$\delta = \frac{5}{48} \frac{M_{max} \cdot l^2}{(EI)r}$$

with

$$\frac{M_{max}}{(EI)r} = k_r \quad \text{and} \quad k_r = \frac{\epsilon_s}{d-x} = \frac{\sigma_s}{E_s(d-x)}$$

it is found that

$$\delta = \frac{5}{48} \frac{\sigma_s l^2}{E_s d (1 - \frac{x}{d})} \tag{11.18}$$

where  $\sigma_s$  is the stress in the longitudinal steel and  $x$  is the height of the compression zone.

In general the requirement  $\delta_{\infty} \leq 0.004 l$  will be governing.

Substituting this equation in (11.1) it is found that

$$\frac{1}{d} < \frac{0.038 E_s (1 - \frac{x}{d})}{\sigma_s} \tag{11.19}$$

For the height  $x$  of the compression zone in the linear elastic cracked state it is known that

$$\frac{x}{d} = -n\rho_1 + \sqrt{(n\rho_1)^2 + 2n\rho_1} \tag{11.20}$$

where  $\rho_1$  = longitudinal reinforcement ratio and  $n = E_s/E_c$

For a concrete strength C20/25 the E-modulus, including creep effects, can be assumed to be  $E_c \cong 9000$  MPa, so that  $n \cong 200,000/9000 = 22,2$

For lightweight concrete  $E_{lc} = \eta_E \cdot E_c$ , where  $\eta_E$  is defined as

$$\eta_E = \left( \frac{\rho}{2200} \right)^2, \text{ see Eq. 11.2 in prEN1992-1-1} \tag{11.21}$$

In Table 11.1 the values for  $x/d$  are calculated on the basis of Eq. (11.19), as a function of  $\rho_1(\%)$  and  $\eta_E$

**Table 11.1** values for  $x/d$  calculated on the basis of Eq. (11.19), as a function of  $\rho_1(\%)$  and  $\eta_E$

		$\rho(\text{kg/m}^3) \geq 2200$	2000	1800	1600
		$\eta_E = 1$	0,82	0,67	0,53
$\rho_1 =$	0.2%	$x/d = 0.26$	0.235	0.217	0.20
	0.3%	$x/d = 0.30$	0.28	0.26	0.24
	0.4%	$x/d = 0.34$	0.31	0.29	0.27
	0.5%	$x/d = 0.37$	0.34	0.32	0.29
	1.0%	$x/d = 0.48$	0.45	0.42	0.38

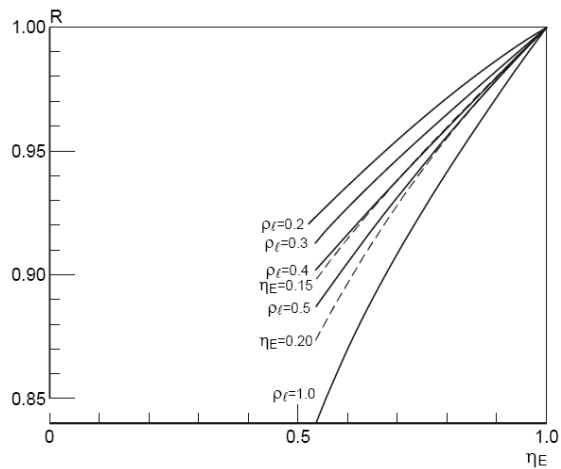
The values  $x/d$  being known as  $(1-x/d)$  is known; on the basis of Eq. 11.19 the change of  $l/d$  can be calculated.

Table 11.2 gives the reduction factors for  $l/d$  obtained in this way

**Table 11.2.** reduction factors for  $l/d$

		Reduction factor R for $l/d$			
		$\eta_E=1$	$\eta_E=0.82$	$\eta_E=0.67$	$\eta_E=0.53$
$\rho_1 =$	0.2	1	0.974	0.950	0.925
	0.3	1	0.972	0.946	0.921
	0.4	1	0.96	0.93	0.90
	0.5	1	0.95	0.93	0.89
	1.0	1	0.95	0.89	0.84

Fig. 11.9 shows the results graphically. In practical design the reinforcement ratio is generally between 0.15 and 0.50%. It can be seen that the reduction factor  $\eta_E^{0.15}$  covers the calculated values quite well.



**Figure 11.9.** Reduction factor R for  $l/d$  as a function of  $\eta_E$  and  $\rho_1$

## REFERENCES

1. fib-Task Group 8.1, "Lightweight Aggregate Concrete: Codes and Standards", State-of-the-Art Report, Lausanne, Aug. 1999, 40 pages
2. fib-Task Group 8.1, "Structural Lightweight Aggregate Concrete: Recommended Extensions to Model Code 90", 35 pages, to be published in 2000.
3. European Union – Brite Euram III, "Definitions and International Consensus Report", Eurolightcon Project, Document BE96-3942/R1, April 1998.
4. European Union – Brite Euram III, LWAC Material Properties State-of-the-Art", Document BE96-3942/R2, December 1998.
5. Kordina, K, "Experiments on the influence of the mineralogical character of aggregate on the creep of concrete", Rilem Bulletin, Paris, 1960, No. 6, pp 7-22.
6. Neville, A.M., Dilger, W.H., Brooks, J.J., "Creep of plain and structural concrete" Construction Press, London.
7. CEB-FIP Manual on Lightweight Aggregate Concrete, the Construction Press, London, 1977
8. Cembureau (1974), Lightweight aggregate concrete – Technology and World applications, Editor G. Bologna.
9. Hoffmann, P., Stöckl, S., "Tests on creep and shrinkage of high strength lightweight aggregate concrete", Deutscher Ausschuss für Stahlbeton, Nr. 343, pp. 1-20 (in German).
10. Theissing, E.M., et al. "Lightweight concrete", CUR report 48, 208 p., 1971.
11. Probst, P., Stöckl, S., "Experiments on creep and shrinkage of high strength lightweight concrete", Deutscher Ausschuss für Stahlbeton, Nr. 313, pp. 58-81 (in German).
12. Ivey, D.L., Buth, E., "Shear capacity of lightweight concrete beams", ACI Journal, Proceedings, Oct. 1967.
13. Walraven, J.C., "The influence of depth on the shear strength of lightweight concrete beams without shear reinforcement", Report 5-78-4, Delft University of Technology, 1978.
14. Hanson, J.A., Tensile strength and diagonal tension resistance of structural lightweight concrete, ACI Journal Proceedings, Vol. 58, July 1961, pp. 1-40.
15. Taylor, R., Brewer, R.S., "The effects of the type of aggregate on the diagonal cracking of reinforced concrete beams", Magazine of Concrete Research, July 1963, pp. 87-92.
16. Evans, R.H., Dongre, A.V., "The suitability of lightweight aggregate (Aglite) for structural concrete", Magazine of Concrete Research, Vol 15, No. 44, July 1963, pp. 93-97.
17. Thorenfeld, E., Drangshold, G., "Shear Capacity of Reinforced High Strength Concrete Beams", High Strength Concrete, Second International Symposium, May 1990, Berkely 1990, ACI-SP-121.
18. Thorenfeld, E., Stemland, H., "Shear capacity of lightweight concrete beams without shear reinforcement", International Symposium on Structural Lightweight Concrete, 20-24 June 1995, Sandefjord, Norway, Proceedings, pp. 244-255.
19. König, G., Fisher, "Model uncertainties concerning design equations for shear capacity of concrete members without shear reinforcement", CEB-Bulletin 224, Model Unvertainties, July 1995, pp. 100.
20. Taerwe, L., "Towards a consistent treatment of model uncertainties in reliability formats for concrete structures", CEB Bulletin 219, 1993, pp. 5-61.
21. Walraven, J.C., Al-Zubi, N., "Shear capacity of lightweight concrete beams with shear reinforcement", International Symposium on Structural Lightweight Concrete, 20-24 June 1995, Sandefjord, Norway, Proceedings, pp. 91-104.
22. Hamadi, Y.D., Regan, P.E., "Behaviour of normal and lightweight aggregate beams with shear cracks", The Structural Engineer, Vol 58B, No. 4, December 1980, pp. 71-79.
23. Thorenfeld, E., Stemland, H. and Tomaszewicz, A., "Shear Capacity of Large I-Beams", International Symposium on Structural Lightweight Concrete, 20-24 June 1995, Sandefjord, Norway, 1995, Proceedings, pp. 733-744.
24. Tomaszewicz, A., High –Strength Concrete. SP2 – Plates and Shells. Report 2.3 "Punching Shear Capacity of Reinforced Concrete Slabs", Report No. STF70 A93082, SINTEF Structures and Concrete, Trondheim, 36 pp.
25. Regan, P.E., Al-Hussaini, A., Ramdane K-E., Xue H-Y., (1993). "Behaviour of High Strength

- Concrete Slabs”, Concrete 2000. Proceedings of International Conference, University of Dundee, Scotland, UK, September 7-9, Vol. 1, E&FN Spon, Cambridge, pp. 761-773.
26. Hognestad, E., Elstner, R.C., Hanson, J.A., “Shear strength of reinforced structural lightweight aggregate concrete slabs”, ACI Journal, June 1964, PP. 643-656.
  27. Corley, W.G., Hawkins, N.M., Shearhead reinforcement for slabs”, ACI-Journal, October 1968, pp. 811-824.
  28. Ivy, C.B., Ivey, D.L., Buth, E., Shear capacity of lightweight concrete flat slabs”, ACI-Journal, June 1969, pp. 490-494.
  29. Aster, H., Koch, R., “Untersuchungen an dicken Stahlbetonplatten”, Universität Stuttgart, 1974,
  30. Faust, T., “Recommended extensions to Model Code 90 for light-weight aggregate concrete”, fib news, 2000, No. 3, pp. 153-156.
  31. Walraven, J.C., den Uijl. J.A., Stroband, J., Al-Zubi, N., Gijsbers, J. and Naaktgeboren, M., “Structural Lightweight Concrete: Recent Research”, Heron, 1995, 40, No. 1, pp. 5 – 30.

**See example 11.1, 11.2**